Electrospray ionization mass spectrometry and its environmental applications
by Jesse MacArthur Long

A thesis submitted in partial fulfillment of the requirements for the degree of Doctor of Philosophy in Chemistry
Montana State University
© Copyright by Jesse MacArthur Long (1993)

Abstract:
An electrospray ionization (ESI) source was designed, fabricated and then installed on a VG TRIO-2 quadrupole mass spectrometer. A gold coated 50-/μm fused silica capillary was used instead of the conventional stainless steel needle. Analytes are desorbed into the gas phase via a heated metal transport capillary and are focused through a set of five electrostatic lenses into the analyzer region of the mass spectrometer.

Environmentally significant compounds (~ 100 - 500 Da) such as pesticides and herbicides that are polar, nonvolatile and thermally labile are not readily analyzed by conventional gas chromatography/mass spectrometry (GC/MS). A viable alternative is ESI/MS. Thirty pesticides from the 13 classes of carbamate, organophosphorus, organochlorine, bipyridyl, phthalimide, urea, carboxyllic acid, hydroxycoumarin, triazine, indandione, dinitroaniline, pyrethrin, and thiocarbamate were analyzed using this method.

Analysis of these samples in the neat form at a pH of 5.5 and acidified to a pH of 3.0 showed that addition of acid to the neat sample did not appreciably increase the protonated analyte signal nor the total ion current for any of the samples analyzed. This observation together with the extremely low pKa values of these pesticides, calculated by SPARC, indicates that the protonated analytes are formed in the gas rather than in the condensed phase.

Sodium and ammonium ions were added to these pesticides but in no case was the total ion current increased over that from the neat sample.

Solvent studies showed that 50/50 mixtures of methanol/water and acetonitrile/water are both suitable solvent systems but that a methanol fraction of 30% appears to be ideal for some of the pesticides studied. Evidence of radical cation formation was observed when pure acetonitrile was used.

It was demonstrated, by spiking 5 carbamate pesticides into Yellowstone River water, that ESI/MS by the direct injection method is a potential candidate as a rapid screening method for pesticides in natural waters.

This work is significant because the data suggests that the protonated molecular ions from many of the compounds studied are formed in the gas phase. Also, ESI/.MS shows promise as a multi-class analytical technique for pesticides.

ELECTROSPRAY IONIZATION MASS SPECTROMETRY AND ITS ENVIRONMENTAL APPLICATIONS

by

Jesse MacArthur Long

A thesis submitted in partial fulfillment
of the requirements for the degree

of

Doctor of Philosophy

in

Chemistry

MONTANA STATE UNIVERSITY
Bozeman, Montana

April 1993

D378
L8522

APPROVAL

of a thesis submitted by

Jesse MacArthur Long

This thesis has been read by each member of the thesis committee and has been found to be satisfactory regarding content, English usage, format, citations, bibliographic style, and consistency, and is ready for submission to the College of Graduate Studies.

4-6-93
Date

L Joseph Seaver
Edwin H. Abbott
Chairperson, Graduate Committee

Approved for the Major Department

4-6-93
Date

John R Emens
Head, Major Department

Approved for the College of Graduate Studies

4/6/93
Date

R L Brown
Graduate Dean

STATEMENT OF PERMISSION TO USE

In presenting this thesis in partial fulfillment of the requirements for a doctoral degree at Montana State University, I agree that the Library shall make it available to borrowers under rules of the Library. I further agree that copying of this thesis is allowable only for scholarly purposes, consistent with "fair use" as prescribed in the U.S. Copyright Law. Requests for extensive copying or reproduction of this thesis should be referred to University Microfilms International, 300 North Zeeb Road, Ann Arbor, Michigan 48106, to whom I have granted "the exclusive right to reproduce and distribute my dissertation for sale in and from microform or electronic format, along with the right to reproduce and distribute by abstract in any format in whole or in part."

Signature Jesse MacArthur Long

Date April 6, 1993

This dissertation is written in memory of my sister, Frances, who always laughed easily, worked hard and enjoyed the simple things in life.

ACKNOWLEDGMENTS

I wish to thank Dr. L. Joseph Sears for his guidance and instruction during the course of this work, especially for giving me the opportunity to work in the area of electrospray ionization mass spectrometry. I thank Dr. Edwin H. Abbott for coordinating all the business matters associated with the cooperative agreement under which I completed this work and also for his ever present optimism and encouragement. I am appreciative of the advice and encouragement given by Drs. Jan Sunner and Robert V. Thurston during this work. Additionally, Drs. Patrik R. Callis, Reed A. Howald and Lee H. Spangler deserve credit for contributing significantly to my having a better understanding of physical phenomena.

I am grateful to Dr. Rosemarie C. Russo and the U. S. Environmental Protection Agency for supporting this research.

A special acknowledgment is extended to Nan, my wife and best friend, for her unfaltering encouragement and support throughout my tenure at Montana State University. Her support and sense of adventure contributed profoundly to the success of this work.

TABLE OF CONTENTS

Page

1. INTRODUCTION 1

Background 1
Analytical Methods 3
Gas Chromatography/Mass Spectrometry (GC/MS) 3
High Performance Liquid Chromatography/Mass Spectrometry (HPLC/MS) 4
HPLC/MAGIC/MS 5
HPLC/TS/MS 5
HPLC/ES/MS 6
Electrospray Ionization 9
Mass Analysis 12
Statement of the Problem 12

2. EXPERIMENTAL 16

Instrumentation 16
Electrospray Ionization Interface 16
Ion Signal Optimization 24
Electrostatic Lens System 24
Ion Kinetic Energy 29
Signal Amplification 29
VG Trio-2 Quadrupole Mass Spectrometer 29
Data System 29
Vacuum System 31
Pesticide Analysis 31
Pesticide Samples 31
Sample Preparation 35
pH Studies 37
Adduct Studies 37
Solvent Study 38
Rapid Method 38

3. RESULTS AND DISCUSSION 40

Electrospray Ionization Interface 40
Calibration 47

TABLE OF CONTENTS - Continued

Page

Pesticide Analysis 50
Triazine Pesticides 61
Carbamate Pesticides 64
Dimethyl Urea Pesticides 66
Organophosphorus Pesticides 66
Hydroxycoumarin Pesticides 66
Carboxyllic Acid Pesticides 67
Other Classes of Pesticides 67
pH Studies 76
Sodium Adduct Study 77
Ammonium Acetate Study 78
Solvent Study 78
Rapid Method by Direct Injection 84
Sensitivity 85

4. CONCLUSIONS 89

LITERATURE CITED 91

APPENDICES 96

Appendix A - Pesticide Reference Spectra 97
Appendix B - Chemical Structures and pKa's of the Pesticides 129
Appendix C - Collision-Activated Dissociation Spectra 142
Appendix D - Neat Pesticide Response as a Function of Potential Difference 167
Appendix E - pH/Sodium Studies 182
Appendix F - Sodium Adduct Study 194
Appendix G - Ammonium Acetate Study 204
Appendix H - Solvent Study 211
Appendix I - Rapid Method 220

LIST OF TABLES

Table Page

1. SIMION Contour Intervals (Original Design) 24
2. SIMION Contour Intervals (Final Design) 26
3. Pesticide Nomenclature, CAS Numbers and Estimated Discharge Levels 32
4. Spray Needle/Transport Capillary Potential Difference 37
5. Polyethylene Glycol Reference Masses 52
6. Chemical/Physical Properties of the Pesticides 54
7. Pesticide Reference Samples 59
8. Major Ions (and Intensity) Generated by Electrospray Ionization Mass Spectrometry 62
9. Percent Ionization as a Function of pKa 71
10. Chemical/Physical Properties of the Solvents 79
11. Total Ion Current as a Function of Needle Diameter 87
12. Sensitivity Study 88

LIST OF FIGURES

Figure Page

1. Sketch of the Three Steps in ES/MS 7
2. Electrospray Ionization Interface. Scale: 1 cm = 1.33 cm. 17
3. Electrical Feedthrough Connections 18
4. DC Power Supply 19
5. Heater Construction 20
6. VARIAC Transformer Calibration 21
7. Heater Calibration 23
8. SIMION Simulation of Ion Trajectories in Original Lens System Design 25
9. SIMION Simulation of Ion Trajectories in Final Lens System Design 27
10. Pressure and Signal/Noise as Function of Capillary/Skimmer Distance 28
11. Signal Amplification Before and After Installation of Pre-Amplifier 30
12. Home-Built Electrospray Ion Source for the VG TRIO 2 Mass Spectrometer 41
13. Intensity as a Function of Heater Temperature 44
14. Needle Current as a Function of Needle Voltage 46
15. Electrospray Ionization Mass Spectrum of PEG (1000 M.W.) P. D. 35 Volts 48
16. Electrospray Ionization Mass Spectrum of PEG (1000 M.W.) P. D. 200 Volts 49
17. Electrospray Ionization Mass Spectrum of Calibration Standard 51
18. Electrospray Ionization Mass Spectrum of Protonated PEG (200 M.W.) 53
19. First Electrospray Ionization Mass Spectrum of PEG 57
20. First Electrospray Ionization Mass Spectrum of Propoxur 58
21. Resonance Stabilization in the Aromatic Carbamate Pesticides 65
22. Possible Structures of the Diquat Ions 68
23. Possible Structures for the Folpet Ions 68
24. Ion Intensity as a Function of Capillary/Skimmer Potential Difference 75
25. Solvent Effects (Methanol/Water, Methanol) on Total Ion Current 80
26. Solvent Effects (Acetonitrile/Water) on Total Ion Current 81
27. Free Energy of Solvation as a Function of Cluster Radius 83

LIST OF FIGURES - Continued

Figure Page

28. Electrospray Ionization Mass Spectrum of Yellowstone River Water Spike with 5 Carbamate Pesticides 86
29. Electrospray Ionization Mass Spectrum of Amitrole. P. D. 75 Volts 98
30. Electrospray Ionization Mass Spectrum of Anilazine. P. D. 65 Volts 99
31. Electrospray Ionization Mass Spectrum of Antu. P. D. 65 Volts 100
32. Electrospray Ionization Mass Spectrum of Carbaryl. P. D. 55 Volts 101
33. Electrospray Ionization Mass Spectrum of Carbofuran. P. D. 75 Volts 102
34. Electrospray Ionization Mass Spectrum of Chloramben. P. D. 75 Volts 103
35. Electrospray Ionization Mass Spectrum of Chlorpyrifos. P. D. 75 Volts 104
36. Electrospray Ionization Mass Spectrum of Coumafuryl. P. D. 75 Volts 105
37. Electrospray Ionization Mass Spectrum of Diphacinone. P. D. 45 Volts 106
38. Electrospray Ionization Mass Spectrum of Diquat Dibromide. P. D. 75 Volts 107
39. Electrospray Ionization Mass Spectrum of Diuron. P. D. 55 Volts 108
40. Electrospray Ionization Mass Spectrum of Endosulfan. P. D. 55 Volts 109
41. Electrospray Ionization Mass Spectrum of Endothall. P. D. 65 Volts 110
42. Electrospray Ionization Mass Spectrum of Ethion. P. D. 75 Volts 111
43. Electrospray Ionization Mass Spectrum of Folpet. P. D. 65 Volts 112
44. Electrospray Ionization Mass Spectrum of Glyphosate. P. D. 35 Volts 113
45. Electrospray Ionization Mass Spectrum of Linuron. P. D. 85 Volts 114
46. Electrospray Ionization Mass Spectrum of Mephosfolan. P. D. 85 Volts 115
47. Electrospray Ionization Mass Spectrum of Methidathion. P. D. 75 Volts 116

LIST OF FIGURES - Continued

Figure Page

48. Electrospray Ionization Mass Spectrum of Mehiocarb. P. D. 65 Volts 117
49. Electrospray Ionization Mass Spectrum of Methomyl. P. D. 55 Volts 118
50. Electrospray Ionization Mass Spectrum of Mexacarbate. P. D. 75 Volts 119
51. Electrospray Ionization Mass Spectrum of Molinate. P. D. 85 Volts 120
52. Electrospray Ionization Mass Spectrum of Phosfolan. P. D. 85 Volts 121
53. Electrospray Ionization Mass Spectrum of Propoxur. P. D. 55 Volts 122
54. Electrospray Ionization Mass Spectrum of Pyrethrin I & II. P. D. 65 Volts 123
55. Electrospray Ionization Mass Spectrum of Rotenone. P. D. 65 Volts 124
56. Electrospray Ionization Mass Spectrum of Siduron. P. D. 75 Volts 125
57. Electrospray Ionization Mass Spectrum of Thiometon. P. D. 45 Volts 126
58. Electrospray Ionization Mass Spectrum of Trifluralin. P. D. 35 Volts 127
59. Electrospray Ionization Mass Spectrum of Warfarin. P. D. 75 Volts 128
60. Chemical Structures of the Pesticides 130
61. Chemical Structures and pKa's of the Pesticides 136
62. Collision-Activated Dissociation Spectrum of Chloramben. P. D. 35 Volts 143
63. Collision-Activated Dissociation Spectrum of Chloramben. P. D. 85 Volts 144
64. Collision-Activated Dissociation Spectrum of Endothall. P. D. 45 Volts 145
65. Collision-Activated Dissociation Spectrum of Endothall. P. D. 85 Volts 146
66. Collision-Activated Dissociation Spectrum of Carbofuran. P. D. 35 Volts 147
67. Collision-Activated Dissociation Spectrum of Carbofuran. P. D. 85 Volts 148

LIST OF FIGURES - Continued

Figure Page

68. Collision-Activated Dissociation Spectrum of Propoxur. P. D. 35 Volts 149
69. Collision-Activated Dissociation Spectrum of Propoxur. P. D. 75 Volts 150
70. Collision-Activated Dissociation Spectrum of Amitrole. P. D. 35 Volts 151
71. Collision-Activated Dissociation Spectrum of Amitrole. P. D. 135 Volts 152
72. Collision-Activated Dissociation Spectrum of Anilazine. P. D. 35 Volts 153
73. Collision-Activated Dissociation Spectrum of Anilazine. P. D. 85 Volts 154
74. Collision-Activated Dissociation Spectrum of Ethion. P. D. 45 Volts 155
75. Collision-Activated Dissociation Spectrum of Ethion. P. D. 85 Volts 156
76. Collision-Activated Dissociation Spectrum of Methidathion. P. D. 45 Volts 157
77. Collision-Activated Dissociation Spectrum of Methidathion. P. D. 85 Volts 158
78. Collision-Activated Dissociation Spectrum of Diuron. P. D. 45 Volts 159
79. Collision-Activated Dissociation Spectrum of Diuron. P. D. 75 Volts 160
80. Collision-Activated Dissociation Spectrum of Linuron. P. D. 45 Volts 161
81. Collision-Activated Dissociation Spectrum of Linuron. P. D. 95 Volts 162
82. Collision-Activated Dissociation Spectrum of Coumafuryl. P. D. 55 Volts 163
83. Collision-Activated Dissociation Spectrum of Coumafuryl. P. D. 85 Volts 164
84. Collision-Activated Dissociation Spectrum of Rotenone. P. D. 55 Volts 165
85. Collision-Activated Dissociation Spectrum of Rotenone. P. D. 120 Volts 166
86. Amitrole (2.54E-4 M) Ion Intensity as a Function of Potential Difference 168
87. Chlorpyrifos (5.88E-5 M) Ion Intensity as a Function of Potential Difference 169

LIST OF FIGURES - Continued

Figure Page

88. Ethion (1.44E-5 M) Ion Intensity as a Function of Potential Difference 170
89. Mephosfolan (2.28E-5 M) Ion Intensity as a Function of Potential Difference 171
90. Methiocarb (9.98E-5 M) Ion Intensity as a Function of Potential Difference 172
91. Mexacarbate (8.96E-5 M) Ion Intensity as a Function of Potential Difference 173
92. Phosfolan (7.90E-5 M) Ion Intensity as a Function of Potential Difference 174
93. Propoxur (5.51E-5 M) Ion Intensity as a Function of Potential Difference 175
94. Linuron (8.40E-5 M) Ion Intensity as a Function of Potential Difference 176
95. Methidathion (6.66E-5 M) Ion Intensity as a Function of Potential Difference 177
96. Coumafuryl (6.46E-5 M) Ion Intensity as a Function of Potential Difference 178
97. Antu (9.85E-5 M) Ion Intensity as a Function of Potential Difference 179
98. Carbofuran (9.38E-5 M) Ion Intensity as a Function of Potential Difference 180
99. Endothall (1.00E-4 M) Ion Intensity as a Function of Potential Differnce 181
100. Ethion (1.14E-5 M) Ion Intensity as a Function of Potential Difference 183
101. Glyphosate (9.48E-5 M) Ion Intensity as a Function of Potential Difference 184
102. Carbofuran (7.41E-5 M) Ion Intensity as a Function of Potential Difference 185
103. Linuron (6.64E-5 M) Ion Intensity as a Function of Potential Difference 186
104. Methiocarb (7.88E-5 M) Ion Intensity as a Function of Potential Difference 187
105. Methidathion (5.26E-5 M) Ion Intensity as a Function of Potential Difference 188
106. Mephosfolan (1.80E-5 M) Ion Intensity as a Function of Potential Difference 189
107. Coumafuryl (5.10E-5 M) Ion Intensity as a Function of Potential Difference 190

LIST OF FIGURES - Continued

Figure Page

108. Total Ion Current as a Function of pH. Thiometon Concentration 1.2E-5 M 191
109. Total Ion Current as a Function of pH. Propoxur Concentration 5.0E-5 M 192
110. Intensity as a Function of pH. Phosfolan Concentration 1.58E-5 M 193
111. Diuron (1.73E-5 M) [M+H]+ Ion Intensity as a Function of NaI Concentration 195
112. Diuron (1.73E-5 M) [M+Na]+ Ion Intensity as a Function of NaI Concentration 196
113. Diuron (1.73E-5 M) Total Ion Current as a Function of NaI Concentration 197
114. Methomyl (2.53E-5 M) [M+H]+ Ion Intensity as a Function of NaI Concentration 198
115. Methomyl (2.53E-5 M) [M+Na]+ Ion Intensity as a Function of NaI Concentration 199
116. Methomyl (2.53E-5 M) Total Ion Current as a Function of NaI Concentration 200
117. Siduron (1.79E-5 M) [M+H]+ Ion Intensity as a Function of NaI Concentration 201
118. Siduron (1.79E-5 M) [M+Na]+ Ion Intensity as a Function of NaI Concentration 202
119. Siduron (1.79E-5 M) Total Ion Current as a Function of NaI Concentration 203
120. Endothall (8.00E-5 M) [M+H]+ Ion Intensity as a Function of Potential Difference 205
121. Linuron (6.72E-5 M) Ion Intensities as a Function of Potential Difference 206
122. Coumafuryl (5.17E-5 M) Ion Intensities as a Function of Potential Difference 207
123. Antu (7.88E-5 M) Ion Intensities as a Function of Potential Difference 208
124. Carbofuran (7.50E-5 M) Ion Intensities as a Function of Potential Difference 209
125. Propoxur (4.41E-5 M) Ion Intensities as a Function of Potential Difference 210
126. Methomyl (2.53E-5 M) Ion Intensity as a Function of Methanol Fraction 212
127. Methomyl (2.53E-5 M) [M+Na]+ Ion Intensity as a Function of Methanol Fraction 213

LIST OF FIGURES - Continued

Figure Page

128. Methomyl (2.53E-5 M) Total Ion Current as a Function of Methanol Fraction 214
129. Phosfolan (1.58E-5 M) [M+H]+ Ion Intensity as a Function of Methanol Fraction 215
130. Phosfolan (1.58E-5 M) [M+Na]+ Ion Intensity as a Function of Methanol Fraction 216
131. Phosfolan (1.58E-5 M) Total Ion Current as a Function of Methanol Fraction 217
132. Folpet (1.43E-5 M) Total Ion Current as a Function of Methanol Fraction 218
133. Trifluralin (1.25E-5 M) Total Ion Current as a Function of Methanol Fraction 219
134. Standard Curve for Carbaryl Generated by Electrospray Ionization 221
135. Standard Curve for Carbofuran Generated by Electrospray Ionization 222
136. Standard Curve for Methiocarb Generated by Electrospray Ionization 223
137. Standard Curve for Methomyl Generated by Electrospray Ionization 224
138. Standard Curve for Propoxur Generated by Electrospray Ionization 225
139. Standard Curve for Carbaryl in Mixture Generated by Electrospray 226
140. Standard Curve for Carbofuran in Mixture Generated by Electrospray 227
141. Standard Curve for Methiocarb in Mixture Generated by Electrospray 228
142. Standard Curve for Methomyl in Mixture Generated by Electrospray 229
143. Standard Curve for Propoxur in Mixture Generated by Electrospray 230

ABSTRACT

An electrospray ionization (ESI) source was designed, fabricated and then installed on a VG TRIO-2 quadrupole mass spectrometer. A gold coated 50-μm fused silica capillary was used instead of the conventional stainless steel needle. Analytes are desorbed into the gas phase via a heated metal transport capillary and are focused through a set of five electrostatic lenses into the analyzer region of the mass spectrometer.

Environmentally significant compounds ($\sim$100 - 500 Da) such as pesticides and herbicides that are polar, nonvolatile and thermally labile are not readily analyzed by conventional gas chromatography/mass spectrometry (GC/MS). A viable alternative is ESI/MS. Thirty pesticides from the 13 classes of carbamate, organophosphorus, organochlorine, bipyridyl, phthalimide, urea, carboxyllic acid, hydroxycoumarin, triazine, indandione, dinitroaniline, pyrethrin, and thiocarbamate were analyzed using this method.

Analysis of these samples in the neat form at a pH of 5.5 and acidified to a pH of 3.0 showed that addition of acid to the neat sample did not appreciably increase the protonated analyte signal nor the total ion current for any of the samples analyzed. This observation together with the extremely low pKa values of these pesticides, calculated by SPARC, indicates that the protonated analytes are formed in the gas rather than in the condensed phase.

Sodium and ammonium ions were added to these pesticides but in no case was the total ion current increased over that from the neat sample.

Solvent studies showed that 50/50 mixtures of methanol/water and acetonitrile/water are both suitable solvent systems but that a methanol fraction of 30% appears to be ideal for some of the pesticides studied. Evidence of radical cation formation was observed when pure acetonitrile was used.

It was demonstrated, by spiking 5 carbamate pesticides into Yellowstone River water, that ESI/MS by the direct injection method is a potential candidate as a rapid screening method for pesticides in natural waters.

This work is significant because the data suggests that the protonated molecular ions from many of the compounds studied are formed in the gas phase. Also, ESI/MS shows promise as a multi-class analytical technique for pesticides.

CHAPTER 1

INTRODUCTION

Background

"That miraculous DDT powder" ... or the "elixir of death" (1)? This question represents the two diametrically opposed viewpoints of pesticide chemicals used in our culture. The first quote was by Sir Winston Churchill in a speech in 1944 in which he recognized the role that DDT played in stopping an outbreak of typhus among allied troops in Naples. The second was by Rachel Carson in her book, Silent Spring,(2) expressing concern over the adverse effects of pesticides on birds of prey, farmers, other segments of the environment and the general populace.

Pesticides are released into the environment during manufacture, transport, handling, and application to crops. Because of their widespread use, pesticide residues have been found in groundwater (3, 4), surface waters (5), rain (6), and fog water (7).

Most available residue methods have been devised for the analysis of only a single pesticide or pesticide class. Public health concerns require continued research aimed at extending the available multiclass, multiresidue methods, and finding new methods to include many more of the pesticides being used worldwide, as well as their polar and conjugated metabolites. This problem was highlighted in a feature article in *Analytical Chemistry*, entitled "The Great Fruit Scares of 1989" (8), which discussed the near panic that occurred in the U. S. when residues of the plant growth regulator daminozide (Alar)

were found in apples and cyanide in grapes. The article states that multiresidue methods used by the FDA to routinely check foods for contaminants can pick up 40% of the pesticides likely to leave residues and that Alar is among those pesticides that slip past the routine screens. The article further describes the single residue methods used to detect and determine this compound and also elaborates on efforts taken to devise and test new methods for analyzing cyanide in fruit.

In 1985 U. S. farmers applied 335,000 metric tons (9) of pesticides to agricultural land, almost tripling the amount of pesticide used in the U. S. in 1965. The U. S. Environmental Protection Agency (USEPA) has estimated (10) that approximately 750,000 chemicals are now in use in homes, industry and agriculture. This does not include pesticides, pharmaceuticals and food additives nor the estimated 1500 different ingredients used in pesticides.

The staggering number and amount of chemicals used daily in this country explains the vested interest that the USEPA has in developing and maintaining state-of-the-art arsenal of analytical methodologies for analyzing these chemicals that are of potential danger to the environment.

Implementation of the Clean Water Act and the 1986 Amendments to the Comprehensive Environmental Response, Compensation, and Liability Act requires the USEPA to list chemicals that should be regulated in industrial wastewaters and hazardous waste landfills. Additionally, knowledge of the distribution of chemicals likely to reach the ambient environment is required for implementation of the Toxic Substance Control Act and Resource Conservation and Recovery Act. This knowledge facilitates the setting

of priorities for reviewing existing toxic chemicals and performing risk assessments for chemicals that may pose leaching problems from new and existing landfill operations. A major consideration in listing chemicals for regulations is the probability of their occurrence in the environment to which regulations will be applied. Surveys of chemicals conducted by the Office of Water Regulations and Standards and by the Office of Emergency and Remedial Response record the distribution of chemicals that are already listed and provide raw data from which other chemicals occurring frequently can be identified. During the last decade the responsibility of the Environmental Protection Agency to regulate chemical contamination has significantly increased. Conceivably, the Environmental Protection Agency's responsibility could involve the control of the eight million chemicals in the Chemical Abstracts Services Registry. However, the combined lists of chemicals specifically regulated by EPA amount to fewer than two thousand chemicals. Although there are other factors involved, the major limitation of protecting the environment from these potentially hazardous chemicals is the lack of the analytical methodology required to identify and measure these substances.

Analytical Methods

Gas Chromatography/Mass Spectrometry (GC/MS)

Organic chemical identification is accomplished by the most commonly accepted technique of extracting the chemical into a non-polar solvent and then analyzing the chemical by gas chromatography/mass spectrometry (GC/MS). Compounds that are detected are identified by empirical matching of their spectra with those in the 40- to

100- thousand spectrum libraries. Although occasionally some unmatched compounds can be identified utilizing mass fragmentation theory, most often compounds whose spectra are not in the spectral libraries remain on the unidentified list. Furthermore, the polar (hydrophilic) compounds remain unextracted by the accepted sample preparation techniques for GC/MS analysis and are, therefore, not detected. It is estimated that the most comprehensive files available leave over 25 percent of the extracted compounds unidentified after spectra matching. Furthermore, virtually all of the hydrophilic substances contained in the samples remain unidentified.

Two requirements of GC/MS that restrict the application to the non-volatile fraction are that the analytes of interest must be volatile enough to elute from the chromatographic column and that they must be sufficiently stable to avoid thermal degradation. Unfortunately, many classes of environmentally significant compounds do not meet these criteria and consequently cannot be determined by GC/MS techniques.

High Performance Liquid Chromatography/Mass Spectrometry (HPLC/MS)

High performance liquid chromatography (HPLC) does not have these limitations since this technique is suitable for the direct separation of highly polar and non-volatile compounds without inducing thermal degradation. Among other benefits, LC techniques indicate that the compounds are indigenous to the sample and not formed by pyrolysis during the GC/MS analysis itself.

Three techniques developed recently out of the determination and need to develop better ways to accomplish LC/MS are HPLC/Monodisperse Aerosol-based Interface for

Liquid Chromatography (MAGIC)/MS, also known as HPLC/Particle Beam (PB)/MS, HPLC/Thermospray (TS)/MS, and HPLC/Electrospray (ES)/MS.

HPLC/MAGIC/MS. The MAGIC or PB interface, developed by Browner and Willoughby (11), directs a nebulizing gas orthogonal to the flow of HPLC effluent and this results in the generation of highly uniform-sized droplets. A dispersion gas is used to prevent clustering of the droplets as they are passed through a desolvation region on their way to the MS ion source. The desolvation chamber is maintained at atmospheric pressure while an aerosol beam separator connects it to the high vacuum region of the mass spectrometer. Flow rates of 0.1-0.5 mL/minute are optimal and the complete separation of the sample from the HPLC eluent provides a choice between electron impact (EI) and chemical ionization (CI) mass spectra.

HPLC/TS/MS. HPLC/TS/MS was developed by Vestal (12) and involves the direct heating of a metal capillary tube through which HPLC eluent is flowing. This process, discovered serendipitously, results in the formation of ions without the use of an external source of ionizing electrons. Aqueous mobile phases containing an electrolyte such as ammonium acetate are passed at flow rates from 1 to 2 mL/minute through an electrically heated stainless steel capillary situated in a specially heated ion source with an auxiliary pumping line situated opposite the capillary. This results in a supersonic jet of vapor containing a fine mist of droplets or particles. The aerosol beam contains equal numbers of positively and negatively charged droplets. As the droplets travel through the heated source they continue to vaporize from the heat input from the

surrounding hot vapor. As the size of the charged droplet is reduced, the electrical field at the liquid surface increases until ions present in the liquid phase are ejected from the droplet. The ions are then sampled through a conical exit aperture in the mass analyzer.

HPLC/ES/MS. The generation in air at atmospheric pressure of a charged aerosol beam by electrospray was first reported in the scientific literature in 1917 (13) but experiments performed as early as 1745 have been referenced (14). Malcolm Dole and co-workers reported their work on producing macro ions from polymer solutions by ES about 25 years ago (15-18) and John Fenn renewed interest in ES when he first published results of electrospray ionization mass spectra of large molecules having molecular weights up to 40 kilodaltons (19). Fenn and his colleagues at Yale University initially began the development of ES as a mass spectrometric technique starting in the early 1980's (20, 21) and later went on to prove its capabilities for extensive multiple charging (22) and for the mass spectrometry of large biomolecules (19).

Electrospray mass spectrometry can be briefly described as taking place in three consecutive steps as shown in Figure 1: (1) the spray produces small highly charged droplets, (2) ion desorption produces pseudo-molecular ions and (3) sampling into vacuum produces an ion beam for analysis by a mass spectrometer.

In addition to the work done by Fenn the applications of ES/MS were demonstrated by Smith (23) at Battelle, Pacific Northwest Laboratories, Henion (24) at Cornell, and Nikolaev (25) of Leningrad U.S.S.R.

The liquid containing the analyte is sprayed from the needle tip of a hypodermic needle maintained at several kilovolts. Charge is deposited on the surface of the

emerging liquid resulting in the production of Coulomb repulsion forces that are sufficient to overcome surface tension so that the liquid containing the analyte is dispersed in an ultrafine spray. It is thought that the analyte molecules attach to adduct ions in solution and desorb out of the droplet under the influence of the self generated electric field of the droplet. Pseudo-molecular ions are further desolvated in countercurrent drying gas and then sampled into the vacuum via a glass capillary. In the free jet expansion at the exit of the capillary energy can be imparted to the ions by changing the potential of the capillary exit relative to the skimmer. The ion beam is then transmitted to a mass analyzer.

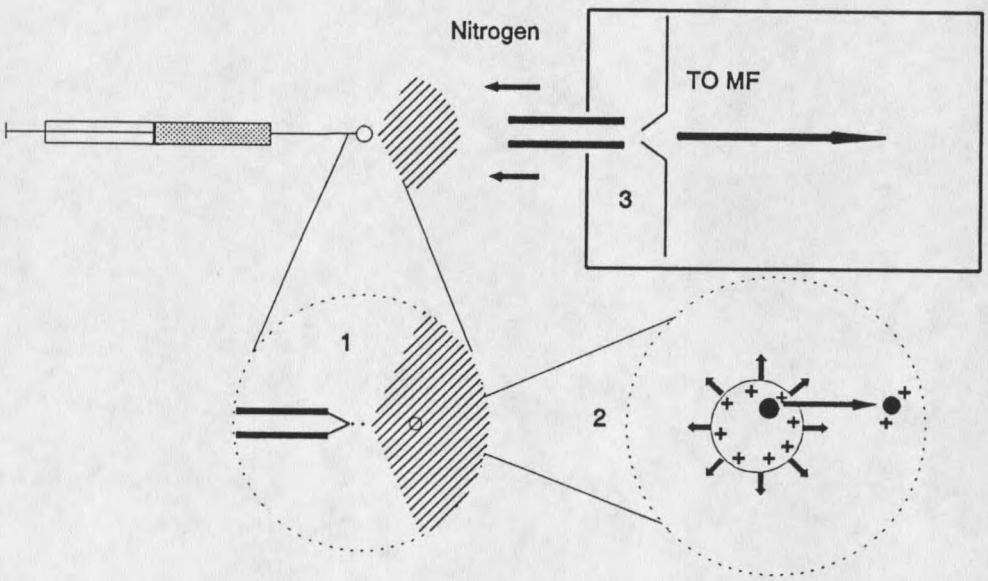


Figure 1. Sketch of the Three Steps in ES/MS

Once a stable spray has been established, ion desorption from a charged droplet is the key that determines which molecules can be efficiently analyzed by ES/MS. By

some unknown mechanism, depending on the analyte flow rate and the potential of the needle tip, the analyte molecules come to be in a multiple charged state.

The ES technique enables spectra to be obtained from mass spectrometrically difficult compounds such as gramicidin S for example (26). The electrospray process works best with flow rates in the range of 5-10 μL/minute and is very well suited to the use of micro or capillary liquid chromatograph packed columns.

The USEPA has been evaluating high performance liquid chromatography (HPLC)/particle beam (PB) mass spectrometry (MS) as one of several broad spectrum analytical methods for the determination of nonvolatile organic compounds in environmental samples. As stated earlier, this analytical technique was developed in the early 1980's (11) and later improved (27). One of the major reasons the USEPA selected this technique for evaluation in analyzing the non-volatile organics is that EI-like fragmentation and hence EI-like spectra are generated from this mode of analysis.

Although HPLC/PB/MS has been used successfully to analyze environmentally important chemicals such as pesticides and herbicides (28) it is generally recognized that this technique does not provide adequate sensitivity and specificity for the analysis of a broad range of compound classes.

Thermospray has also been used but because this ionization technique generally produces little if any fragmentation it is usually not considered as the ultimate analytical technique. The temperature required in the thermospray process is higher than that necessary in electrospray ionization and this factor must be considered in determining which process is most suitable for the analysis in mind.

Electrospray Ionization

Many theories regarding ion production are in existence. The hypodermic needle tip used to generate the spray is maintained at a few kilovolts and the resulting electrical field at the needle tip charges the surface of the emerging liquid and causes the liquid to be dispersed by Coulomb forces into a fine spray of charged droplets. These charged droplets consist of the solvent containing positive and negative ions and the predominant charge is determined by the induced potential. Under the influence of the electric field the droplets migrate toward the glass capillary inlet. It is thought that the charge density on the surface of the liquid droplet increases until the Rayleigh limit is reached and the Coulomb repulsion has the same magnitude as that of the droplet surface tension. This instability, referred to as a "Coulomb explosion", tears the droplet apart and produces charged daughter droplets that also evaporate. This sequence repeats itself until the radius of curvature of the daughter droplet becomes small enough that the field due to the surface charge density is strong enough to desorb ions from the droplet. In other words, repulsive forces within these daughter droplets appear to cause a field induced ion evaporation of the dissolved analyte ion, which effectively transfers the ion from the condensed to the gas phase. Production of these gas phase ions is desirable because it precludes introducing liquids directly into the mass spectrometer. These desorbing ions include cations or anions to which are attached solvent or solute species that are not themselves ions, thus producing "quasi-molecular" ions suitable for mass analysis. This idea of ion production is depicted in Figure 1.

This model of ion formation, based on that of Dole *et al* to some degree, was first

proposed by Iribarne and Thompson (29). They make the assumption based on the thermodynamic relationship, $\frac{Ne^2}{R} = -\Delta G^{\circ}_{s}$ (N=number of elementary charges; e=elementary charge; R=radius of droplet; ΔG°_{s}=free enthalpy of solvation), ions could begin to be released when R reaches a value of 0.06 μm. R_R is given by $\frac{N^2e^2}{R_R} = 16\pi\sigma R_R^2$ (N, e=same as above; σ=surface tension; R_R=Rayleigh instability radius). Therefore their critical value of R_E is given by $R_E > R_R = \left(\frac{N^2e^2}{16\pi\sigma}\right)^{1/3} = 3.979N^{2/3}$ Å (N, e, R_R, σ= same as above; R_E=droplet radius at onset of ion evaporation) . The relationship for R_E is given by $R = A + \sqrt{A^2 + B}$, where $A = 1/2\left(\frac{-e^2}{\Delta G^{\circ}_{s} + \Delta G^{\neq}}(\sqrt{N} - 0.25) + d\right)$ (N, e, ΔG°_{s}=same as above; $\Delta G^{\neq}$=barrier height; d=distance beneath surface of droplet from equilibrium position) and $B = \frac{-e^2d}{\Delta G^{\circ}_{s} + \Delta G^{\neq}}(\sqrt{N} - 0.5)^2$ (e, N, ΔG°_{s}, $\Delta G^{\neq}$, d=same as above).

Additionally, they postulate that for ion evaporation to be possible the critical radius R_E must be reached before the radius R_R at which the droplet may become disrupted due to Rayleigh instability. Assuming values of ΔG°_{s} = -56 and -64 kcal/mol for small and large clusters, respectively, and $\Delta G^{\neq}$ = 9 kcal/mol they determine that positive ions in the range of 55-135 Å and negative ions in the range of 80-190 Å would be in the Rayleigh instability limits.

This model has not been proved and has been questioned by Rollgen *et al* (30, 31) among others. Rollgen argued that the fields necessary for ion desorption in the model cannot be attained and that hydrodynamic instability would occur after an ion had left the droplet.

Although there is no theory that can be used as a guide, there are several features

established experimentally about the desorption process (32). The ionization step involves moderate temperature (60 degrees C) and ion desorption takes place from a liquid matrix probably with at least one solvation shell. Also, it is known that the ionization efficiency should be promoted by small size of droplets, high charge, high deformation and weak solvation by a volatile solvent (33). Methanol and acetonitrile are preferred over water for the best ionization efficiency.

Whatever the correct model of ion formation, the average charge state for large polymeric compounds is almost always such that the ions come to lie in an m/z window between 500 and 2500. One big advantage of ES/MS is that the m/z of the mass analyzer need not be large because, as a result of multiple charging, ions above 2500 are rarely observed. This multiple charging effect extends the molecular weight range of the analyzer by a factor equal to the number of charges. Although the mass spectral data produced by this multiple charging effect has quite an unfamiliar appearance compared to conventional electron impact spectra, data interpretation is fairly straightforward. Several algorithms for extracting molecular mass information from spectra showing sequences of peaks due to ions with varying numbers of charges have been proposed (23, 34, 35). To date most of the ES work done has been performed on quadrupole mass spectrometers which are relatively inexpensive and easy to use. However, results using ES combined with magnetic sector instruments have been reported (36, 37). Also, the first on-line coupling of microbore high performance liquid chromatography with an ion trap mass spectrometer equipped for sampling ions formed by ES at atmospheric pressure was recently reported (38).

Mass Analysis

The overall sensitivity of an ES/MS system is determined by the number of analyte ions that can be introduced into the mass analyzer. One problem common to atmospheric pressure ion sources, including the electrospray source, is the clustering of the analyte ions by water molecules during the free-jet expansion stage before they are sampled into the vacuum region of the mass spectrometer. Ions are drawn toward the skimmer orifice by an electric field. Sample, solvent and other background ions are formed as clusters with neutrals in the ionization region and are admitted through the ion sampling orifice of the skimmer. This clustering can lead to broadening, on the high mass side, of the low resolution mass spectra. By varying not only the distance between the transfer capillary and skimmer, but also the potential on the skimmer, collision induced dissociation of these clusters can be effected. Mild collisions are sufficient to break hydrogen bonds in cluster ions but vigorous collisions, however, can cause fragmentation of sample ions (25). Presently the transmission of ions from the source at atmospheric pressure to the analyzer is in the 10^{-5} to 10^{-6} range. There is much room for improvement in ES/MS sensitivity.

Statement of the Problem

It is obvious from the foregoing discussion that there is a real need for analytical methodologies that can be used to analyze more than one class of pesticide chemicals. Most of the techniques being employed are specific to one class of compounds.

Therefore, the major objective of this work was to evaluate electrospray ionization

mass spectrometry as an analytical technique for determining environmentally important chemicals using a home-built electrospray ionization source. Included in this work is the study of highly polar and non-volatile pesticides and herbicides. The following compounds are of specific interest (39, 40) and were included: Aldicarb, Carbaryl, Carbofuran, Methiocarb, Methomyl, Mexacarbate, Diuron, Linuron, Siduron, Rotenone, Chlorpyrifos, Ethion, Pyrethrin I, Molinate, Trifluralin, Amitrole, Warfarin, Diphacinone, Antu, Anilazine, Propoxur, Endosulfan I, Courmafuryl, Folpet, Chloramben, Endothall, Thiometon, Phosfolan, Mephosfolan, Methidathion, and Glyphosate.

Although no systematic studies have been done as to which classes of molecules can be ionized with electrospray it is generally recognized that satisfactory analyses are obtained on polar molecules but not on non polar ones such as hydrocarbons. Also successful analyses are common on the large molecules such as proteins, nucleotides and carbohydrates.

To date, most of the work using electrospray ionization has involved the very large molecules. Little, if any, work has involved analyzing the environmentally important samples such as pesticides and herbicides in the molecular weight ranges of 300-500 Daltons. However, work using "ion spray", a variation of electrospray, to analyze sulfonated azo dyes has been reported (41).

Although high pressure liquid chromatography was not included in this work, the utility of front-ending electrospray ionization with liquid chromatography is recognized and several comments are worthy of note. The conventional liquid chromatographic

column internal diameter is 4.6 mm. Although miniaturization in various forms has been in existence for many years it has not gained wide acceptance. There are many advantages of using capillary LC over conventional practices: better permeability, better efficiency, lower optimum flow rate, high mass sensitivity, savings in solvent and stationery phase, better column-to-column reproducibility, faster instrument start up, fewer problems with spent solvents, good column life expectancy, and easy column maintenance, chemical inertness and better quantitation (42).

Aside from the analytical advantages, the economics of using a capillary approach are worthy of consideration (43). A comparison of cost per year and disposal volume per year was done based on the liquid chromatographic column internal diameter used. Using a column diameter of 0.5 mm the cost per year is $7.83; the disposal volume per year is 1.4 L. Using the conventional LC column diameter of 4.6 mm the cost per year is $524.16; the disposal volume per year is 93.6 L. The cost is based on 32 injections per day or 8320 injections per year of 60:40 (v/v) acetonitrile/water.

Included in the work were pH studies to determine if the response is enhanced by the addition of acid. Also the effect of adding ions such as sodium and ammonium was studied. One of the most important variables in electrospray ionization mass spectrometry is choice of solvent system. The solvents methanol and acetonitrile were studied as solvent mediums for these pesticide solutions both in the pure form and in various fractions mixed with water.

The utility of using electrospray ionization by the direct injection method was studied as a rapid method candidate by spiking five of the carbamate pesticides into

Yellowstone River water and then by running standard curves to determine what kind of response the spiked river samples generate.

Finally, the sensitivity of the electrospray ionization technique is discussed in conjunction with improving the efficiency of mass transport of ions through the transport capillary.

The successful achievement of these objectives would indicate that ES/MS is a broad analytical technique capable of analyzing not only the large bio-molecules in the 10-40 kilodalton range but also environmentally important compounds, i.e. pesticides, in the 300-500 Dalton range. Hopefully, this research will augment the arsenal of analytical methodologies to be used in the continuing struggle to protect the environment.

CHAPTER 2

EXPERIMENTAL

Instrumentation

Electrospray Ionization Interface

The electrospray ionization interface drawn to scale in Figure 2 was designed in the Montana State University's (MSU) Chemistry Department, fabricated by the MSU Engineering Department and then installed on a VG TRIO 2 quadrupole mass spectrometer.

The electrical feeder consists of a 12-pin connector. Attached to each pin is an electrical wire (22 AWG, 0.32 mm^2, tin/copper, Lot #F805, Belden, Geneva, Il.) which is inserted into a metal tube containing an insulating glass tube (86 mm in length, 2 mm o. d., 1 mm i. d.). This tubing extends from the electrical feeder to the front plate of the interface. The wires protrude from the tube assembly and are attached to the various electrostatic lenses to apply desired potentials through the electrical feeder. Epoxy was used to close the openings in the ends of the metal and glass tubing as required by the vacuum system.

Shown in Figure 3 is the schematic diagram depicting the arrangement of these electrical connections between the electrical feeder and the electrostatic lenses.

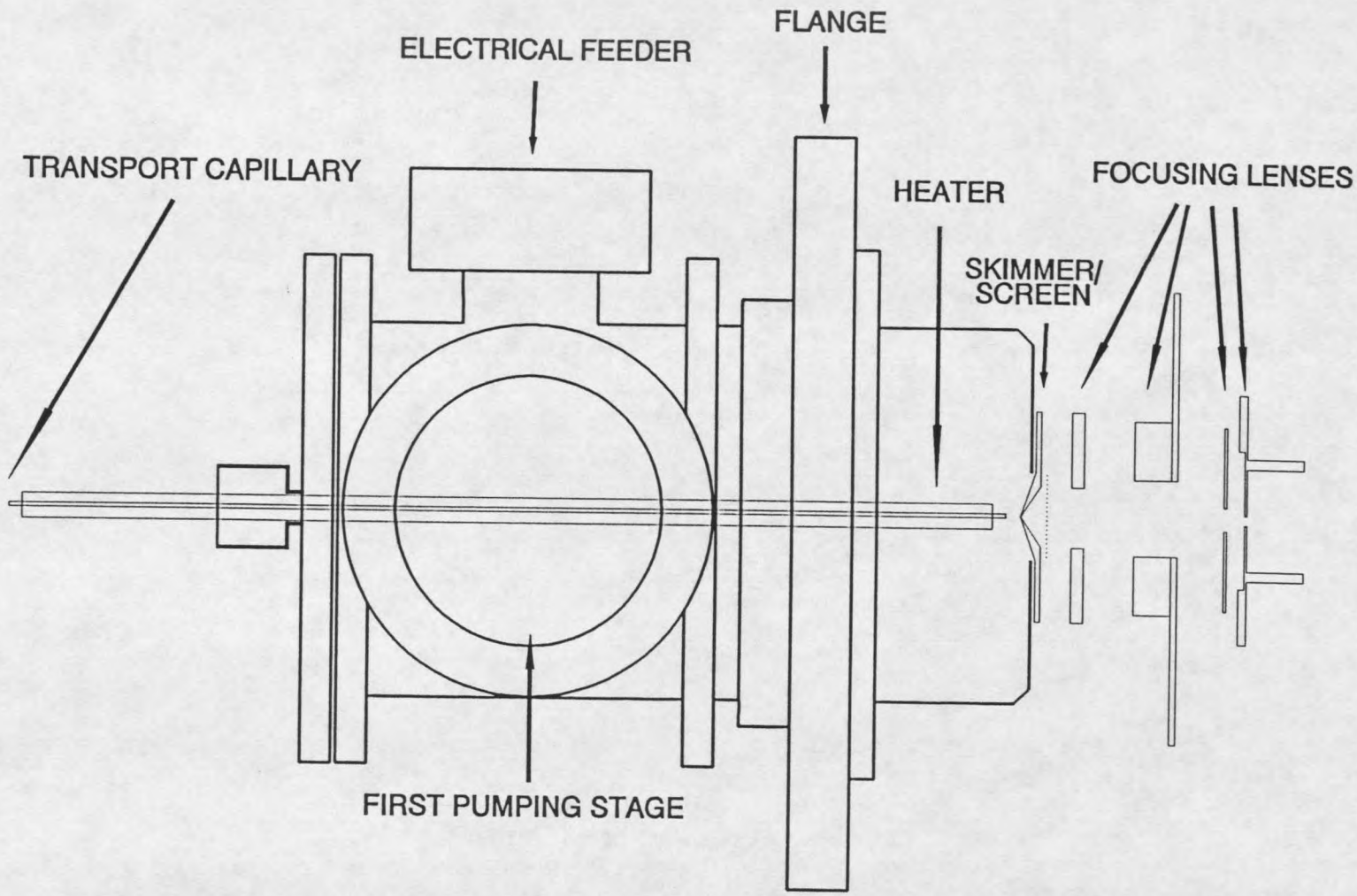


Figure 2. Electrospray Ionization Interface. Scale: 1 cm = 1.33 cm.

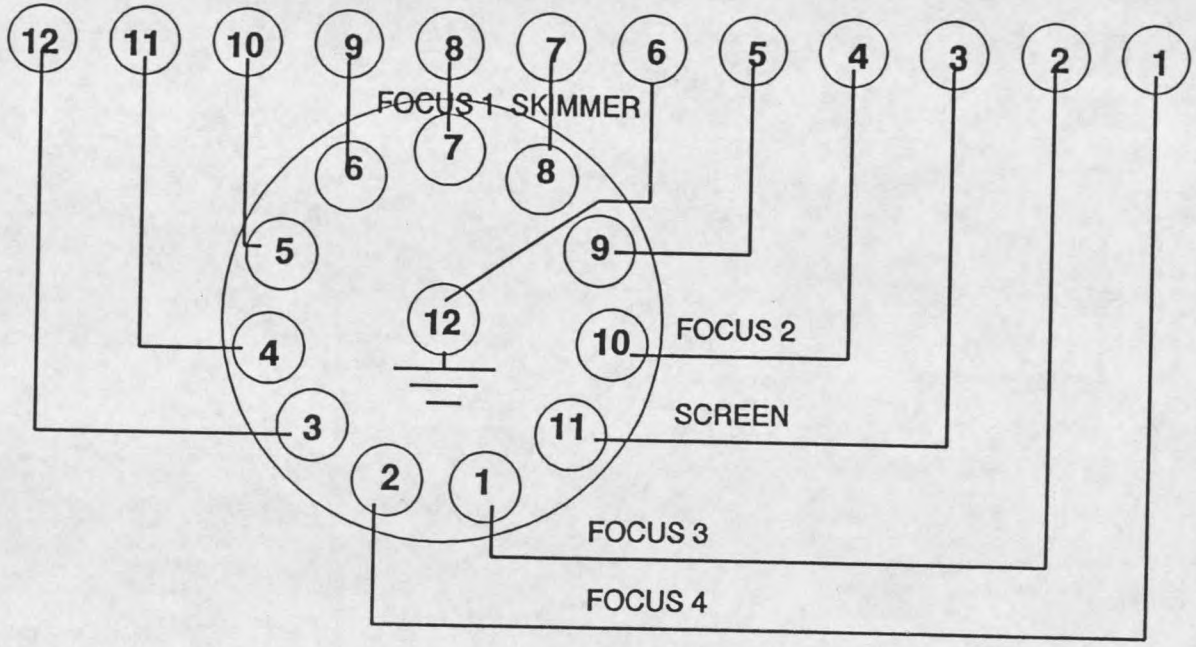


Figure 3. Electrical Feedthrough Connections.

A control box was designed to contain the DC power supply (6 9-volt battery stacks), 6 3-way switches for positive/negative voltage and 6 potentiometers (Clarostat 100kΩ, 10-turn, Newark Electronics, Chicago, IL) for regulating the lens potentials. Figure 4 shows the configuration of the DC power supply.

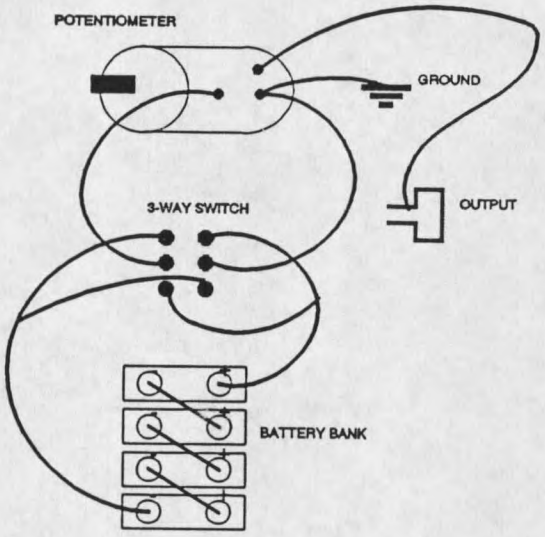


Figure 4. DC Power Supply.

A coaxial cable was used to make connections between the power supply and the electrical feeder pins. This insured minimization of noise in electrospray signal generation. A DC digital voltmeter was used to monitor the applied potentials. Prior to designing the control box the VG TRIO 2 power supply was used by inserting leads into the power outlet and attaching them to the electrical feeder of the interface. The potentials then were selected by using the computerized EI+ control panel accessible through the keyboard.

Heater construction involved taking 22 inches of 0.010 inch diameter nichrome wire, folding the wire in half to form an 11 inch double strand and then wrapping this double strand of wire clockwise around the length of a ceramic tube insulator (19.05 cm length, 2.39 mm o. d., 1.57 mm i. d., Scientific Instrument Service, Ringoes, NJ). Figure 5 shows how the wire is wrapped around the ceramic tube.

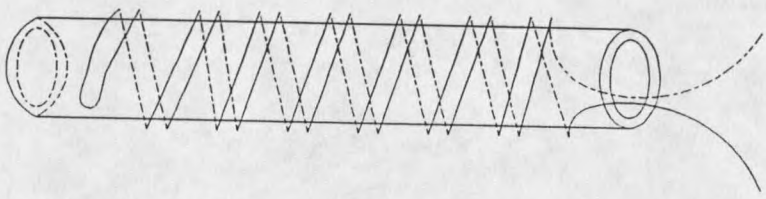


Figure 5. Heater Construction

Extreme caution must be exercised during the wrapping process to insure that the double strands of wire don't touch and short out the system. This is achieved by spreading a thin film of epoxy over the strand of wire as it is wrapped. This wrapped ceramic tube is then inserted into another ceramic tube (18.42 cm in length, 4.78 mm o. d., 3.18 mm i. d.), and this assembly is inserted into a stainless steel tube (17.5 cm in length, 6.5 mm o. d., 4.5 mm i. d.). The stainless steel transport capillary (20 cm in length, 0.6 mm o. d., 0.5 mm i. d.) is inserted into this assembly. Epoxy is then used to seal any air space between the ends of the ceramic and metal tubes. A VARIAC voltage transformer is then connected to the two ends of nichrome wire; passing voltage through this nichrome wire causes resistive heating. The VARIAC transformer was calibrated so that a correlation could be observed between the transformer dial and the actual voltage produced. Figure 6 shows this correlation. Each of the heaters was calibrated by measuring the temperature of nitrogen gas (100 kPa) exiting the end of the

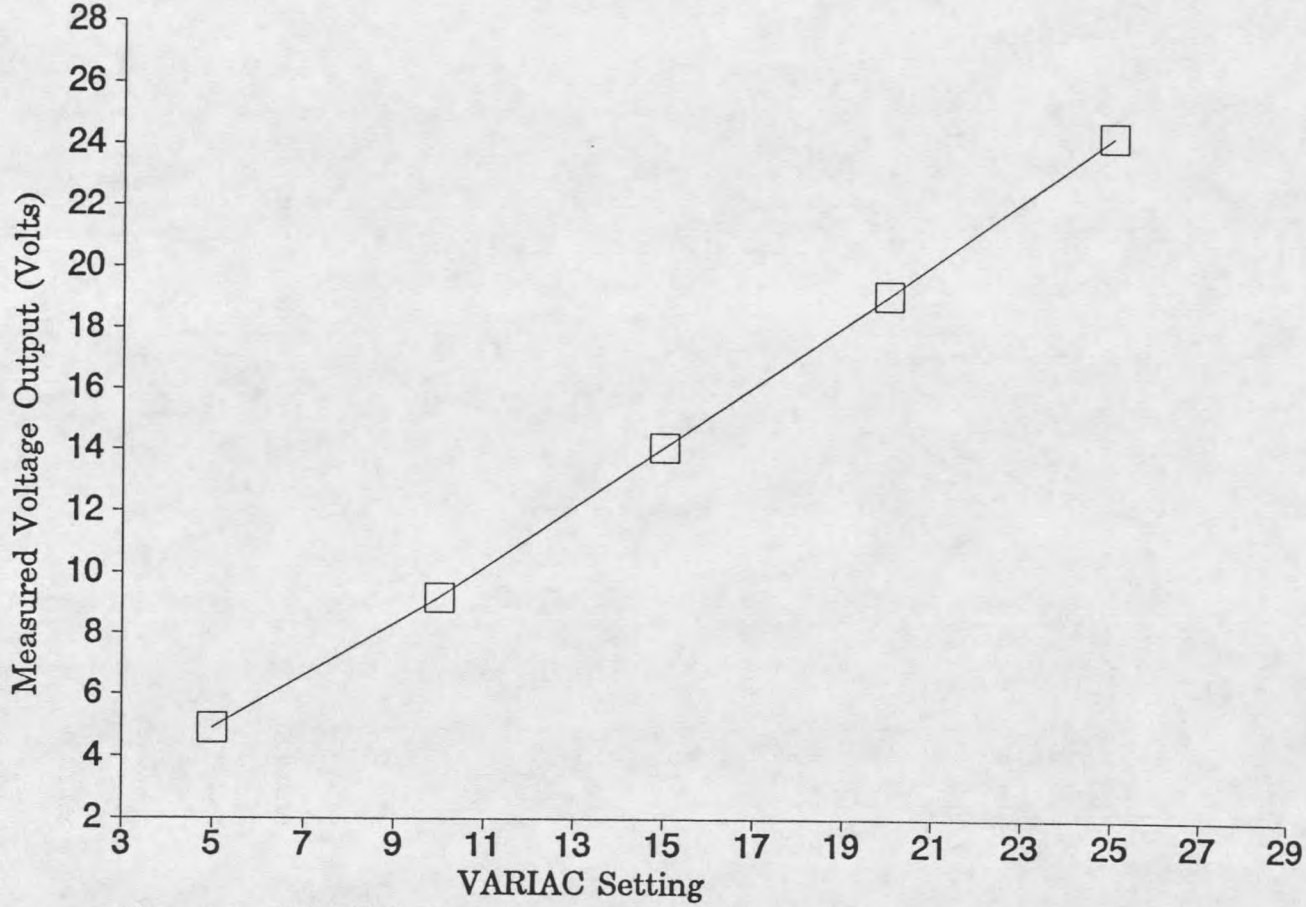


Figure 6. VARIAC Transformer Calibration

transport capillary with a thermocouple. Contact time was 20 minutes for each Variac setting. Figure 7 shows a typical calibration curve for these home made heaters.

Potential was supplied to the transport capillary with a high voltage DC module power supply (MJ Series 15 Watt, 10 kV output, Regulated High Voltage DC Module Power Supply, Glassman High Voltage Inc., Whitehouse Station, New Jersey). Potential was supplied to the electrospray needle with a similar power supply with a higher wattage rating (MK Series 75 Watt, 15 kV output, Regulated High Voltage DC Module Power Supply (Glassman).

Using an ISI sputter coater a layer of gold ~400 Å thick was deposited on a length of 50 μm i. d. fused silica capillary tubing. The fused silica tubing was then inserted into the 129 μm i. d. stainless steel needle until the fused silica tubing protruded 1 - 2 mm past the metal tip. The other end of the capillary was inserted into the Rheodyne injector valve. During the early stages of this work a spray needle with an i. d. of 0.5 mm was used.

A syringe pump (Model 355, Sage Instrument Inc., Cambridge, MA) was used to provide a constant flow of solvent through the needle. This pump was calibrated periodically to ensure accurate flow rate readings.

The first pumping stage, located in the interface, is evacuated by a rotary pump (Alcatel 2033, pumping speed 700 L/minute, Hanover, MA) that maintains a pressure of approximately 2 torr in the vicinity of the transport capillary. However, based on calculations, the pumping speed required to maintain this pressure is on the order of only 200 L/minute.

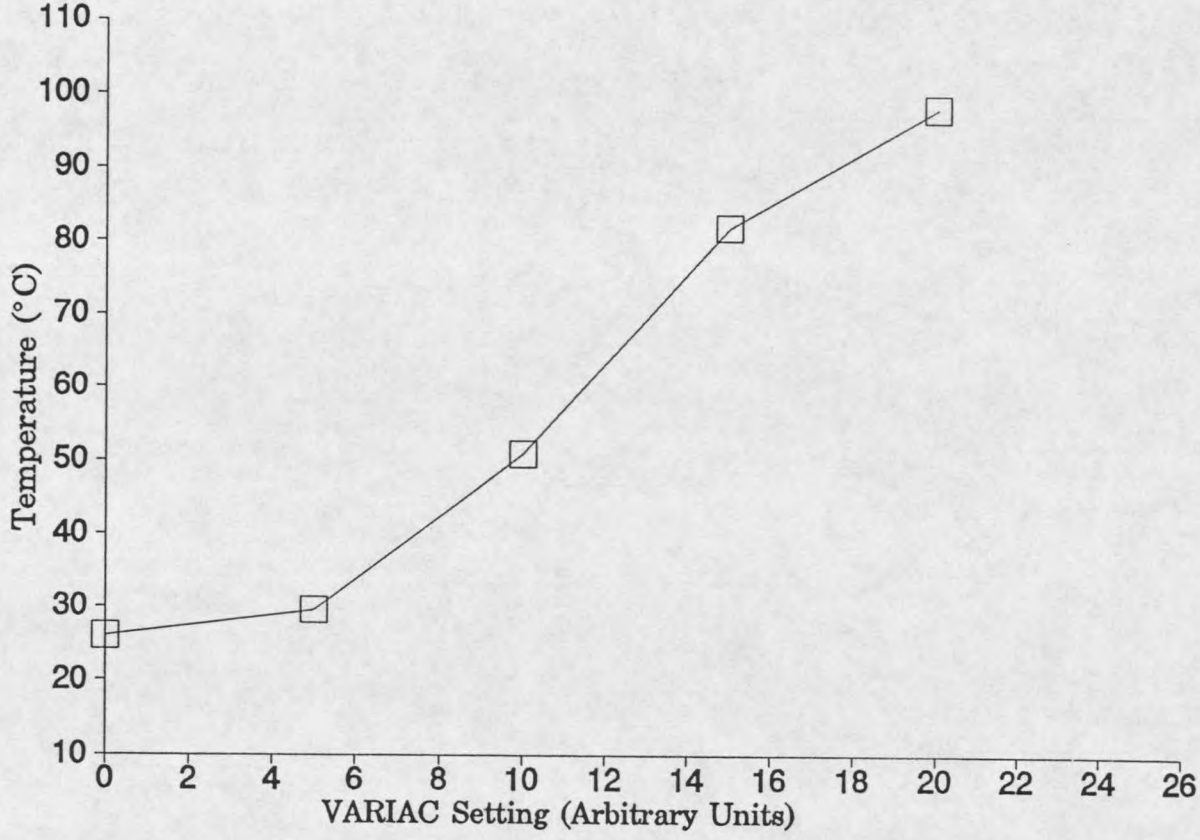


Figure 7. Heater Calibration

Ion Signal Optimization

Electrostatic Lens System. The SIMION program (44) was used in the early stage of developing the design of the lens system for the electrospray interface. Figure 8 shows a SIMION simulation for the initial design of the interface which did not include the first focusing lens shown in Figure 2. For the simulation the kinetic energy of the ions are estimated to be 10 eV with a mass of 200 amu. Ten trajectories are shown in increments of 2 degrees off axis. The potentials assigned to the lens system are the following: skimmer: +18 volts (V); screen: -40 V; focus 1: +14 V; focus 2: -50 V; and focus 3: -35 V. The thirteen potential contours used to determine these trajectories are shown in Table 1.

Table 1. SIMION CONTOUR INTERVALS[a]

INTERVAL	VALUE (Volts)
1	-50.00
2	-49.00
3	-41.00
4	-40.00
5	-39.50
6	-35.50
7	-35.00
8	-30.10
9	9.10
10	14.00
11	14.40
12	17.60
13	18.00
14	20.70
15	42.30
16	45.00

[a]original design

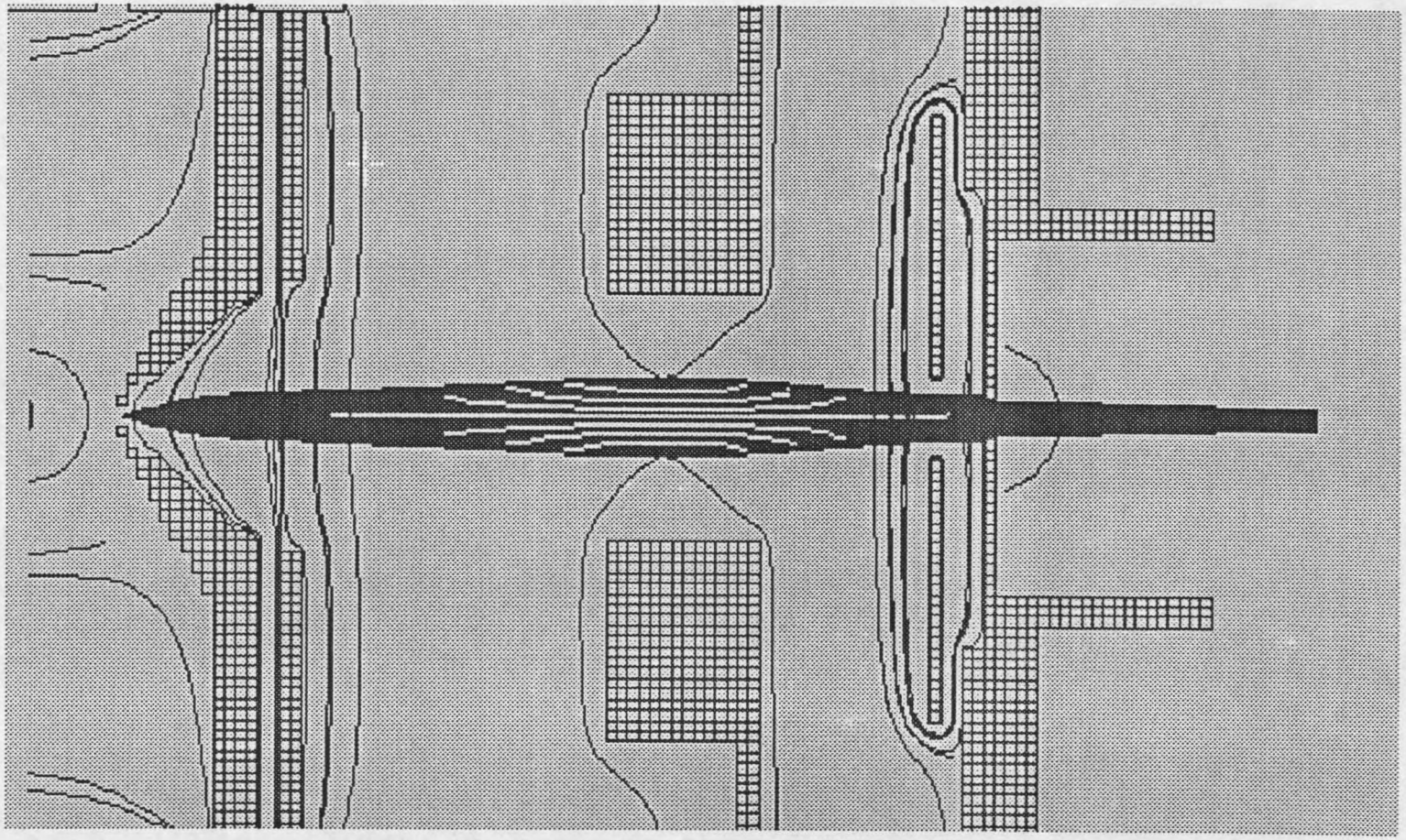


Figure 8. SIMION Simulation of Ion Trajectories in Original Lens System Design.

After the design of the lens system was modified by inserting the first focusing lens shown in Figure 2, the potentials used in routine sample analysis were experimentally determined by methodically adjusting the lens potentials while maximizing an analyte response on the oscilloscope. These potentials are skimmer: +11 V; screen: -16 V; focus 1: +6 V; focus 2: +11 V; focus 3: -80 V; and focus 4: -18 V. Figure 9 shows the SIMION simulation for these potentials. Table 2 shows the potential contours used in the simulation.

Table 2. SIMION CONTOUR INTERVALS[a]

INTERVAL	VALUE (Volts)
1	-80.00
2	-73.80
3	-24.20
4	-18.00
5	-17.80
6	-16.20
7	-16.00
8	-13.80
9	3.80
10	6.00
11	6.50
12	10.50
13	11.00
14	14.40
15	41.60
16	45.00

[a]final design

Using polyethylene glycol as the analyte, the distance between the transport capillary and the skimmer was optimized and as shown in Figure 10 a distance of ~ 4.5

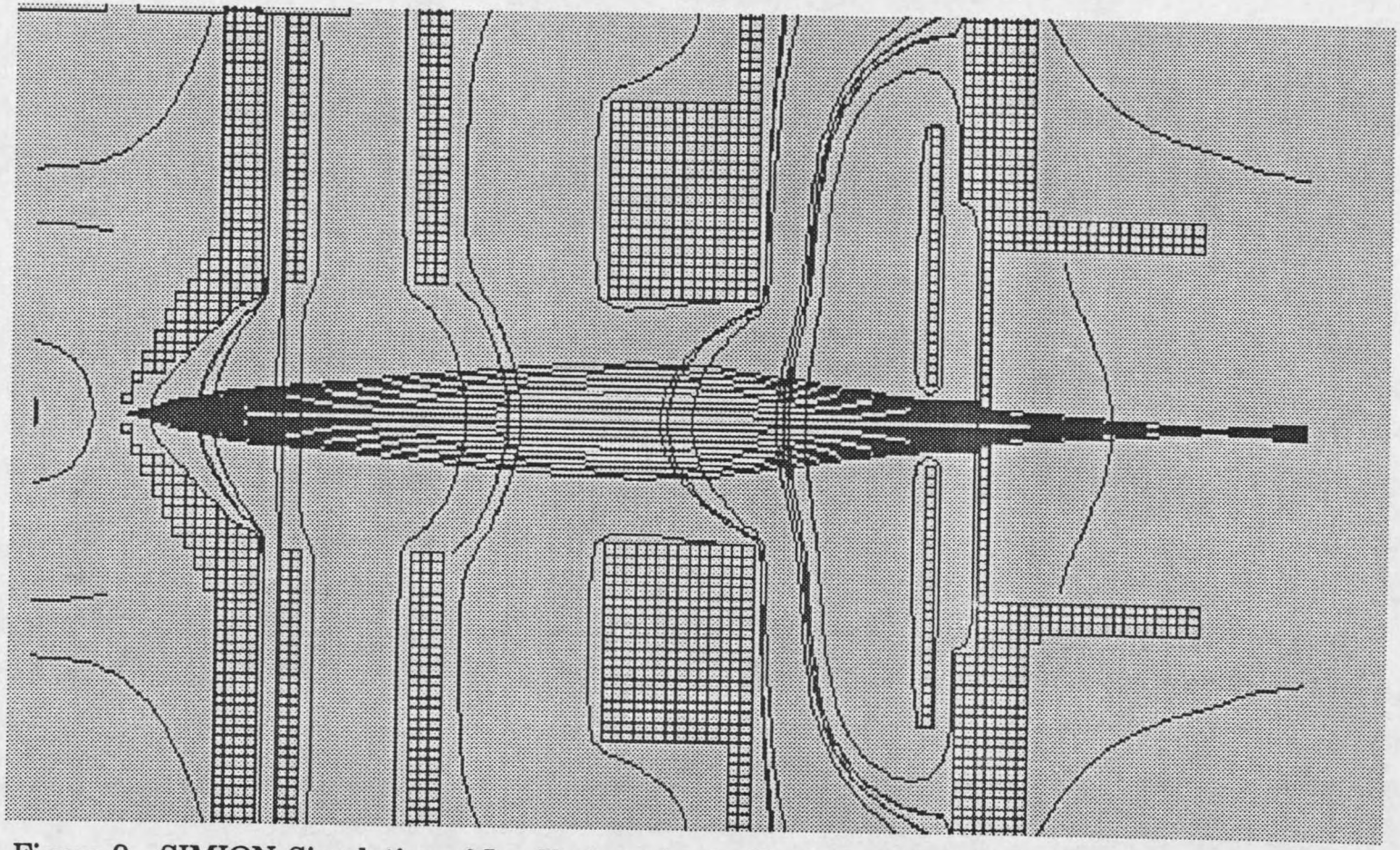


Figure 9. SIMION Simulation of Ion Trajectories in Final Lens System Design.

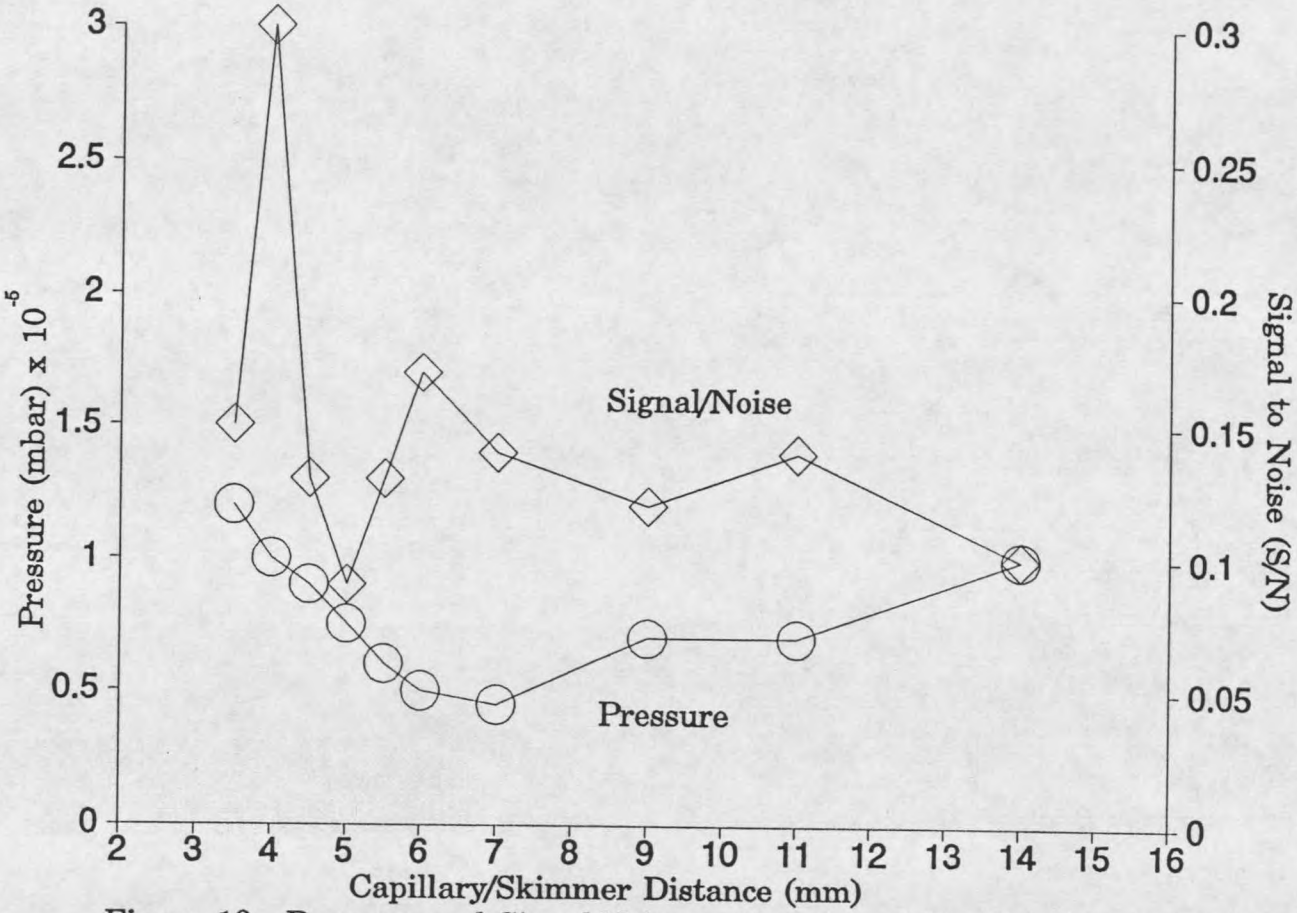


Figure 10. Pressure and Signal/Noise as Function of Capillary/Skimmer Distance

mm between these components produces a maximum in signal to noise and an acceptable vacuum level in the analyzer region.

Ion Kinetic Energy. While viewing the signal response on the oscilloscope the lens potentials were optimized by spraying polyethylene glycol. The potential on the skimmer lens was +14 V and -35 V on the focus 3 lens. The potential was gradually made more and more positive until the signal was attenuated to ~ 5 % of the maximum value for mass 1098 amu. The potential on the focus 3 lens that attenuated the signal to this level was +3 V. This same procedure was repeated several times and the same results were obtained. From this simple experiment it can be estimated the ion kinetic energy was 10 - 11 eV.

In other words an entrance to exit (skimmer to focus 3) potential gradient of 10 - 11 V will stop ions that have a kinetic energy equal to 10 - 11 eV. Of course, this procedure gives only a rough approximation to the kinetic energy of the ions.

Signal Amplification. A preamplification system (VG F16, FA 3) was installed on the VG TRIO 2 to enhance the signal level. Figure 11 shows the original and modified design of the amplification system. The modified design provided additional range selection of 10^{-6}, 10^{-7} and 10^{-8} amps full scale as compared to the 10^{-5} amps full scale on the original head-amp.

VG Trio-2 Quadrupole Mass Spectrometer

Data System. The data acquisition interface was connected to the system

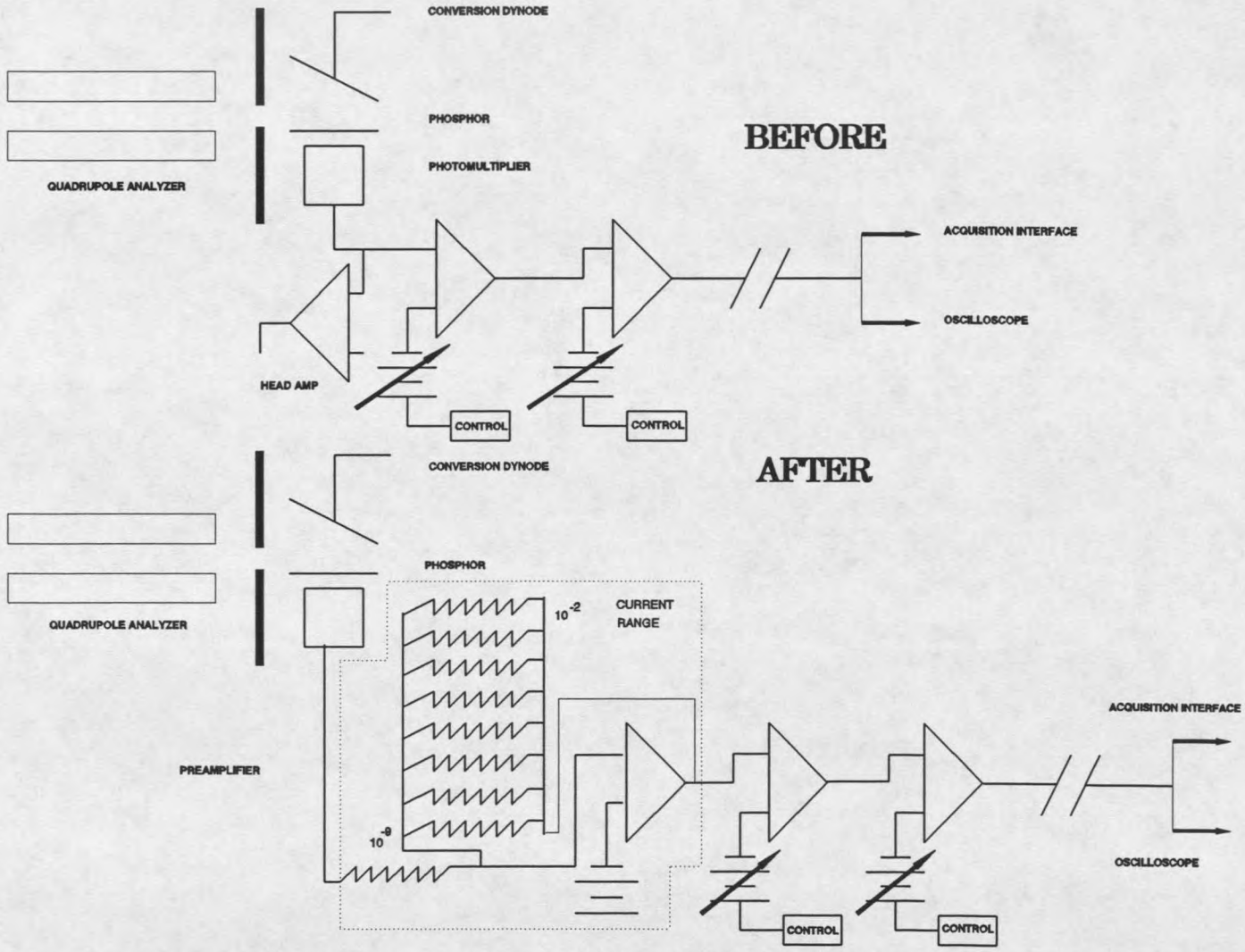


Figure 11. Signal Amplification Before and After Installation of Pre-Amplifier.

computer which is a DEC PDP 11/73 with a 71 Mbyte hard disk. Twenty five Mbytes are occupied by the operating systems. Data was archived on TK-50 streamer tapes and a Printronix MVP-2 printer was used for hardcopying data.

Vacuum System. The focusing lens area of the electrospray ionization interface was maintained at about $2x10^{-3}$ torr by a four inch oil diffusion pump (Edwards, West Sussex, England, Diffstak-100/300M, pumping speed 280 L/second-air.) The mass filter area was maintained at $2x10^{-5}$ torr by a three inch oil diffusion pump (Edwards, West Sussex, England, Diffstak-63/150M, pumping speed 135 L/second-air.) The source and analyzer diffusion pumps were backed by rotary pumps (Edwards, E2M8; pumping speed 190 L/minute and E2M2; 60 L/minute, respectively.)

Pesticide Analysis

Pesticide Samples

The pesticide samples shown in Table 3 were obtained from the USEPA Repository of Toxic Substances. Shown in this table are the pesticide names, trade names, chemical abstracts name, CAS number and the discharge levels of pesticide active ingredients by pesticide formulators and packagers as estimated by the USEPA. These chemicals were selected for study because they represent a variety of pesticide/herbicide classes and because of the high discharge levels reported by USEPA in August 1989.

Many of these pesticides deactivate or inhibit the enzyme cholinesterase. In neurotransmission the ester acetylcholine is released to trigger a muscle contraction. The

Table 3. Pesticide Nomenclature, CAS Numbers and Estimated Discharge Levels

Pesticide	Trade Name	Chemical Abstracts Name[a]	CAS Number	Discharge Levels[b]
Amitrole (H)[c]	*Cytrol	1H-1,2,4-Triazol-3-amine	61-82-5	N/A
Anilazine (FF)	*Dyrene	4,6-Dichloro-N-(2-chlorophenyl)-1,3,5-triazin-2-amine	101-05-3	422
Antu (R)	*Rattrack	1-Naphthalenylthiourea	86-88-4	N/A
Carbaryl (I)	*Sevin	1-Naphthalenol methycarbamate	63-25-2	10,546
Carbofuran (I)	*Furadan	2,3-Dihydro-2,2-dimethyl-7-benzo-furanol methylcarbamate	1563-66-2	422
Chloramben (H)	*Amiben	3-Amino-2,5-dichlorobenzoic acid	133-90-4	1,350
Chlorpyrifos (I)	*Dursban	Phosphorothioic acid *O,O*-diethyl *O*-(3,5,6 trichloro-2-pyridinyl) ester	2921-88-2	15,945
Coumafuryl (R)	*Fumarin	3-[1-(2-Furanyl)-3-oxobutyl]-4-hydroxy-2H-1-benzopyran-2-one	117-52-2	N/A
Diphacinone (R)	*Ramik	2-(diphenylacetyl)-(1,3)(2H)-dione	82-66-6	1,350
Diquat Dibromide (H)	*Reglone	6,7-Dihydrodipyrido[1,2-a:2',1'-c]pyrazinediium dibromide	6385-62-2	N/A
Diuron (H)	*Drexel	N'-(3,4-Dichlorophenyl)-N,N-dimethyl-urea	330-54-1	1,265
Endosulfan I (H)	*Thiodan I	6,7,8,9,10,10-Hexachloro-1,5,5a,6,9-9a-hexahydro-6,9-methano 2,4,3-benzodioxathiepin 3-oxide	959-98-8	1,687
Endothall (H)	*Endothall	7-Oxabicyclo[2.2.1]heptane-2,3-dicarboxylic acid	145-73-3	422
Ethion (I)	*Bladan	Phosphorodithioic acid S,S'-methylene *O,O,O',O'*-tetraethyl ester	563-12-2	591
Folpet (FF)	*Phaltan	2-[(Trichloromethyl)thio]-1H-isoindole-1,3(2H)-dione	137-07-3	3,037
Glyphosate (H)	*Roundup	N-(Phosphonomethyl)glycine	1071-83-6	2,194
Linuron (H)	*Lorox	N'-(3,4-Dichlorophenyl)-N-methoxy-N-methylurea	330-55-2	675
Mephosfolan (I)	*Cytrolane	(4-Methyl-1,3-dithiolan-2-ylid-ene)phosphoramidic acid diethytl ester	950-10-7	N/A
Methidathion (I)	*Supracide	Phosphorodithioic acid S-[(5-methoxy-2-oxo-1,3,4-thiadiazol-3(2H)-yl)methyl] *O,O*-dimethyl ester	950-37-8	84

Table 3. Pesticide Nomenclature, CAS Numbers and Estimated Discharge Levels (Continued)

Pesticide	Trade Name	Chemical Abstracts Name	CAS Number	Discharge Levels[b]
Methiocarb (I)	*Mesurol	3,5-Dimethyl-4-(methylthio)phenol methylcarbamate	2032-65-7	506
Methomyl (I)	*Lannate	N-[[(Methylamino)carbonyl]oxy]ethan-imidothioic acid methyl ester	16752-77-5	506
Mexacarbate (I)	*Zectran	4-(Dimethylamino)-3,5-dimethyl-phenol methylcarbamate (ester)	315-18-4	84
Molinate (H)	*Ordram	Hexahydro S-ethyl ester (1H)azepine-1-carbothioic acid	2212-67-1	253
Phosfolan (I)	*Cyolane	1,3-Dithiolan-2-ylidenephosphoramidic acid diethyl ester	947-02-4	N/A
Propoxur (I)	*Baygon	2-(1-Methylethoxy)phenol methylcarbamate	114-26-1	10,377
Pyrethrins I (I)[d]	*Pyrethrins	2,2-dimethyl-3-(2-methyl-1-propenyl)cyclopropanecarboxylic acid 2-methyl-4-oxo-3-(2,4-pentadienyl)-2-cyclopen-1-yl ester chrysanthemummono-carboxylic acid pyrethrolone ester	8003-34-7	34,084
Rotenone (I)	*Mexide	[2R-(2α,6aα,12aα)]-1,2,12,12a-Tetra-hydro-8,9-dimethoxy-2-(1-methylethenyl)-[1]benzopyrano-[3,4-b]furo[2,3-h][1]benzopyran-6(6aH)-one	83-79-4	3,965
Siduron (H)	*Tupersan	N-(2-Methylcyclohexyl)-N'-phenylurea	1982-49-6	675
Thiometon (I)	*Ekatin	S-(2-(ethylthio)ethyl) *O,O*-dimethyl ester phosphorodithioic acid	640-15-3	N/A
Trifluralin (H)	*Treflan	2,6-Dinitro-N,N-dipropyl-4-(trifluromethyl)benzenamine	1582-09-8	17,464
Warfarin (R)	*Ratox	4-Hydroxy-3-(3-oxo-1-phenylbutyl)-2H-1-benzopyran-2-one	81-81-2	3,628

[a] Uninverted Chemical Abstracts Registry Name.

[b] U.S.E.P.A.'s estimated discharge (lbs./yr.) of pesticide active ingredients by pesticide formulators and packagers. Preliminary Data Summary for the Pesticide Chemicals Point Source Category, Office of Water Regulations and Standards, EPA 440/1-89/060-e, August 1989.

Table 3. Pesticide Nomenclature, CAS Numbers and Estimated Discharge Levels (Continued)

[c] Abbreviations:

FF	foliar fungicide
H	herbicide
I	insecticide
R	rodenticide

[d] Pyrethrin II name: 3-(3-methoxy-2-methyl-3-oxo-1-propenyl)-2,2-dimethylcyclopropanecarboxylic acid 2-methyl-4-oxo-3-(2,4-pentadienyl)-2-cyclopenten-1-yl ester, chrysanthemum dicarboxylic acid monomethyl ester prethrolone ester.

enzyme cholinesterase hydrolyzes the ester to end the process. The hydrolysis is a transesterification in which the acetyl group is transferred to a hydroxy group of the enzyme. An electrophilic compound, such as many of these pesticides, can be the receptor for the nucleophilic cholinesterase. Once the cholinesterase has reacted with the pesticide it cannot function to hydrolyze acetylcholine. The muscle contraction continues and results in death.

Sample Preparation

Stock solutions of these pesticides were prepared by diluting 10 mg of each pesticide to a 5-mL volume in pure methanol. Working solutions were then prepared by diluting 1 mL of the stock solution to volume in 100-mL volumetric flasks with 50/50 methanol/water. The organic solvents used were Fisher HPLC grade and were used without further purification. The water used was from a Barnstead Nano Pure System, Series 550, that contained a triple filtration system: anion/cation resin, carbon resin and a bacteria filter. All solvents were filtered (0.45-μm nylon membrane, Alltech Associates, Inc.) and degassed by ultrasound under reduced pressure before use.

The calibration compound used was a mixture of 200 and 400 molecular weight polyethylene glycol, sodium iodide, potassium iodide, rubidium iodide, and cesium iodide. One mL of the 200 molecular weight and 4 mL of the 400 molecular weight polyethylene glycols, respectively, were diluted to volume in a 100 mL flask with a 50/50 mixture of methanol and water. One mL of this solution, 0.01523 g of sodium iodide, 0.01 g potassium iodide, 0.01 g rubidium iodide, and 0.01 g cesium iodide were

diluted to volume with methanol/water. The resulting solution concentration is ~ $1x10^{-4}$ M with respect to the polyethylene glycols and ~ $1x10^{-3}$ M with respect to sodium, potassium, rubidium and cesium ions.

The acetic acid/ammonium acetate buffer was prepared by diluting 10 mL of a mixture of 0.174 M acetic acid and 0.2387 g of ammonium acetate to volume in a 100 mL volumetric flask with 50/50 methanol/water solution. The resulting buffer concentrations are 0.0174 M acetic acid and 0.031 M ammonium acetate.

Each of the pesticides in Table 3 was sprayed using 50/50 methanol water as the solvent. Using a sample flow rate of 2 μL per minute each of the pesticides were injected into the Rheodyne injector valve (Model 7120 with *ca.* 100 μL fused silica sample loop) and ultimately reached the needle held at high voltage. A mass range of 40 to 400 was generally used. Scan rate was set at 20-second scans with interscan time of 0.1 seconds. Normally 5 scans were accumulated for each run after the signal stabilized. The potential difference between the transport capillary and the skimmer lens was varied from 35 volts to 135 volts and each sample was run at the following transport capillary/skimmer potential differences: 35, 45, 55, 65, 75, 85, 95, 105, and 135 volts. These values are illustrated in Table 4.

A potential of approximately 3.15 kilovolts was applied to the spray needle for the first run with a transport capillary/skimmer potential difference of 35 volts. In subsequent runs the high voltage on the needle was adjusted so that the potential difference between the needle and the transport capillary remained constant.

Table 4. Spray Needle/Transport Capillary Potential Difference

Transport Voltage (V)	Needle Voltage (kV)
46	3.15
56	3.16
66	3.17
76	3.18
86	3.19
96	3.20
106	3.21
146	3.25
200	3.30

pH Studies

After 0.3 mL of 0.174 M acetic acid was added to 1.0 mL of the pesticide sample, this solution was injected into the injector valve and the same routine was carried out for the acidified sample as was for the neat sample. Additionally, hydrochloric acid was added instead of the acetic acid to selected pesticide samples.

Adduct Studies

To determine the influence of adding ions such as Na^+, Cs^+, and NH_4^+, samples were sprayed that had been spiked with these cations individually or together. For the sodium study 0.5 mL of $1x10^{-3}$ M sodium iodide was mixed with 2.0 mL of the pesticide sample. Again, the same procedure is carried out on the sodiated sample as on the neat and acidified sample. The same procedure was used for the cesium study. For the ammonium adduct study 0.5 mL of $3.7x10^{-4}$ M ammonium acetate was added to 2.0 mL

of the selected pesticide sample.

Diuron, Methomyl and Siduron were used to do an additional adduct study with sodium. The concentration of each of these pesticides was held constant and the sodium ion concentration was varied from about 10^{-6} M to 10^{-3} M. Each of the samples was injected individually into the injector valve leading to the electrospray needle and the several different transport capillary/skimmer potential differences were used for each of the sample injections.

Solvent Study

One of the most important parameters in electrospray ionization mass spectrometry is the choice of solvent. Amitrole, Diphacinone, Propoxur and Rotenone were selected and run in pure methanol, 50/50 methanol/water, pure acetonitrile, and 50/50 acetonitrile/water.

Folpet, Methomyl, Phosfolan and Trifluralin were selected to study the effects of the signal by varying the solvent composition. Methanol/water was used and the methanol content was varied from 10% to 90% by volume. Several runs were carried out at several different transport capillary/skimmer potential differences for both of these sets of pesticides.

Rapid Method

Electrospray ionization was tested as a rapid method for quantitatively determining carbamate pesticides in natural waters. The following carbamate pesticides were spiked into Yellowstone River Water. The procedure was to spike 100 mL of the Yellowstone

River water, collected at Greycliff, Montana, with 1.0 mL of the pesticide and 1.0 mL of an acetic acid ammonium acetate buffer ($1.74x10^{-2}$ M acetic acid/$3.1x10^{-2}$ M ammonium acetate in methanol/water) and then filter this through 0.45 μm Millipore filter paper. The buffer was designed to maintain the solutions at a pH of 5 to minimize matrix effects. Standard curves were generated for the pesticides in methanol/water both individually and collectively and then various spikes within the analytical range of 0.1 to 20 ng/μL were analyzed similarly. Without using any separation techniques the samples, after filtration, were injected directly into the electrospray ionization interface through the Rheodyne injector valve connected to a 50-μm i. d. gold coated transport capillary that was 20 cm in length.

CHAPTER 3

RESULTS AND DISCUSSION

Electrospray Ionization Interface

The electrospray ionization interface was installed on a VG Quadrupole Trio-2 mass spectrometer and a schematic representation is shown below in Figure 12. This interface was designed in a similar fashion to that of Whitehouse (26). The analyte solution is electrosprayed from a 1-mL syringe through a gold coated fused silica capillary, 50 μm i. d. inserted into a 0.129 mm i. d. stainless steel needle that is held at a potential of 3.15 kV relative to the metal transport capillary tube through which analyte ions, solvents and gases enter the mass spectrometer. A syringe pump is used to maintain a constant flow of solvent through the needle at a flow rate of 2 - 3 μL per minute. Whitehouse used a 100 μm i. d. needle with a flow rate of 5 - 10 μL per minute. Solvent continually flows through the needle in order to avoid stabilization problems with the solvent flow. The syringe is connected to a Rheodyne injection valve which in turn routes the solvent to the needle through a 50-μm i. d. fused silica capillary tubing that is 20 cm in length. The injector valve has a 250-μm i. d. injection loop that is 10 cm long that is used for introducing the analyte into the system. The quality of the mass spectrum is strongly dependent on the quality of the spray from the needle. The quality of the spray is in large part dependent on the flow rate stability. Filling the

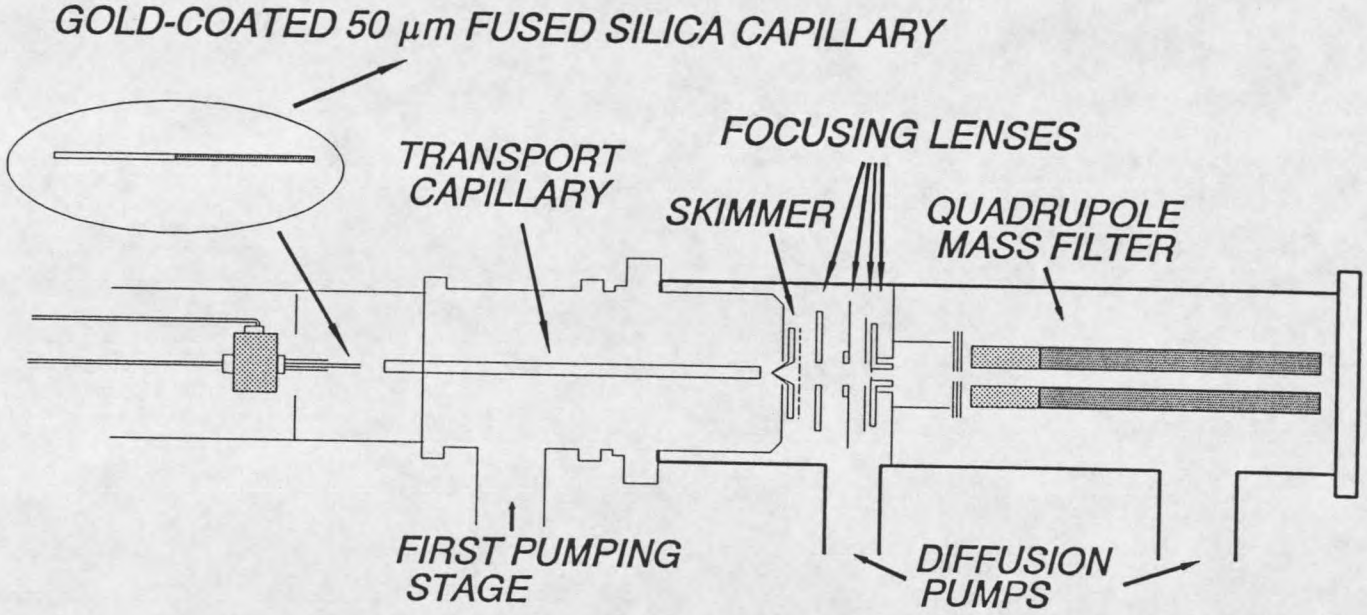


Figure 12. Home-Built Electrospray Ion Source for the VG TRIO 2 Mass Spectrometer

syringe with solvent and allowing the flow to stabilize before the analyte is injected is tantamount to obtaining good spectra. If the injector valve is not used the flow rate must be stabilized each time a new analyte is introduced by the syringe.

Electrospraying of the analyte solution produces highly charged droplets that generally follow the electric field lines and migrate toward the metal transport capillary (1.5 mm o. d., 0.5 mm i. d., 20 cm long). The optimum distance between the end of the transport capillary and the skimmer lens was determined to be 4.5 mm. Whitehouse *et al* used a glass capillary tube (0.2 mm i. d., 6 cm in length) metallized on each end.

The first pumping stage is evacuated by a rotary pump (580 L/min pumping speed) that maintains a pressure of approximately 2 torr in the vicinity of the transport capillary. Based on the dimensions of the transport capillary and the pressure differential at the inlet (640 torr) and exit (1 torr) of the capillary, a pump having a pumping speed calculated to be 200 L/minute is required (45). The first pumping stage of the Whitehouse design incorporates an oil diffusion pump with a pumping speed of about 1000 L/s. The pressure is maintained at $< 5 \times 10^{-4}$ torr in this region. A very small fraction of the charged droplets emanating from the needle enter the transport capillary and move through it due to the large pressure differential between transport capillary extremities. The metal transport capillary is encased in a homemade resistive heater that can maintain temperatures in the range of 70 - 120 °C. The Whitehouse design uses a heated nitrogen bath gas at a pressure of 1000 torr, a temperature of 50 °C to 80 °C or more and a flow rate typically in the range of 150 cm^3/s. The bath gas flows countercurrent to the migrating charged droplets. The elevated temperature of the heated

transport capillary helps to desolvate the ionized droplets and solvated ions as they migrate through the capillary and emerge in the near-supersonic free jet of gaseous material leaving the capillary.

The importance of heating the transport capillary in our design can be seen from Figure 13. The ion signal increases exponentially for the compound Antu at a temperature starting at about 85 °C. Because the life of the home-built heaters was extremely short when maintained at or above this temperature, most of this work was done with a temperature around 80 °C. It should be noted that some of the pesticides included in this work are thermally labile and care must be taken not to maintain too high a temperature setting.

In one of the experiments using the pesticide, Propoxur, the heater temperature setting was around 85 °C. The spectrum at this temperature showed evidence of thermal degradation by the increased intensity of the methyl isocyanate group which is the major degradation product of Propoxur.

A small fraction of the material emerging from the transport capillary in the free jet enters the second vacuum stage through a coaxial 0.64 mm diameter orifice in the skimmer lens. The transport capillary and skimmer are isolated electrically in order to maintain an electric field between them. The potential difference maintained between the transport capillary and the skimmer primarily determines the energy available from collisional activation which can further desolvate analyte ions and even effect analyte ion fragmentation. Furthermore, the degree of this fragmentation process can be controlled by varying this potential difference. Potential is supplied to the transport capillary

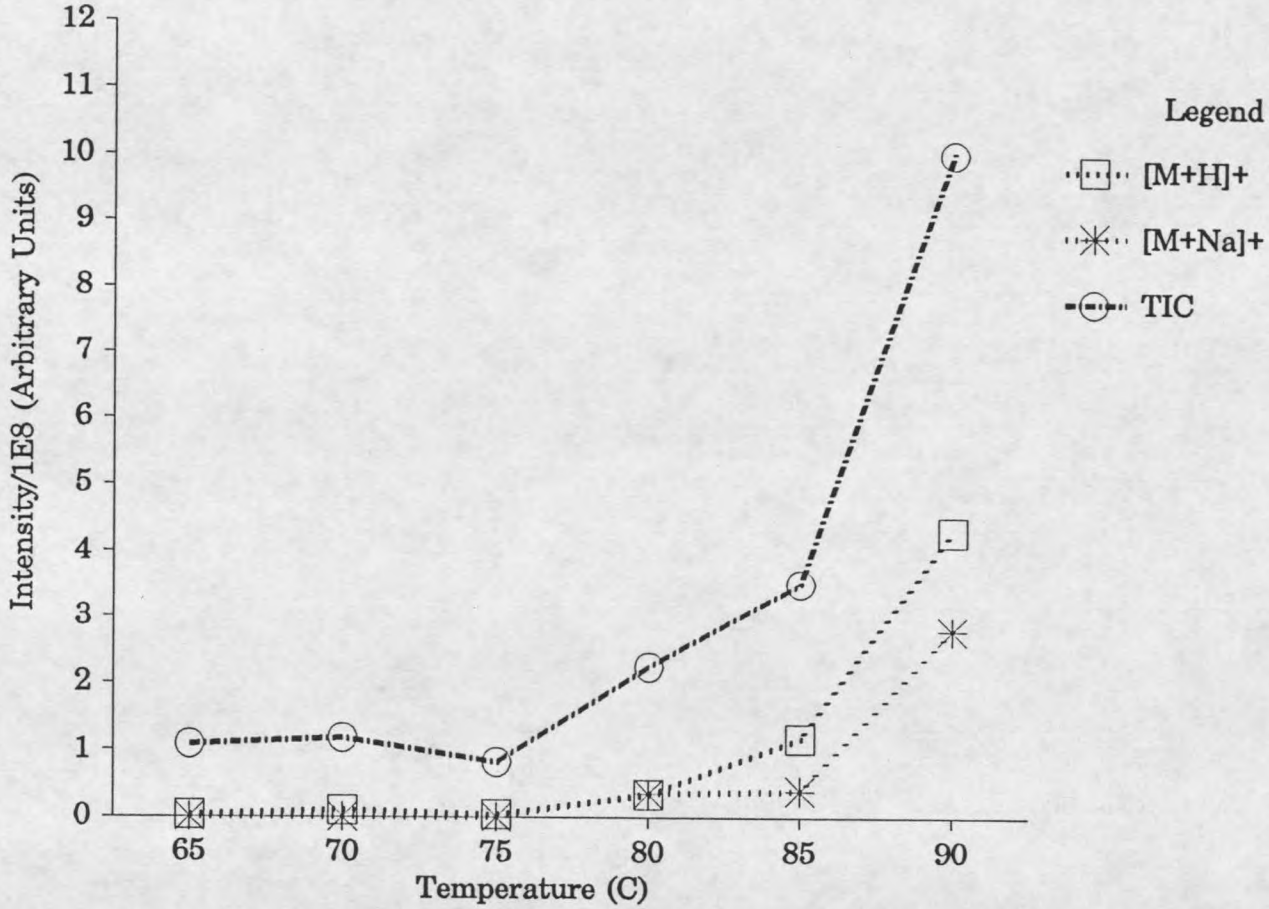


Figure 13. Intensity as a Function of Heater Temperature

with a high voltage DC module power supply. Figure 14 shows an example of the needle current as a function of needle voltage applied. The pesticide Methomyl at a concentration of 1.15×10^{-5} M was sprayed using a flow rate of 2 μL/minute. The spray was directed at a rectangular piece of metal in series with an ammeter. It is interesting to note that the current on the outermost focusing lens was measured with a picoammeter to be only a few picoamps. This is indicative of the very low efficiency of transporting the ions through the transport capillary into the analyzer region of the mass spectrometer.

The pressure in the focusing lens area of our design was maintained at about 2×10^{-3} torr by an oil diffusion pump (280 L/s pumping speed). The mass analyzer region is maintained at a pressure of 2×10^{-5} torr by a second diffusion pump (135 L/s pumping speed. The pressure in this region of the Whitehouse system is substantially lower at 10^{-6} torr.

A bank of 9-volt batteries was used to supply potentials to the six electrostatic lenses and was arranged so that the potentials could be easily monitored. The normal operating potentials were: spray needle (3.15 kilovolts), skimmer (+11 volts), screen (-16 volts), focus 1 (+6 volts), focus 2 (+11 volts), focus 3 (-80 volts), and focus 4 (-18 volts). The voltage applied to the metal transport capillary was normally varied between 45 and 145 volts depending on the degree of analyte ion fragmentation required. In the Whitehouse design the needle was held at ground and was surrounded by a cylindrical electrode that was held at -3500 volts. The metalized inlet and exit of the glass transport capillary were held at -4500 volts and +40 volts respectively. An aperture between the first and second vacuum stages was held at -20 volts and the quadrupole was maintained

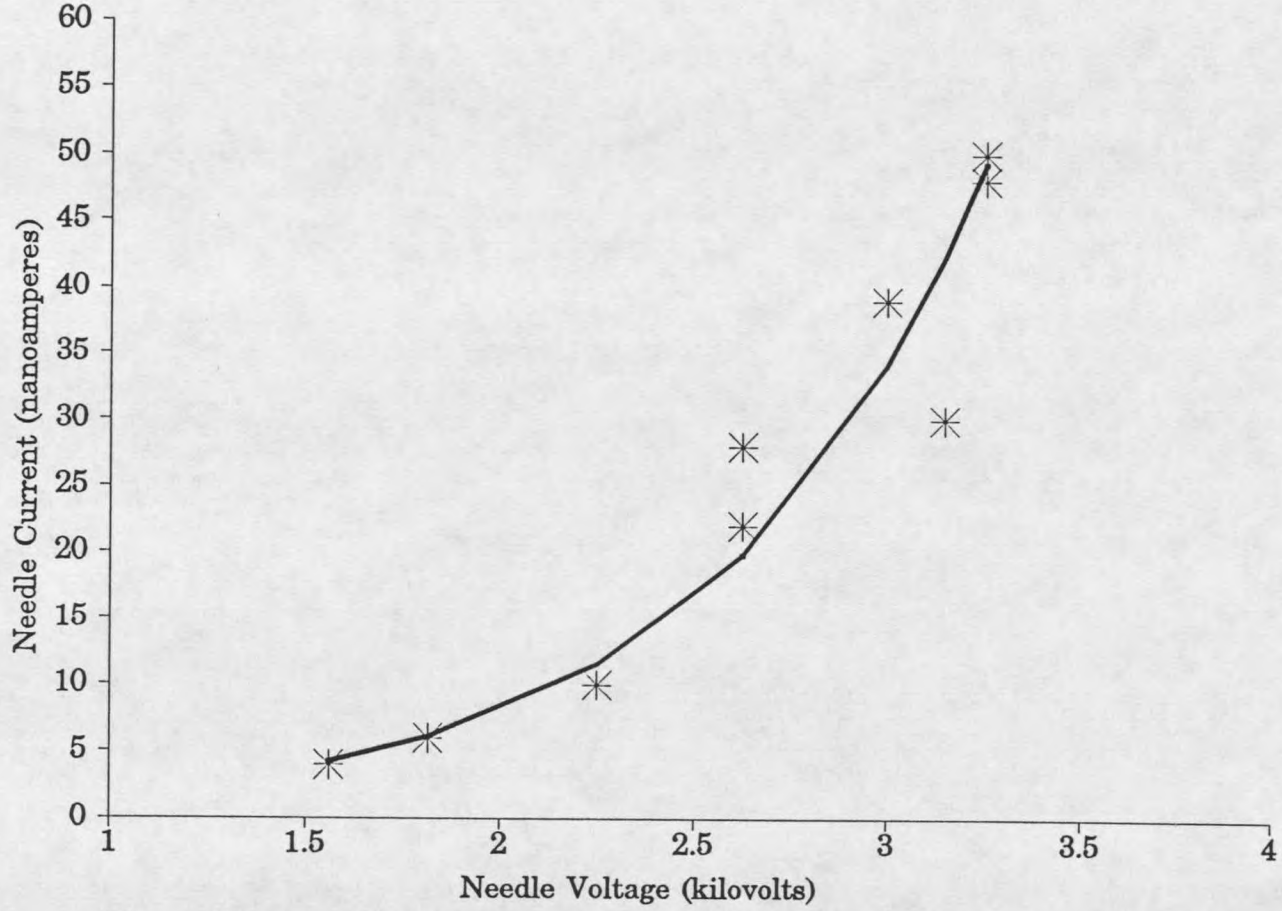


Figure 14. Needle Current as a Function of Needle Voltage

at -100 volts.

The ions that emerge through the skimmer orifice in our system are focused by a set of six electrostatic lenses into the quadrupole mass filter region through a 1.67 mm circular orifice in the outermost focusing lens.

When the field at the tip of the spray needle exceeds a critical value that is largely determined by pressure, temperature, solution composition, electrode configuration, and possibly others, electrical breakdown occurs and results in a corona discharge. This corona discharge occurs normally when the voltage applied to the spray needle is on the order of 3 - 4 kilovolts. Under this high voltage condition the spectra generated are markedly different and are characterized by an attenuation in the parent analyte peaks together with the appearance of other peaks corresponding to species found in discharges as a result of ion molecule reactions. All of the spectra obtained in this study were obtained using conditions that prevented the corona discharge phenomena.

Calibration

Polyethylene glycol (M. W. 1000) was used early in this work to generate electrospray signals for a variety of purposes such as to determine the optimum level of signal response. Figures 15 and 16 show the singly and doubly charged sites of polyethylene glycol with a transport capillary/skimmer potential difference of 35 volts and 200 volts, respectively. Figure 16 shows that the high potential difference imparts energy sufficient to destroy the doubly charged states and the distribution of ions shifts toward the singly charged state.

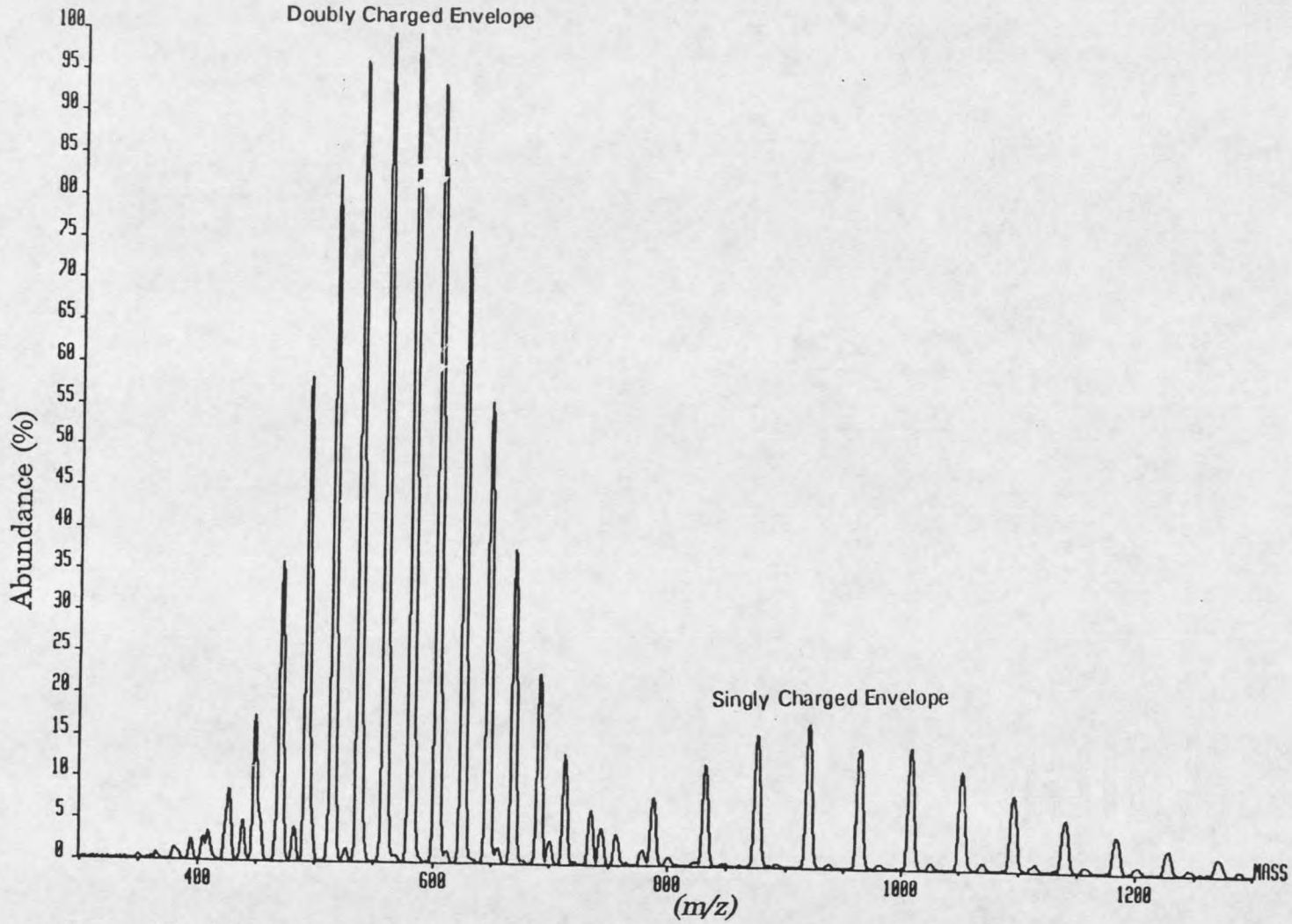


Figure 15. Electrospray Ionization Mass Spectrum of PEG (1000 M. W.). P. D. 35 Volts.

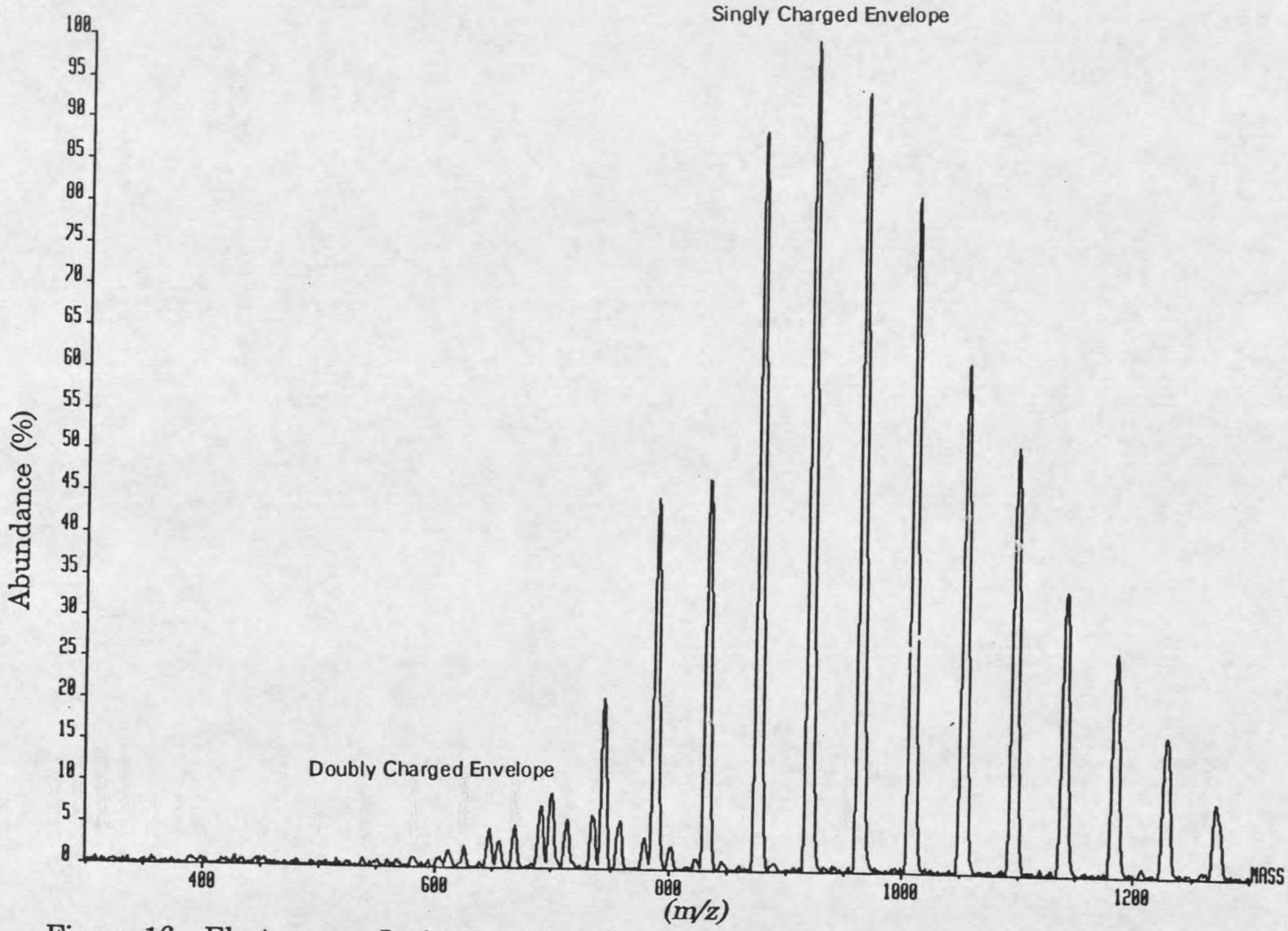


Figure 16. Electrospray Ionization Mass Spectrum of PEG (1000 M. W.). P. D. 200 Volts.

Because of the low molecular weight range of the pesticides (100 - 400 Da) a mixture of 200 M. W. and 400 M. W. polyethylene glycols was selected as a calibration sample for these pesticides. Sodium, rubidium and cesium also were added to the calibration sample and a typical electrospray spectrum is shown in Figure 17. Table 5 contains the masses of the reference ions used.

In the process of developing a calibration sample with a suitable mass range for these pesticide samples it was accidentally discovered that polyethylene glycol (M. W. 200) could be protonated by the addition of hydrochloric acid. For reasons unknown, protonated polyethylene glycol spectra have not appeared in the literature. Figure 18 shows an electrospray spectrum of the protonated polyethylene glycol. The masses in the spectrum can be found in Table 5, a listing of reference masses for polyethylene glycol.

Pesticide Analysis

Very little work has been done to study the feasibility of using electrospray ionization mass spectrometry to analyze pesticide/herbicide samples. There have been two studies (46, 47) carried out to study a narrow class of compounds using atmospheric pressure ionization techniques. Both studies report full scan detection levels as nanogram quantities for the pesticides studied. The majority of pesticides listed in Table 6 were selected from the classes of triazine, phenyl urea, carbamate, thoicarbamate, hydroxycoumarin, organophosphorus and carboxyllic acid. Other classes represented are bipyridyl, organochlorine, pyrethrin, dinitroaniline, indandione and phthalimide. Stock

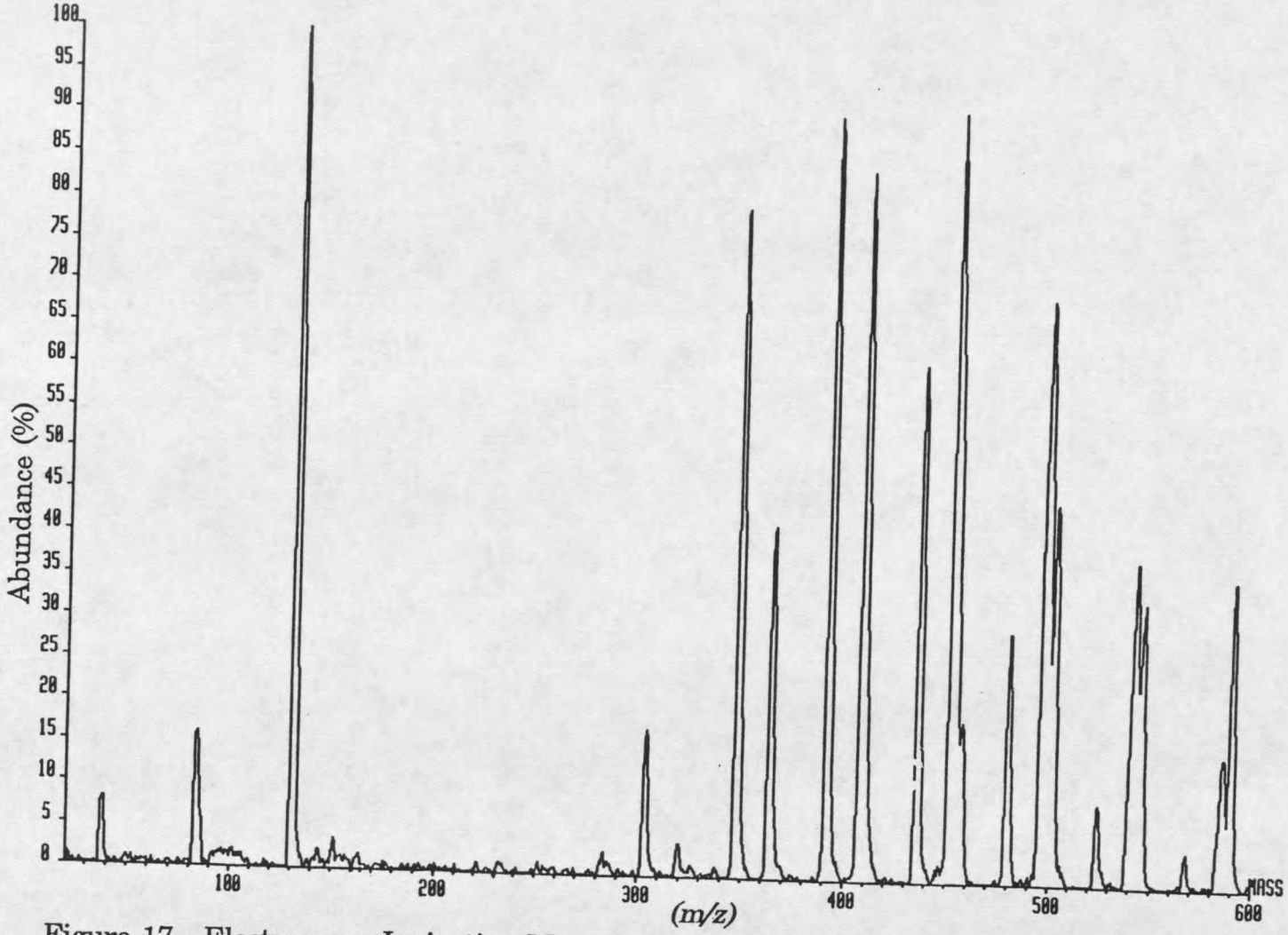


Figure 17. Electrospray Ionization Mass Spectrum of Calibration Standard.

Table 5. Polyethylene Glycol Reference Masses

C 12.011 H 1.0079 O 15.9994 Na 22.9898 H(OCH2CH2)nOH 44.053

	SINGLY CHARGED IONS				DOUBLY CHARGED IONS		
N	M	M+H	M+Na	M+K	M+2H	M+2Na	M+2K
1	62.068	63.076	85.058	101.158	32.042	54.024	70.124
2	106.121	107.129	129.111	145.211	54.069	76.051	92.151
3	150.174	151.182	173.164	189.264	76.095	98.077	114.177
4	194.227	195.235	217.217	233.317	98.122	120.104	136.204
5	238.280	239.288	261.270	277.370	120.148	142.130	158.230
6	282.333	283.341	305.323	321.423	142.175	164.157	180.257
7	326.386	327.394	349.376	365.476	164.201	186.183	202.283
8	370.439	371.447	393.429	409.529	186.228	208.210	224.310
9	414.492	415.500	437.482	453.582	208.254	230.236	246.336
10	458.545	459.553	481.535	497.635	230.281	252.263	268.363
11	502.598	503.606	525.588	541.688	252.307	274.289	290.389
12	546.651	547.659	569.641	585.741	274.334	296.316	312.416
13	590.704	591.712	613.694	629.794	296.360	318.342	334.442
14	634.757	635.765	657.747	673.847	318.387	340.369	356.469
15	678.810	679.818	701.800	717.900	340.413	362.395	378.495
16	722.863	723.871	745.853	761.953	362.440	384.422	400.522
17	766.916	767.924	789.906	806.006	384.466	406.448	422.548
18	810.969	811.977	833.959	850.059	406.493	428.475	444.575
19	855.022	856.030	878.012	894.112	428.519	450.501	466.601
20	899.075	900.083	922.065	938.165	450.546	472.528	488.627
21	943.128	944.136	966.118	982.218	472.572	494.554	510.654
22	987.181	988.189	1010.171	1026.271	494.599	516.581	532.681
23	1031.234	1032.242	1054.224	1070.324	516.625	538.607	554.707
24	1075.287	1076.295	1098.277	1114.377	538.652	560.634	576.734
25	1119.340	1120.348	1142.330	1158.430	560.678	582.660	598.760
26	1163.393	1164.401	1186.383	1202.483	582.705	604.687	620.787
27	1207.446	1208.454	1230.436	1246.536	604.731	626.713	642.813
28	1251.499	1252.507	1274.489	1290.589	626.758	648.740	664.840
29	1295.552	1296.560	1318.542	1334.642	648.784	670.766	686.866
30	1339.605	1340.613	1362.595	1378.695	670.811	692.793	708.893
31	1383.658	1384.666	1406.648	1422.748	692.837	714.819	730.919
32	1427.711	1428.719	1450.701	1466.801	714.864	736.846	752.946
33	1471.764	1472.772	1494.754	1510.854	736.890	758.872	774.972
34	1515.817	1516.825	1538.807	1554.907	758.917	780.899	796.999
35	1559.870	1560.878	1582.860	1598.960	780.943	802.925	819.025
36	1603.923	1604.931	1626.913	1643.013	802.970	824.952	841.052
37	1647.976	1648.984	1670.966	1687.066	824.996	846.978	863.078
38	1692.029	1693.037	1715.019	1731.119	847.023	869.005	885.105
39	1736.082	1737.090	1759.072	1775.172	869.049	891.031	907.131
40	1780.135	1781.143	1803.125	1819.225	891.076	913.058	929.158
41	1824.188	1825.196	1847.178	1863.278	913.102	935.084	951.184
42	1868.241	1869.249	1891.231	1907.331	935.129	957.111	973.211
43	1912.294	1913.302	1935.284	1951.384	957.155	979.137	995.237
44	1956.347	1957.355	1979.337	1995.437	979.182	1001.163	1017.264
45	2000.400	2001.408	2023.390	2039.490	1001.208	1023.190	1039.290
46	2044.453	2045.461	2067.443	2083.543	1023.235	1045.217	1061.317
47	2088.506	2089.514	2111.496	2127.596	1045.261	1067.243	1083.343
48	2132.559	2133.567	2155.549	2171.649	1067.288	1089.270	1105.370
49	2176.612	2177.620	2199.602	2215.702	1089.314	1111.296	1127.396
50	2220.665	2221.673	2243.655	2259.755	1111.341	1133.323	1149.423

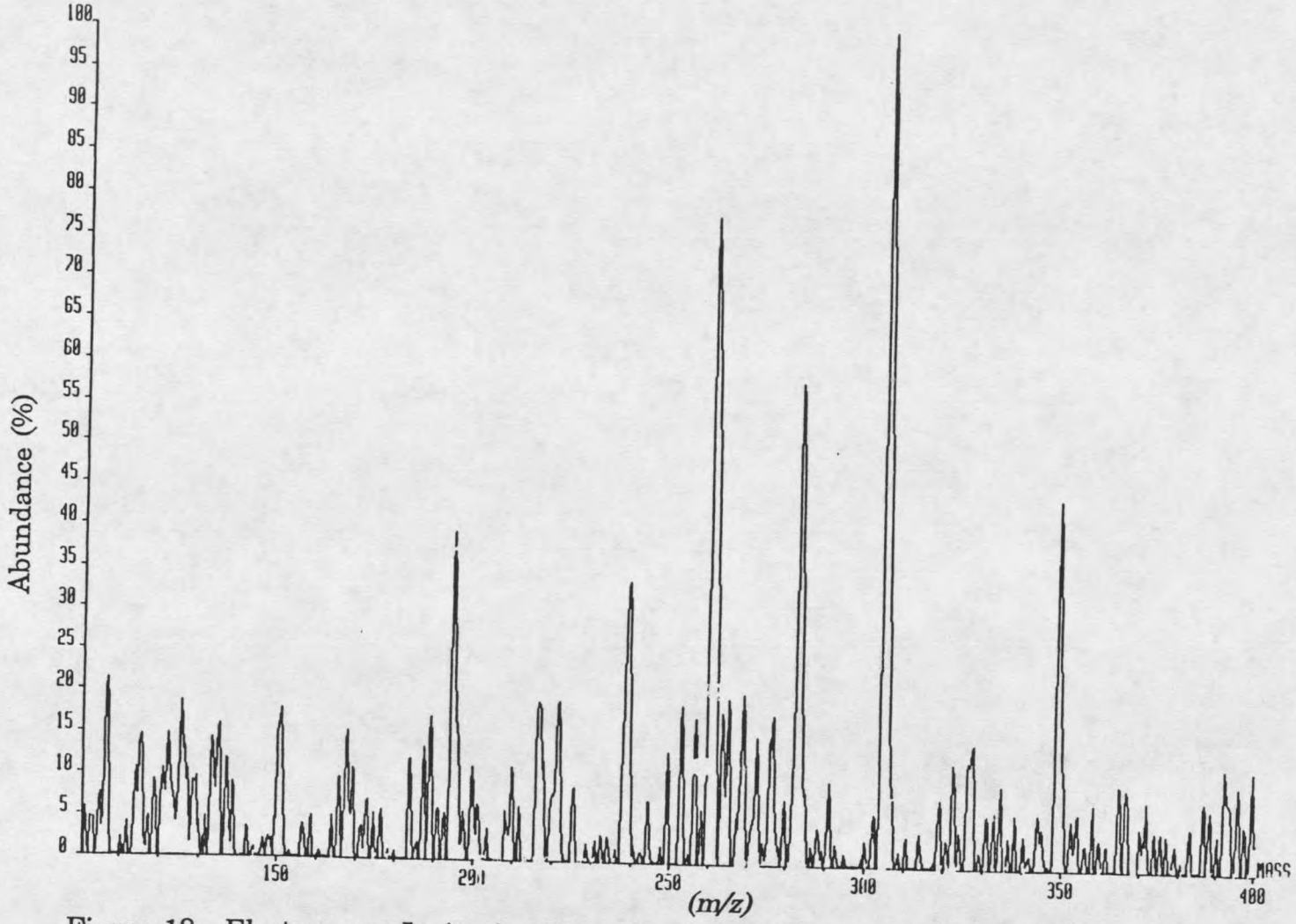


Figure 18. Electrospray Ionization Mass Spectrum of Protonated PEG (200 M. W.).

Table 6. Chemical/Physical Properties of the Pesticides

Pesticide	Family	Molecular Formula	Molecular Weight[a]	Solubility (H_2O)[b]	Specific Gravity[c]	Vapor Pressure[d]	pK_a[e]	pK_a[f]
Amitrole	Triazine	$C_2H_4N_4$	84.08	280,000	N/A	$4.4x10^{-7}$	4.2	5.6
Anilazine	Triazine	$C_9H_5N_4Cl_3$	275.52	8	N/A	$6.2x10^{-9}$	N/A	-6.9
Antu	Thiourea	$C_{11}H_{10}N_2S$	202.27	600	N/A	N/A	N/A	1.1
Carbaryl	Carbamate	$C_{12}H_{11}NO_2$	201.22	40	1.23	$1.2x10^{-6}$	N/A	-1.9
Carbofuran	Carbamate	$C_{12}H_{15}NO_3$	221.26	311	N/A	$6.0x10^{-7}$	N/A	-1.7
Chloramben	Benzoic acid	$C_7H_5NO_2Cl_2$	206.03	slightly	N/A	$7.0x10^{-3}$	3.4	2.8
Chlorpyrifos	Phosphorothioate	$C_9H_{11}Cl_3NO_3PS$	350.58	0.4	1.40	$1.9x10^{-5}$	N/A	-4.1
Coumafuryl	Hydroxycoumarin	$C_{17}H_{14}O_5$	298.30	insoluble	N/A	N/A	N/A	4.5
Diphacinone	Indandione	$C_{23}H_{16}O_3$	340.38	17	N/A	$1.0x10^{-8}$	N/A	-5.9
Diquat Dibromide	Bipyridyl	$C_{12}H_{12}N_2Br_2$	344.05	700,000	1.25	0	4.0	NR[g]
Diuron	Dimethyl urea	$C_9H_{10}Cl_2N_2O$	233.10	42	N/A	$6.9x10^{-8}$	N/A	-1.2
Endosulfan	Alicyclic halogen	$C_9H_6Cl_6O_3S$	406.92	0.32	N/A	$1.7x10^{-7}$	N/A	NR
Endothall	Dicarboxyllic	$C_8H_{10}O_5$	186.16	100,000	1.43	N/A	N/A	4.0
Ethion	Organophosphorus	$C_9H_{22}O_4P_2S_4$	384.46	2	1.22	$2.4x10^{-6}$	N/A	NR
Folpet	Phthalimide	$C_9H_4Cl_3NO_2S$	296.56	2	N/A	$4.0x10^{-5}$	N/A	-4.9
Glyphosate	Organophosphorus	$C_3H_8NO_5P$	169.07	20,000	1.74	$1.9x10^{-7}$	5.6	6.9
Linuron	Dimethyl urea	$C_9H_{10}Cl_2N_2O_2$	249.10	75	N/A	$1.5x10^{-5}$	N/A	-3.7
Mephosfolan	Phosphoramidate	$C_8H_{16}NO_3PS_2$	269.31	60,000	1.23	N/A	N/A	4.3
Methidathion	Organophosphorus	$C_6H_{11}N_2O_4PS_3$	302.32	240	1.21	$3.4x10^{-6}$	N/A	-0.9
Methiocarb	Carbamate	$C_{11}H_{15}NO_2S$	225.31	10	N/A	$1.2x10^{-4}$	N/A	-1.8

Table 6. Chemical/Physical Properties of the Pesticides (Continued)

Pesticide	Family	Molecular Formula	Molecular Weight[a]	Solubility (H_2O)[b]	Specific Gravity[c]	Vapor Pressure[d]	pK_a[e]	pK_a[f]
Methomyl	Carbamate	$C_5H_{10}N_2O_2S$	162.21	58,000	1.29	$5.0x10^{-5}$	N/A	-2.5
Mexacarbate	Carbamate	$C_{12}H_{18}N_2O_2$	222.29	100	N/A	$1.0x10^{-1}$	N/A	5.7
Molinate	Thiocarbamate	$C_9H_{17}NOS$	187.30	800	1.06	$5.6x10^{-3}$	N/A	0.2
Phosfolan	Organophosphorus	$C_7H_{14}NO_3PS_2$	255.29	650,000	N/A	N/A	N/A	4.3
Propoxur	Carbamate	$C_{11}H_{15}NO_3$	209.25	2,000	N/A	$9.7x10^{-6}$	N/A	-1.9
Pyrethrin[h]	Pyrethrin	$C_{21}H_{28}O_3$	328.45	insoluble	0.84	N/A	N/A	NR
Rotenone	Hydroxycoumarin	$C_{23}H_{22}O_6$	394.42	15	1.27	N/A	N/A	-4.9
Siduron	Urea	$C_{14}H_{20}N_2O$	232.33	18	N/A	$4.0x10^{-9}$	N/A	-0.4
Thiometon	Thiophosphate	$C_6H_{15}O_2PS_3$	246.34	200	1.21	$3.0x10^{-4}$	N/A	NR
Trifluralin	Dinitroaniline	$C_{13}H_{16}F_3N_3O_4$	335.28	0.3	N/A	$1.1x10^{-4}$	N/A	-5.5
Warfarin	Hydroxycoumarin	$C_{19}H_{16}O_4$	308.33	4	N/A	N/A	N/A	4.4

[a] chemical masses
[b] at 20 - 25 °C, units ppm
[c] at 20 °C
[d] at 20 - 25 °C, units of mm Hg
[e] pK_a's found in the literature
[f] pK_a's calculated using SPARC
[g] no reactive site found by SPARC
[h] mixture of Pyrethrins I and II (chemical mass 372.46)

solutions (2 mg/mL) of the compounds listed in Table 6 were prepared in pure methanol and kept under cold storage and subsequently diluted to volume with freshly filtered and degassed methanol/water. Each of the neat pesticides was electrosprayed using a flow rate of 2 μL per minute and various transport capillary/skimmer potential differences were employed. Reference spectra from these pesticides are located in Appendix A. Chemical structures of these pesticides are located in Appendix B.

Five twenty-second scans, with 0.1 second interscan times, were collected from each neat pesticide in the continuum mode. The transport capillary/skimmer potential difference used to generate these reference spectra varied from compound to compound. The potential difference was adjusted to maximize the $[M+H]^+$ ion and still invoke fragmentation to the extent that these patterns can be used diagnostically to determine compound identification.

Figures 19 and 20 of polyethylene glycol and Propoxur, respectively, are among the first electrospray ionization spectra generated on our system. Although the quality of these spectra is very poor, the peaks in both spectra are identifiable.

The concentration of all these reference compounds used to generate the spectra are shown in Table 7 and the majority are on the order of 10^{-5} M. The amount of pesticide used to generate each spectrum is shown also in Table 7. A twenty-microliter volume of pesticide solution was injected and allowed to spray for three to five minutes before data acquisition began. This was done to insure a stable flow rate and spray. Then five scans were collected. Based on the flow rate, pesticide concentration and total scan time the amount of pesticide consumed was calculated.

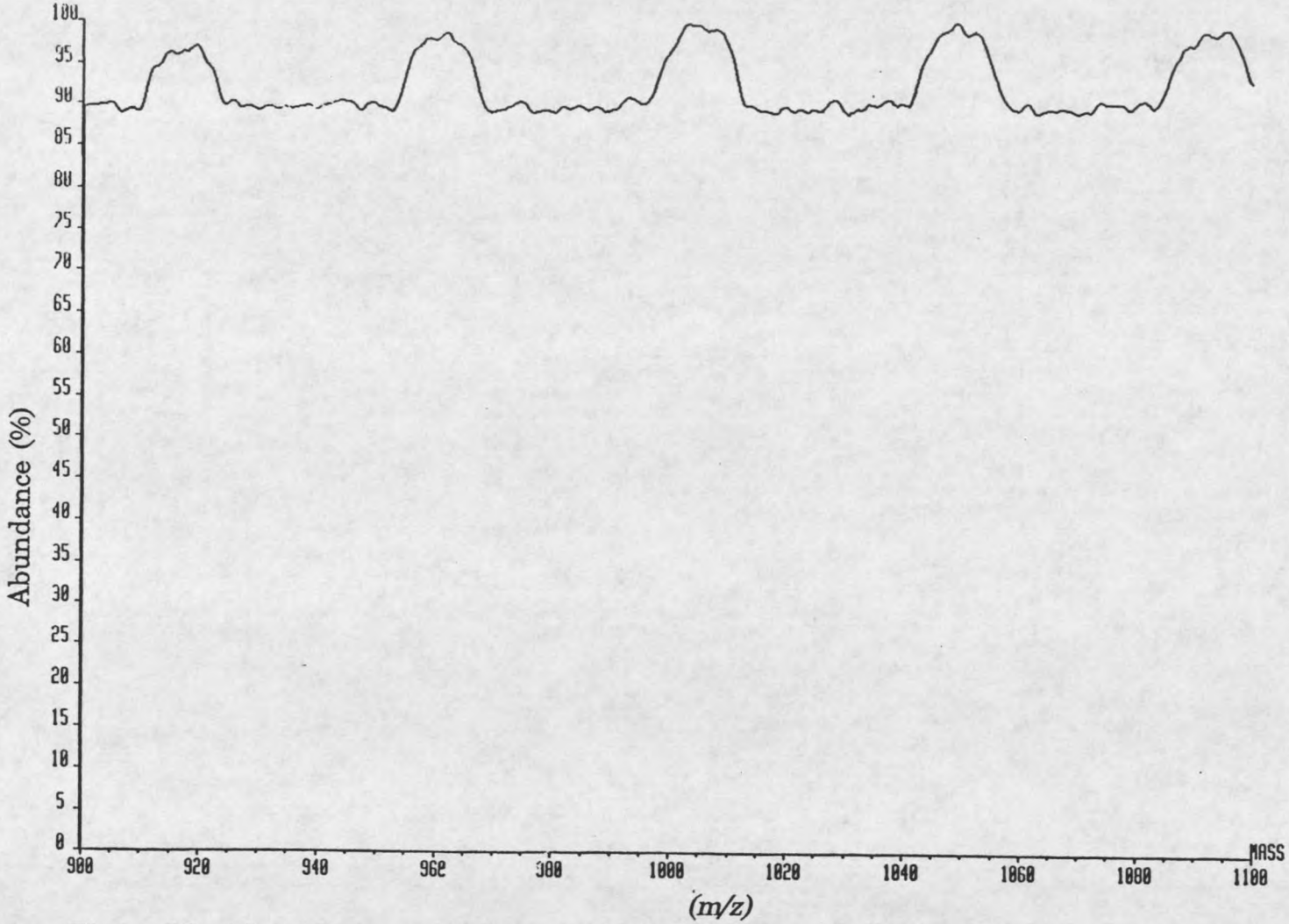


Figure 19. First Electrospray Ionization Mass Spectrum of PEG.

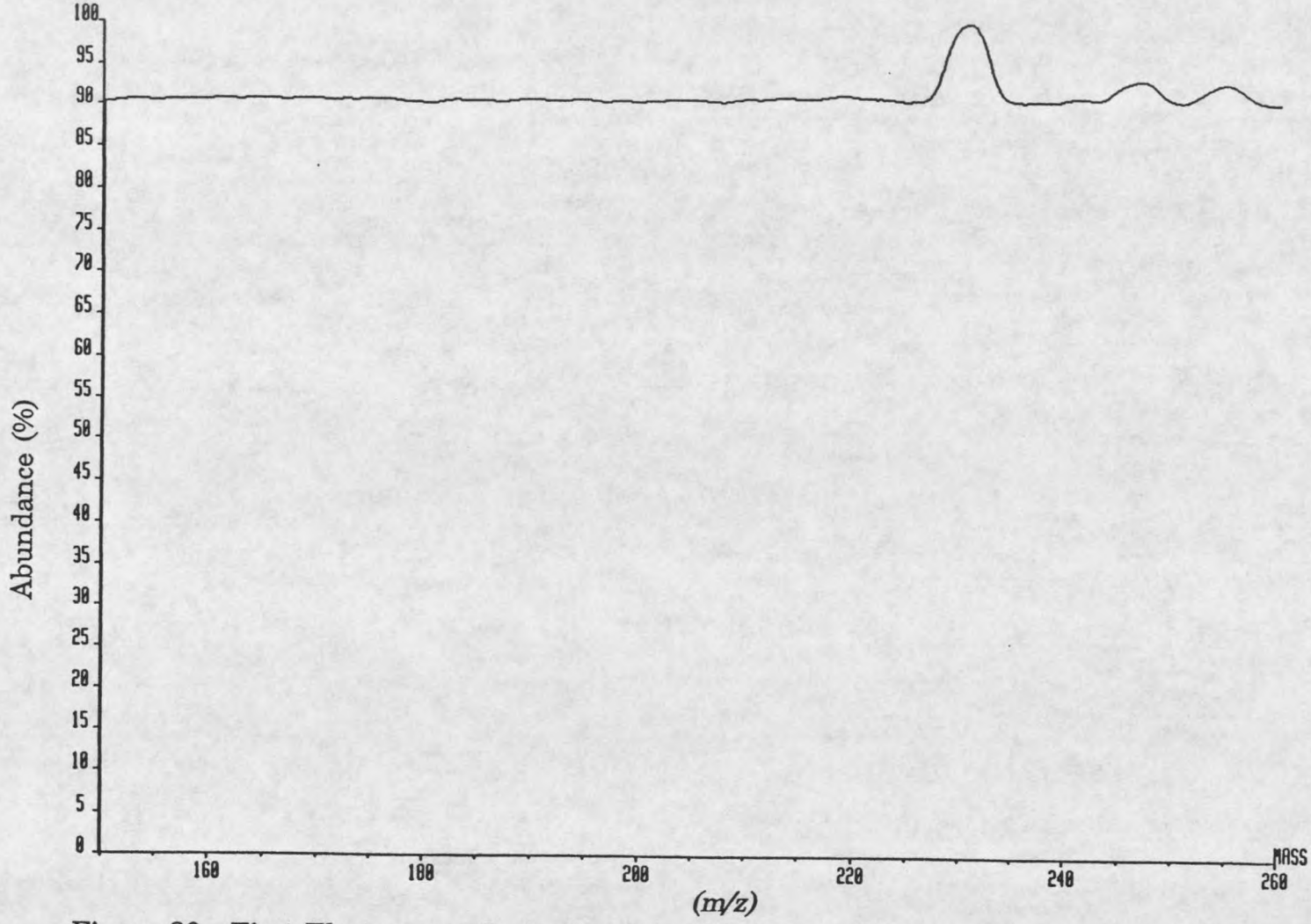


Figure 20. First Electrospray Ionization Mass Spectrum of Propoxur.

Table 7. Pesticide Reference Samples

Pesticide	Molecular Formula	Molecular Weight[a]	Purity (%)	Melting Point(°C)	Reference Concentration (M)	Quantity Consumed (ng)
Amitrole	$C_2H_4N_4$	84.08	99.2	159	$2.54x10^{-4}$	71
Anilazine	$C_9H_5N_4Cl_3$	275.52	99.9	160	$7.47x10^{-5}$	69
Antu	$C_{11}H_{10}N_2S$	202.27	95.0	198	$9.85x10^{-5}$	67
Carbaryl	$C_{12}H_{11}NO_2$	201.22	99.9	142	$9.93x10^{-5}$	67
Carbofuran	$C_{12}H_{15}NO_3$	221.26	99.9	151	$9.38x10^{-5}$	69
Chloramben	$C_7H_5NO_2Cl_2$	206.03	97.0	200	$1.10x10^{-4}$	75
Chlorpyrifos	$C_9H_{11}Cl_3NO_3P$	350.58	99.8	42	$5.88x10^{-5}$	69
Coumafuryl	$C_{17}H_{14}O_5$	298.30	96.3	124	$6.46x10^{-5}$	64
Diphacinone	$C_{23}H_{16}O_3$	340.38	99.7	145	$6.27x10^{-5}$	71
Diquat Dibromide	$C_{12}H_{12}N_2Br_2$	344.05	99.9	300	$5.69x10^{-5}$	65
Diuron	$C_9H_{10}Cl_2N_2O$	233.10	99.9	159	$8.63x10^{-5}$	67
Endosulfan	$C_9H_6Cl_6O_3S$	406.92	99.5	10	$5.06x10^{-5}$	69
Endothall	$C_8H_{10}O_5$	186.16	99.9	44	$1.00x10^{-4}$	62
Ethion	$C_9H_{22}O_4P_2S_4$	384.46	90.8	15	$1.44x10^{-5}$	19
Folpet	$C_9H_4Cl_3NO_2S$	296.56	99.3	178	$7.15x10^{-5}$	71
Glyphosate	$C_3H_8NO_5P$	169.07	97.3	200	$1.20x10^{-4}$	68
Linuron	$C_9H_{10}Cl_2N_2O_2$	249.10	99.4	94	$8.40x10^{-5}$	70
Mephosfolan	$C_8H_{16}NO_3PS_2$	269.31	99.8	0	$2.28x10^{-5}$	21
Methidathion	$C_6H_{11}N_2O_4PS_3$	302.32	99.5	40	$6.66x10^{-5}$	67
Methiocarb	$C_{11}H_{15}NO_2S$	225.31	99.3	121	$9.98x10^{-5}$	75

Table 7. Pesticide Reference Samples (Continued)

Pesticide	Molecular Formula	Molecular Weight	Purity (%)	Melting Point (C)	Reference Concentration (M)	Quantity Consumed (ng)
Methomyl	$C_5H_{10}N_2O_2S$	162.21	99.4	78	$1.27x10^{-4}$	69
Mexacarbate	$C_{12}H_{18}N_2O_2$	222.29	99.6	85	$8.96x10^{-5}$	67
Molinate	$C_9H_{17}NOS$	187.30	99.9	N/A	$2.84x10^{-5}$	18
Phosfolan	$C_7H_{14}NO_3PS_2$	255.29	99.6	37	$7.90x10^{-5}$	68
Propoxur	$C_{11}H_{15}NO_3$	209.25	98.9	92	$5.51x10^{-5}$	39
Pyrethrins[b]	$C_{21}H_{28}O_3$	328.45	10.5	N/A	$1.34x10^{-6}$	7
Rotenone	$C_{23}H_{22}O_6$	394.42	99.0	166	$5.67x10^{-5}$	75
Siduron	$C_{14}H_{20}N_2O$	232.33	99.7	135	$8.93x10^{-5}$	69
Thiometon	$C_6H_{15}O_2PS_3$	246.34	49.3	110	$1.21x10^{-5}$	10
Trifluralin	$C_{13}H_{16}F_3N_3O_4$	335.28	99.5	47	$6.26x10^{-5}$	70
Warfarin	$C_{19}H_{16}O_4$	308.33	99.5	161	$6.65x10^{-5}$	69

[a] chemical masses

[b] mixture of Pyrethrins I and II (chemical mass 372.46, purity 9.71%, molarity $1.10x10^{-6}$)

It should be noted from Table 7, with two exceptions, that the pesticide purity ranged from 95% to 99.9%. Although these purities are high it should be noted that a 1% impurity corresponds to 10,000 ppm in the neat sample and may give rise to peaks in these spectra that are not readily identifiable.

Because the purity of the pyrethrin pesticide was so low no attempt was made to identify spectral peaks.

Table 8 summarizes the spectral information from these neat pesticide samples. It was observed that the protonated analyte molecules, $[M+H]^+$, were obtained for the majority of pesticides with intensities ranging from 0 to 100%. Also the majority of samples exhibited an $[M+Na]^+$ peak although no sodium was added to these samples. The sodium originated from impurities in the methanol/water medium not only from being stored in glass containers but also because sodium chloride is an impurity in methanol. Sodium has been estimated to be present as an external contaminant with a concentration on the order of 10^{-6} M (48).

It is generally accepted that in electrospray ionization mass spectrometry even electron ions are produced both as the protonated analyte and as the fragment ions. In both cases neutral losses occur. The electrospray ionization process is such a soft ionization process that the physical separation of an electron pair to form a radical cation is not an energetically favored process although there is some evidence for formation of these radical cations from certain classes of compounds (49).

Triazine Pesticides

Amitrole has a fairly high solubility in water while Anilazine has a relatively low

Table 8. Major Ions (and Intensity) Generated by Electrospray Ionization Mass Spectrometry

Pesticide	$[M+Na^+]$	$[M+H^+]$	Other Major Ions
Amitrole	107(-0-)	85(100)	221(9) 58(1) 46(8)
Anilazine	299(-0-)	277(-0-)	363(8) 289(4) 269(15) 267(17) 171(6) 149(9) 135(16) 65(23)
Antu	225(46)	203(100)	186(2) 144(2)
Carbaryl	224(32)	202(-0-)	234(100) 216(25) 195(60) 181(25) 174(49) 151(11)
Carbofuran	244(16)	222(74)	165(100) 157(7) 149(2) 123(2) 73(5)
Chloramben	229(-0-)	207(-0-)	174(18) 172(100) 138(2)
Chlorpyrifos	374(100)	352(30)	324(11) 296(8) 200(23) 153(15) 133(87)
Coumafuryl	321(23)	299(6)	335(23) 299(6) 241(100) 163(3) 137(8)
Diphacinone	363(-0-)	341(4)	256(11) 240(10) 217(69) 212(100) 173(48) 168(92) 151(5) 105(47)
Diquat Dibromide	367(-0-)	345(-0-)	183(7) 157(14) 149(5) 92(100) 85(71) 73(29) 45(60)
Diuron	256(69)	234(100)	217(57) 195(6) 173(16) 150(5) 133(4) 111(6) 90(6)
Endosulfan	430(21)	408(4)	475(23) 458(9) 429(21) 374(90) 352(2) 323(62) 287(26) 133(100) 99(29)
Endothall	209(5)	187(2)	223(2) 183(11) 169(15) 135(35) 73(91) 45(54)
Ethion	407(100)	385(11)	359(10) 199(21) 171(43) 157(25) 135(9) 73(29) 71(62) 57(34)
Folpet	310(-0-)	299(4)	292(89) 202(13) 179(12) 177(14) 171(33) 163(100) 157(42) 149(27) 135(73) 73(13) 65(58)

Table 8. Major Ions (and Intensity) Generated by Electrospray Ionization Mass Spectrometry (Continued)

Pesticide	$[M+Na^+]$	$[M+H^+]$	Other Major Ions
Glyphosate	192(-0-)	170(6)	245(4) 223(8) 152(12) 119(37) 114(13) 105(28) 97(27) 87(49) 82(62) 73(9) 50(100)
Linuron	272(3)	250(48)	251(29) 162(8) 160(10) 149(11) 73(69) 45(100)
Mephosfolan	292(100)	270(89)	242(2) 196(20) 168(2) 149(2) 133(2)
Methidathion	325(100)	303(70)	320(12) 267(3) 229(3) 171(2) 145(88) 85(4) 23(20) 18(39)
Methiocarb	248(21)	226(100)	177(5) 171(24) 169(88) 157(56) 149(5) 135(11) 113(1) 89(4) 73(52) 45(26)
Methomyl	185(58)	163(26)	386(14) 347(11) 273(38) 261(15) 240(15) 217(93) 208(28) 195(19) 185(58) 173(21) 163(26) 88(61)
Mexacarbate	245(-0-)	223(100)	166(55) 151(5) 46(5)
Molinate	210(5)	188(75)	177(17) 149(13) 126(32) 89(11) 73(74) 45(100)
Phosfolan	278(20)	256(28)	228(10) 221(100) 217(10) 196(7) 169(7) 141(4) 45(13)
Propoxur	232(53)	210(17)	168(100) 153(16) 111(71) 46(22)
Rotenone	417(-0-)	395(100)	217(10) 195(54) 151(23) 42(26)
Siduron	264(-0-)	233(12)	211(5) 197(24) 177(3) 149(3) 108(100) 86(1)
Thiometon	269(100)	247(-0-)	261(14) 217(76) 195(7) 185(11) 173(12) 90(91)
Trifluralin	358(-0-)	336(56)	309(9) 256(10) 119(7) 91(10) 73(28)
Warfarin	331(30)	309(100)	323(30) 251(11) 197(6) 163(5) 108(8)

water solubility. However, in both cases there is evidence in the spectra for both of these pesticides that there is a solvated analyte ion even though the potential difference between the transport capillary and skimmer is on the order of 75 volts. In the Amitrole spectrum the ion at *m/z* 223 represents a sodiated Amitrole dimer with a methanol molecule attached. The protonated analyte molecule at *m/z* 85 is the most abundant ion in the spectrum.

Also in the Anilazine spectrum is evidence of a solvated analyte molecule at *m/z* 363. In fact this mass represents a cluster ion consisting of a sodiated anilazine molecule to which is attached two methanol molecules. The two methanol molecules may be indicative of the fairly low water solubility exhibited by Anilazine.

Carbamate Pesticides

Six carbamate pesticides were included in this study: carbaryl, carbofuran, methiocarb, methomyl, mexacarbate and propoxur. The loss of methyl isocyanate, $OCNCH_3$ is evident in the spectrum from each of these carbamate pesticides (46). The ions that are formed in the case of aromatic compounds must be resonance stabilized as depicted in Figure 21.

In the Carbaryl spectrum the ion at *m/z* 181 results from the cluster, consisting of $[M+H+2H_2O]^+$, losing the methyl isocyanate group. Also the ion at *m/z* 195 represents the same loss from the cluster $[M+H+CH_3OH]^+$. The ion at *m/z* 195 can be formed from the sodiated parent analyte losing $HNCH_2$. Ion at *m/z* 173 results from the protonated parent ion losing this same moiety. The ion at *m/z* 151 results from ion *m/z*

195 losing carbon dioxide.

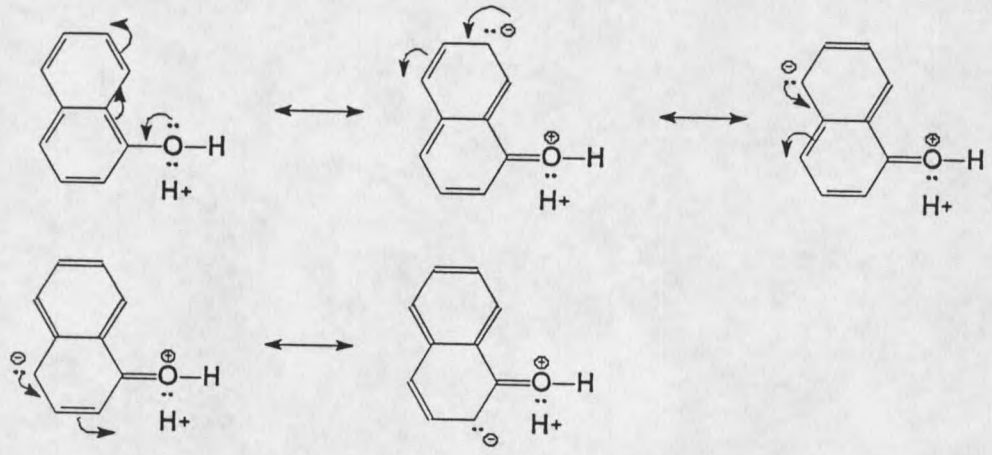


Figure 21. Resonance Stabilization in the Aromatic Carbamate Pesticides.

In the Carbofuran spectrum the ion *m/z* 165 is the most abundant ion and is formed by the loss of the methyl isocyanate group from $[M+H]^+$.

The Methiocarb spectrum shows the protonated parent $[M+H]^+$ to be the predominant ion. The ion at *m/z* 169 results from the loss methyl isocyanate from $[M+H]^+$.

Methomyl shows this same loss at *m/z* 106, $[M+H]^+ - OCNCH_3$. The ion at *m/z* 217 represents $[M+Na+CH_3OH]^+$. The ion at *m/z* 347 represents a sodiated dimer, $[2M+Na]^+$. The ion at *m/z* 386 represents $[2M-H+Na+K]^+$. It is not uncommon to find potassium as an impurity in these solutions.

The Mexacarbate spectrum shows the loss of the methyl isocyanate group at the *m/z* 106. The ion at *m/z* 150 results from the protonated parent ion losing the methyl carbamate group.

The Propoxur spectrum indicates the loss of the methyl isocyanate group as the ion at *m/z* 153. The ion at *m/z* 168 represents $[M+H]^+ - C_3H_6$. The ion at *m/z* 111 results from the protonated parent analyte losing C_3H_6 and then the methyl isocyanate group. Occasionally an ion at *m/z* 93 is observed in the spectrum of this pesticide and is due to the ion at *m/z* 111 losing a water molecule.

Dimethyl Urea Pesticides

Diuron, in the dimethyl urea class, loses methane, $[M+H]^+ - CH_4$, to form the ion at *m/z* 217. Then through some kind of rearrangement the ion at *m/z* 217 loses $HNNCH_3$.

In the Linuron spectrum ion *m/z* 160 represents the almost simultaneous loss of methanol and $HONCH_3$.

Organophosphorus Pesticides

The Mephosfolan spectrum, in addition to the presence of $[M+H]^+$ and $[M+Na]^+$, shows an *m/z* at 242, $[M+H]^+ - C_2H_4$ and an *m/z* at 196 which represents $[[M+H]^+ - C_2H_4 - CH_3CH_2OH$. The protonated Phosfolan molecule shows a similar loss of C_2H_4 to form *m/z* at 228, $[M+H]^+ - C_2H_4$. The most abundant ion at *m/z* 222 results from the sodiated parent ion losing two ethylene molecules, $[M+Na]^+ - C_2H_4 - C_2H_4$.

Hydroxycoumarin Pesticides

Three hydroxycoumarin compounds were included in this work: Coumafuryl,

Rotenone and Warfarin. The ion at *m/z* 241 in the Coumafuryl spectrum results from $(CH_3)_2CO$ being lost from the protonated parent, $[M+H]^+ - (CH_3)_2CO$. Ions at *m/z*'s 163 and 137 result from the Coumafuryl molecule fragmenting into the coumarin and furan moieties. The Warfarin molecule also fragments to form the protonated coumarin moiety. The ion at *m/z* 251 results from the loss of dimethyl ketone or acetone. The Rotenone spectrum contains the protonated parent ion as the most abundant ion, $[M+H]^+$.

Carboxyllic Acid Pesticides

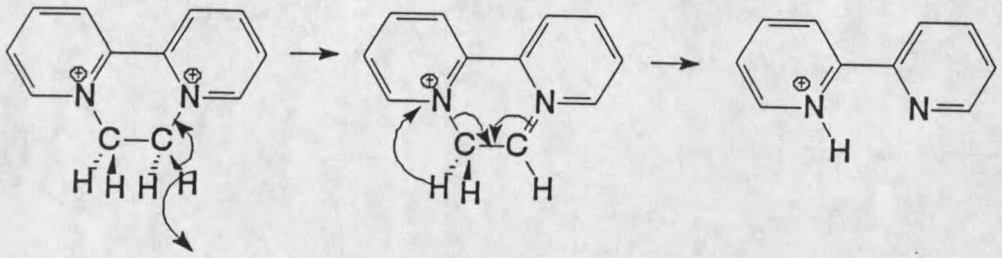
The Endothall spectrum shows evidence of a solvated cluster, $[M+H]^+ + 2\ H_2O$, at an *m/z* of 223. The ion at *m/z* 169 results from the loss of water, $[M+H]^+ - H_2O$. The ion at *m/z* 73 is a protonated epoxide, $[C_2O_3H]^+$. The ion at *m/z* 45 is a protonated carbon dioxide molecule. The ion at *m/z* at 135 results from the loss of water and then the loss of hydrogen peroxide, $[M+H]^+ - H_2O - H_2O_2$.

The Chloramben spectrum contains the $[M+H]^+ - H_2O_2$ ion as the predominant ion. The ion at *m/z* 174 is due to the ^{37}Cl isotope.

Other Classes of Pesticides

Diquat dibromide, a bipyridyl compound, exhibits an interesting spectrum. The ions in this spectrum are shown being formed in Figure 22.

The Endosulfan spectrum contains *m/z* of 133 as the predominant ion which results from the dissection of the two rings. This ion has the composition of

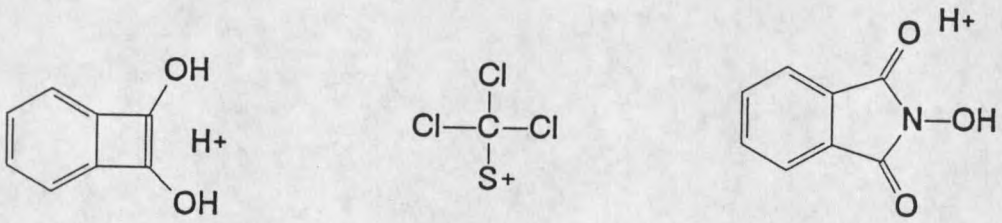


m/z 184/2 = m/z 92 m/z 183 m/z 157

Figure 22. Possible Structures of the Diquat Ions

$C_4H_4O_3SH^+$. The ion at *m/z* 374 results from the protonated parent losing H_2O_2; the ion at *m/z* 323 is $[M+H]^+ - CH_2Cl_2$. Hydrogen chloride is then lost to form the ion at *m/z* 287.

Folpet, a phthalimide compound, exhibits ions in its spectrum that appear to be formed from some type of hydrolysis reaction. Possibilities for the structures of the ions at *m/z*'s of 135, 150 and 164 are shown in Figure 23.



m/z 135 m/z 150 m/z 164

Figure 23. Possible Structures for the Folpet Ions.

Molinate, a thiocarbamate compound, contains in its spectrum an ion at *m/z* 126 as one of the major ions which represents the loss of $HSCH_2CH_3$ from the protonated

analyte molecule, $[M+H]^+ - HSCH_2CH_3$.

The protonated Thiometon molecule loses formaldehyde to form the ion at *m/z* 217. The loss of another formaldehyde molecule accounts for the ion at *m/z* of 185. Then the loss of PS_2 results in the formation of the ion at *m/z* 90.

The protonated Trifluralin molecule, a dinitroaniline compound, loses F_2 to form the ion at *m/z* 298 which in turn loses C_3H_6 to form the ion at *m/z* 256.

It is interesting to consider the pK_a's of these pesticides listed in Table 6. Only two or three of these values were available from the literature. The originators of the computer model, SPARC, Karickhoff and Carreira (50), were consulted concerning calculating the pK_a's of these compounds. SPARC stands for "SPARC Performs Automated Reasoning in Chemistry." This expert system is being developed by Karickhoff of the USEPA's Athens Environmental Research Laboratory and Carreira and other scientists at the University of Georgia's Chemistry Department. This system has the capability of crossing chemical boundaries to cover all organic chemicals and uses algorithms based on fundamental chemical structure theory to estimate parameters. Structural groups that influence certain types of chemical reactivity have been established by organic chemists and the effects on reactivity of other constituents appended to the site of reaction have been described. To encode this knowledge base Karickhoff *et al* developed a classification scheme that defines the role of structural constituents in affecting or modifying reactivity. The effects of parameters such as induction, resonance and field effects, commonly used in structure-reactivity analysis, have been quantified by models developed for these mechanistic descriptions. SPARC incorporates a mixture

of computational approaches including the conventional linear free energy theory (LFET) and perturbed molecular orbital (PMO) methods. LFET is used by SPARC to compute thermodynamic properties and PMO is used to describe quantum effects such as delocalization energies or polarizabilities of π electrons. Ultimately SPARC will advance to the point of being able to calculate a value comparable in accuracy to that obtained experimentally but at a fraction of the expense required to measure it. SPARC has the capability of predicting values over a wide range of conditions. For instance, if a user needs parameter values at conditions other than at STP SPARC will compute these at the desired conditions. For example, one may wish to know the solubility of a compound at a certain pressure, temperature and pH. SPARC will be able to calculate this value at the required conditions. In order to have SPARC calculate the pK_a's the pesticides may be defined for the expert system by use of either CAS numbers, SMILES strings (51) or chemical structures. SMILES notation provides a unique identification of a chemical substance based on a connection table that represents the topological structure of the chemical. Therefore, the SMILES notation does have chemical significance. In the SMILES notation the hydrogen atoms are suppressed, aromatic atoms are represented by lower case characters and non aromatic atoms are represented by upper case characters.

Examples of SMILES strings for several of the pesticides used in this work are shown below.

Carbaryl	c1cccc2c1cccc2OC(=O)NC
Carbofuran	c1ccc(OC(=O)NC)c2c1CC(CC)O2

Propoxur	c1c(OC(=O)NC)c(OC(C)C)ccc1
Warfarin	c1cccc2c1OC(=O)C(C(CC(=O)C)c3ccccc3)=C2O

The SPARC program identifies all reactive sites in basic structures that can accommodate a proton and then determines the pK_a's for all these sites. Actually pK_{BH+} may be a better representation. For acidic structures the program calculates pK_a's for proton loss at reactive sites. Bulk water pK_a's were calculated at one atmosphere pressure and a temperature of 25 °C. The calculated pK_a's for the most basic site in each compound is listed in Table 6. Additionally, pK_a values for all reactive sites were calculated and listed on the reactive site in the molecule. These are located in Appendix B.

As indicated in Table 9, with a solution pH of 5.5 the percent ionization of a compound with a $pK_a > 5.5$ is 50%.

Table 9. Percent Ionization as a Function of pK_a

pK_a	% Ionization (pH ~5.5)
>5.5	50
5.0	24
4.5	9
4.0	3
3.5	1
3.0	0.3
2.5	0.1
2.0	0.03
1.5	0.01
1.0	0.003
0.5	0.001
0.0	0.0003

It is extremely interesting to observe that the majority of these pesticides have extremely low pK_a values, with most of them extending in the negative range.

In other words 50% of the compound exists in solution as the protonated specie, BH^+. On the other hand the percent ionization of a compound with a pK_a of 0 is 0.0003. How, then, can it be explained that all of these pesticides with these extremely low pK_a's give good results using electrospray ionization as evidenced by their spectra that were obtained on neat compounds. The thermodynamic explanation offered by Iribarne and Thomson (29) suggest that protonated analyte ions are preformed in solution.

These low pK_a's for the pesticides appear to contradict the idea of preformed ions in solution. Kebarle (48) describes the electrospray ionization process as an electrolysis cell where protons from the reduction of water are the source of positive charges on the surface of the droplets that are formed during the electrospray process.

Perhaps a more logical explanation for the formation of protonated pesticide molecules involves the formation of these protonated ions, not in the condensed phase, but in the gas phase. No proton affinity data can be found for any of these compounds.

The existence of sodiated pesticides even in these neat solutions also tends to support the hypothesis that these protonated analytes are formed in the gas phase while the sodiated ions are formed in the condensed form. Bond strength between sodium ions and oxygen atoms in these pesticides is probably around 2 eV. Many of the pesticide spectra show evidence of both protonated and sodiated dimers. It is logical that sodium, being a larger ion than hydrogen, would be more stable than hydrogen in the dimer state and this is indicated by a more intense signal for the sodiated dimer for most

observations.

Ions undergo collision-activated dissociation in the region between the end of the transport capillary and the skimmer lens. The extent to which the ions undergo dissociation or fragmentation depends on the collision cross section, collision frequency and energy of the ions. Ions emerge from the transport capillary in a free jet expansion produced by the transport capillary having a much larger diameter than the ion mean free path. The capillary diameter is on the order of 2-3 orders of magnitude greater than the mean free path. Based on the mean free path (~ 80 μm) and the number density (3×10^{16}) it is evident that these ions are undergoing multiple collisions with a collision frequency on the order of 5×10^{6}/sec. The collision energy is a function of the potential difference between the end of the transport capillary and skimmer lens. The ions initially have thermal energy of about 0.1 eV when they are formed in the transport capillary. As the ions emerge from the transport capillary they enter the electrical field that decreases in strength from the transport capillary to the skimmer lens. The ions are exposed to the strongest field at the capillary tip but at this point have the shortest mean free path which limits the ion kinetic energy. As the ions move closer to the transport capillary they have a larger mean free path but the electric field is weaker and this also limits the ion kinetic energy. It has been reported (53) that the collision energy between 1 and 24 eV can be imparted to ions between the transport capillary and skimmer lens by simply varying this potential difference.

The collision-activated dissociation spectra (CAD) generated by electrospray ionization are shown in Appendix C for two representative compounds from each of the

six major classes of compounds studied: triazine, carbamate, urea, carboxyllic acid, hydroxycoumarin, and organophosphorus and thiocarbamate. The concentrations of these compounds are found in Table 7. For each compound a spectrum is included that was generated under both a low and a high transport capillary/skimmer potential difference to show the effect of increasing the potential difference.

From a visual inspection of these spectra it is immediately obvious that a greater degree of fragmentation is observed at the higher potential difference. For the same potential difference the degree of fragmentation from compound to compound can be quite different due to the chemical and structural composition of the compound.

Figure 24, showing the distribution of ions from Propoxur at various transport capillary/skimmer potential differences, is fairly representative of all the compounds studied. Generally, a potential difference of approximately 35 volts is sufficient for most compounds studied not only to produce the protonated and sodiated analyte but also to show evidence of fragmentation. In most of the compounds the protonated analyte signal maximizes at a potential difference of approximately 55-65 volts; the sodiated analyte signal maximizes at approximately 75 volts. At a potential difference of around 135 volts most of the ions present are the lower mass ions with little or no protonated analytes. However, the sodiated analyte signal is still present at this potential difference even though it is fairly low. This suggests that the binding energy of sodium to the analyte is fairly substantial: Fenn reports that the binding energy of sodium in polyethylene glycol is approximately equal to 2.05 eV for the bond between sodium and the oxygen atom in dimethoxy ethane (19).

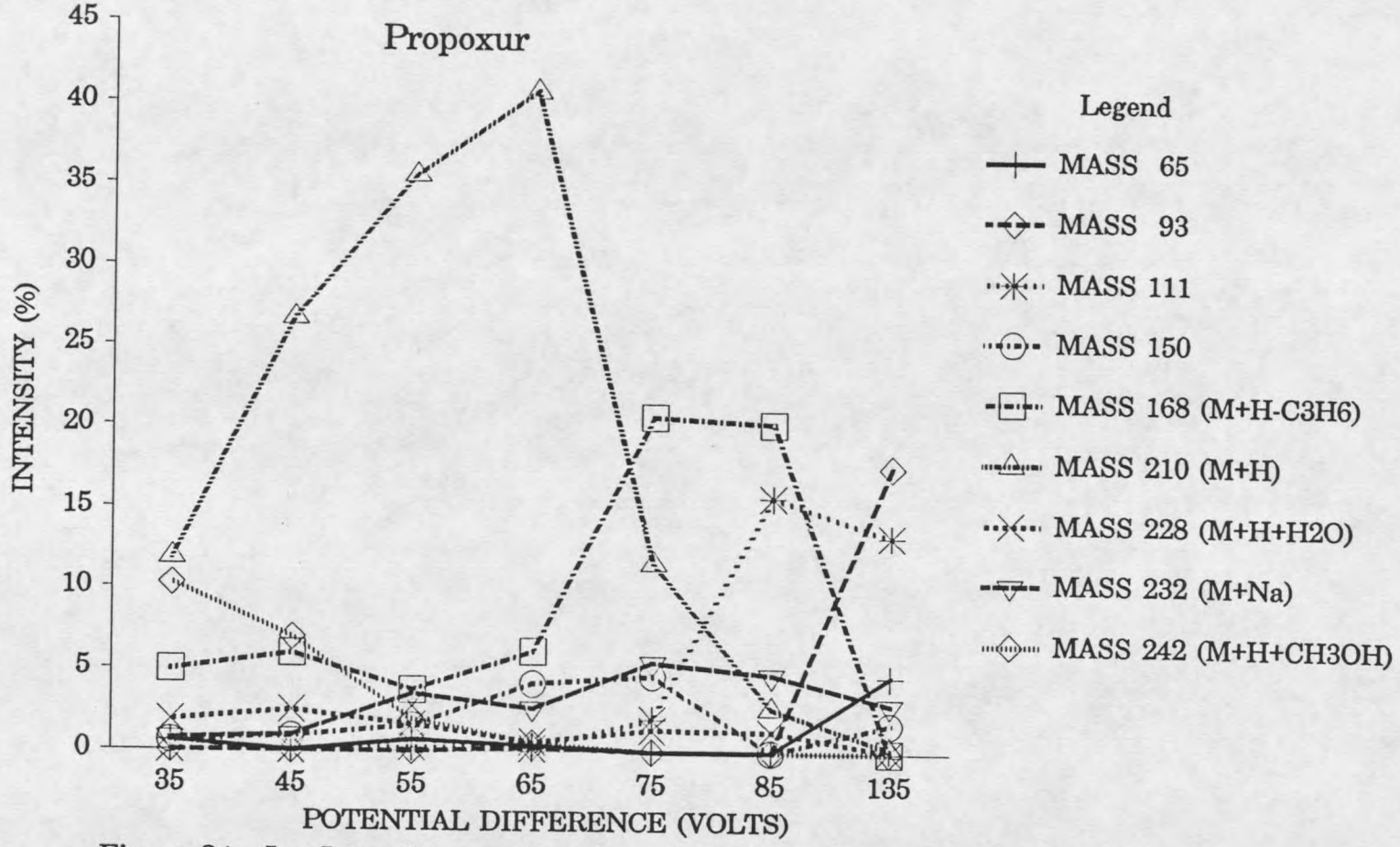


Figure 24. Ion Intensity as a Function of Capillary/Skimmer Potential Difference

pH Studies

Neat solutions of all of the pesticides were analyzed in a 50/50 mixture of methanol/water and the potential difference between the transport capillary and the skimmer lens was varied between 35 and 135 volts. The pH was around 5.5 for these neat solutions as indicated by *colorpHast*® indicator strips. Figures 86 through 99 in Appendix D are representative of the pesticide responses obtained in this work. In each graph the ion intensity is plotted as a function of the transport capillary/skimmer potential difference. Generally, it is observed that the protonated analyte signal is maximized around a potential difference of ~55 volts and the sodiated analyte signal is maximized around 75 volts.

The pH was adjusted to around 3 with acetic acid and the signal response then compared to that of the neat compounds.

Figures 100 - 107 in Appendix E show the response to these compounds as a function of transport capillary/skimmer lens potential difference. Signals for the protonated and sodiated analytes are shown together with the total ion currents. The responses are shown for the neat, acidified and sodiated solutions.

The solutions that were acidified with acetic acid never produced a substantially higher signal for the $[M+H]^+$ or the total ion current than those from the neat solutions. This observation tends to support the suggestion that the protonated ion of the analytes used in this study occurs in the gas rather than the condensed phase.

In addition to the acetic acid study, hydrochloric acid was used to adjust the pH to various values in solutions of Propoxur, Thiometon and Phosfolan. Figures 108 - 110

in Appendix E show that as the pH is increased both the $[M+H]^+$ intensity and the total ion current decrease. The Propoxur signal shows a slight increase in the $[M+H]^+$ signal and total ion current but it is not substantial.

Sodium Adduct Study

Figures 100 - 107 in Appendix E show that addition of sodium with a resulting concentration on the order of 10^{-4} M does not in any case substantially increase the total ion current over that generated by the neat compounds. The sodiated adduct intensity, however, generally shows an increase over that in the neat solutions. Cesium ions were added to only one compound, Propoxur, individually and in combination with sodium ions with a resulting concentration of 10^{-4} M. While the spectrum showed evidence of cesium adduct peaks the signal for the sodium adduct in both cases was the higher.

Three compounds, Diuron, Methomyl, and Siduron, were selected for a second study on sodium adducts. For each of these compounds the signals for $[M+H]^+$, $[M + Na]+$, and total ion current were compared in the neat solution with no sodium added and also in solutions where the final sodium concentrations were $2x10^{-6}$ M, $2x10^{-5}$ M, $2x10^{-4}$ M and $2x10^{-3}$ M. Figures for this study are located in Appendix F. Figure 113 shows that for Diuron the total ion current maximizes at a sodium concentration of 2×10^{-5} M. Figure 111 shows that the $[M+H]^+$ signal is maximized in the neat solution. The $[M+Na]^+$ signal is also a maximum in the neat solution as shown in Figure 112. This finding is in line with the observation that the intensity is either very low or non-existent for both the $[M+H]^+$ and $[M+Na]^+$ for compounds that contain chlorine atoms.

Figure 119 shows that for Siduron, a urea-type compound also, the total ion current maximizes in the $2x10^{-6}$ M sodium. The $[M+H]^+$ signal is maximum in the solution with sodium concentrations of $2x10^{-6}$ M. The $[M+Na]^+$ signal maximizes at a sodium concentration of $2x10^{-4}$ M.

For methomyl Figure 115 shows the $[M+Na]^+$ as a maximum with the sodium concentration at $2x10^{-5}$ M. Figure 114 shows the $[M+H]^+$ at a maximum with the sodium concentration at $2x10^{-6}$ M. Figure 116 shows the total ion current maximized as a sodium concentration of $2x10^{-5}$ M.

Ammonium Acetate Study

Ammonium acetate was added to the following pesticides to determine the effect on the signal response: Endothall, Coumafuryl, Linuron, Antu, Carbofuran, and Propoxur. It was suspected that the addition of ammonium acetate would cause an increase in the protonated analyte signal and also in the total ion current because the following reaction was thought to occur:

$$\text{Analyte} + NH_4^+ = \text{AnalyteH}^+ + NH_3$$

However, from Figures 120 - 125 located in Appendix G it is obvious that neither the $[M+H]^+$ signal nor the total ion current is increased for any of the compounds with the addition of ammonium acetate.

Solvent Study

Although there are many important variables to consider in using electrospray

ionization mass spectrometry, choice of solvent system is one of the most important. Table 10 contains pertinent chemical and physical properties of the solvents used in this work.

Table 10. Chemical/Physical Properties of the Solvents

	Water	Methanol	Acetonitrile
pKa	15.70	15.00	25.00
Dielectric Constant	81.00	33.00	38.00
Dipole Moment (debye)	1.85	1.70	3.92
Surface Tension (dyn/cm)	73.05	22.61	29.30
Boiling Point (°C)	100.00	65.15	81.60
Melting Point (°C)	0.0	-93.90	-45.70
Density (g/mL)	1.00	0.7914	0.7857

Figure 25 shows the total ion current as a function of transport capillary/skimmer potential difference for Amitrole, Diphacinone, Propoxur, and Rotenone analyzed in 50/50 methanol/water and also in 100% methanol. Figure 26 shows total ion current of these four compounds run in 50/50 acetonitrile/water. The total ion current appears to be in the same range in the methanol/water and acetonitrile/water systems and much lower for all four compounds run in pure methanol.

These four compounds were also made up in pure acetonitrile. A signal was obtained for one compound only, Rotenone. The spectrum showed the presence of not a protonated analyte but of a radical cation M^+. Formation of radical cations is not considered unusual in the electrospray ionization for compounds in the PAH category (49).

Kebarle (54) showed that the intensity of the protonated bases used in one of his

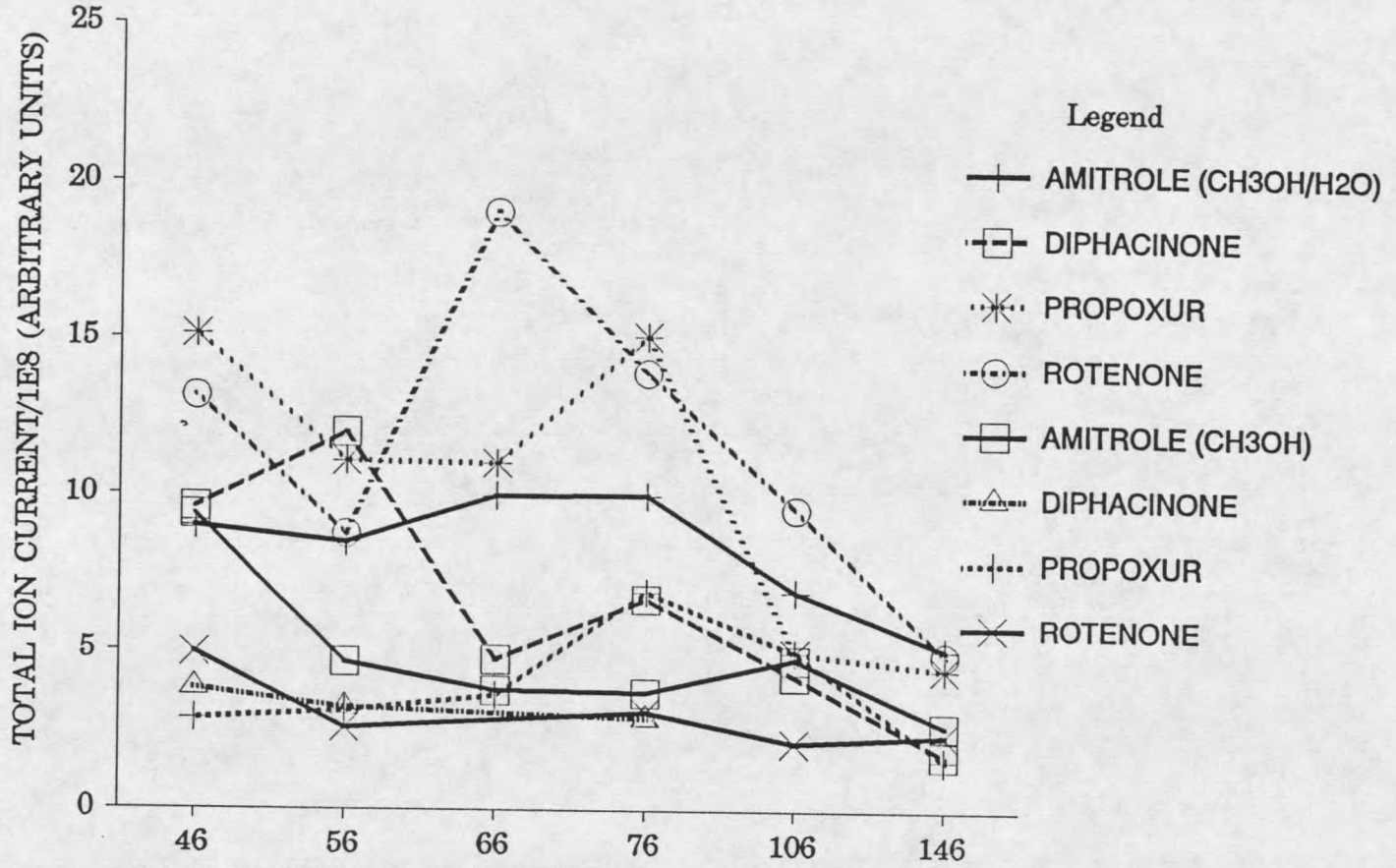


Figure 25. Solvent Effects (Methanol/Water, Methanol) on Total Ion Current

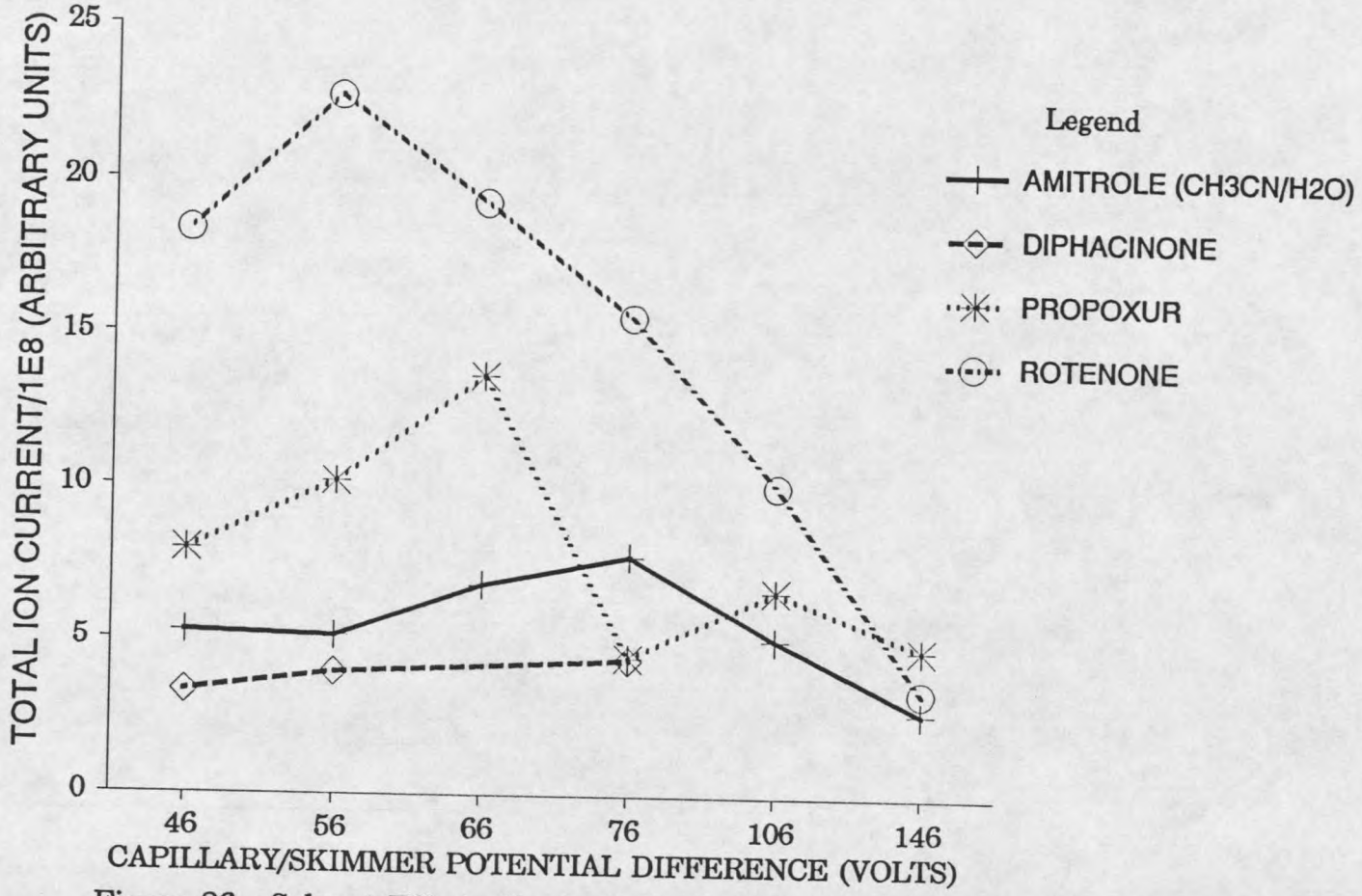


Figure 26. Solvent Effects (Acetonitrile/Water) on Total Ion Current

studies decreased as the percentage of water in the methanol/water mixture increased. He concluded that the ion yield from aqueous droplets is less favorable relative to that from methanol droplets. This is the reverse from conclusions drawn from analyzing Methomyl and Phosfolan in methanol/water mixture where the methanol content was varied from 10% to 90%. See Figures 126 - 131 in Appendix H. In both cases the protonated analyte intensity decreases with increasing fractions of methanol. The total ion current fluctuates in an analogous manner. The sodiated analyte intensity, however, appears to maximize in the solvent with highest methanol content.

Folpet and Trifluralin were also analyzed in methanol/water by varying methanol fractions from 10% to 90%. As noted previously these two compounds do not show protonated analyte peaks in electrospray spectra. The total ion current as shown in Figures 132 and 133 located in Appendix H for both of these compounds appears to increase with an increasing methanol fraction in the solvent mixture.

Kebarle, in the same paper, notes that the activation barrier from analytes in the solvent water is greater than that in methanol. He calculates the free energy of solvation as 65 Kcal/mole in water and 45 Kcal/mole in methanol and suggests that the decrease in the free energy of solvation in methanol should lead to a significant decrease of the activation free energy for methanol and to a higher efficiency of ion evaporation from methanol droplets relative to water. He goes on to predict that an even larger decrease of the free energy of solvation could be predicted for acetonitrile as a solvent. However, if the Born equation is plotted with free energy of solvation versus cluster radius, as shown in Figure 27, it is observed that the free energy of solvation for acetonitrile is not

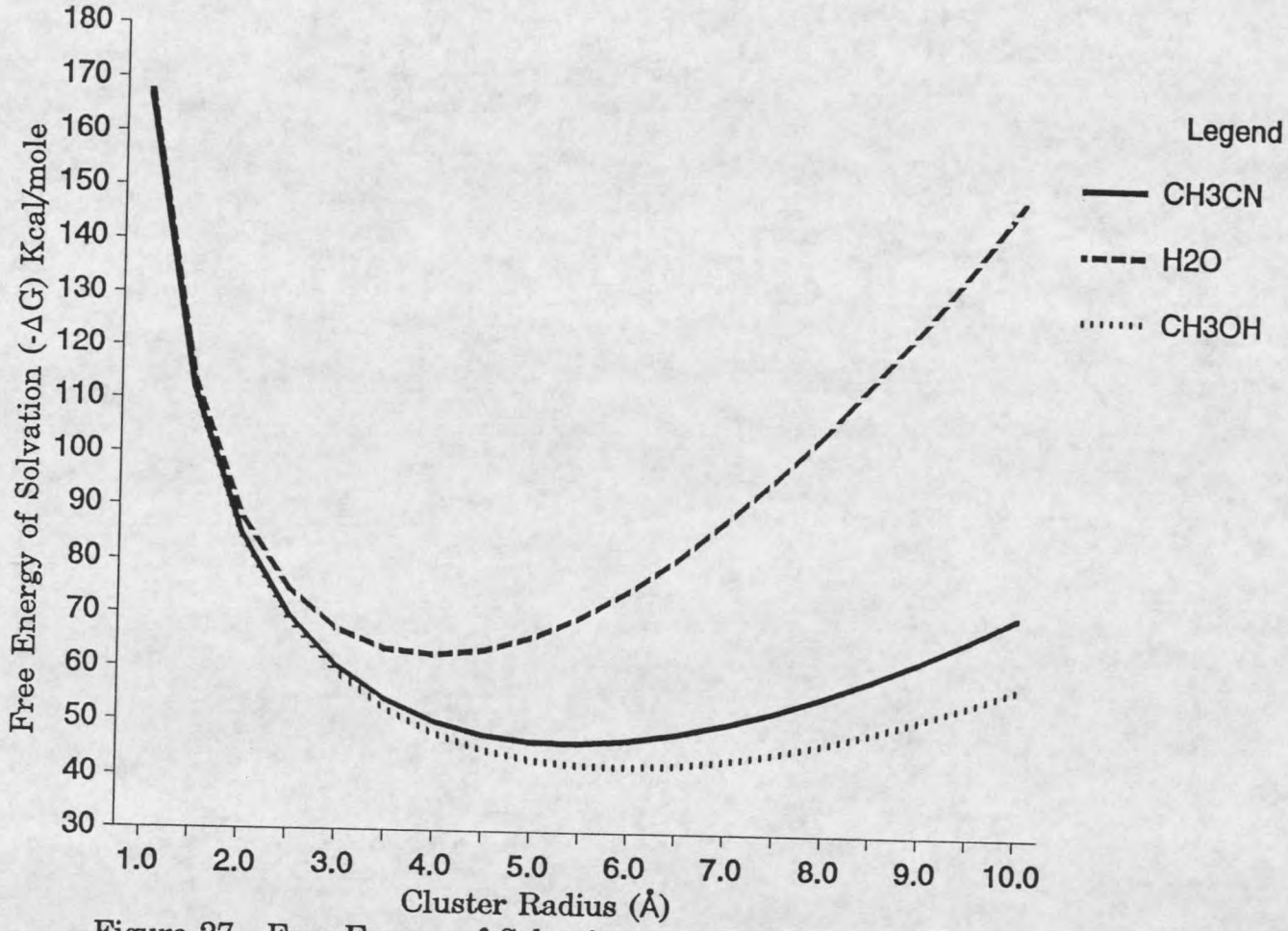


Figure 27. Free Energy of Solvation as a Function of Cluster Radius

lower than that for methanol. This plot shows the optimum cluster radius with water as the solvent as approximately 3.5 Å, with methanol 5.9 Å, and with acetonitrile approximately 5.5 Å. Of course this same radius that produces the minimum free energy of solvation can be determined by differentiating the Born equation with respect to the radius, setting the equation equal to zero and solving for the radius.

Rapid Method by Direct Injection

Standard curves were generated for the pesticides in methanol/water both individually and collectively and the various spikes within the analytical range of approximately 0.1 to 20 mg/ml were analyzed similarly. The concentration ranges of both the standards and spikes were high 10^{-6} M to low 10^{-5} M. Although an attempt was made to use a capillary/skimmer potential difference that maximized the $[M+H]^+$ ion there was some fragmentation observed in these compounds. The counts from the protonated analyte $[M+H]^+$ and all of the fragment ions were summed to get a total count representative of each compound.

The standard curves shown in Figures 134 - 138 in Appendix I show the regression coefficient for the standard curves for the individual pesticides ranged from 0.89 to 0.99. In each figure the spike is represented by a shaded square and the standard by an open square. For the collective standard shown in Figures 138 - 143 in Appendix I the regression coefficient for all curves was greater than 0.95. For the individual spikes this direct injection technique gives a fairly good agreement between the spike and the standard curve. However, this is not the case for most of the spikes done collectively

in the river water. Lack of agreement between the standard curve and the spike concentrations must be due to matrix effects in the river water that were not overcome by the addition of the acetic acid/ammonium acetate buffer. The river water mixed with methanol was analyzed by the electrospray ionization and found to contain no masses corresponding to any of the pesticides but showed a large peak at *m/z* of 60. Figure 28 shows the spectrum containing all of the pesticides spiked into the river water.

Sensitivity

Signals obtained from the use of two spray needle diameters varied dramatically. Table 11 shows the total ion current generated from most of the pesticides studied using both the 0.5 mm i.d. needle and the smaller i.d. needle.

It should be noted that the potential used on the 0.5 mm needle was generally on the order of 3.5 - 3.75 kilovolts while the potential on the smaller i.d. needle was on the order of 3.0 kilovolts. This decreased potential applied to the spray needle allowed a shorter distance between the spray needle and the transport capillary. The ratio of the signal using the two needles shows impressive gains in signal. This gain ranged from a factor of 2 to 800. By using a smaller needle that could be placed closer to the transport capillary, a larger volume of spray entered the transport capillary when using the 0.129 mm i.d. needle as compared to the 0.5 mm i.d. needle. Also, the droplets formed when using the smaller i.d. needle produced smaller droplets and therefore the desorption process is more efficient. These results are interesting in light of the fact that the smaller needle required a lower potential than the larger needle to produce a greater

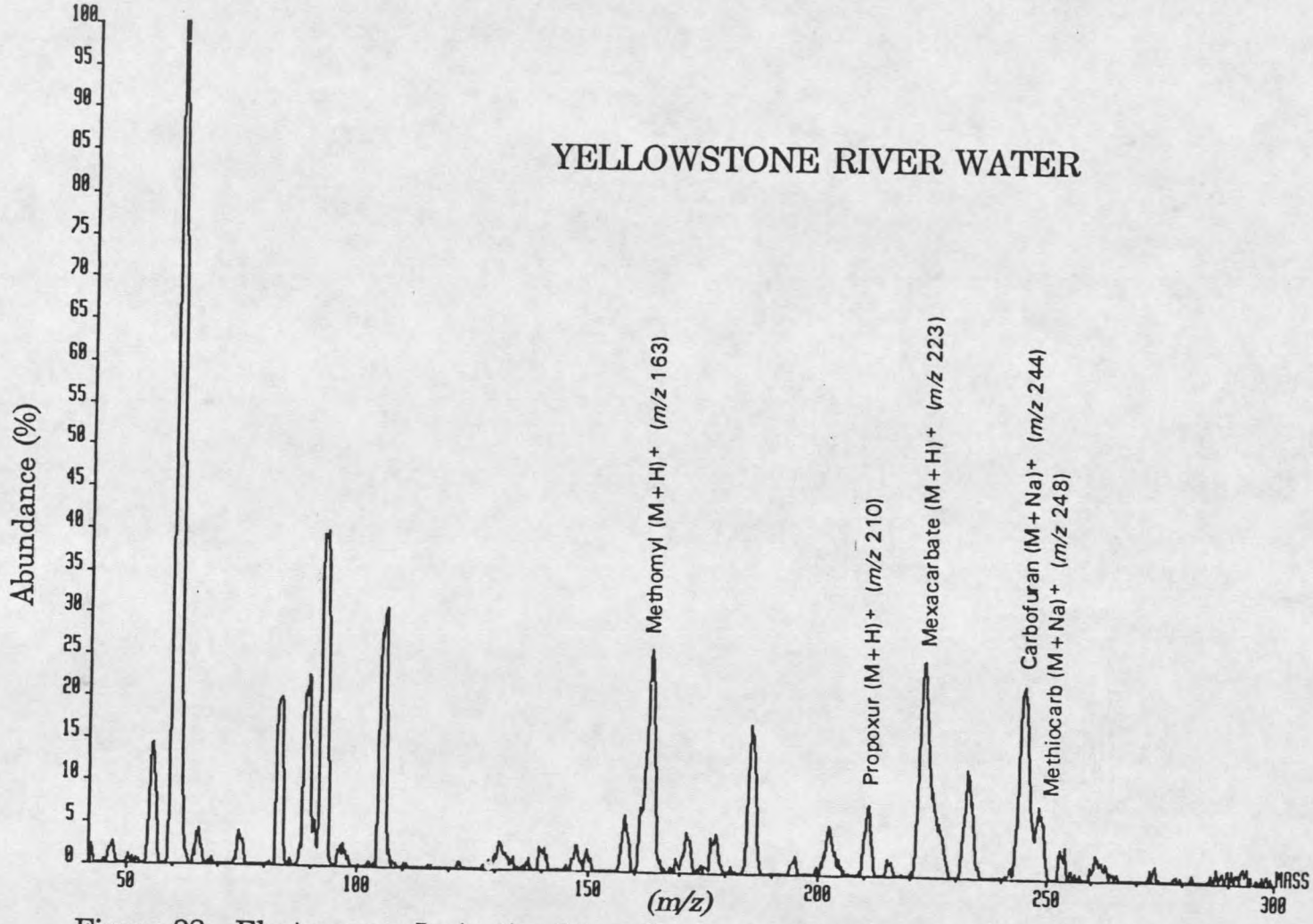


Figure 28. Electrospray Ionization Mass Spectrum of Yellowstone River Water Spiked with 5 Carbamate Pesticides.

total ion current.

Table 11. Total Ion Current as a Function Of Needle Diameter

Compound	TIC 0.5 mm i.d.	TIC 0.129 mm o.d./ 0.05 mm i.d.(Au)	Ratio
Amitrole	0.30×10^8	10×10^8	33
Antu	0.04×10^8	32×10^8	800
Carbaryl	0.40×10^8	26×10^8	65
Carbofuran	0.10×10^8	29×10^8	290
Chloramben	0.50×10^8	22×10^8	44
Chlorpyrifos	0.20×10^8	11×10^8	53
Coumafuryl	0.05×10^8	3×10^8	52
Diphacinone	0.06×10^8	12×10^8	200
Diquat Dibromide	0.30×10^8	33×10^8	110
Diuron	0.06×10^8	23×10^8	383
Endosulfan	0.07×10^8	34×10^8	486
Endothall	0.20×10^8	52×10^8	260
Ethion	33×10^8	436×10^8	13
Glyphosate	8×10^8	219×10^8	27
Mephosfolan	59×10^8	132×10^8	2
Methiocarb	0.07×10^8	38×10^8	543
Phosfolan	0.10×10^8	13×10^8	130
Propoxur	21×10^8	47×10^8	63
Rotenone	0.30×10^8	19×10^8	2
Siduron	0.09×10^8	50×10^8	556

Table 12 shows the sensitivity achieved on some of the pesticides. The picogram quantities are calculated based on the pesticide concentration, molecular weight, flow rate and scan time. All of the values in this table represent calculations based on a single full scan spectrum with the exception of the second entry for Propoxur which results from a single scan over the range of 200 - 220 amu that includes the protonated Propoxur quasi molecular ion. Lower sensitivities are easily achieved for the other pesticides

included in this study by simply scanning over a much narrower mass range, for example, over a 10 - 20 amu mass range.

Table 12. Sensitivity Study

Compound	Quantity (pg)	
Carbofuran	140	
Diquat Dibromide	23	
Endothall	24	
Methomyl	300	
Methiocarb	110	
Phosfolan	200	
Propoxur	10	
Propoxur	2	(200 -220 amu)
Siduron	100	

The sensitivities listed in this table are as good as if not better than those achievable on commercial electrospray ion sources.

CHAPTER 4

CONCLUSIONS

The purpose of this work was to make operational a home-built electrospray ionization source and to evaluate electrospray ionization mass spectrometry as an analytical tool for polar, thermally labile compounds of environmental significance such as pesticides and herbicides. The home-built ionization source rivals those on the commercial market. All of the pesticides/herbicides used in this work gave signals that suggest electrospray ionization should be coupled with micro high pressure liquid chromatography.

It was demonstrated that the degree of fragmentation in these pesticide samples can be controlled by simply varying the potential difference between the transport capillary and skimmer lens.

Analysis of the pesticide samples in the neat form at a pH of ~ 5.5 and at a pH of ~ 3.0 showed that addition of acid to the neat sample did not appreciably increase the protonated analyte signal nor the total ion current for any of the pesticides analyzed. This observation together with the extremely low pKa values of the pesticides, calculated by SPARC, indicates that the protonated analytes of these pesticides are formed in the gas phase rather than in the condensed phase. It should be noted that this is the first reporting of the possibility that electrospray ionization produces the protonated analyte

ions in the gas rather than the condensed phase.

Sodium and ammonium ions were added to these pesticide samples but in no case was the total ion current increased over that resulting from the neat sample.

Solvent studies showed that 50/50 mixtures of methanol/water and acetonitrile/water are suitable solvent systems but that a methanol fraction of 30% appears to be ideal for some of these pesticides.

It was demonstrated by spiking five carbamate pesticides into Yellowstone River water that ESI/MS by the direct injection method is a potential candidate as a rapid screening method for determining pesticides in natural waters.

Because of the success of this work the next step should involve combining high pressure liquid chromatography with electrospray ionization mass spectrometry to analyze natural water for pesticide contamination.

LITERATURE CITED

LITERATURE CITED

1. McEwen, F. L. and S. R. Stephenson, *The Use and Significance of Pesticides in the Environment*, John Wiley & Sons, New York, 1979.

2. Carson, Rachel, *Silent Spring*, Riverside Press, Cambridge, MA, 1972.

3. Anderson, J. L. and D. J. Chesney, *Anal. Chem.* 52, 2156 (1980).

4. Chesney, D. J., J. L. Anderson, D. E. Weisshaar and D. E. Tallman, *Anal. Chim. Acta* 124, 321 (1981).

5. Weisshaar, D. E., D. E. Tallman and J. L. Anderson, *Anal. Chem.* 53, 1809 (1981).

6. Caudill, W. L., J. O. Howell and R. M. Wrightman, *Anal. Chem.* 54, 2532 (1982).

7. Tallman, D. E. and D. E. Weisshaar, *J. Liq. Chromatogr.* 6, 2157 (1983).

8. Newman, A. R., *Anal. Chem.* 6, 861A (1989).

9. Branson, D. H. and M. Sweeney, *Reviews of Environmental Contamination and Toxicology*, Volume 120, Springer Verlag, New York, 1991.

10. Katz, F. W., P. H. Wood and D. P. Baltimore, *Reviews of Environmental Contamination and Toxicology*, Volume 120, Springer Verlag, New York, 1991.

11. Willoughby, R. C. and R. F. Browner, *Anal. Chem.* 56, 2626 (1984).

12. Blakely, C. R. and M. L. Vestal, *Anal. Chem.* 55, 750 (1983).

13. Zeleny, J., *Phys. Rev.* 10, 1 (1917).

14. Drozin, V. G., *J. Colloid Sci.* 10, 158 (1955).

15. Dole, M., L. L. Mach, R. L. Hines, R. C. Mobley, L. P. Ferguson and M. B. Alice, *J. Chem. Phys.* 49, 2240 (1968).

16. Mach, L. L., P. Kralek, A. Rheude and M. Dole, *J. Chem. Phys.* 52, 4977 (1970).

17. Clegg, G. A. and M. Dole, *Biopolymers* 10, 821 (1971).

18. Teer, D. and M. Dole, *J. Polym. Sci.* 13, 985 (1975).

19. Meng, C. K., M. Mann and J. B. Fenn, *Z. Physics* D10, 361 (1988).

20. Yamashita, M. and J. B. Fenn, *J. Phys. Chem.* 88, 4451 (1984).

21. Yamashita, M. and J. B. Fenn, *J. Phys. Chem.* 88, 4471 (1984).

22. Wong, S. F., C. K. Meng and J. B. Fenn, *J. Phys. Chem.* 92, 546 (1988).

23. Smith, R. D., J. A. Loo, C. G. Edmonds, C. J. Barinaga and H. R. Udseth, *Anal. Chem.* 62, 882 (1990).

24. Huang, E. C., T. Wachs, J. J. Conboy and J. D. Henion, *Anal. Chem.* 62, 713A (1990).

25. Alexandrov, M. L., L. N. Gall, M. V. Krasnov, V. I. Nickolaev and V. A. Shkurov, *Zh. Anal. Khim.* 40, 1570 (1985).

26. Whitehouse, C. M., R. N. Dryer, M. Yamashita and J. B. Fenn, *Anal. Chem.* 57, 675 (1985).

27. Winkler, P. C., D. D. Perkins, W. K. Williams, and R. F. Browner, *Anal. Chem.* 60, 489 (1988).

28. Behymer, T. D., T. A. Bellar, and W. L. Budde, *Anal. Chem.* 62, 1686 (1990).

29. Iribarne, J. V. and B. A. Thompson, *J. Chem. Phys.* 64, 2287 (1976).

30. Rollgen, F. W., E. Bramer-Weger and L. Butering, *J. Phys.* (Paris) 48, C6-253 (1987).

31. Schmelgeisen-Redeker, G., L. Butering and F. W. Rollgen, *Int. J. Mass Spectrom. Ion Processes* 90, 139 (1989).

32. Mann, M., *Org. Mass Spectrom.* 25, 575 (1990).

33. Bruins, A. P., *Mass Spectrom. Rev.* 10, 53 (1991).

34. Loo, J. A., H. R. Udseth and R. D. Smith, *Rapid Commun. Mass Spectrom.* 2, 207 (1988).

35. Mann, M., C. K. Meng and J. B Fenn, *Anal. Chem.* 61, 1702 (1989).

36. Allen, M. H. and H. S. Lewis, *Rapid Commun. Mass Spectrom.* 3, 255 (1989).

37. Meng, C. K., C. N. McEwen and B. S. Larsen, *Rapid Commun. Mass Spectrom.* 4, 147 (1990).

38. McLuckey, S. A., G. J. VanBerkel, G. L. Glish, E. C. Huang and J. D. Henion, *Anal. Chem.* 63, 375 (1991).

39. Preliminary Data Summary for the Pesticide Chemicals Point Source Category, United States Environmental Protection Agency, Office of Water Regulations and Standards, EPA 440/1-89/060-e, August 1989.

40. 1988 List of Lists, U. S. Environmental Protection Agency, Industrial Technology Division, Washington, D. C., 1988.

41. Bruins, A. P., T. R. Covey and J. D. Henion, *Anal. Chem.* 59, 2642 (1987).

42. Vergele, M., C. Dewaele and M. DeWeerdt, *LC-GC* 6, 966 (1986).

43. Potter, K. and J. Tehrani, *LC-GC* 8, 862 (1990).

44. Dahl, D. A. and J. E. Delmore, *PC/PS2 SIMION Version 4.0*, Idaho Nuclear Engineering Laboratory, EG&G Idaho; Idaho Falls, ID (1990).

45. Dushman, S., *Scientific Foundations of Vacuum Technology*, J. M. Lafferty, Editor, John Wiley and Sons, New York, 1962.

46. Pleasance, S., J. F. Anacleto, M. R. Bailey and D. H. North, *J. Am. Soc. Mass Spectrom.* 3, 378 (1992).

47. Doerge, D. R. and S. Bajic, *Rapid Commun. Mass Spectrom.* 6, 663 (1992).

48. Blades, A. T., M. G. Ikonomou and P. Kebarle, *Anal. Chem.* 63, 2109 (1991).

49. VanBerkel, G. J., S. A. McLuckey and G. L. Glish, *Anal. Chem.* 64, 1586 (1992).

50. Karickhoff, S. W., V. K. McDaniel, C. Melton, A. N. Vellino, D. E. Nute and L. A. Carreira, *Environmental Toxicology and Chemistry* 10, 1405 (1991).

51. Anderson, E., G. D. Veith and D. Weininger, *USEPA EPA/600/M-87-021*, Duluth, MN (1987).

52. Weininger, D., *J. Chem. Inf. Comput. Sci.* 28, 31 (1988).

53. Voyksner, R. D. and T. Pack, *Rapid Commun. in Mass Spectrom.* 5, 263 (1991).

54. Ikonomou, M. G., A. T. Blades and P. Kebarle, *Anal. Chem.* 63, 1989 (1991).

APPENDICES

APPENDIX A

PESTICIDE REFERENCE SPECTRA

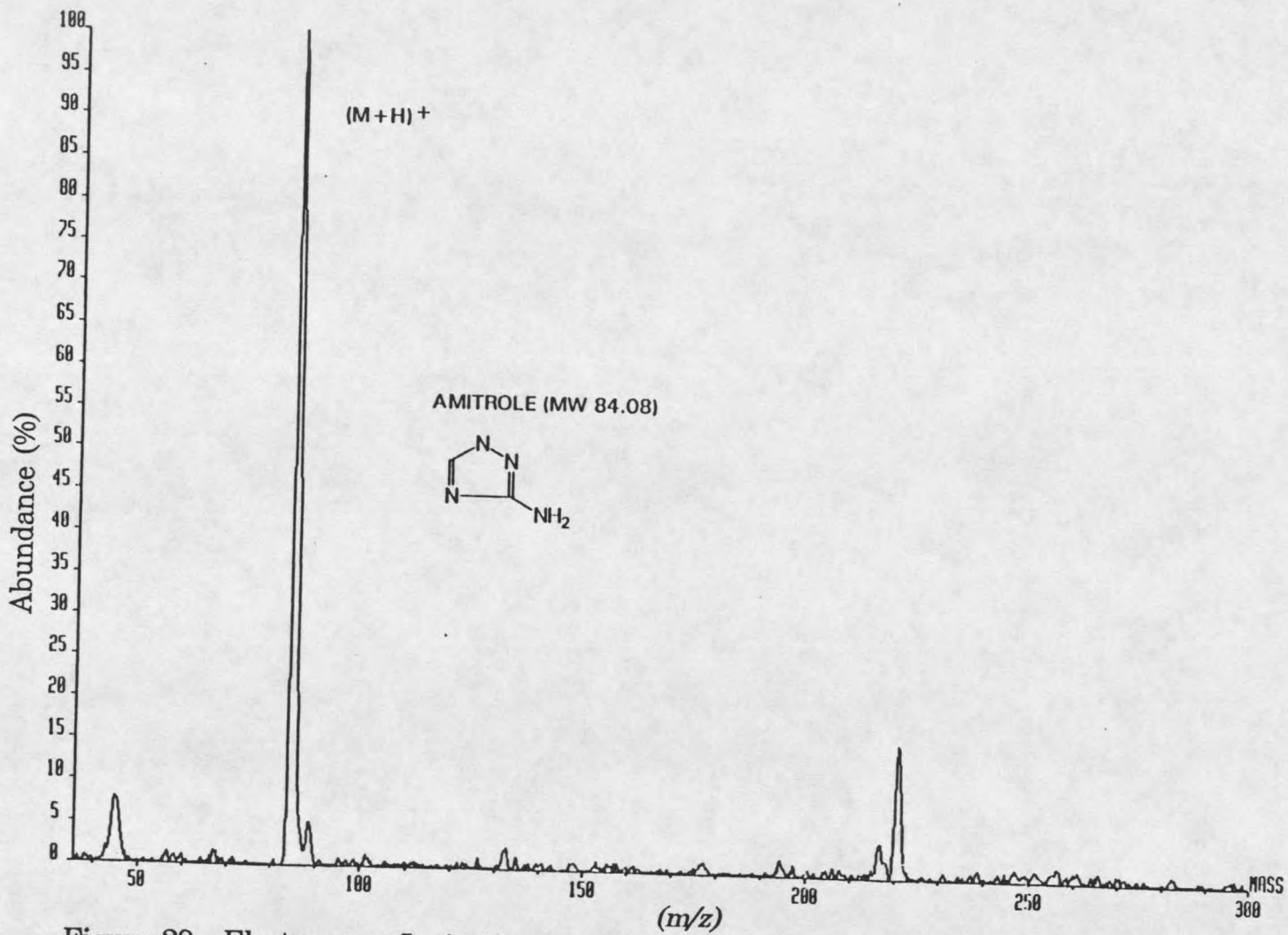


Figure 29. Electrospray Ionization Mass Spectrum of Amitrole. P. D. 75 Volts.

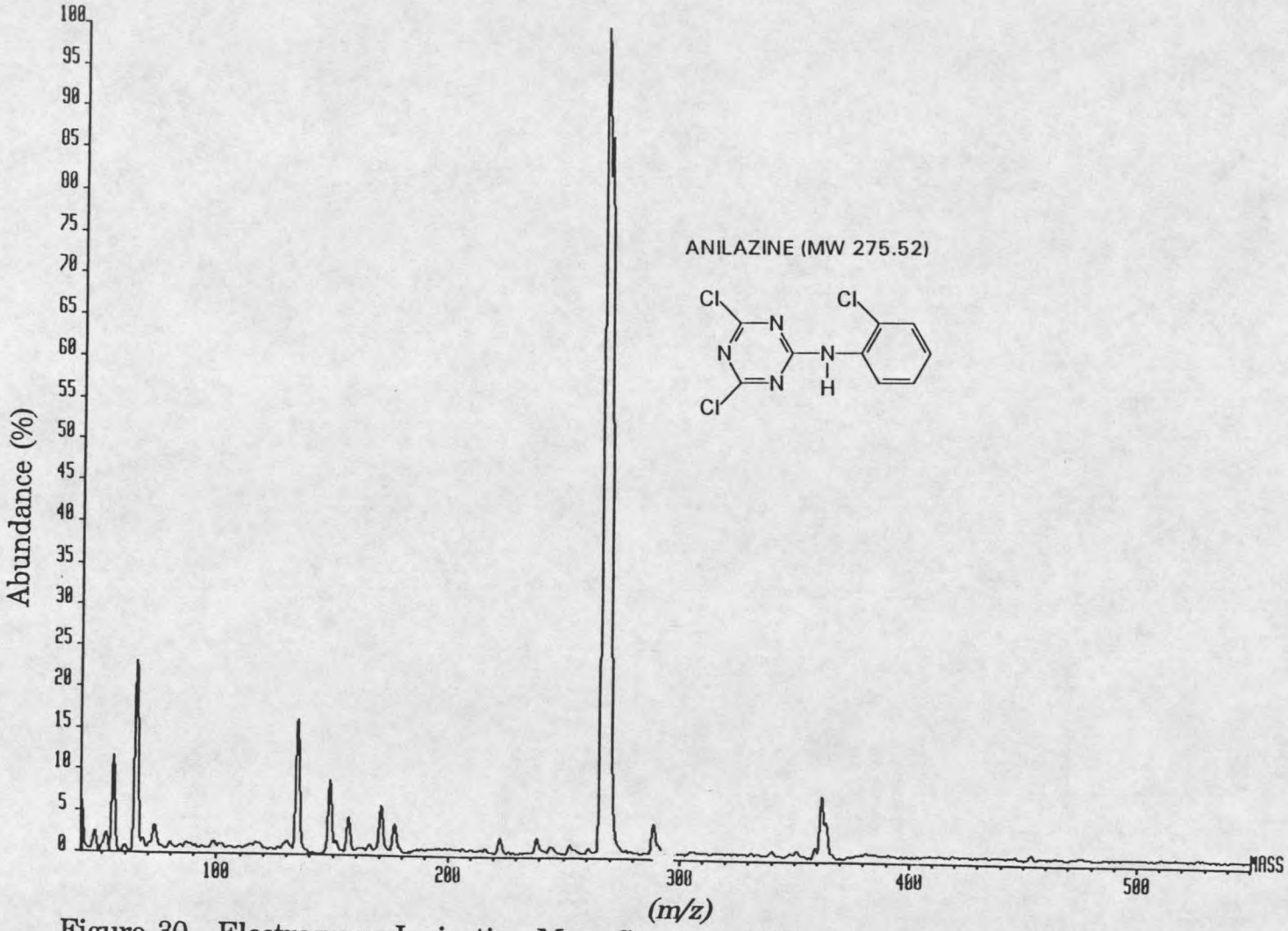


Figure 30. Electrospray Ionization Mass Spectrum of Anilazine. P. D. 65 Volts.

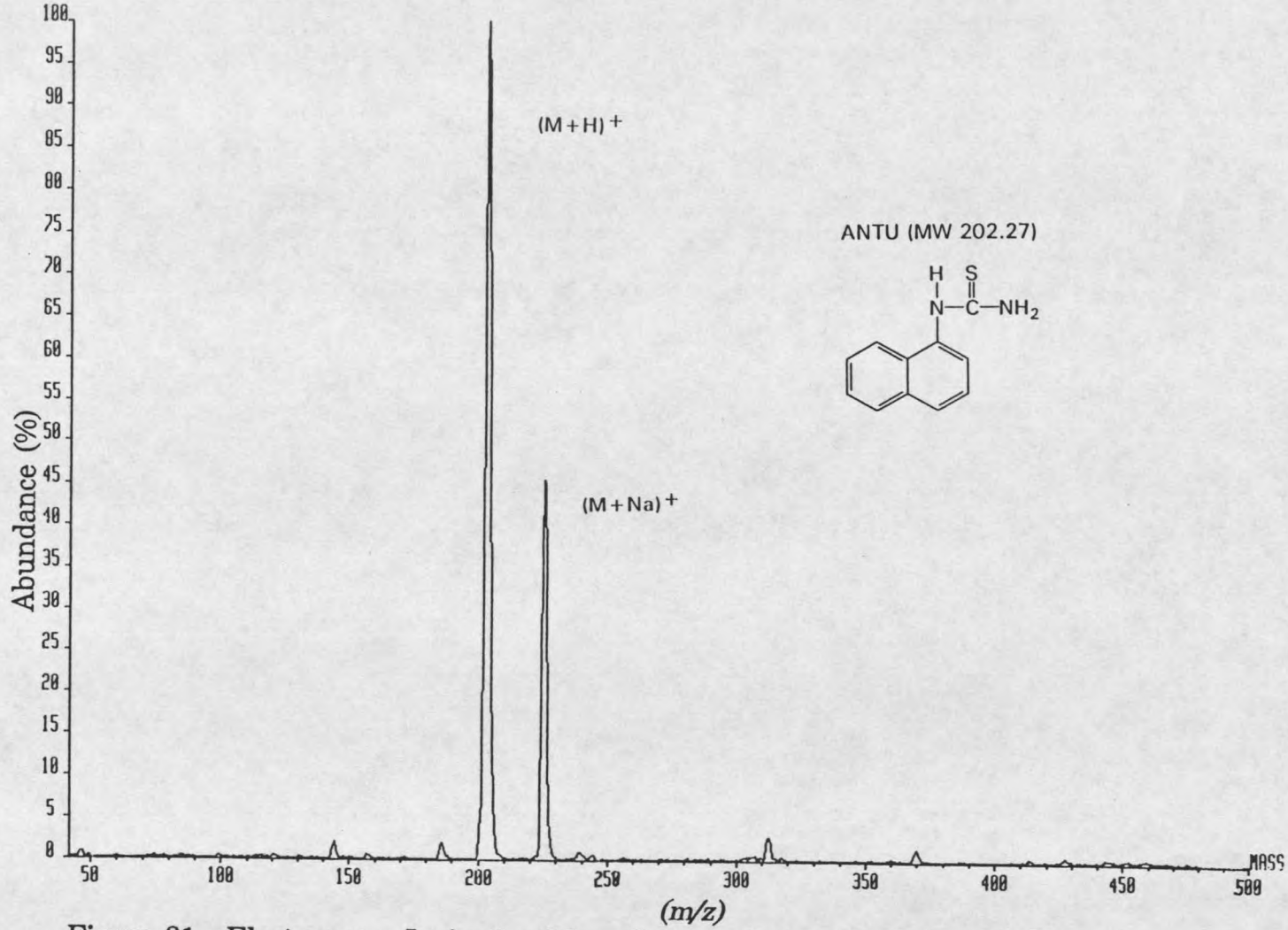


Figure 31. Electrospray Ionization Mass Spectrum of Antu. P. D. 65 Volts.

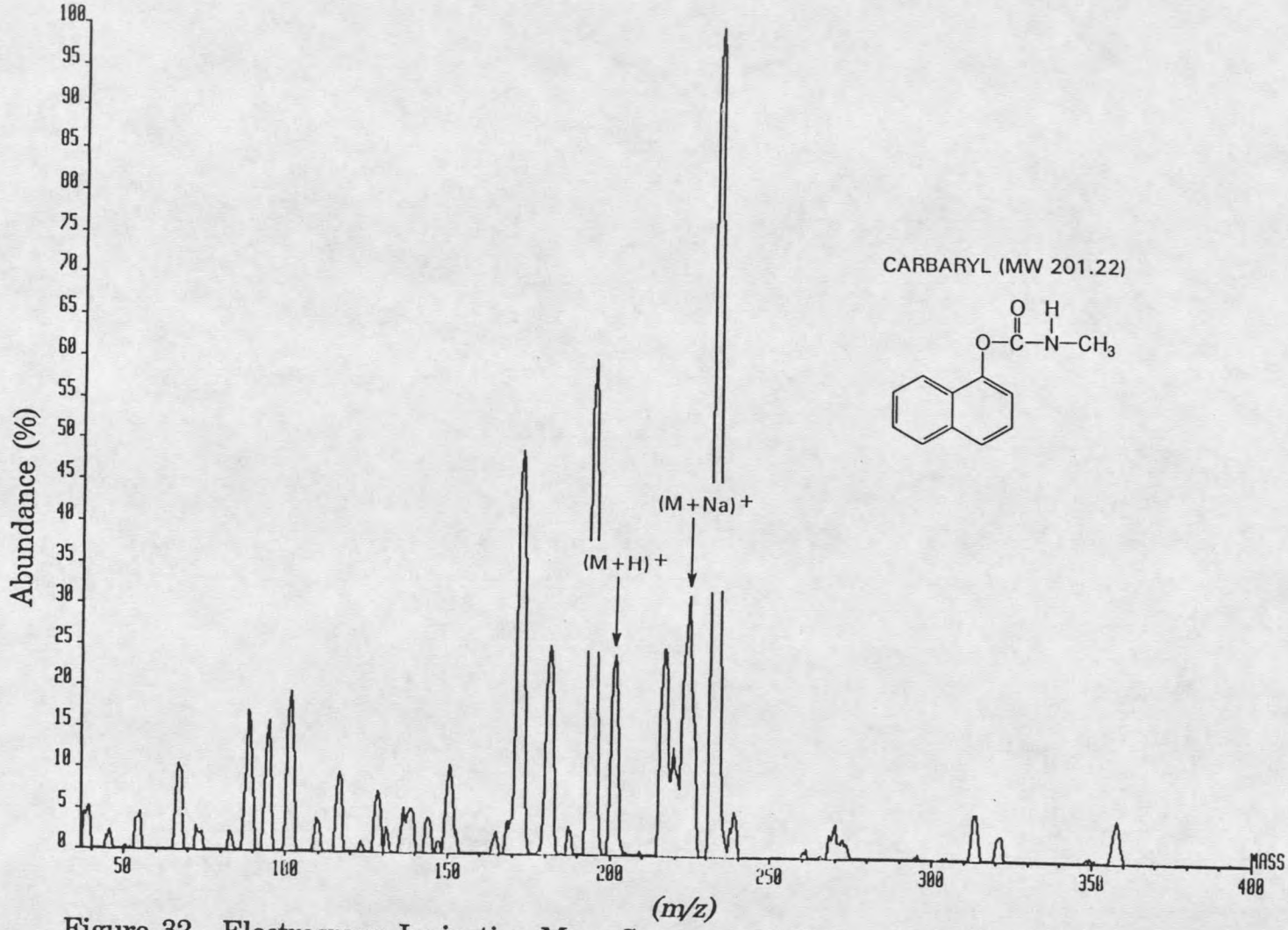


Figure 32. Electrospray Ionization Mass Spectrum of Carbaryl. P. D. 55 Volts.

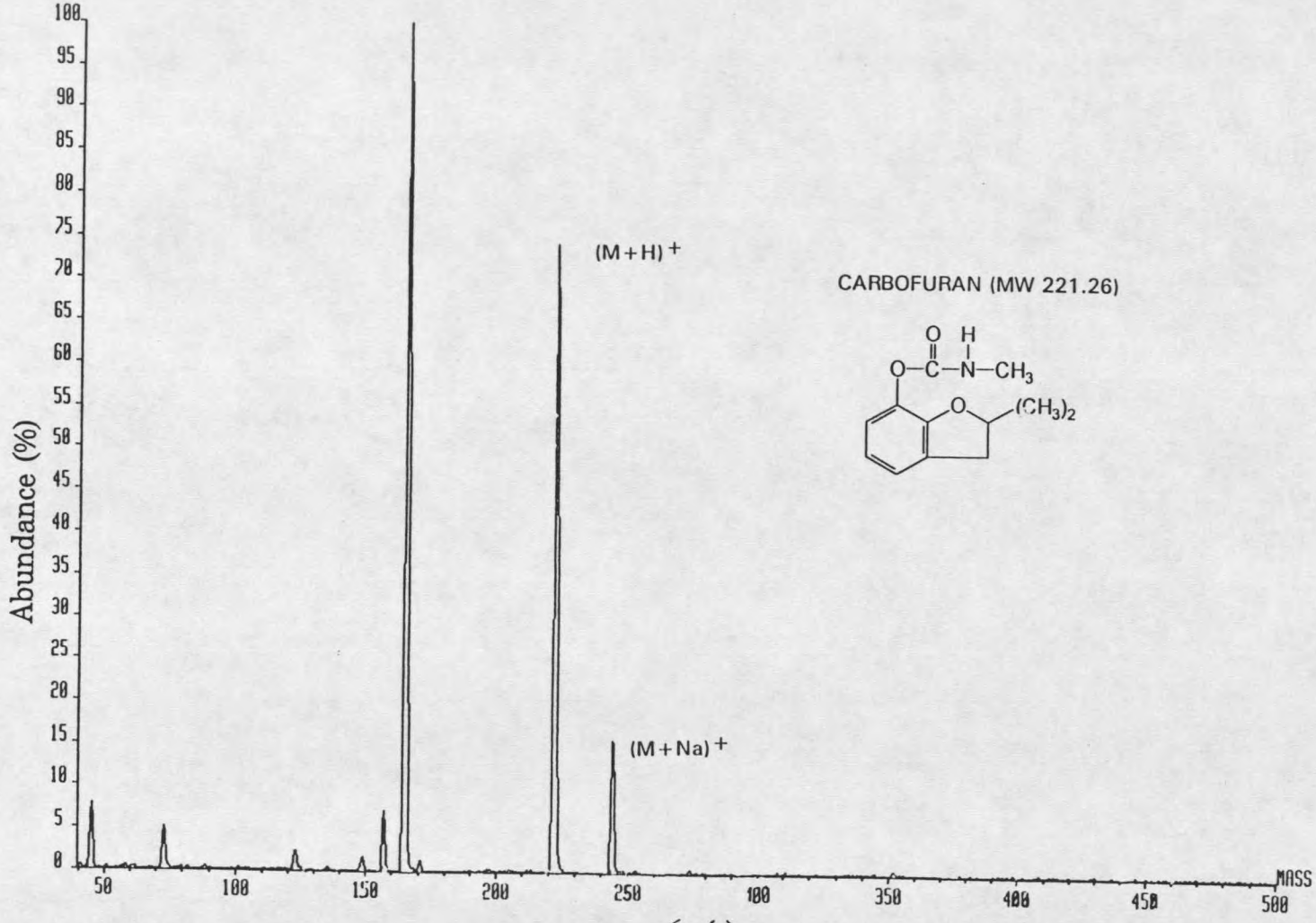


Figure 33. Electrospray Ionization Mass Spectrum of Carbofuran. P. D. 75 Volts.

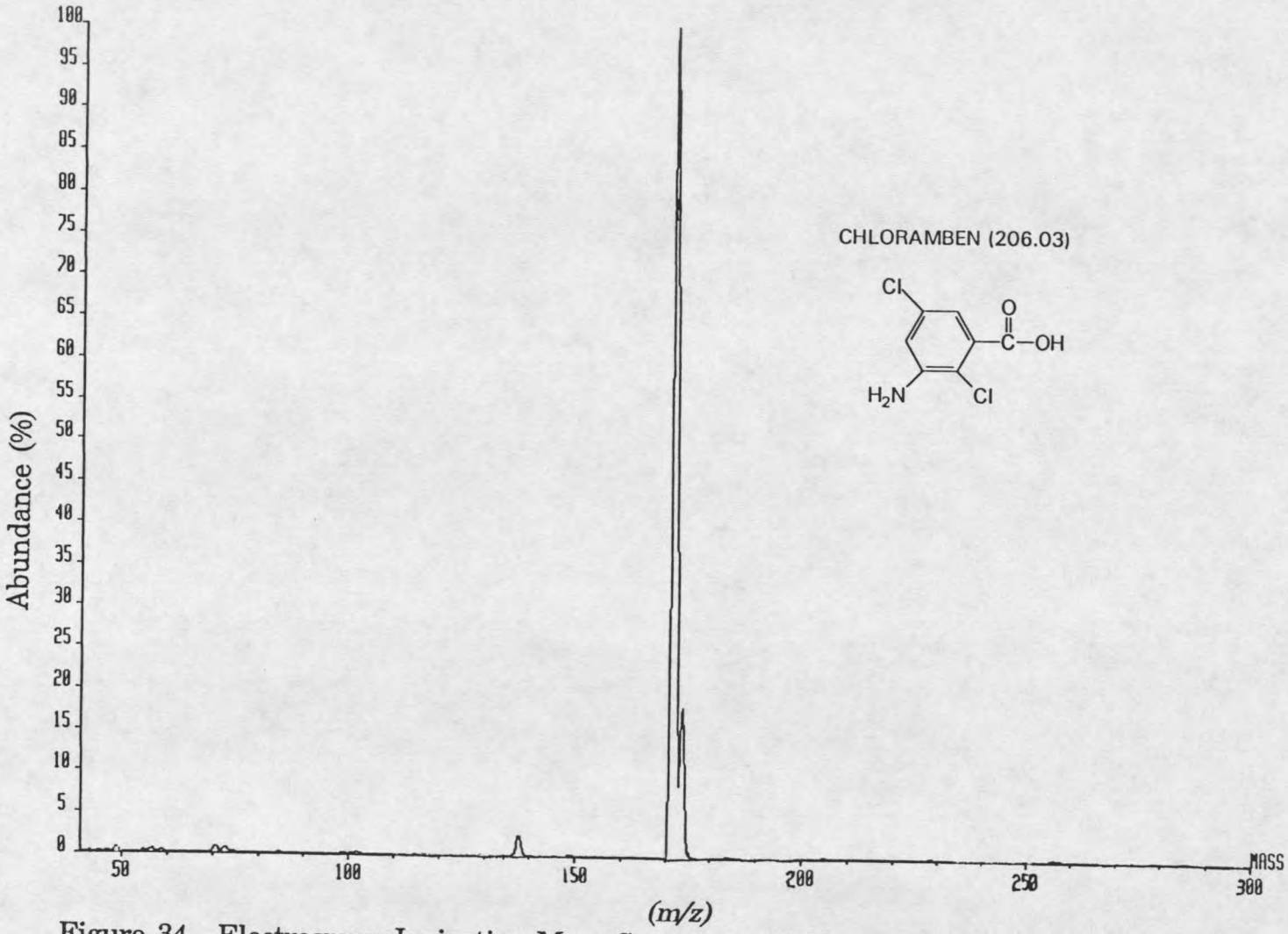


Figure 34. Electrospray Ionization Mass Spectrum of Chloramben. P. D. 75 Volts.

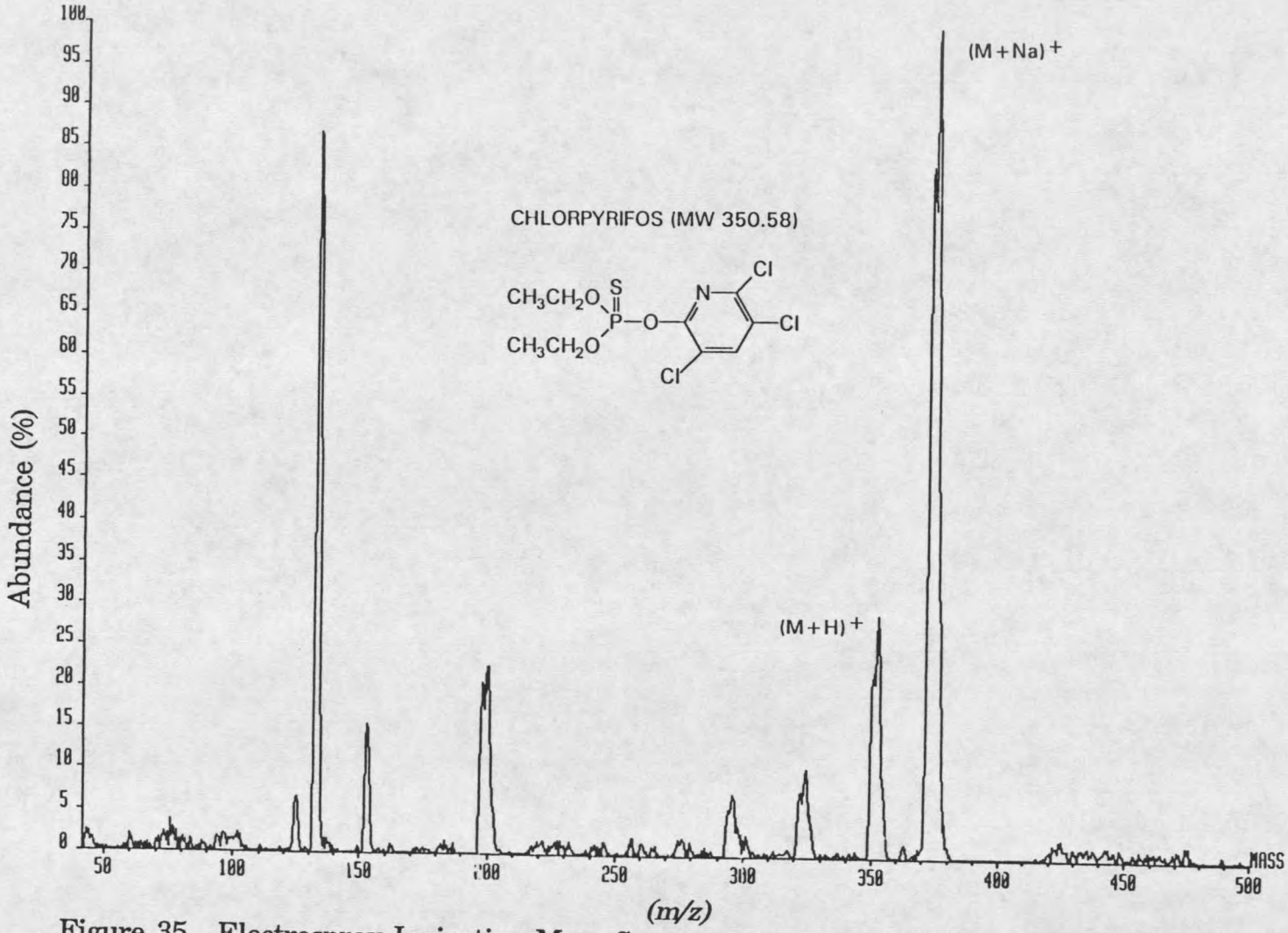


Figure 35. Electrospray Ionization Mass Spectrum of Chlorpyrifos. P. D. 75 Volts.

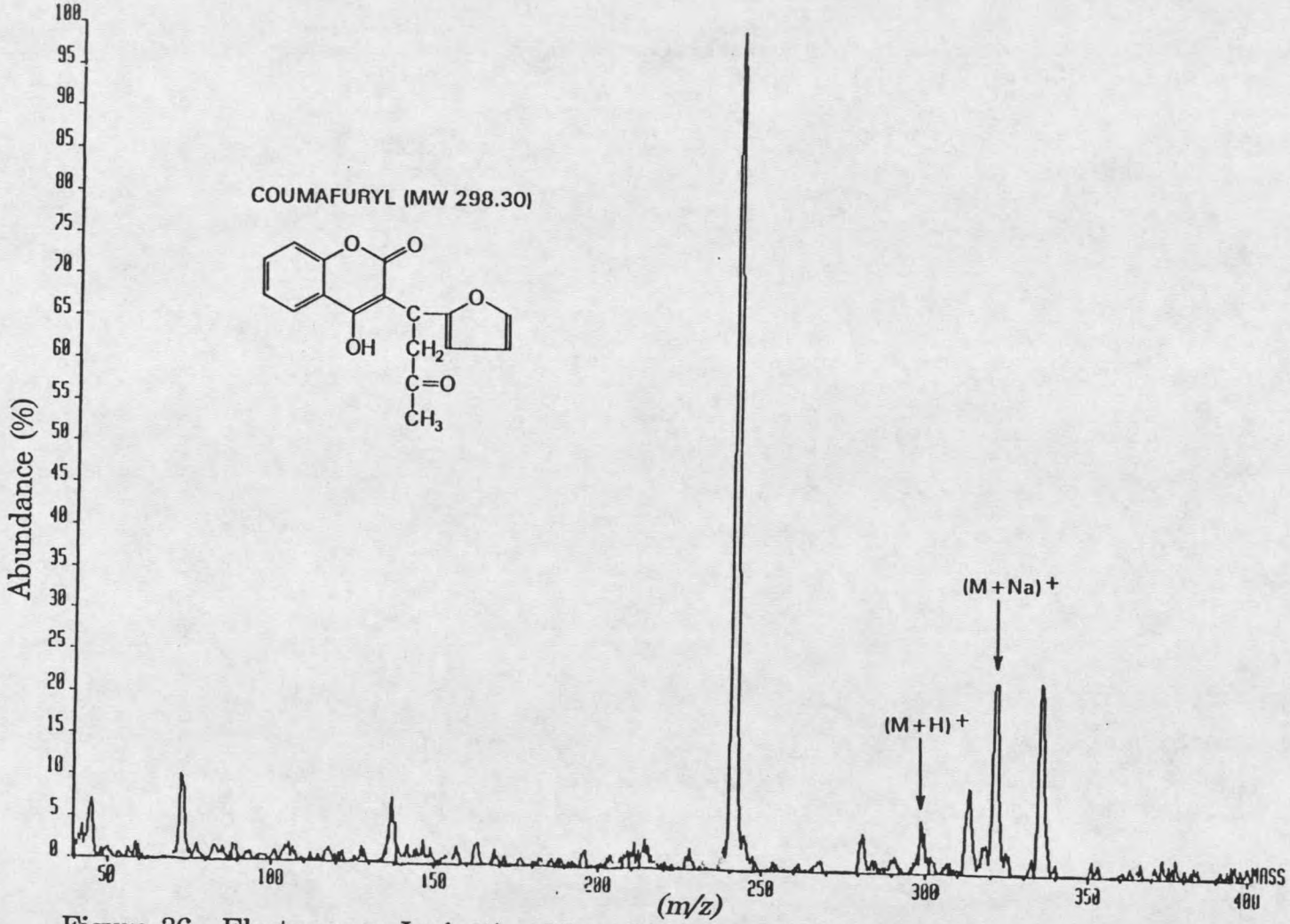


Figure 36. Electrospray Ionization Mass Spectrum of Coumafuryl. P. D. 75 Volts.

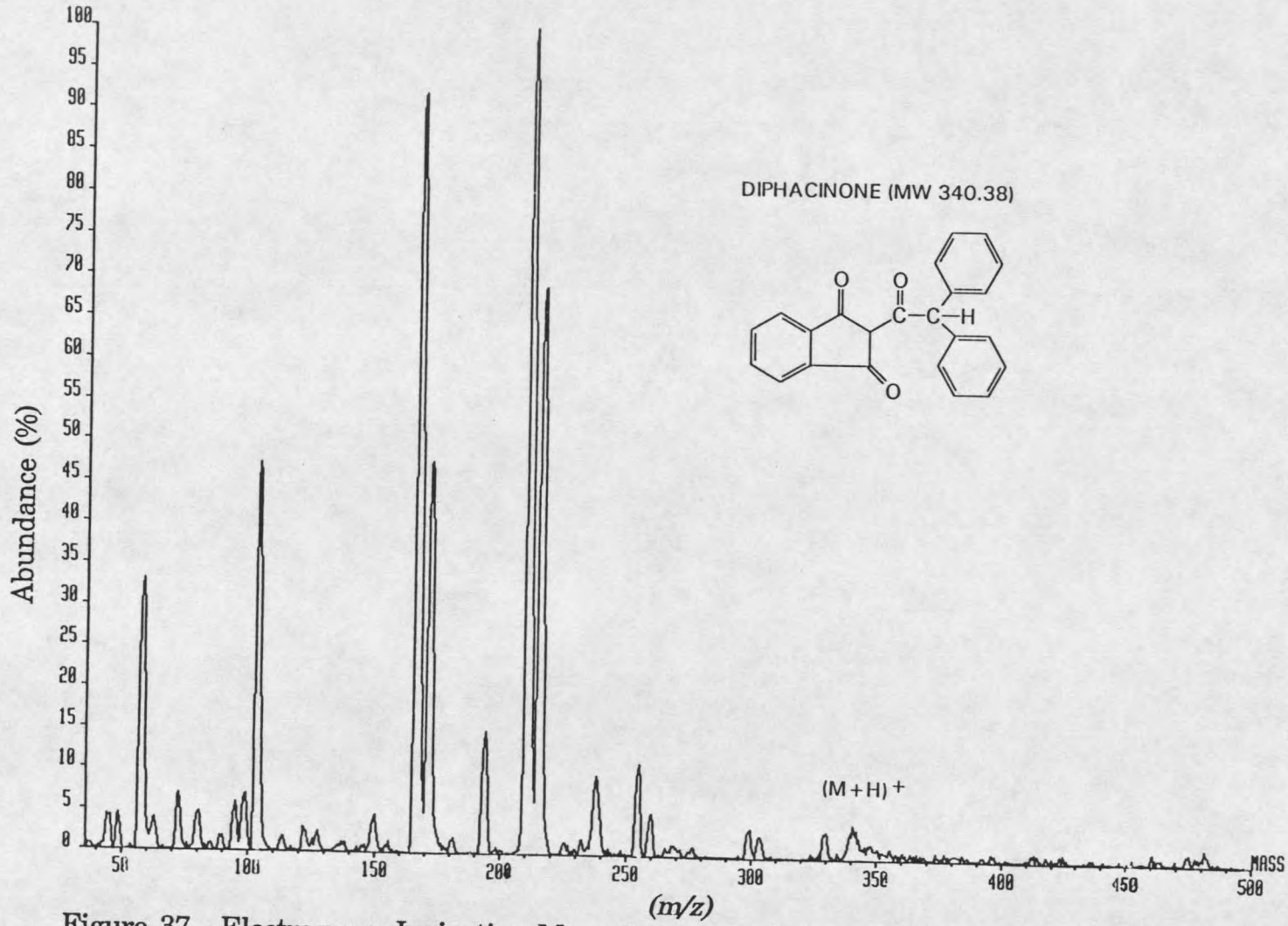


Figure 37. Electrospray Ionization Mass Spectrum of Diphacinone. P. D. 45 Volts.

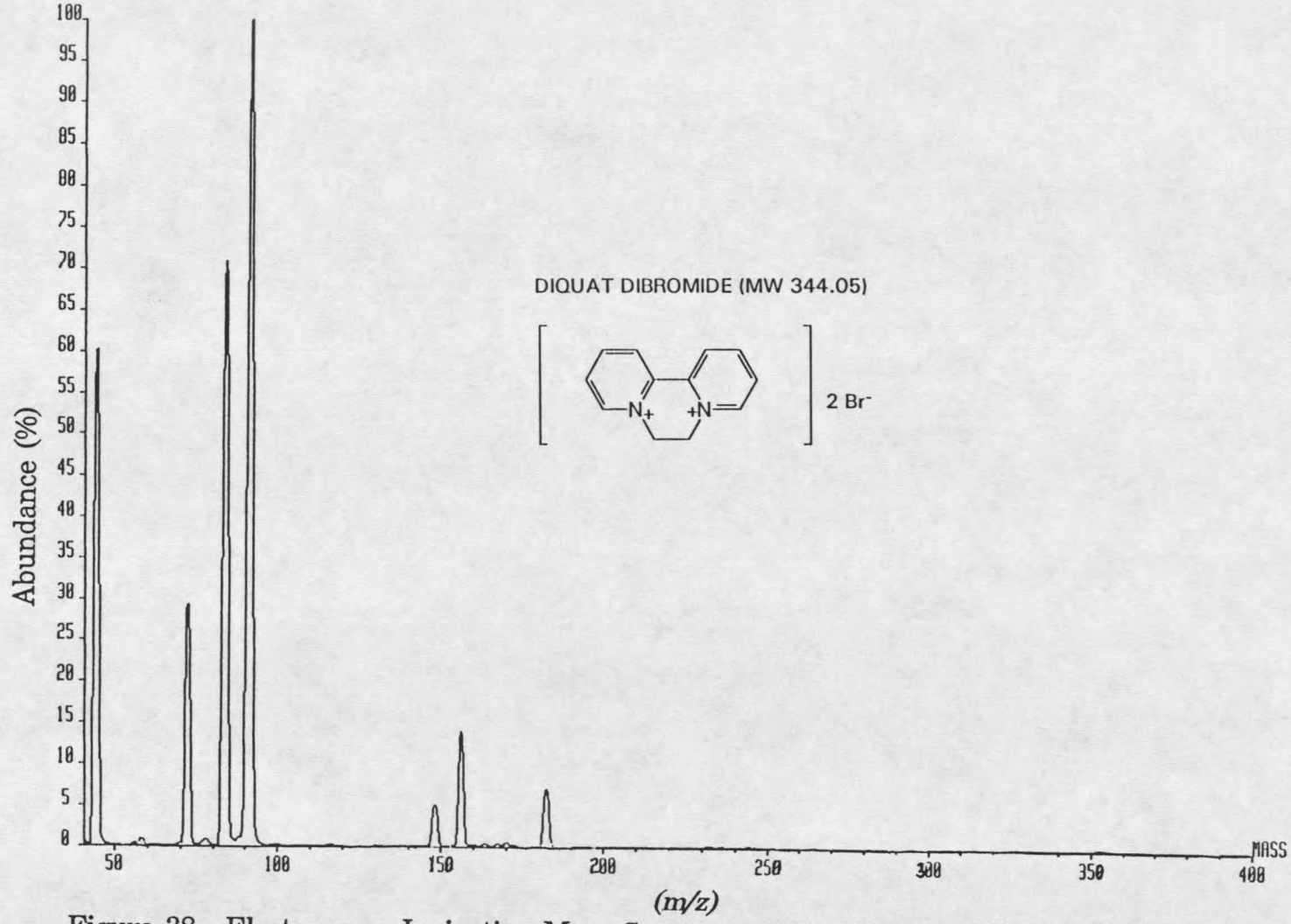


Figure 38. Electrospray Ionization Mass Spectrum of Diquat Dibromide. P. D. 75 Volts.

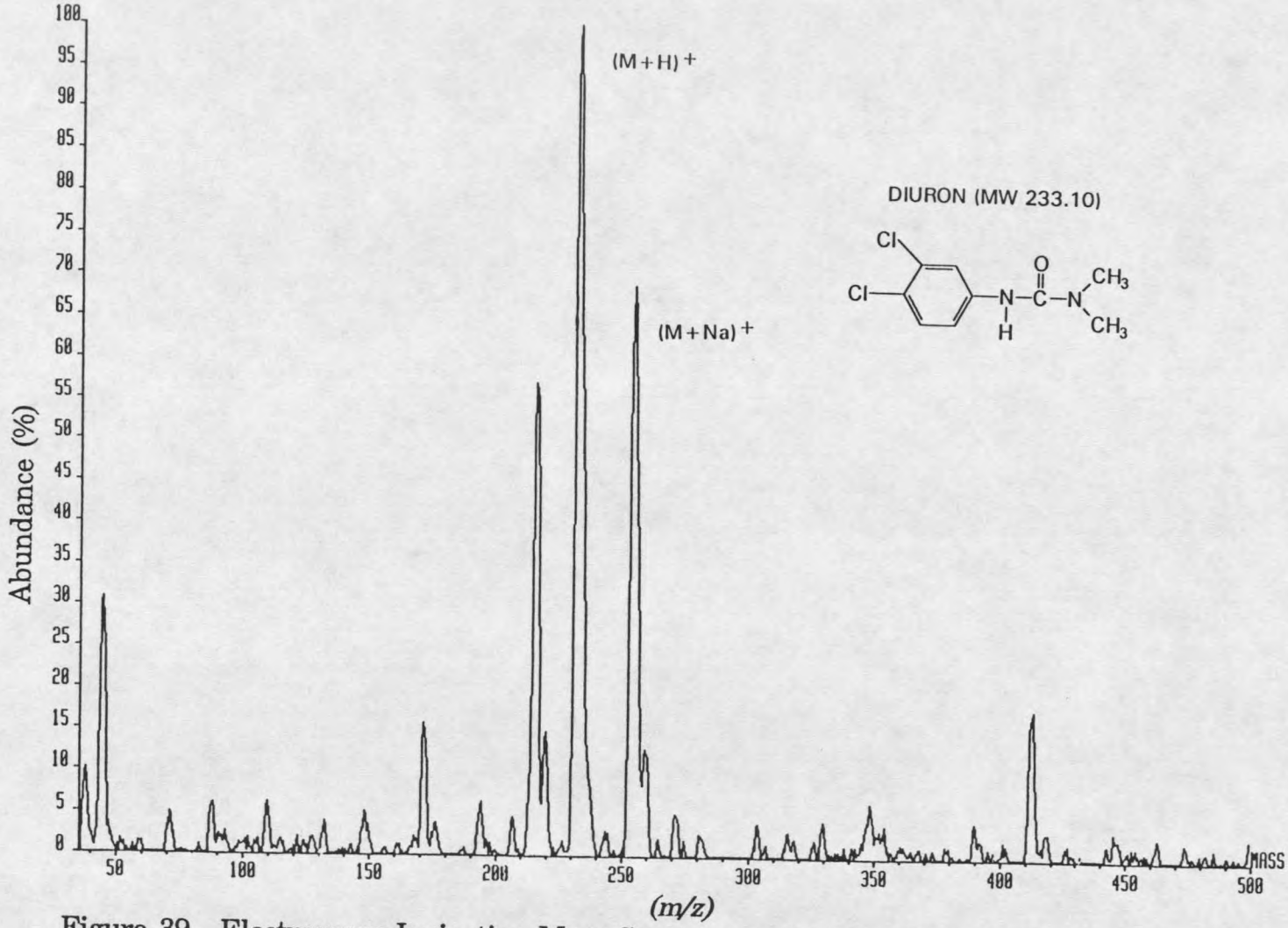


Figure 39. Electrospray Ionization Mass Spectrum of Diuron. P. D. 55 Volts.

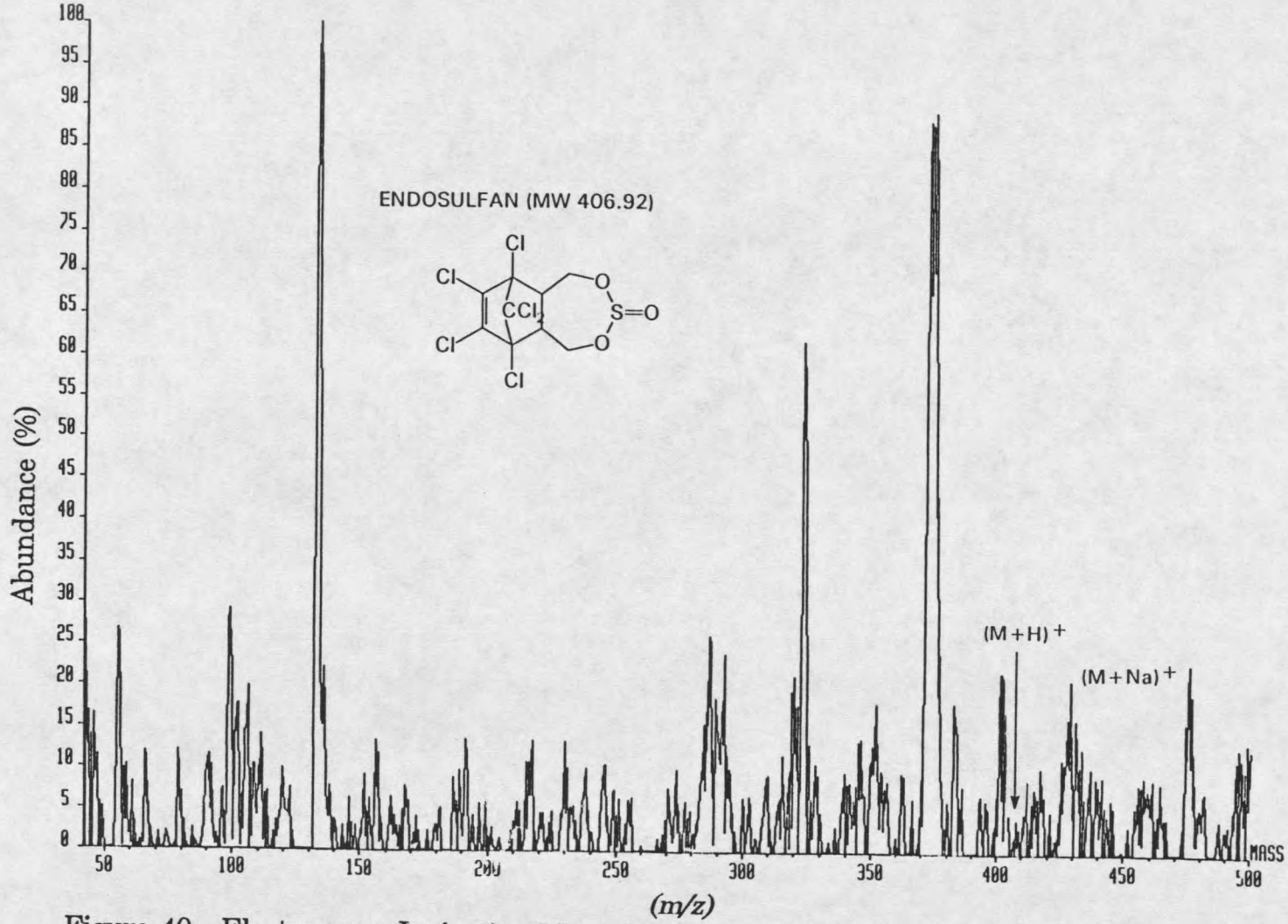


Figure 40. Electrospray Ionization Mass Spectrum of Endosulfan. P. D. 55 Volts.

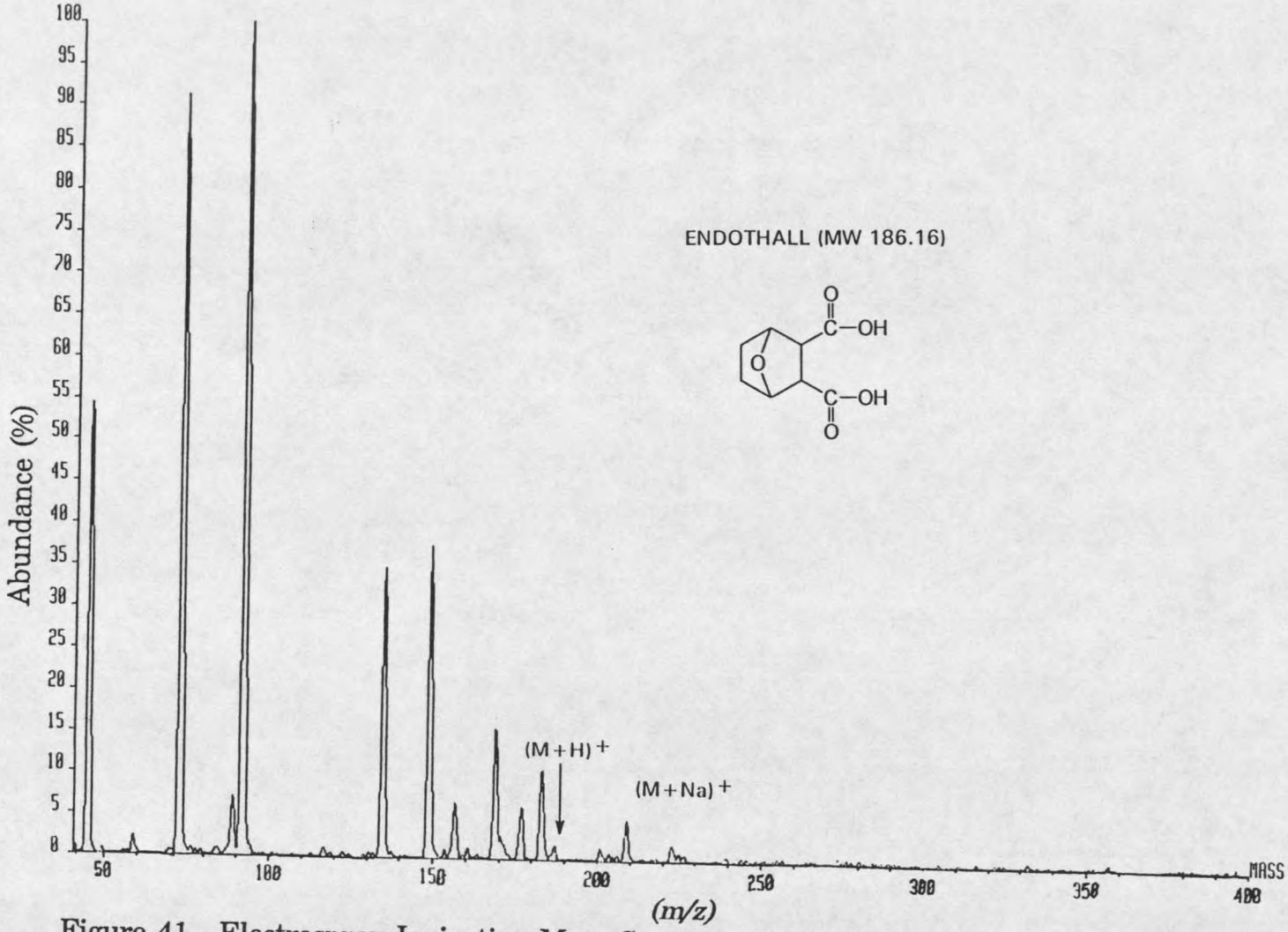


Figure 41. Electrospray Ionization Mass Spectrum of Endothall. P. D. 65 Volts.

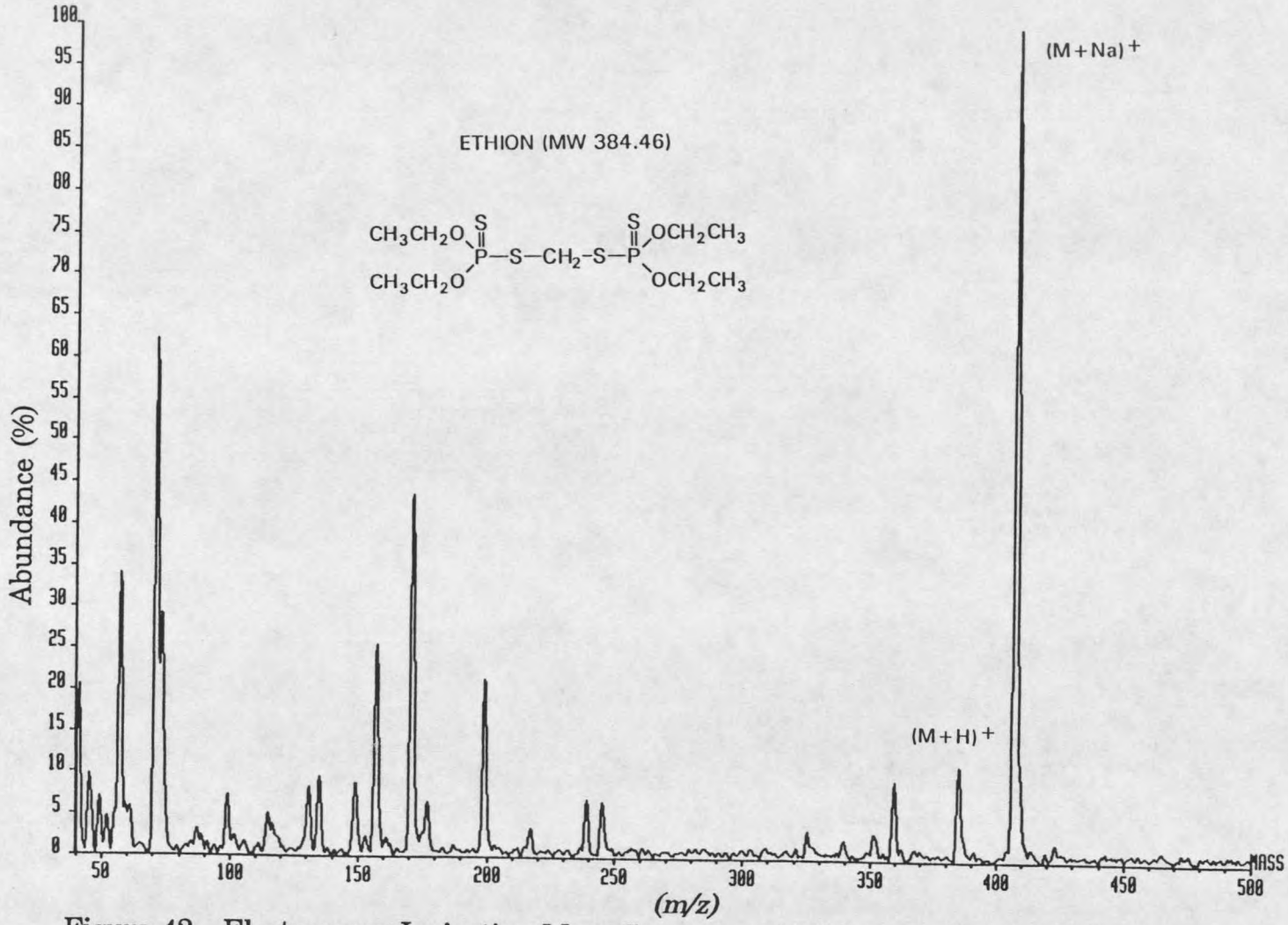


Figure 42. Electrospray Ionization Mass Spectrum of Ethion. P. D. 75 Volts.

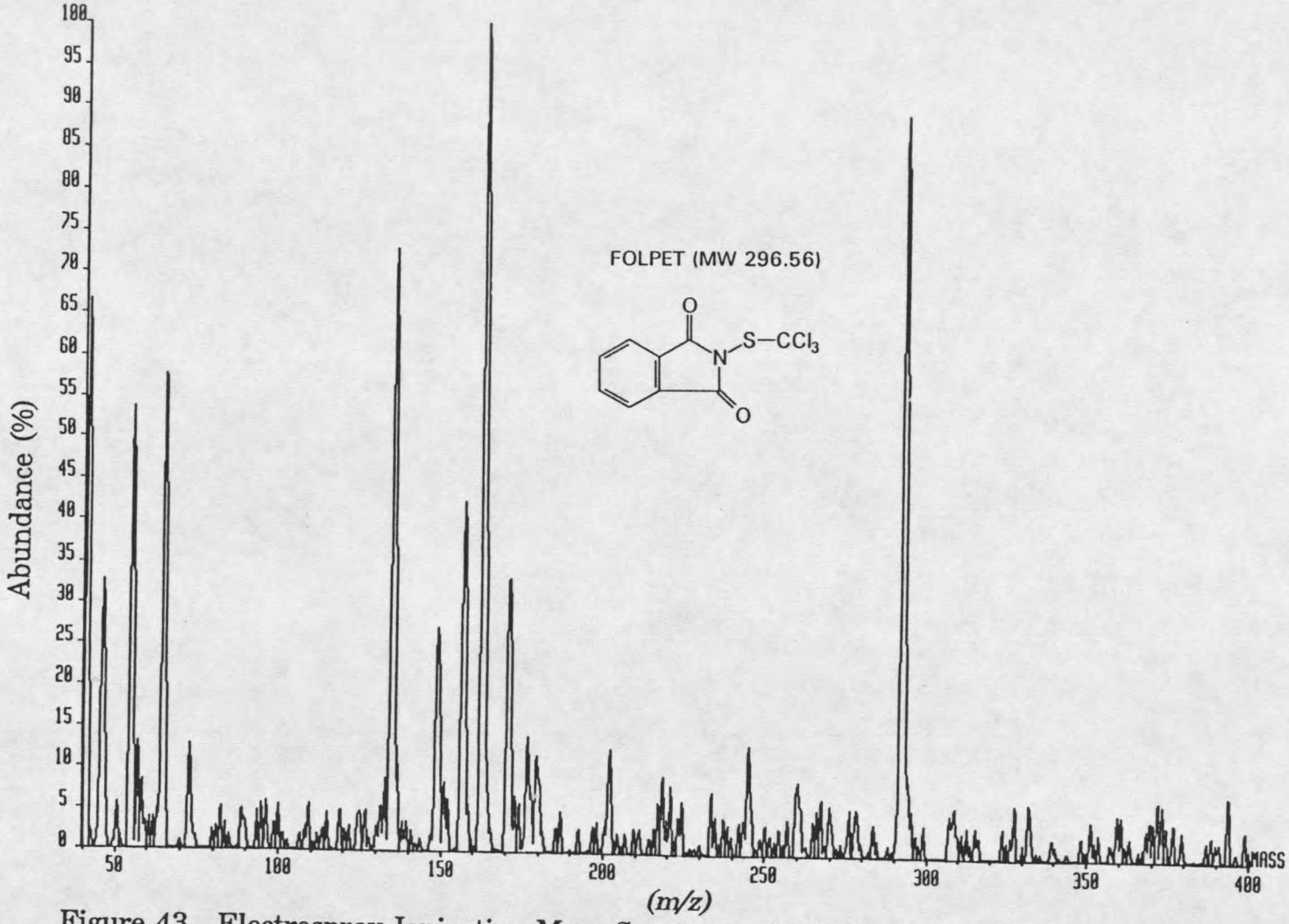


Figure 43. Electrospray Ionization Mass Spectrum of Folpet. P. D. 65 Volts.

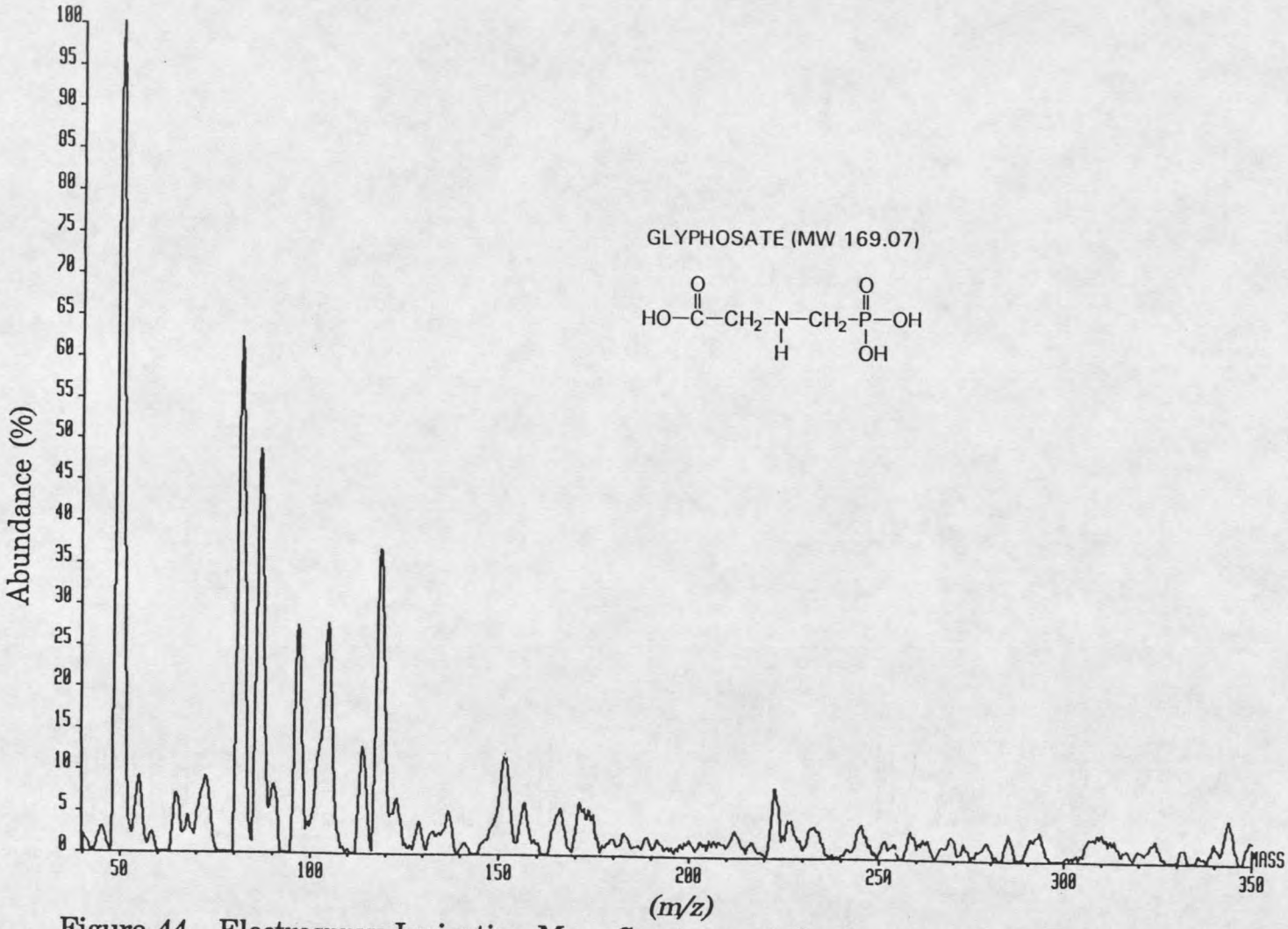


Figure 44. Electrospray Ionization Mass Spectrum of Glyphosate. P. D. 35 Volts.

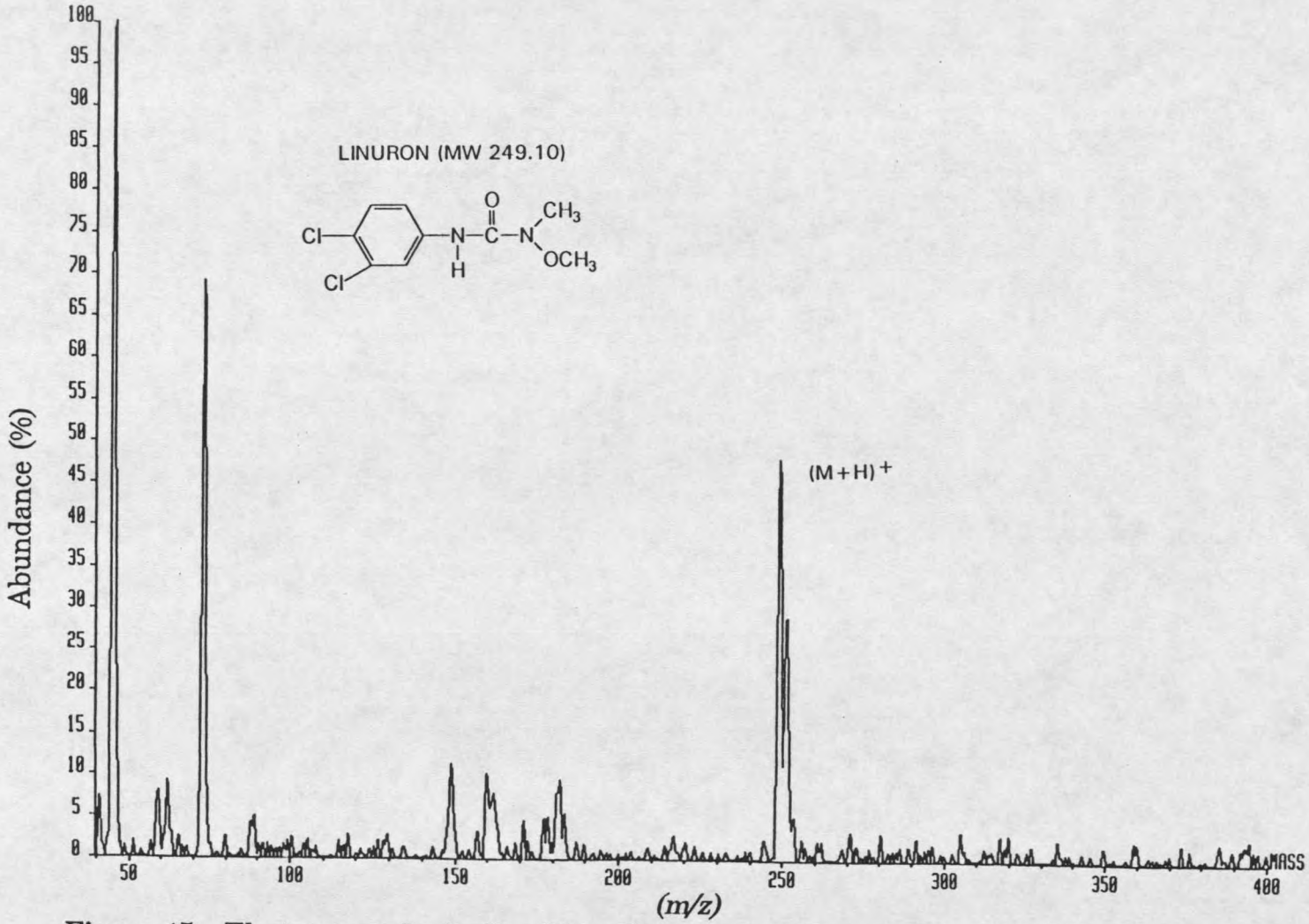


Figure 45. Electrospray Ionization Mass Spectrum of Linuron. P. D. 85 Volts.

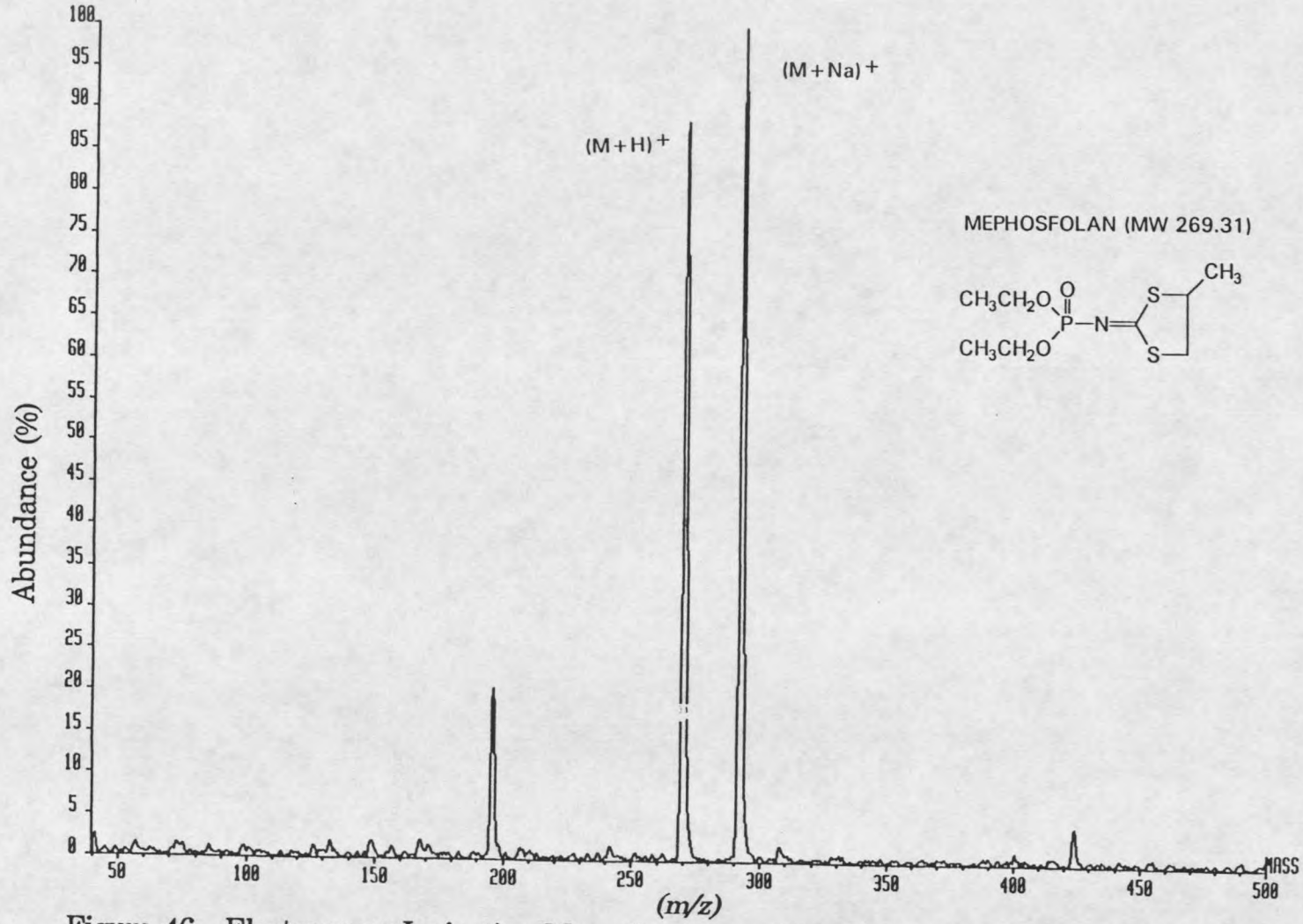


Figure 46. Electrospray Ionization Mass Spectrum of Mephosfolan. P. D. 85 Volts.

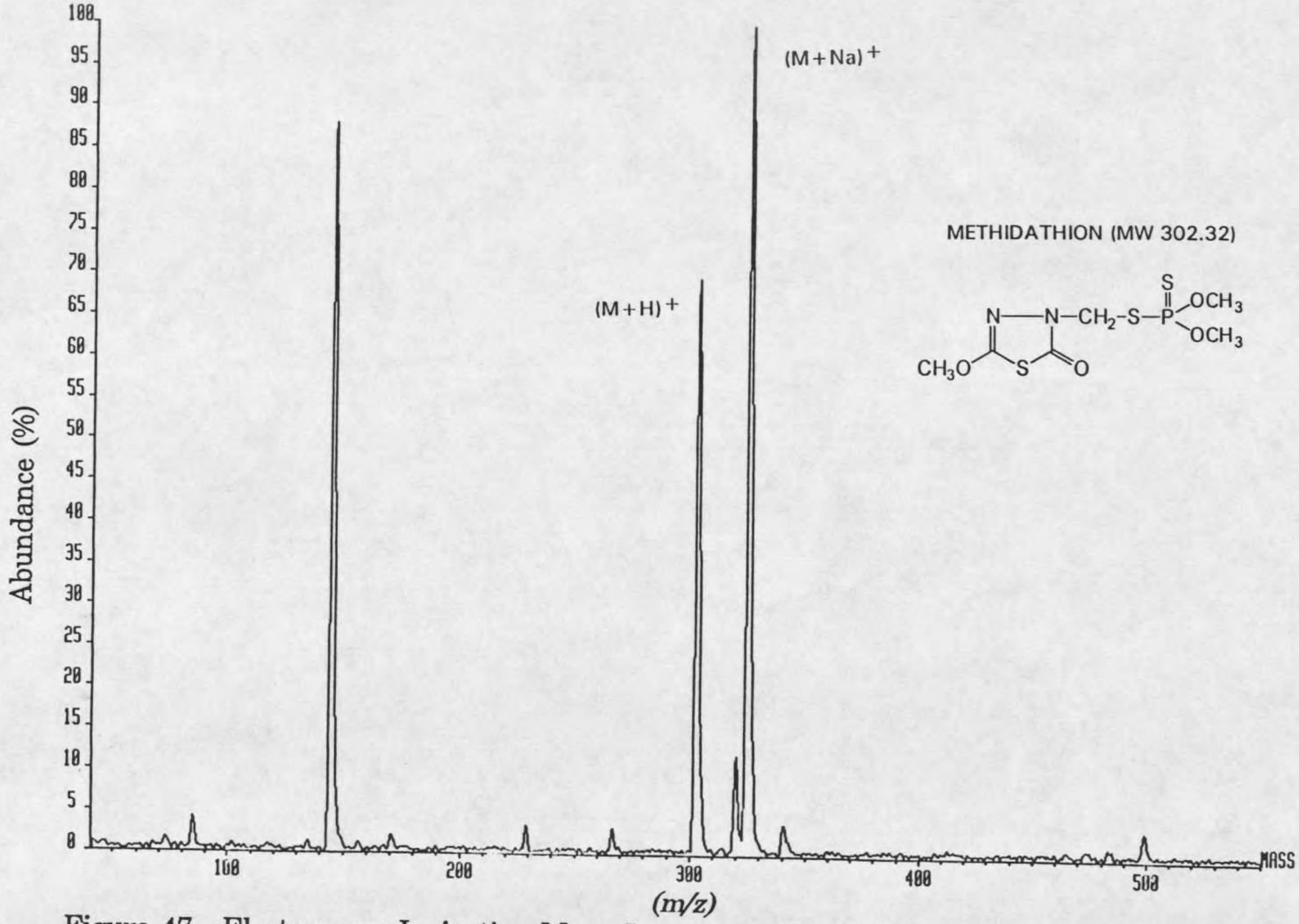


Figure 47. Electrospray Ionization Mass Spectrum of Methidathion. P. D. 75 Volts.

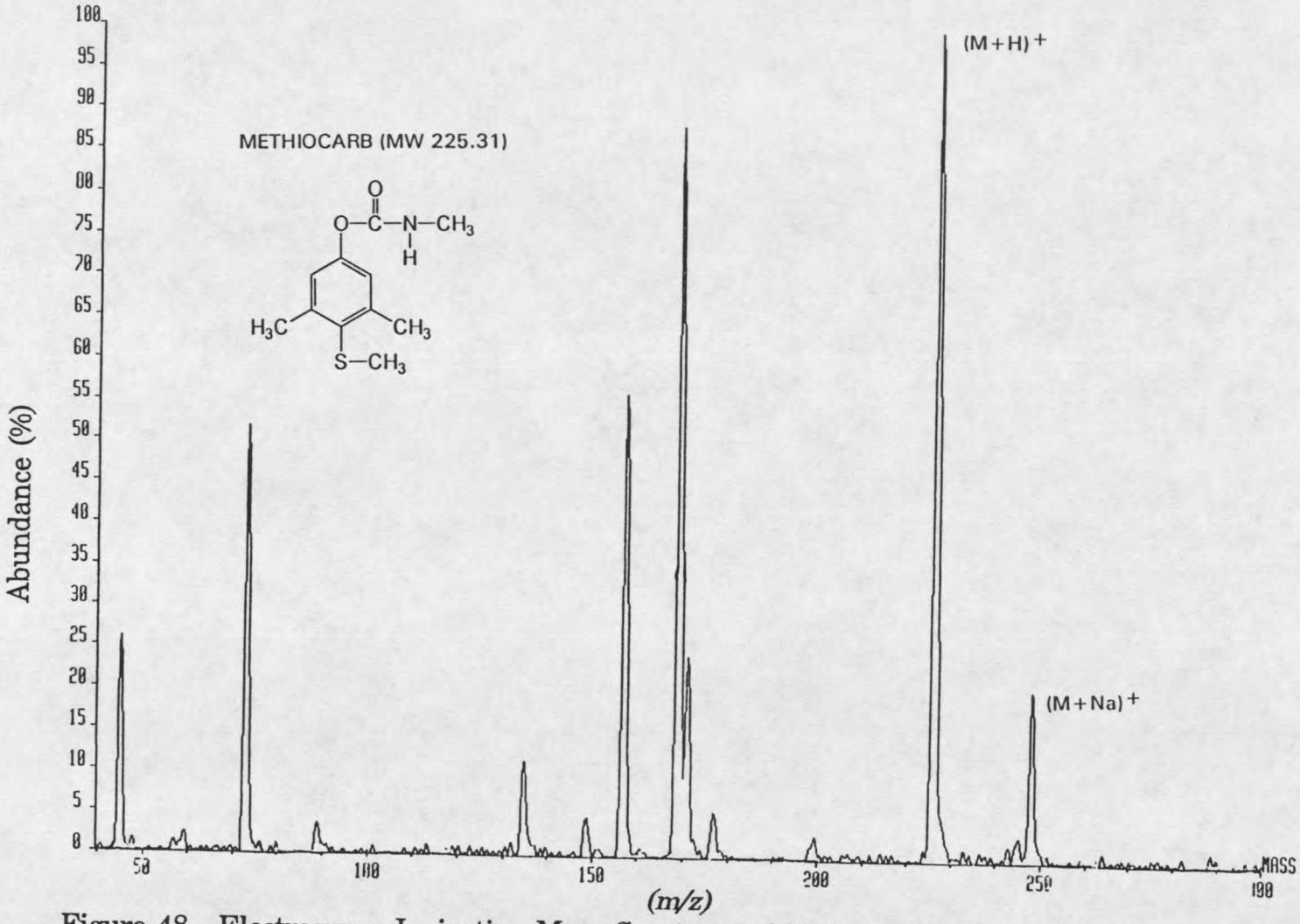


Figure 48. Electrospray Ionization Mass Spectrum of Methiocarb. P. D. 65 Volts.

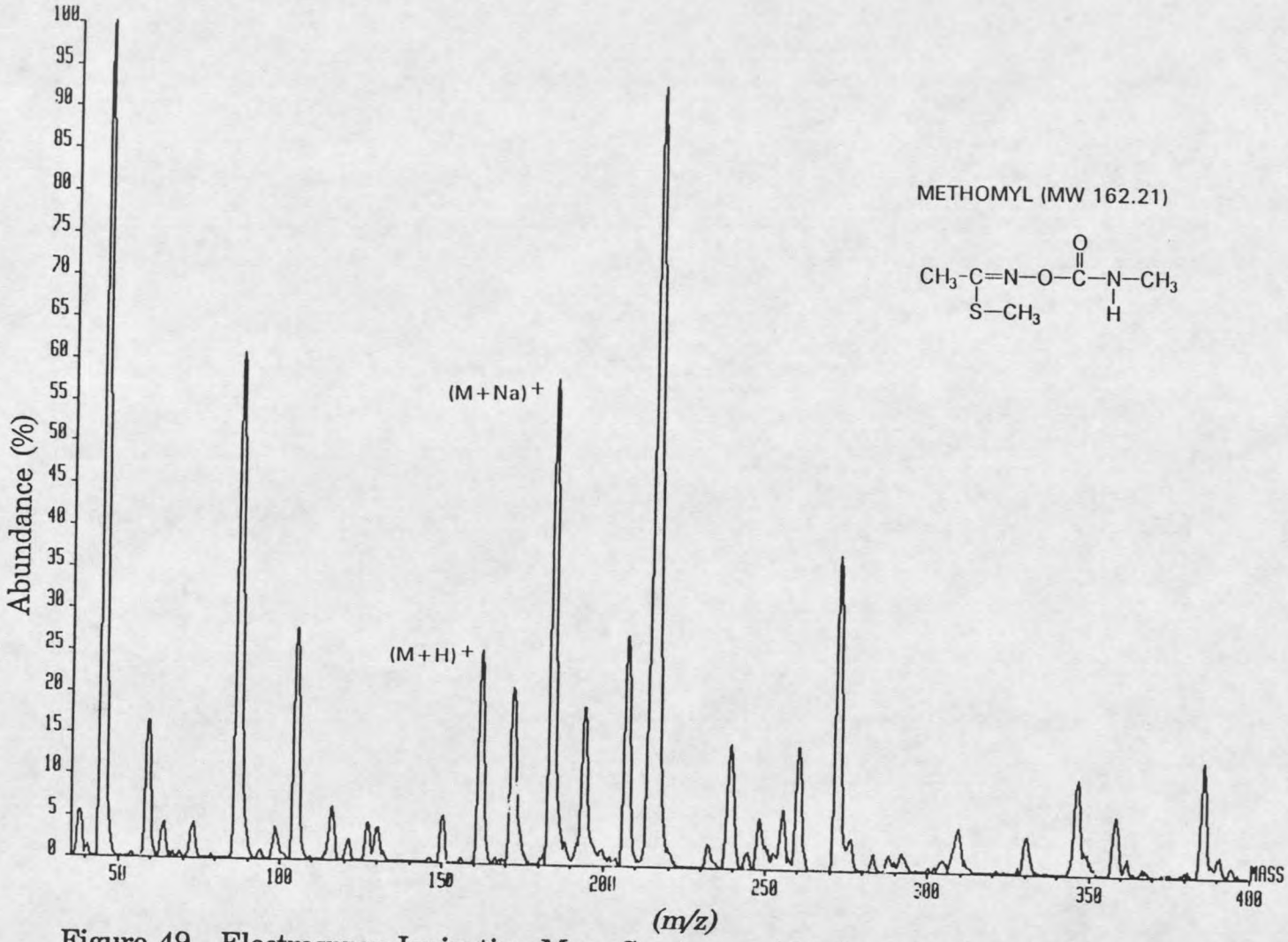


Figure 49. Electrospray Ionization Mass Spectrum of Methomyl. P. D. 55 Volts.

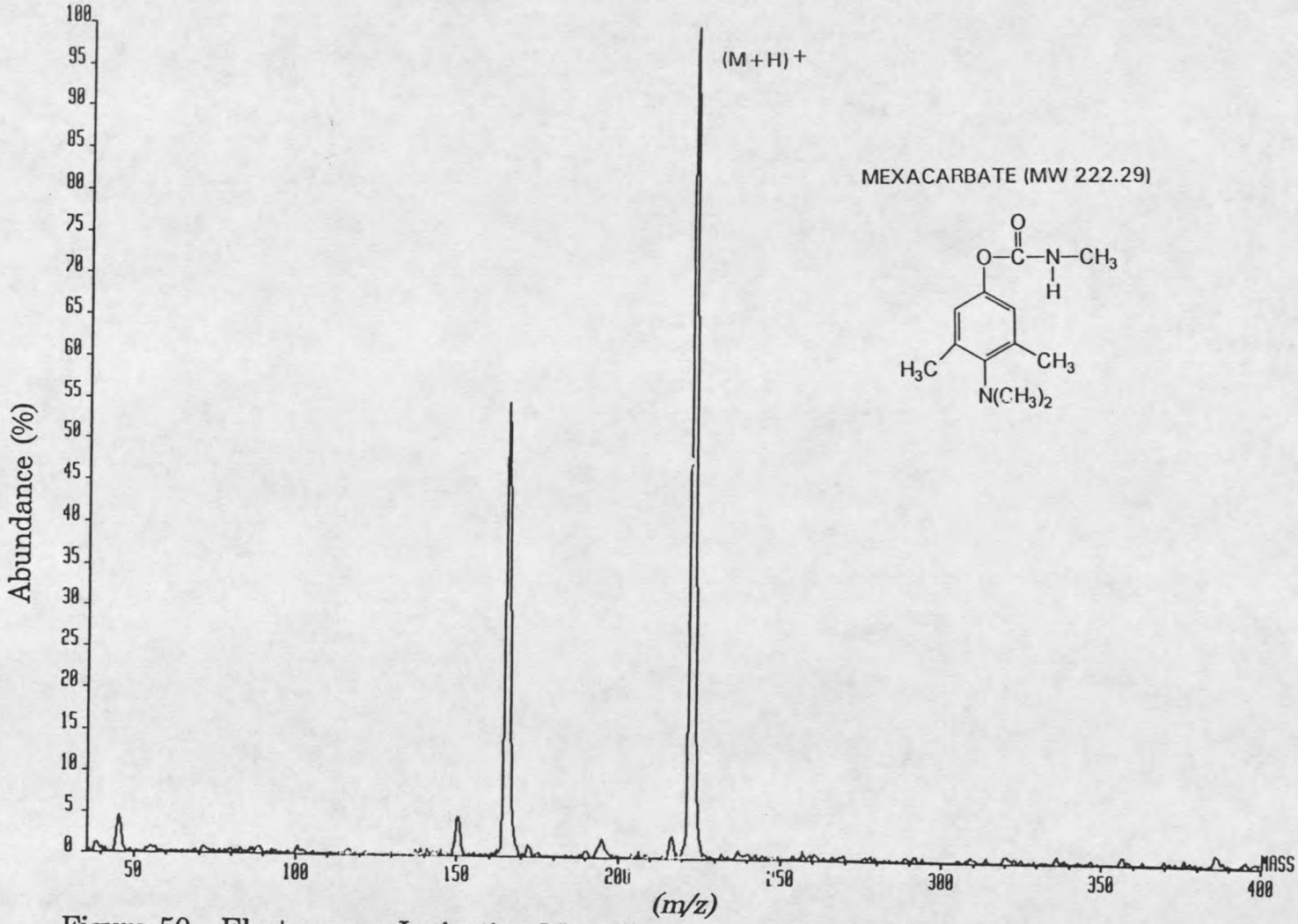


Figure 50. Electrospray Ionization Mass Spectrum of Mexacarbate. P. D. 75 Volts.

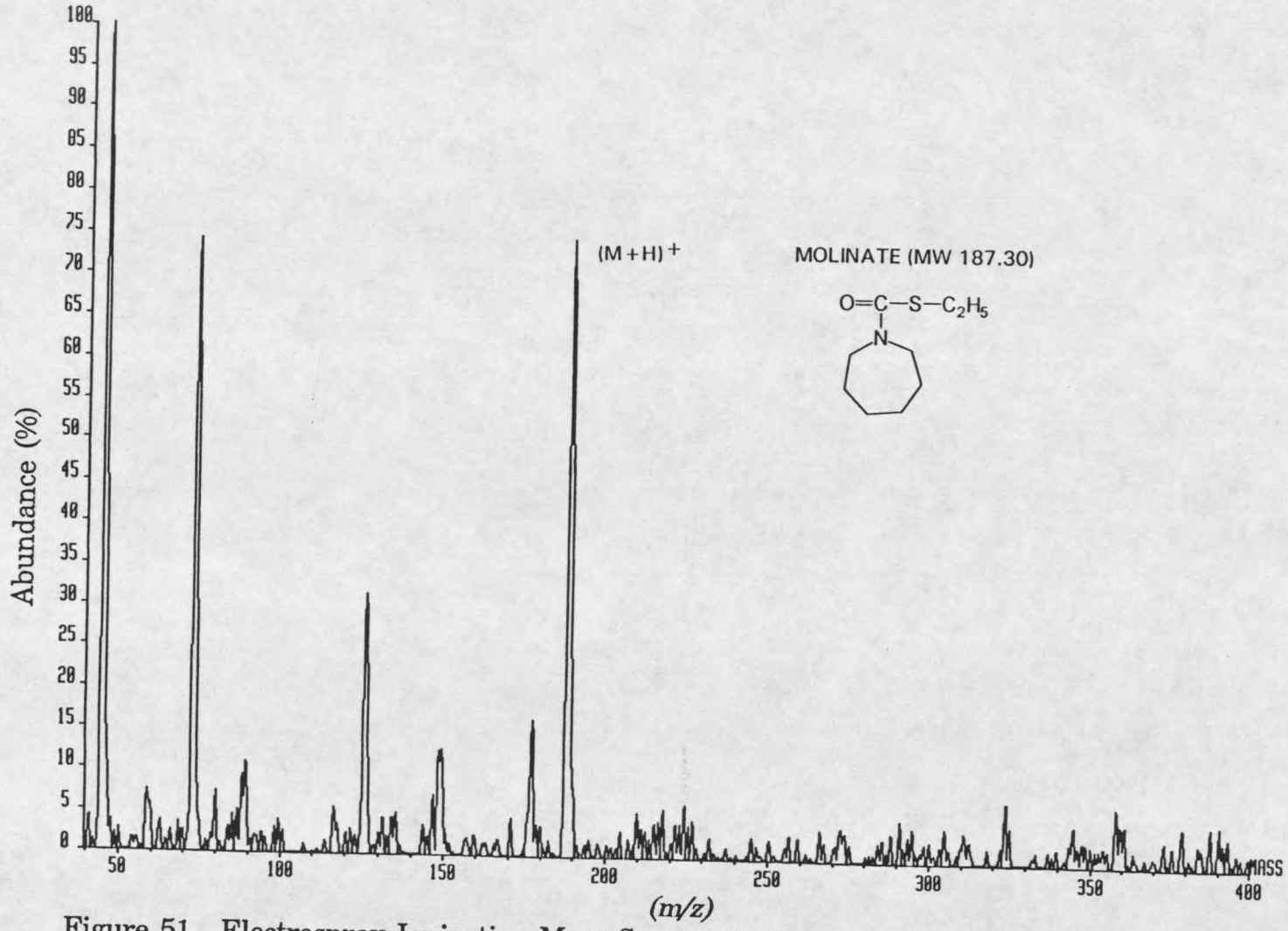


Figure 51. Electrospray Ionization Mass Spectrum of Molinate. P. D. 85 Volts.

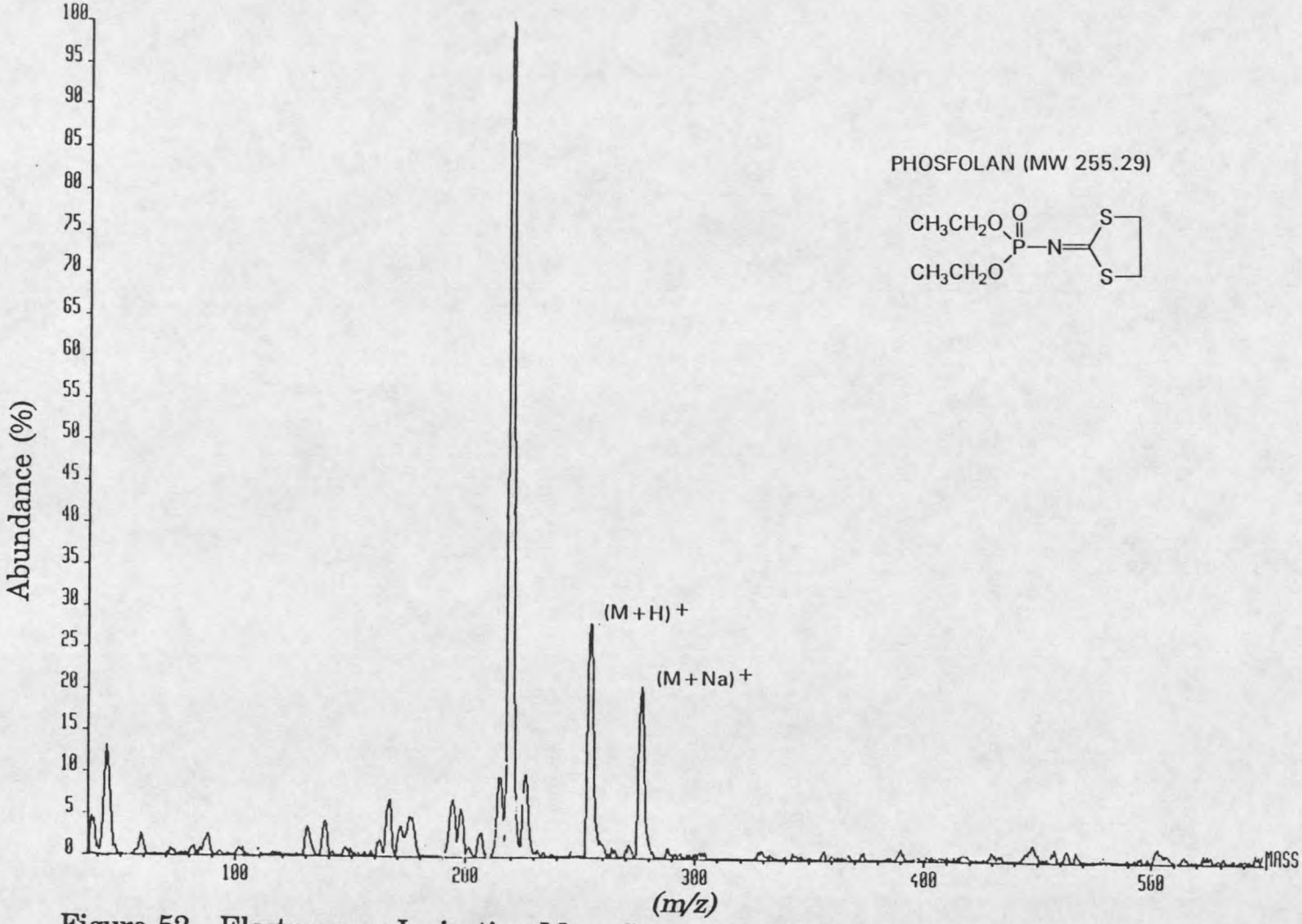


Figure 52. Electrospray Ionization Mass Spectrum of Phosfolan. P. D. 85 Volts.

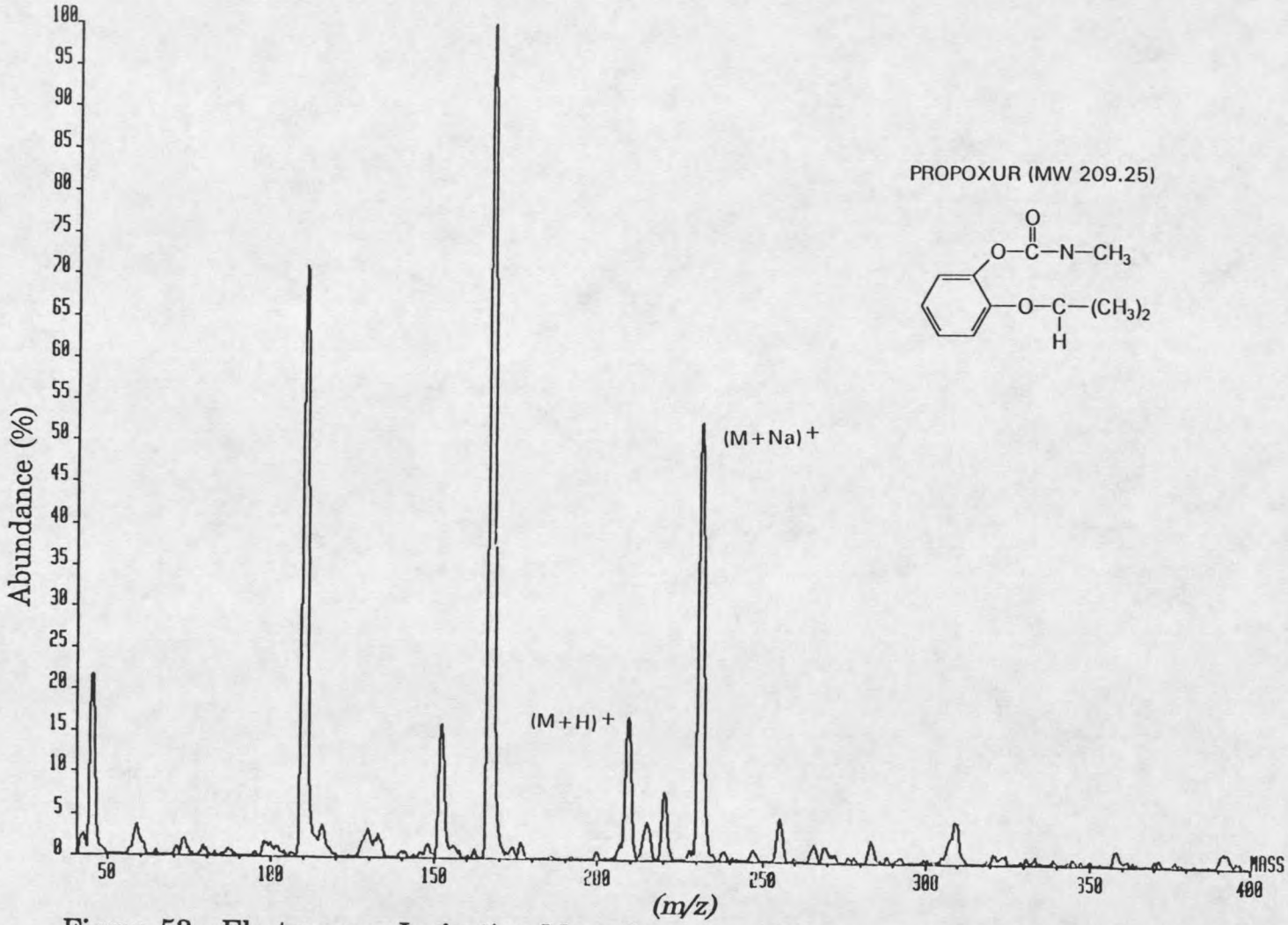


Figure 53. Electrospray Ionization Mass Spectrum of Propoxur. P. D. 55 Volts.

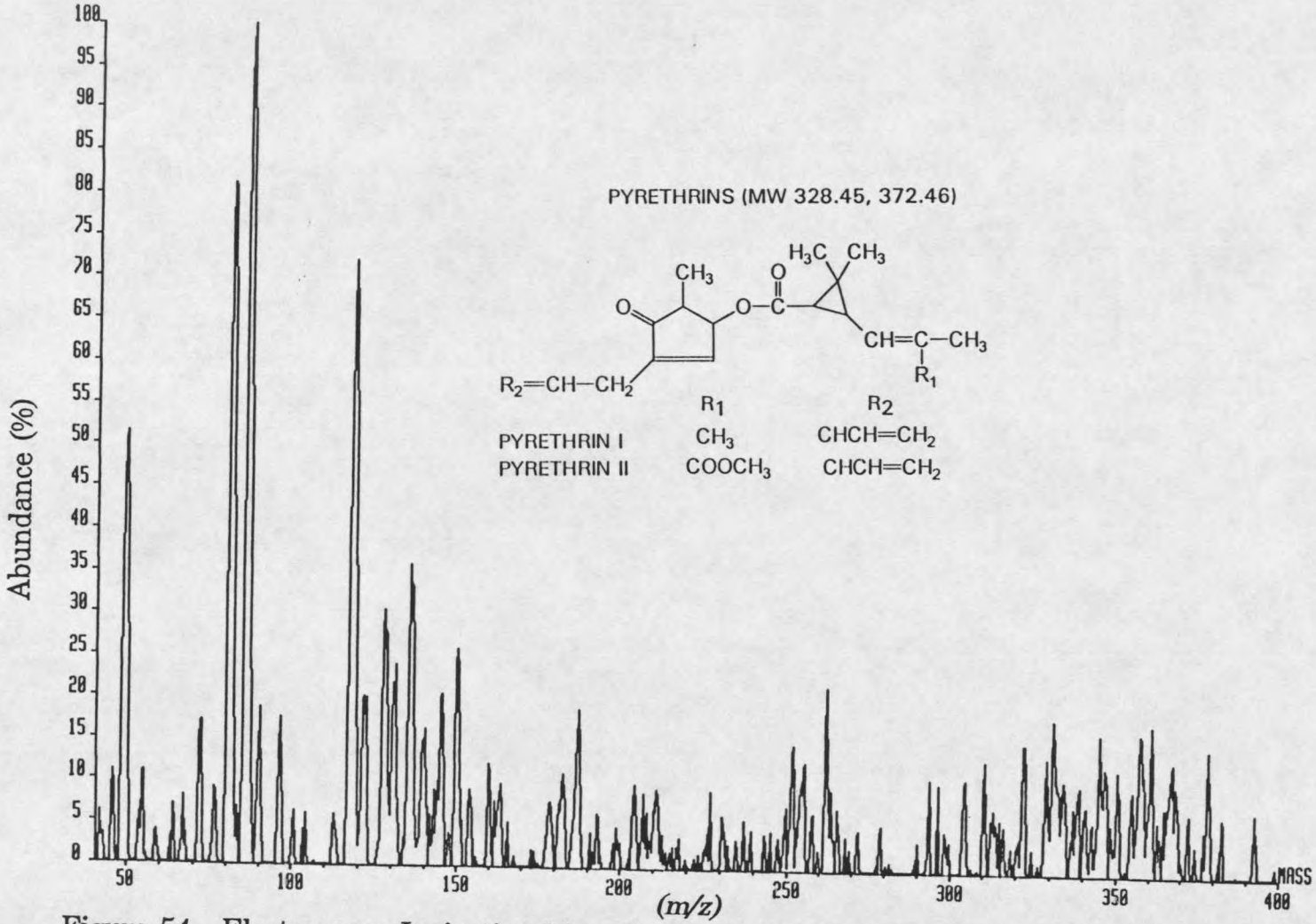


Figure 54. Electrospray Ionization Mass Spectrum of Pyrethrin I & II. P. D. 65 Volts.

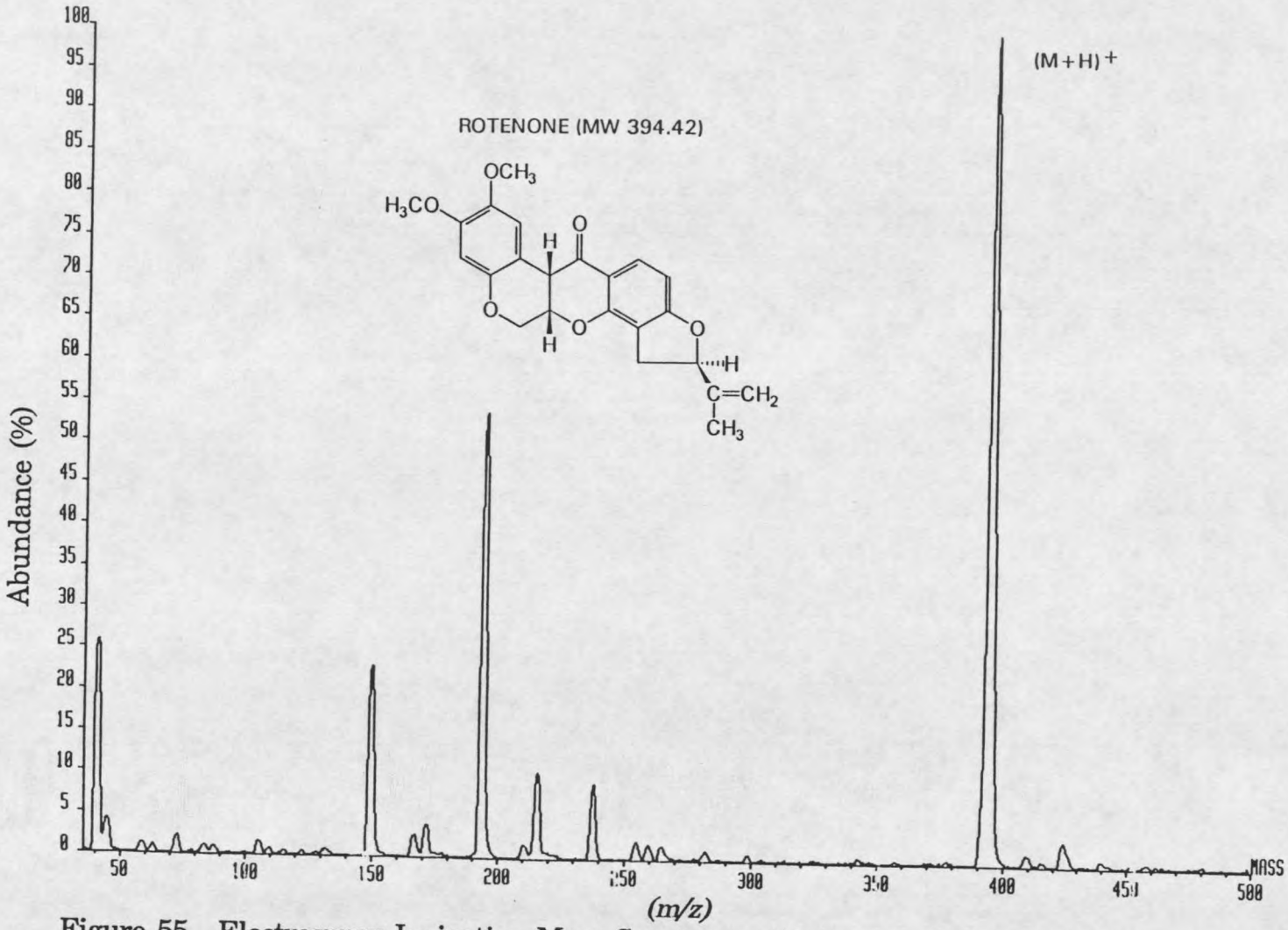


Figure 55. Electrospray Ionization Mass Spectrum of Rotenone. P. D. 65 Volts.

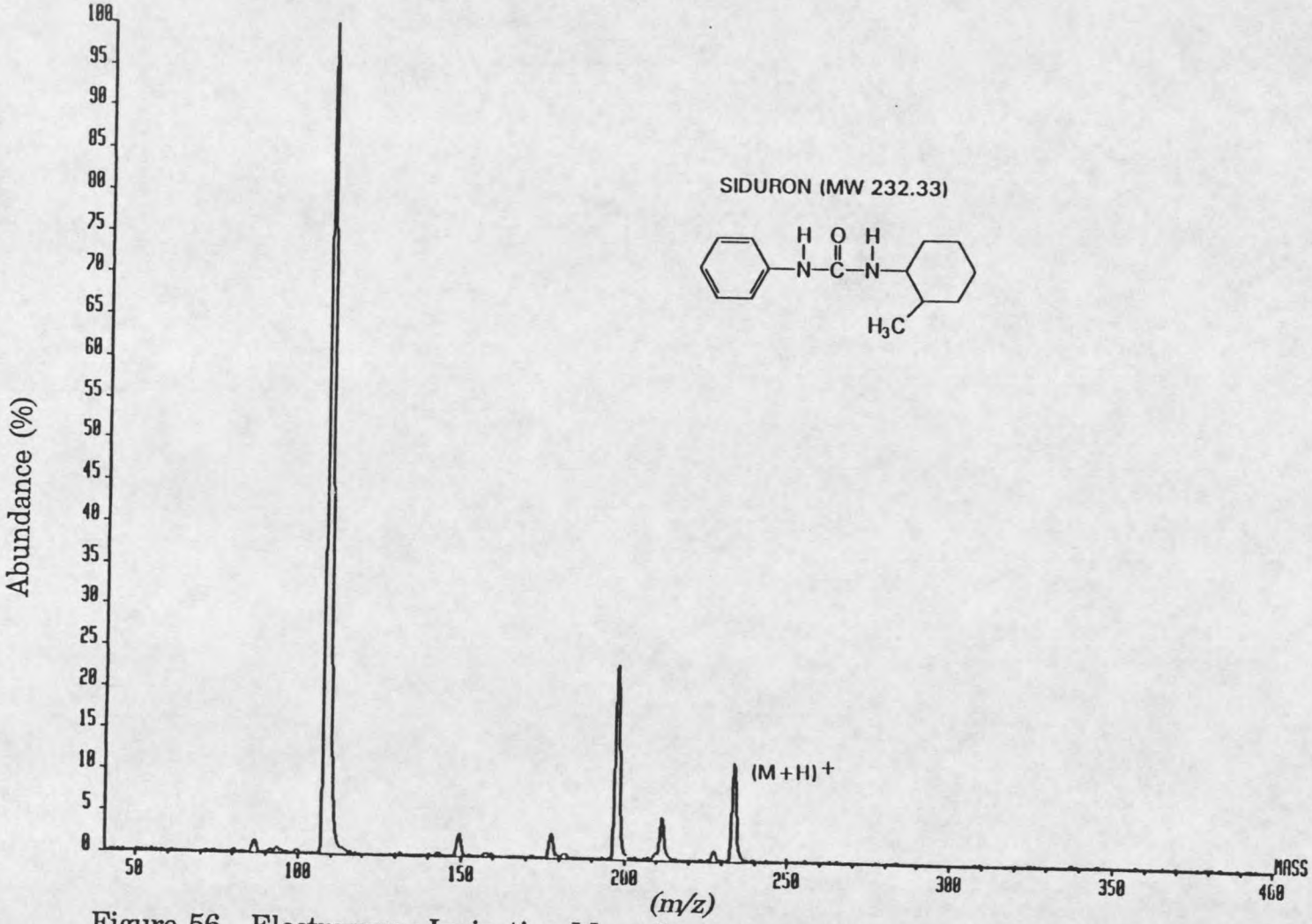


Figure 56. Electrospray Ionization Mass Spectrum of Siduron. P. D. 75 Volts.

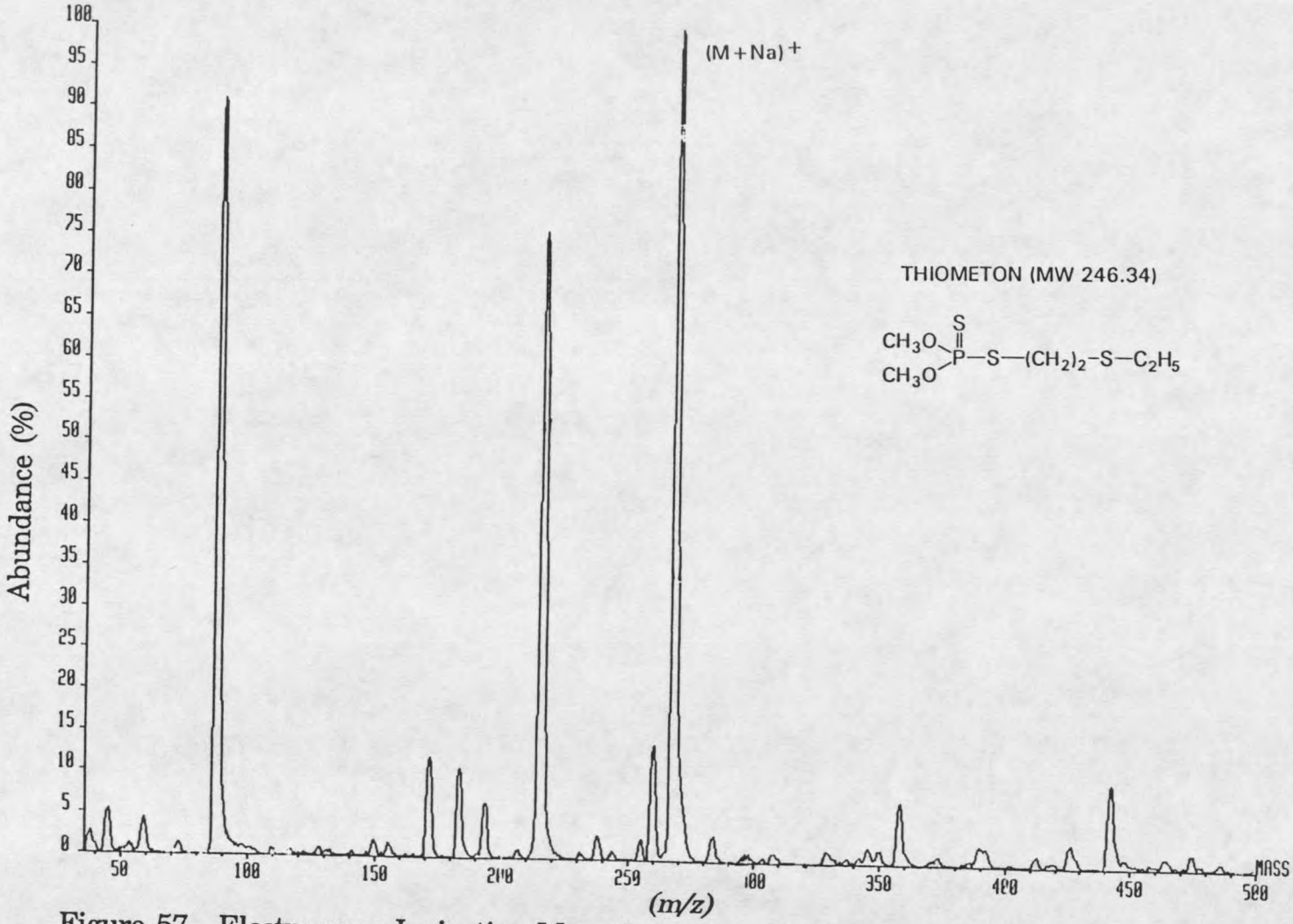


Figure 57. Electrospray Ionization Mass Spectrum of Thiometon. P. D. 45 Volts.

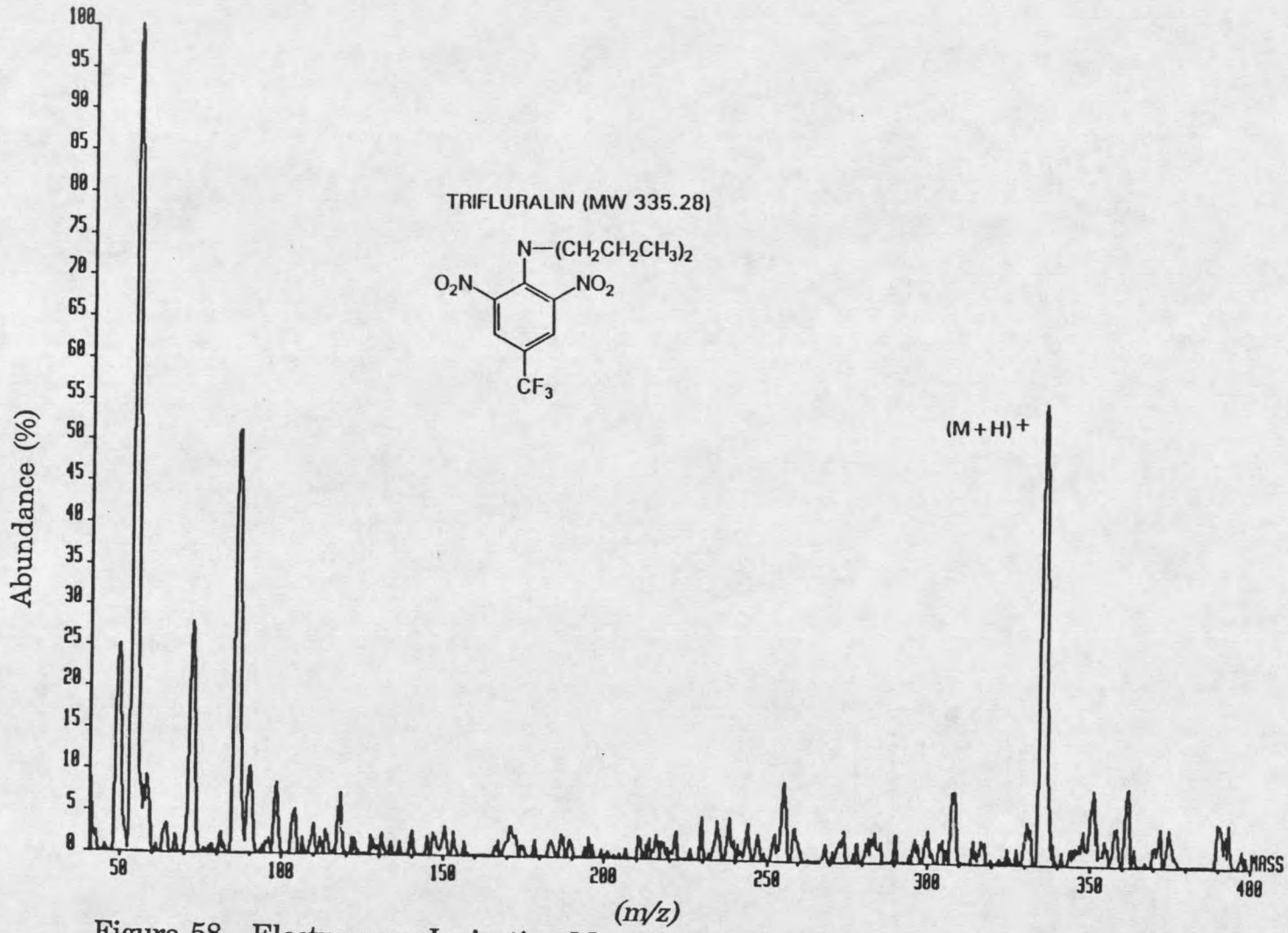


Figure 58. Electrospray Ionization Mass Spectrum of Trifluralin. P. D. 35 Volts.

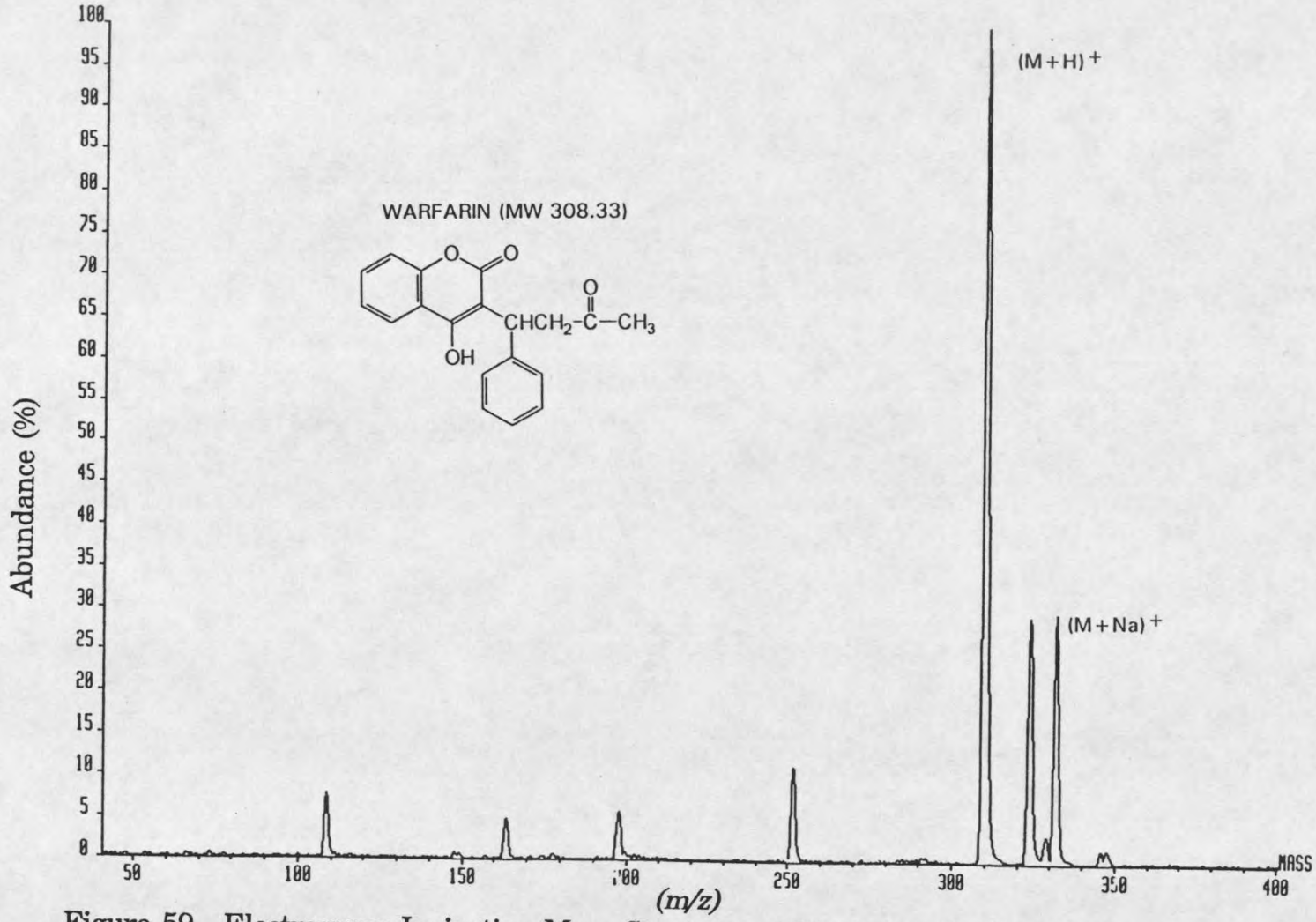


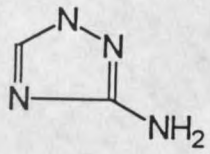
Figure 59. Electrospray Ionization Mass Spectrum of Warfarin. P. D. 75 Volts.

APPENDIX B

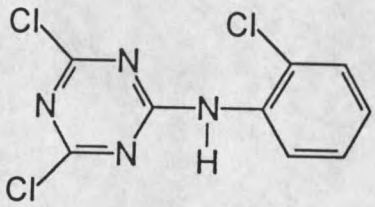
CHEMICAL STRUCTURES AND pKa's OF THE PESTICIDES

Figure 60. Chemical Structures of the Pesticides

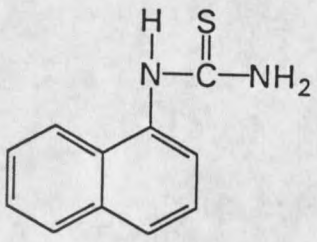
AMITROLE (MW 84.08)



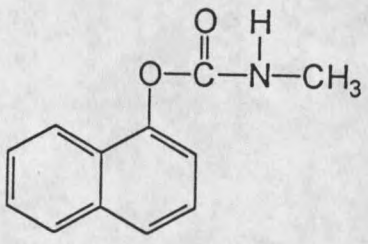
ANILAZINE (MW 275.52)



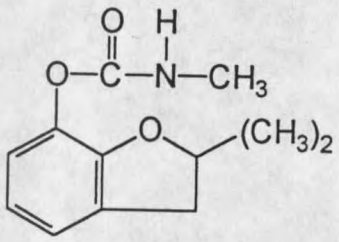
ANTU (MW 202.27)



CARBARYL (MW 201.22)



CARBOFURAN (MW 221.26)



CHLORAMBEN (206.03)

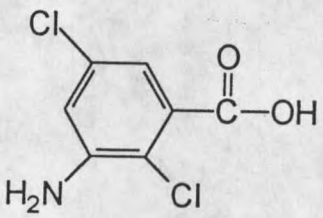
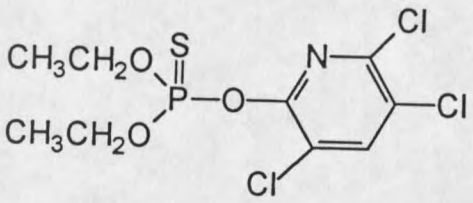
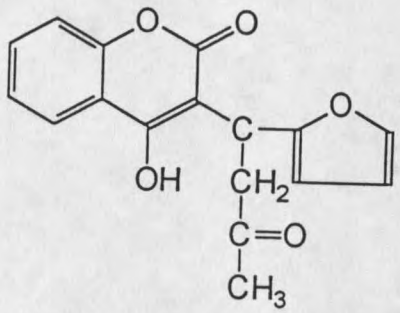


Figure 60. Chemical Structures of the Pesticides (Continued)

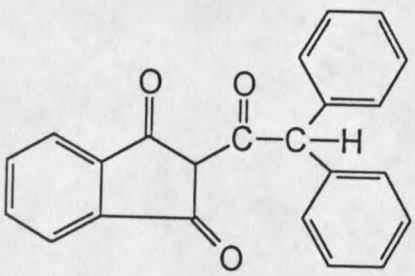
CHLORPYRIFOS (MW 350.58)



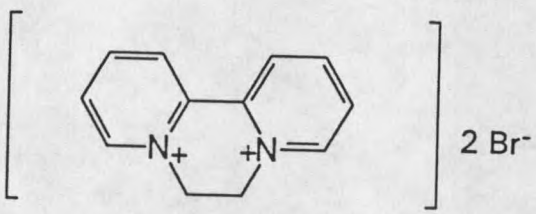
COUMAFURYL (MW 298.30)



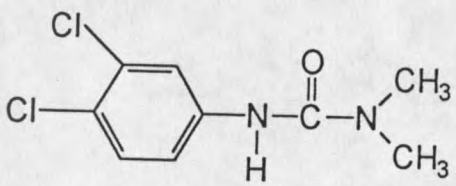
DIPHACINONE (MW 340.38)



DIQUAT DIBROMIDE (MW 344.05)



DIURON (MW 233.10)



ENDOSULFAN (MW 406.92)

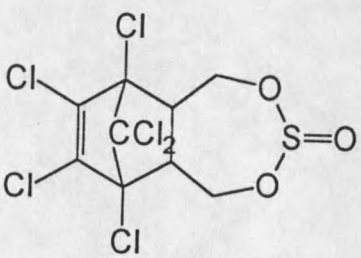
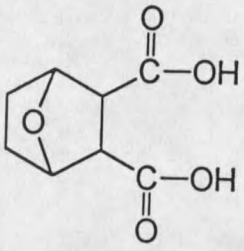
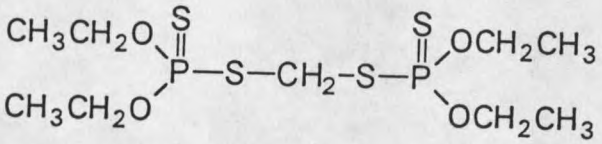


Figure 60. Chemical Structures of the Pesticides (Continued)

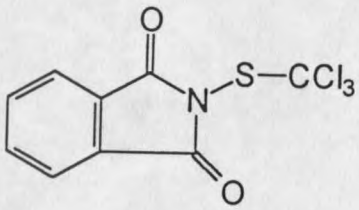
ENDOTHALL (MW 186.16)



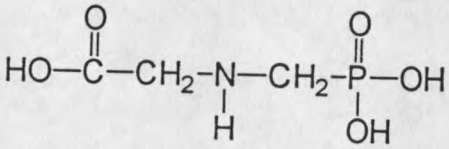
ETHION (MW 384.46)



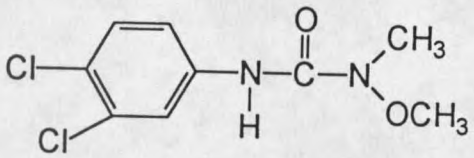
FOLPET (MW 296.56)



GLYPHOSATE (MW 169.07)



LINURON (MW 249.10)



MEPHOSFOLAN (MW 269.31)

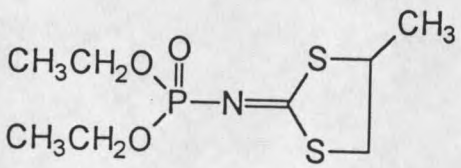
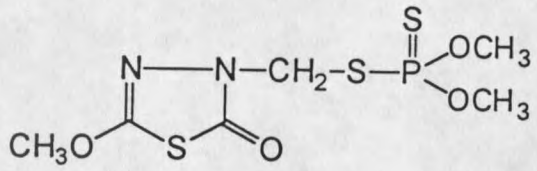
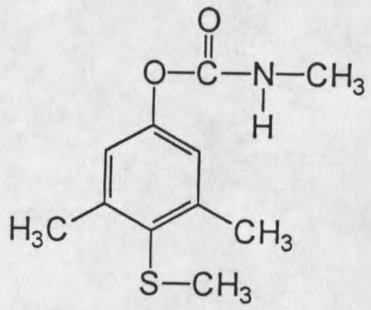


Figure 60. Chemical Structures of the Pesticides (Continued)

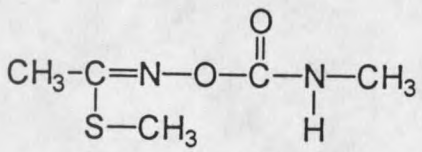
METHIDATHION (MW 302.32)



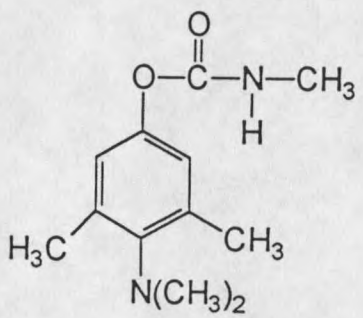
METHIOCARB (MW 225.31)



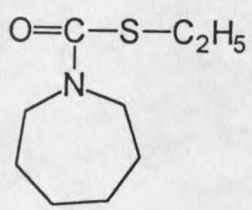
METHOMYL (MW 162.21)



MEXACARBATE (MW 222.29)



MOLINATE (MW 187.30)



PHOSFOLAN (MW 255.29)

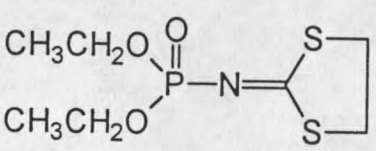
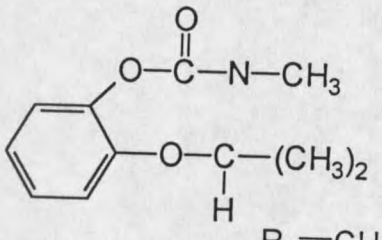
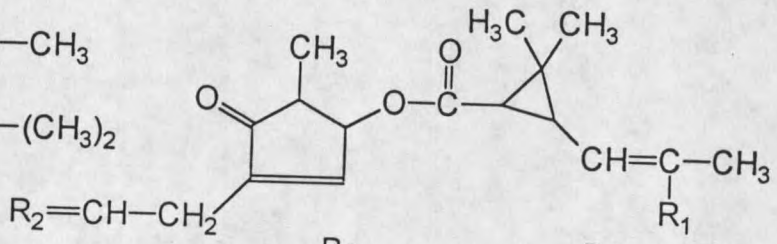


Figure 60. Chemical Structures of the Pesticides (Continued)

PROPOXUR (MW 209.25)

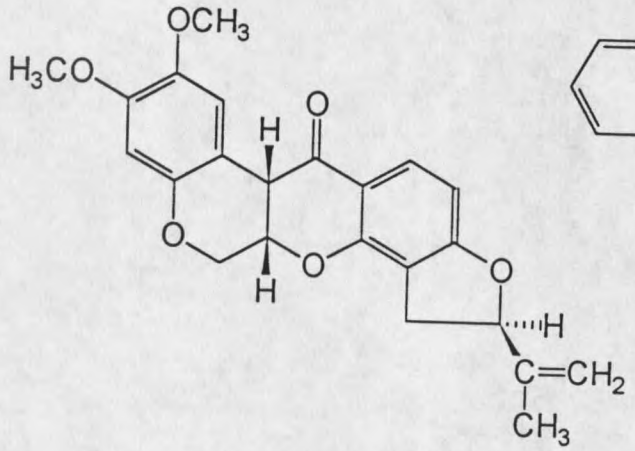


PYRETHRINS (MW 328.45, 372.46)

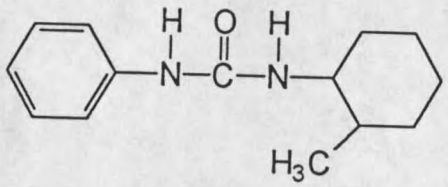


	R_1	R_2
PYRETHRIN I	CH_3	$CHCH{=}CH_2$
PYRETHRIN II	$COOCH_3$	$CHCH{=}CH_2$

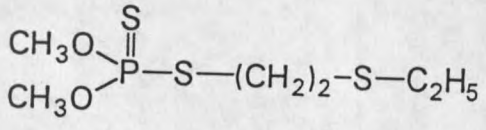
ROTENONE (MW 394.42)



SIDURON (MW 232.33)



THIOMETON (MW 246.34)



TRIFLURALIN (MW 335.28)

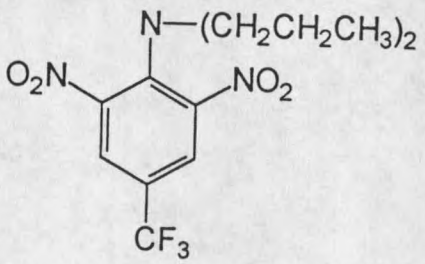


Figure 60. Chemical Structures of the Pesticides (Continued)

WARFARIN (MW 308.33)

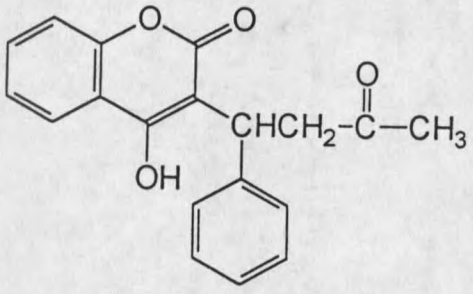
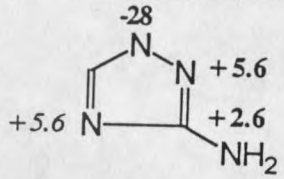
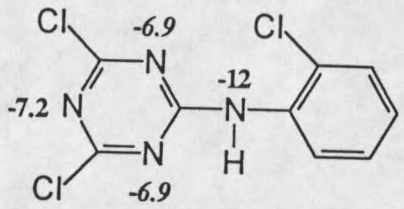


Figure 61. Chemical Structures and pK_a's of the Pesticides

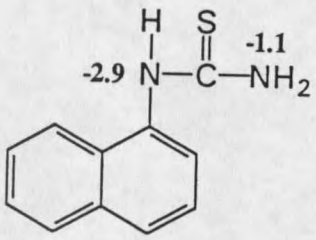
AMITROLE (MW 84.08)



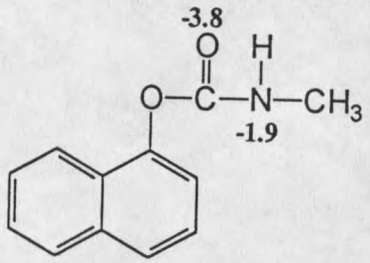
ANILAZINE (MW 275.52)



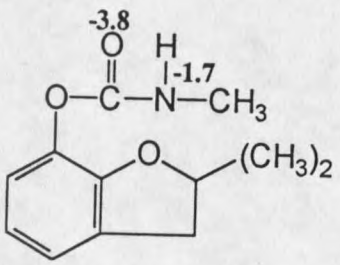
ANTU (MW 202.27)



CARBARYL (MW 201.22)



CARBOFURAN (MW 221.26)



CHLORAMBEN (206.03)

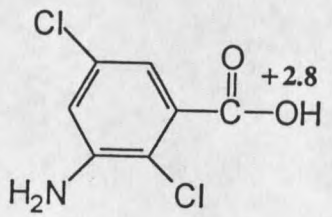
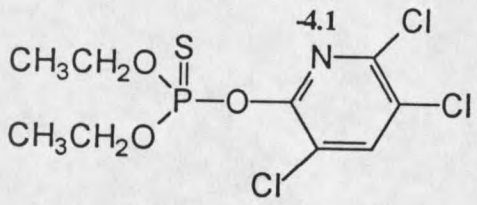
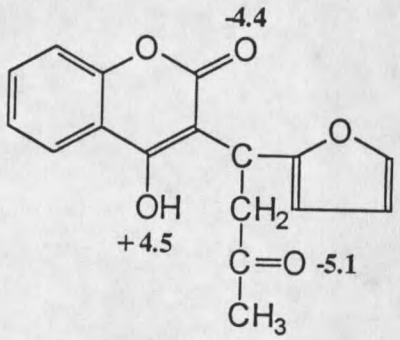


Figure 61. Chemical Structures and pK_a's of the Pesticides (Continued)

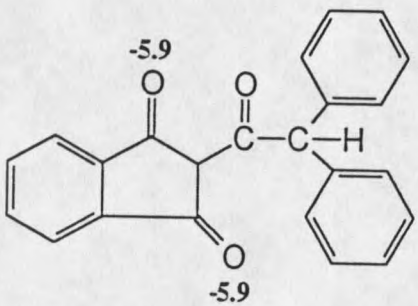
CHLORPYRIFOS (MW 350.58)



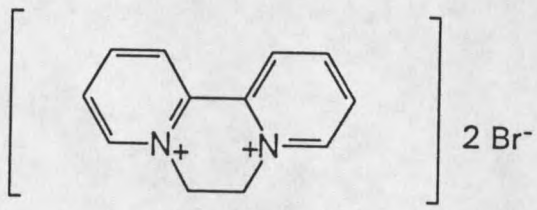
COUMAFURYL (MW 298.30)



DIPHACINONE (MW 340.38)

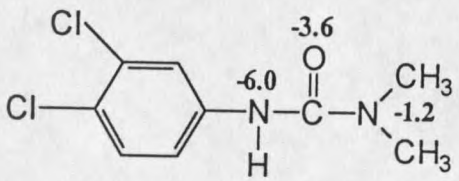


DIQUAT DIBROMIDE (MW 344.05)

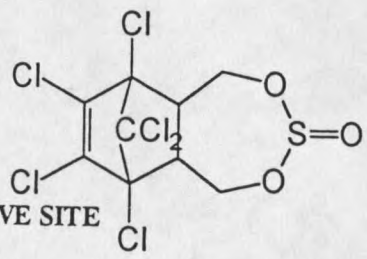


NO REACTIVE SITE

DIURON (MW 233.10)



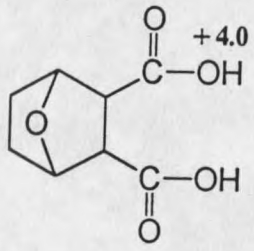
ENDOSULFAN (MW 406.92)



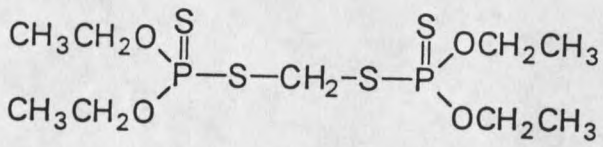
NO REACTIVE SITE

Figure 61. Chemical Structures and pK_a's of the Pesticides (Continued)

ENDOTHALL (MW 186.16)

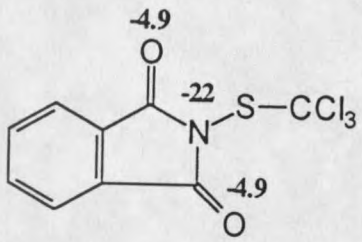


ETHION (MW 384.46)

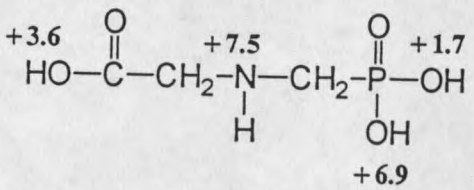


NO REACTIVE SITE

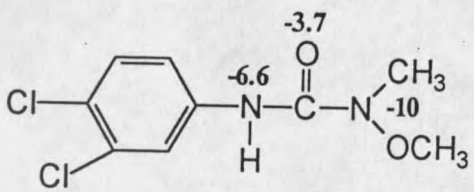
FOLPET (MW 296.56)



GLYPHOSATE (MW 169.07)



LINURON (MW 249.10)



MEPHOSFOLAN (MW 269.31)

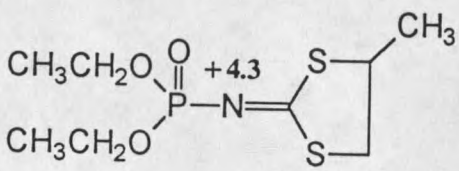
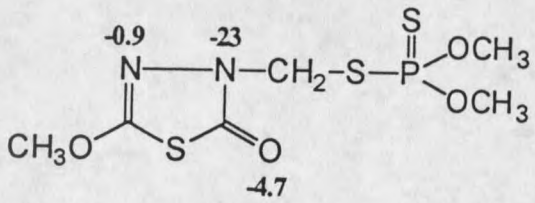
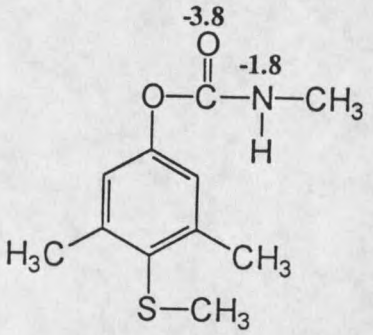


Figure 61. Chemical Structures and pK_a's of the Pesticides (Continued)

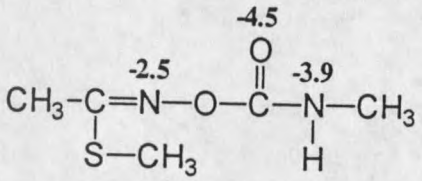
METHIDATHION (MW 302.32)



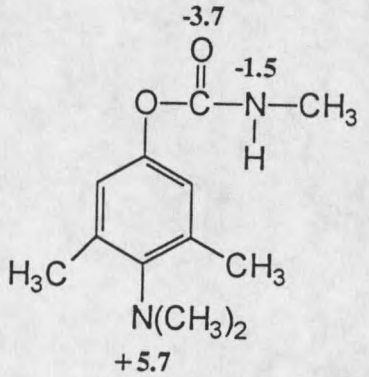
METHIOCARB (MW 225.31)



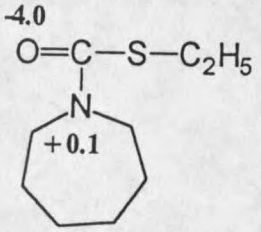
METHOMYL (MW 162.21)



MEXACARBATE (MW 222.29)



MOLINATE (MW 187.30)



PHOSFOLAN (MW 255.29)

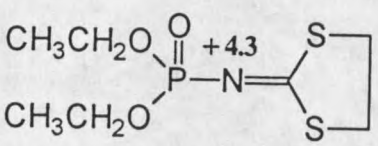
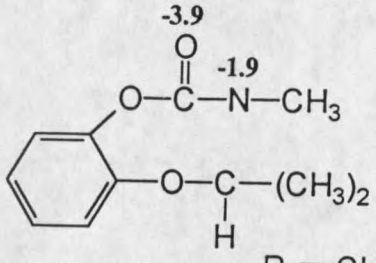
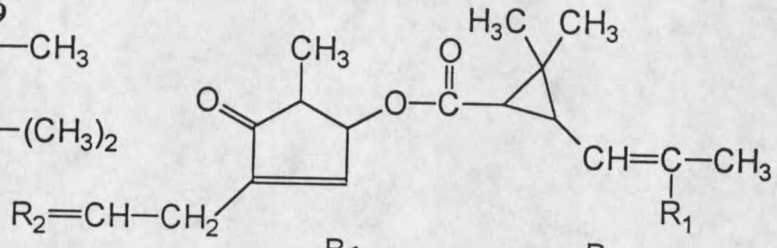


Figure 61. Chemical Structures and pK_a's of the Pesticides (Continued)

PROPOXUR (MW 209.25)

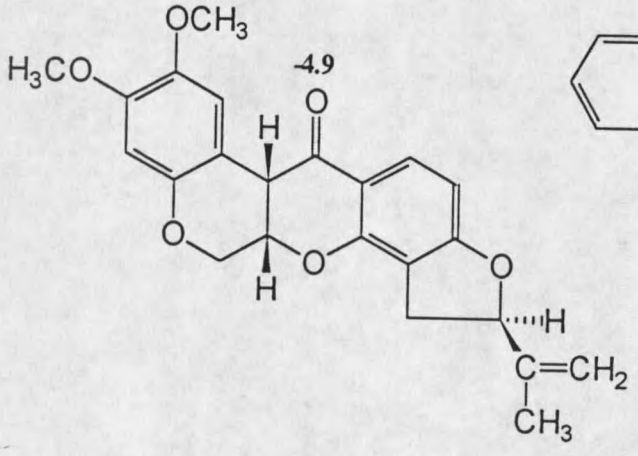


PYRETHRINS (MW 328.45, 372.46)

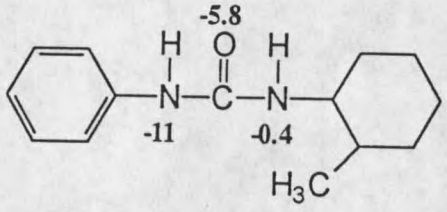


	R_1	R_2
PYRETHRIN I	CH_3	$CHCH{=}CH_2$
PYRETHRIN II	$COOCH_3$	$CHCH{=}CH_2$

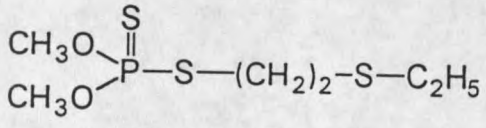
ROTENONE (MW 394.42)



SIDURON (MW 232.33)



THIOMETON (MW 246.34)



NO REACTIVE SITE

TRIFLURALIN (MW 335.28)

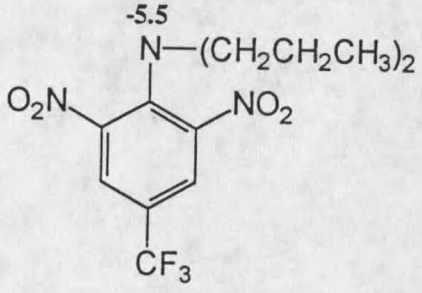
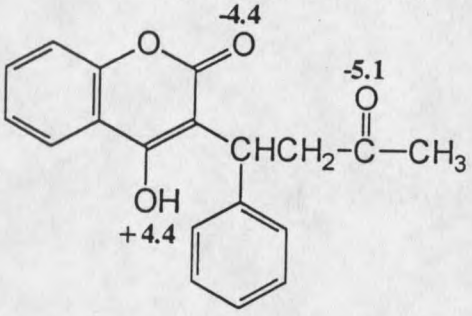


Figure 61. Chemical Structures and pK_a's of the Pesticides (Continued)

WARFARIN (MW 308.33)



APPENDIX C

COLLISION-ACTIVATED DISSOCIATION SPECTRA

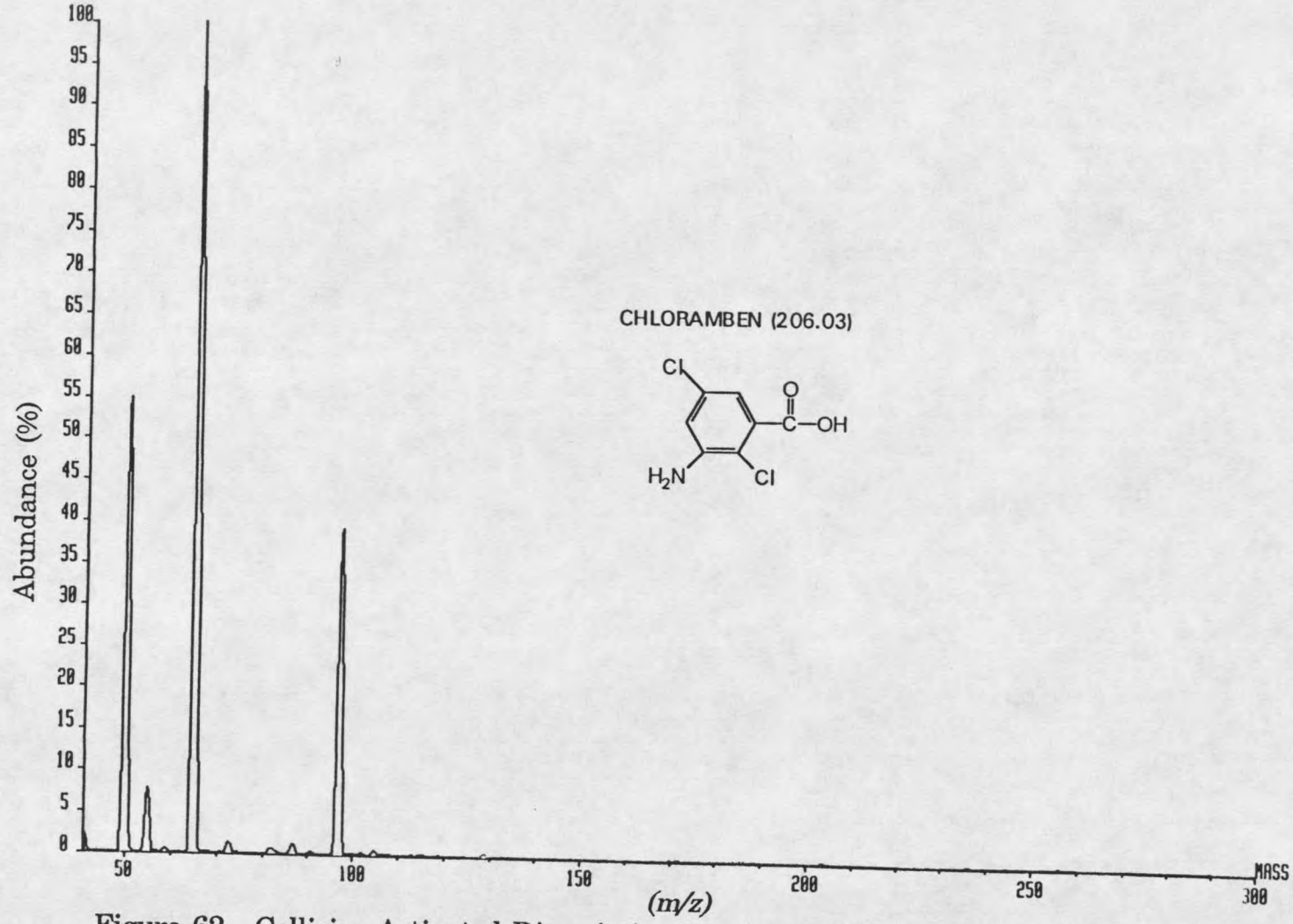


Figure 62. Collision-Activated Dissociation Spectrum of Chloramben. P. D. 35 Volts.

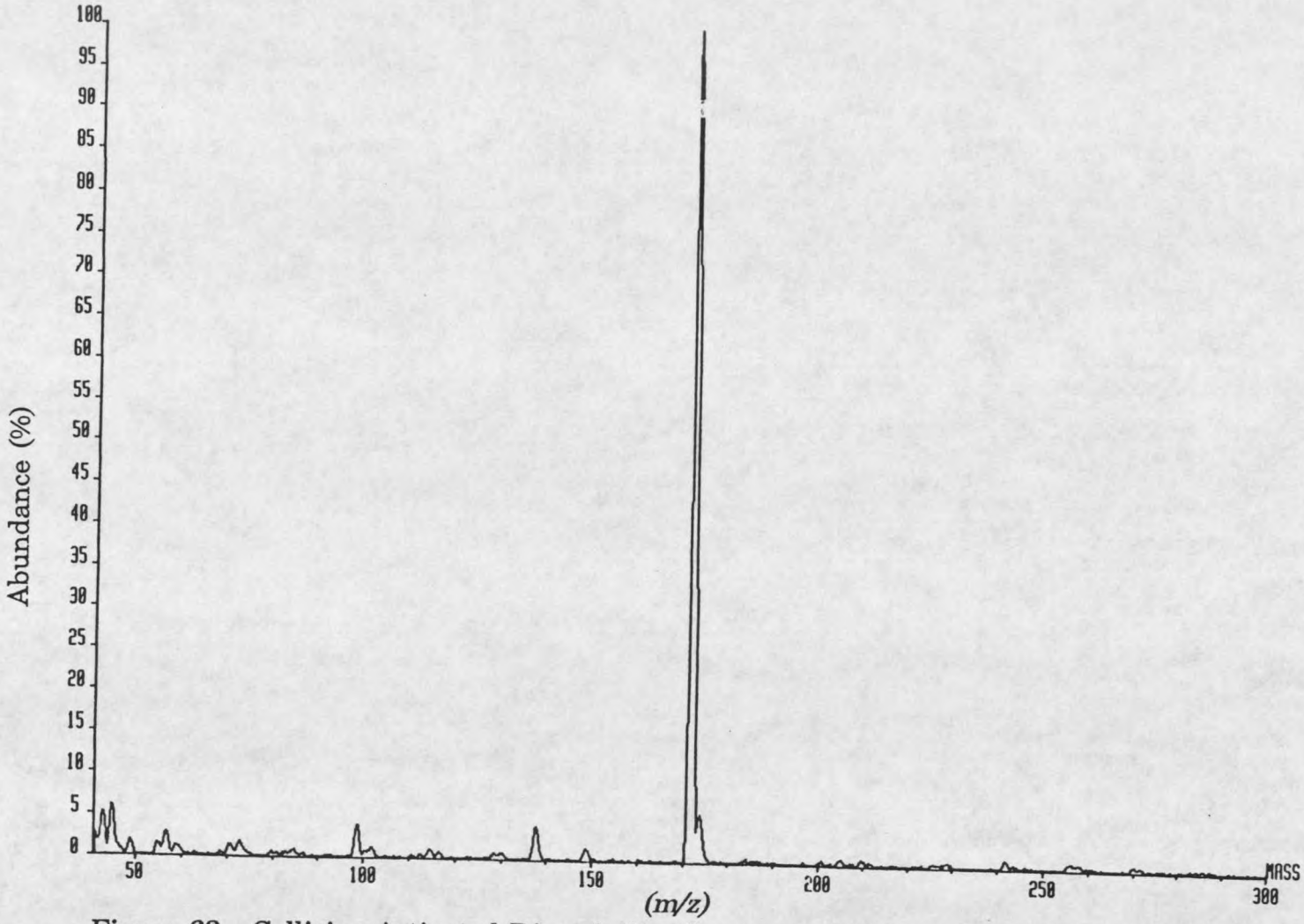


Figure 63. Collision-Activated Dissociation Spectrum of Chloramben. P. D. 85 Volts.

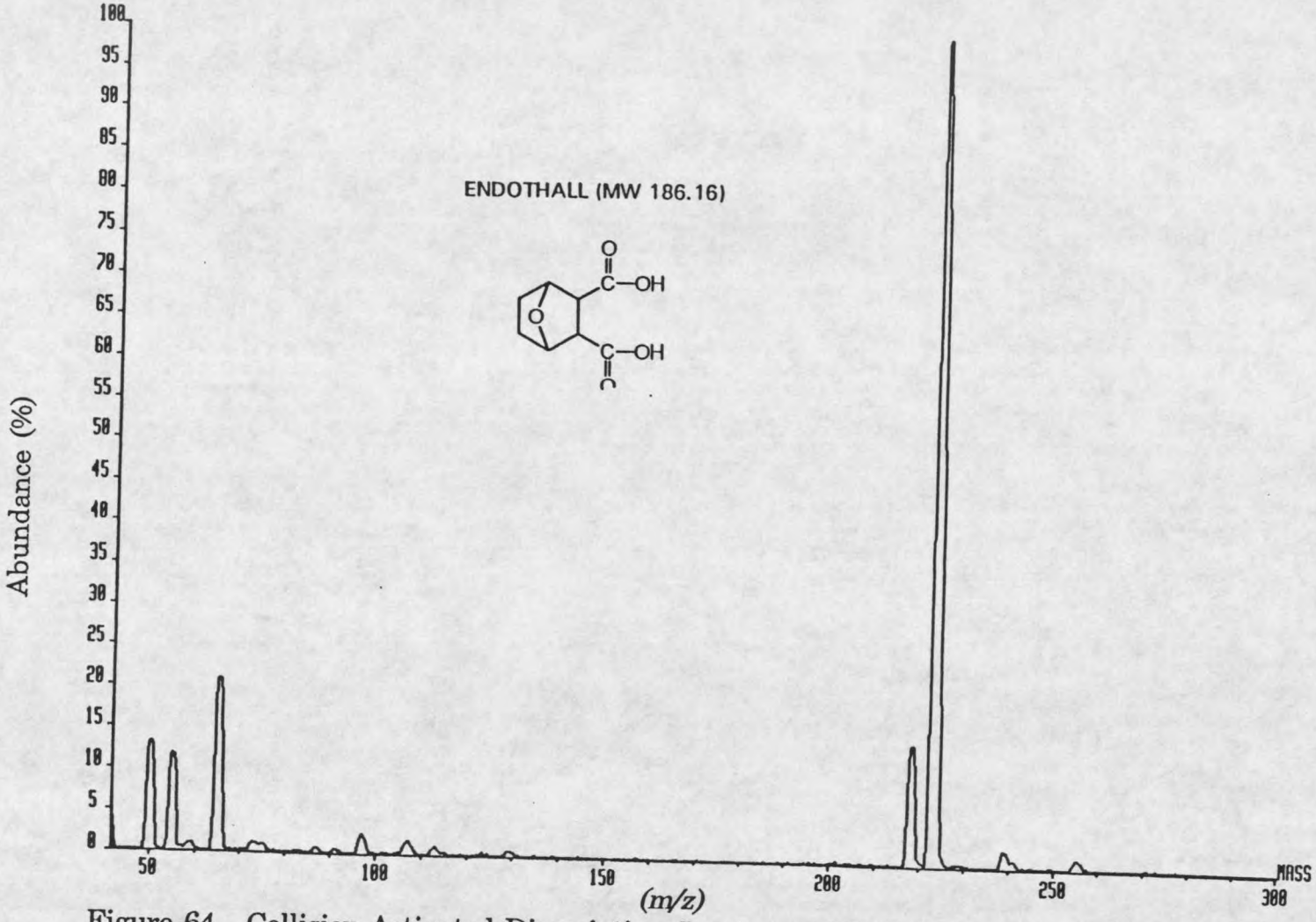


Figure 64. Collision-Activated Dissociation Spectrum of Endothall. P. D. 45 Volts.

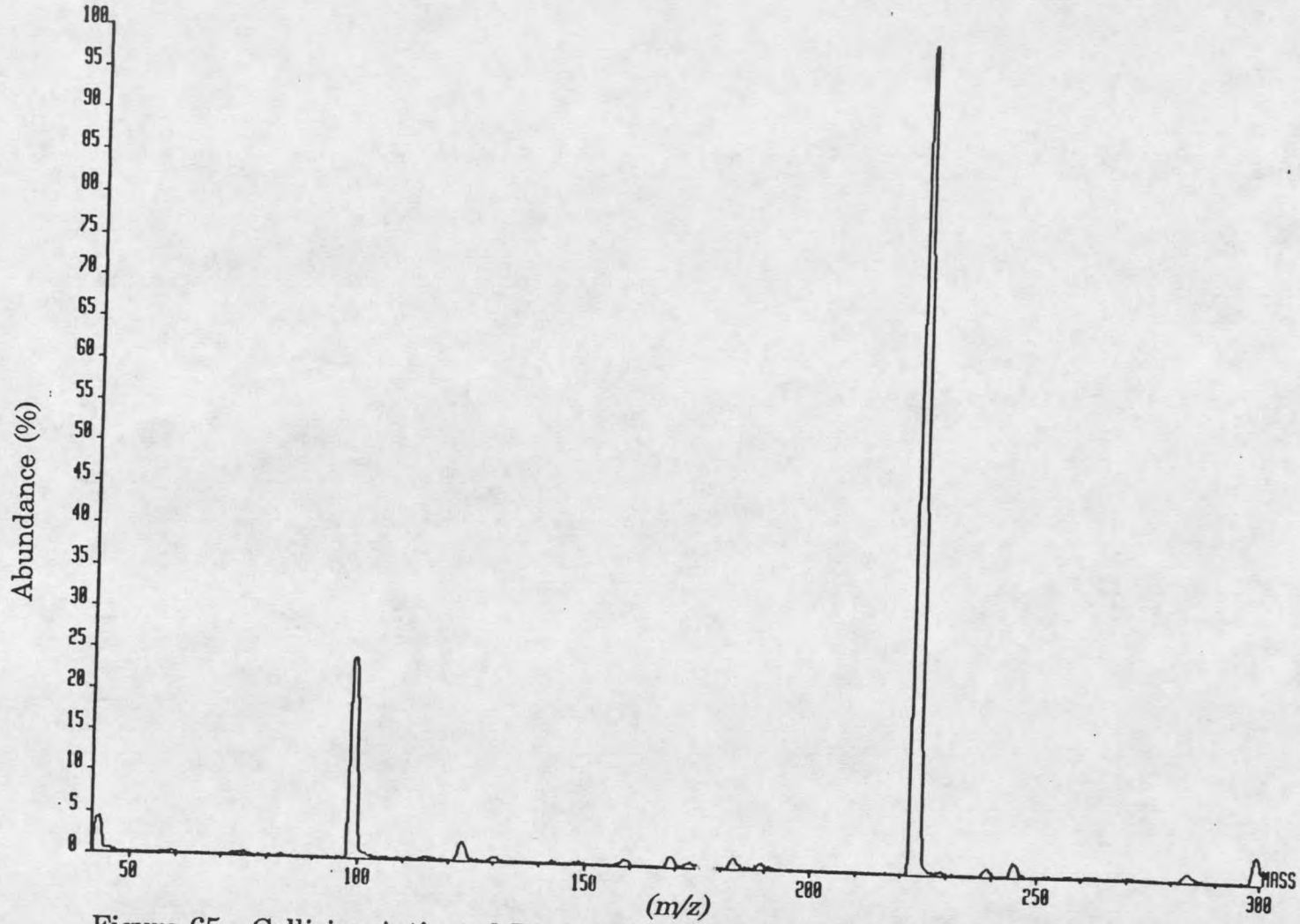


Figure 65. Collision-Activated Dissociation Spectrum of Endothall. P. D. 85 Volts.

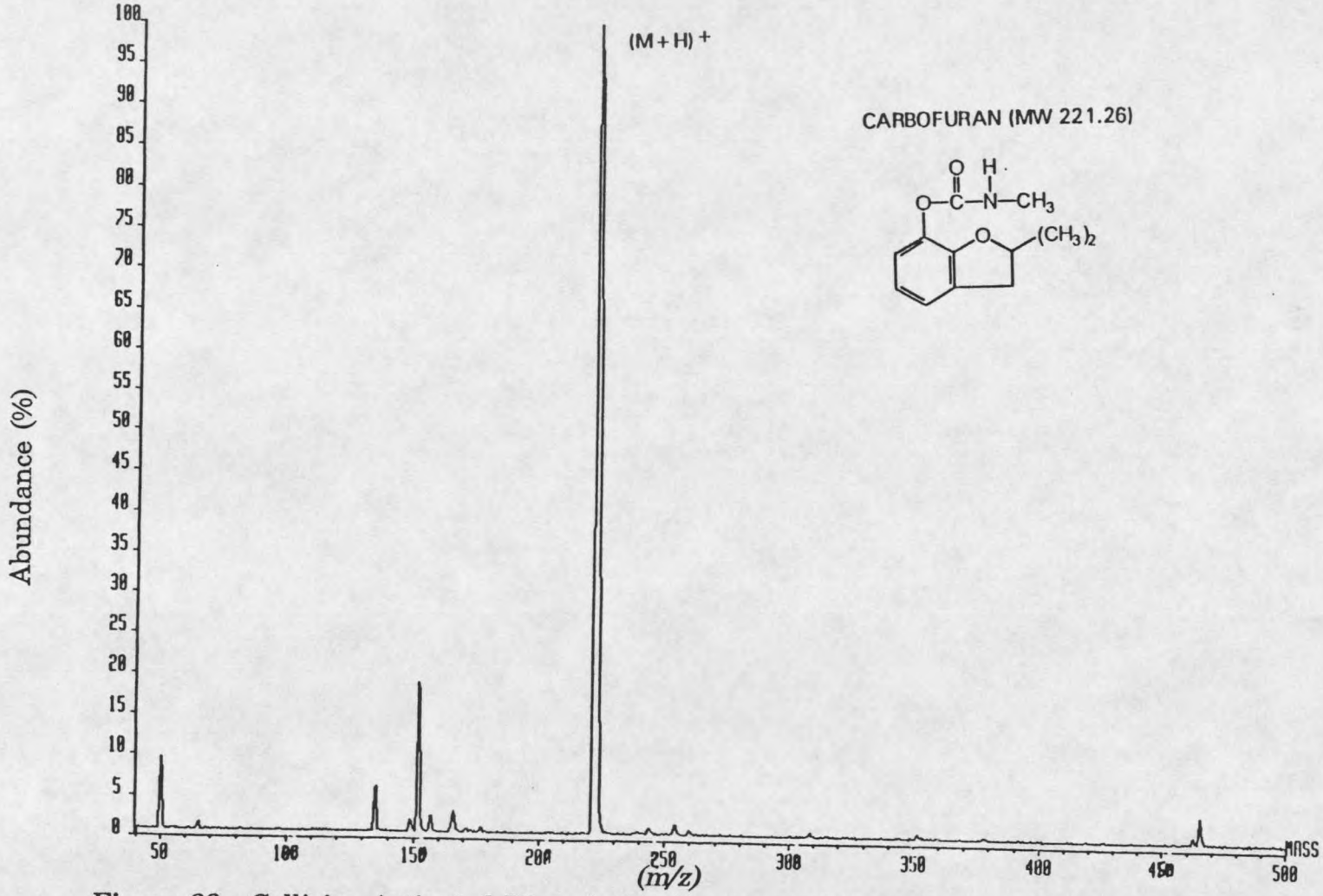


Figure 66. Collision-Activated Dissociation Spectrum of Carbofuran. P. D. 35 Volts.

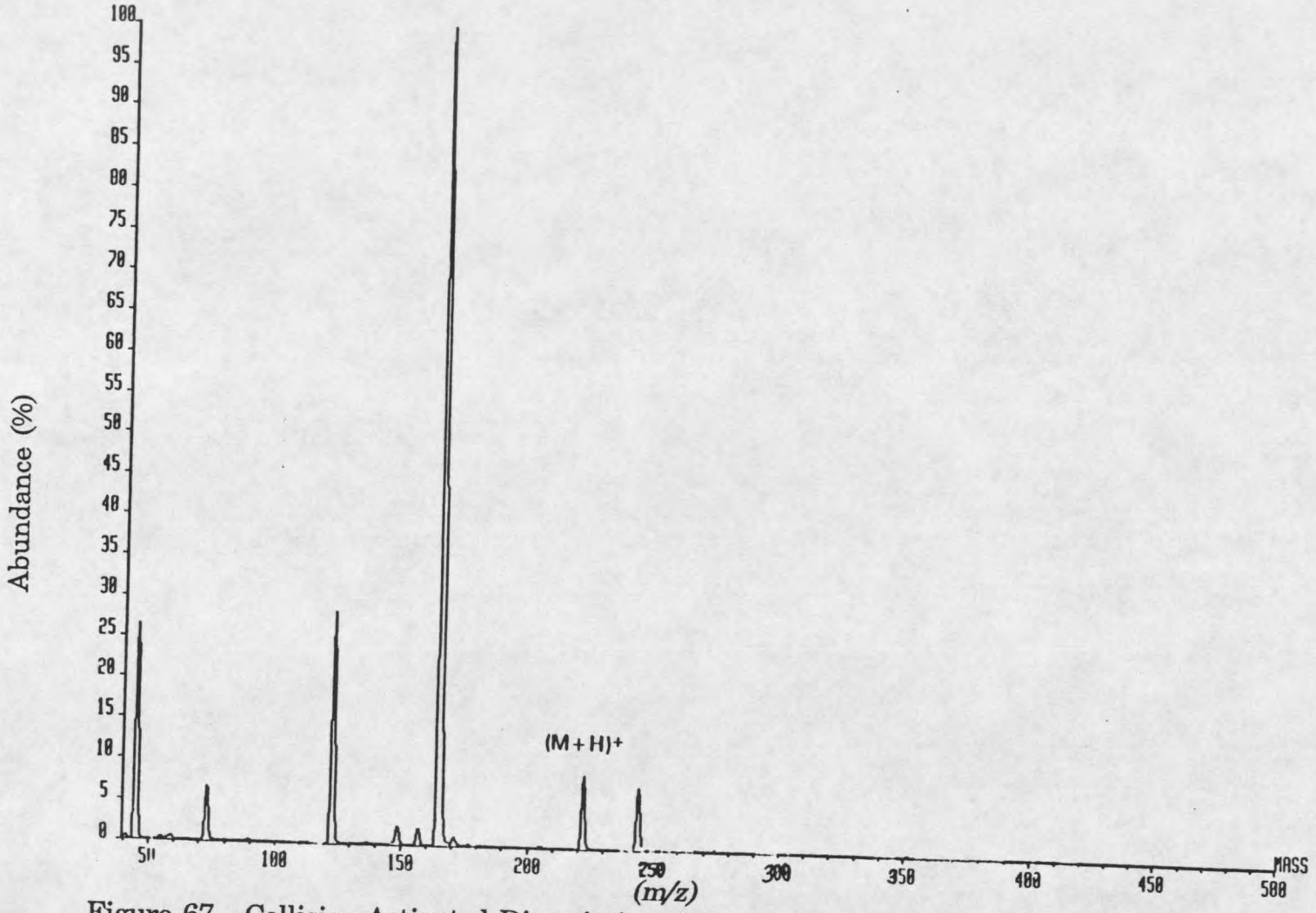


Figure 67. Collision-Activated Dissociation Spectrum of Carbofuran. P. D. 85 Volts.

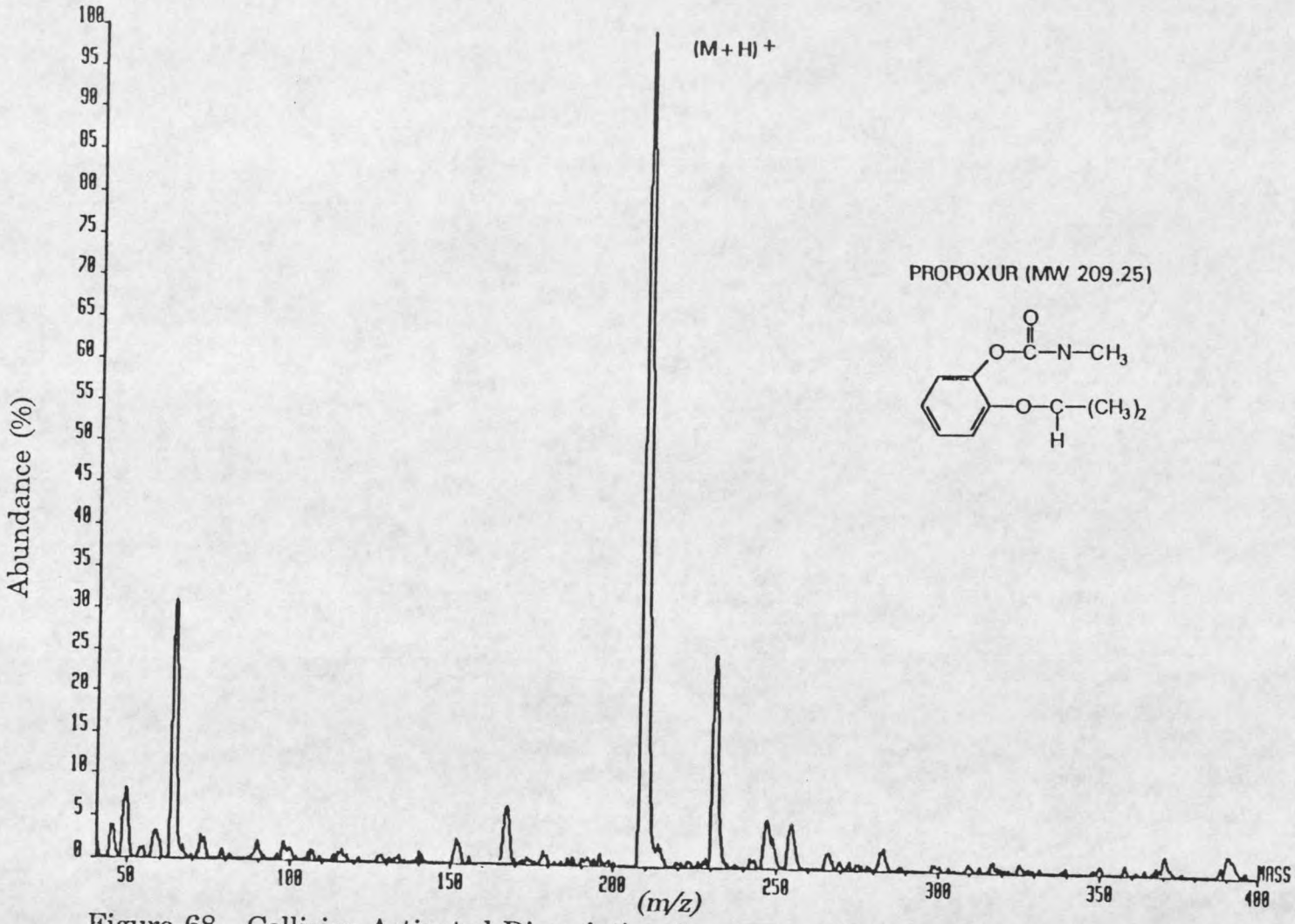


Figure 68. Collision-Activated Dissociation Spectrum of Propoxur. P. D. 35 Volts.

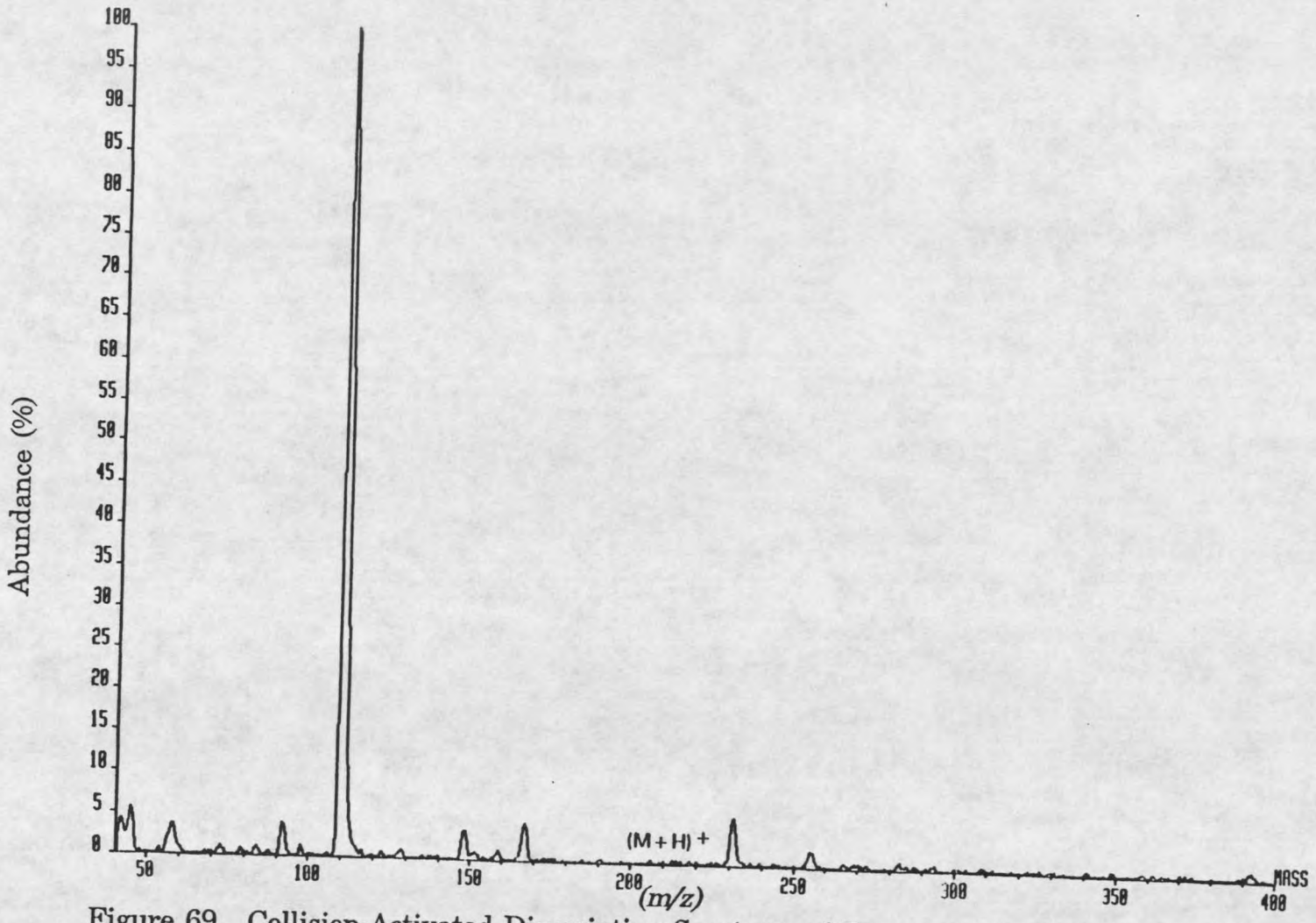


Figure 69. Collision-Activated Dissociation Spectrum of Propoxur. P. D. 75 Volts.

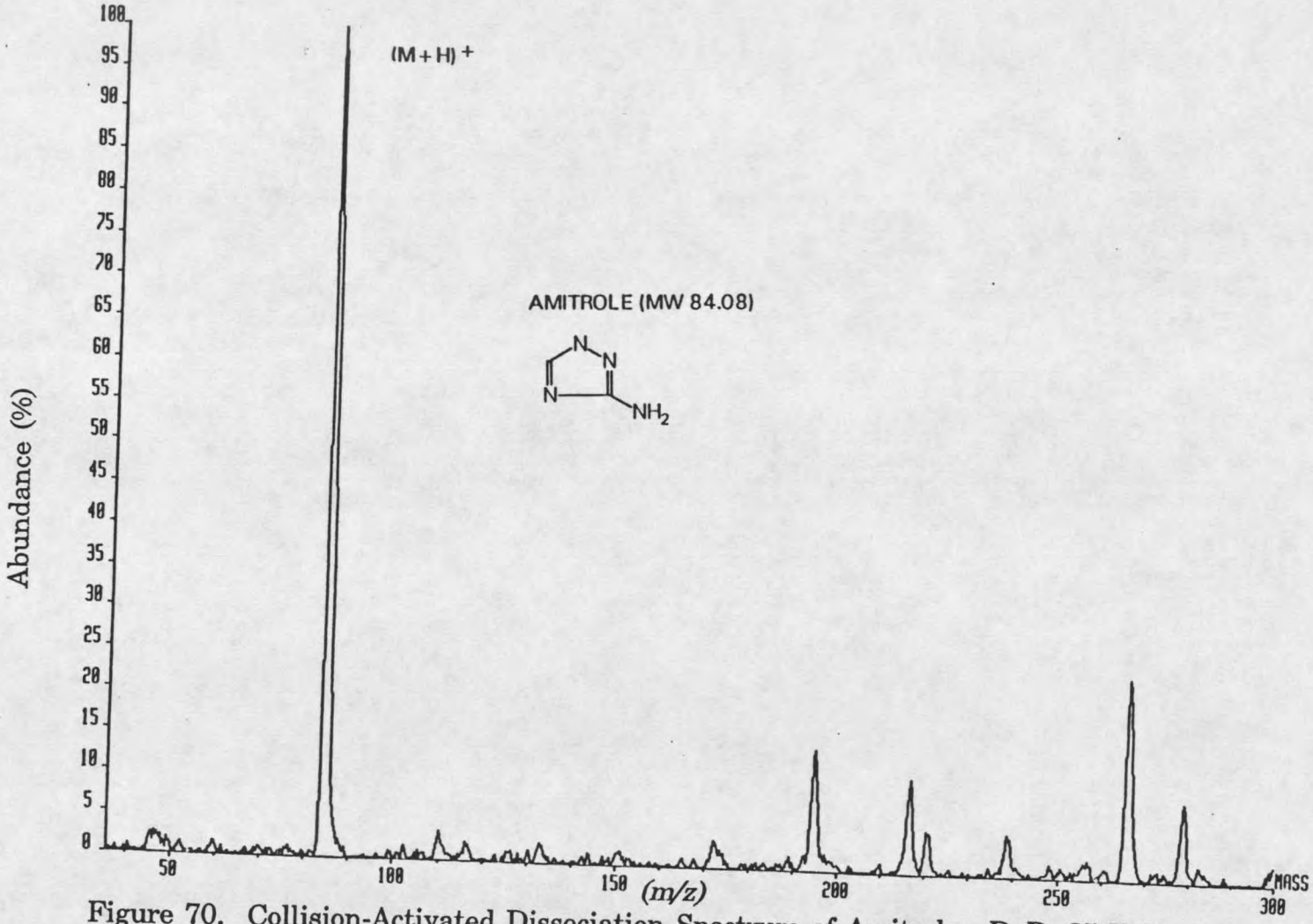


Figure 70. Collision-Activated Dissociation Spectrum of Amitrole. P. D. 35 Volts.

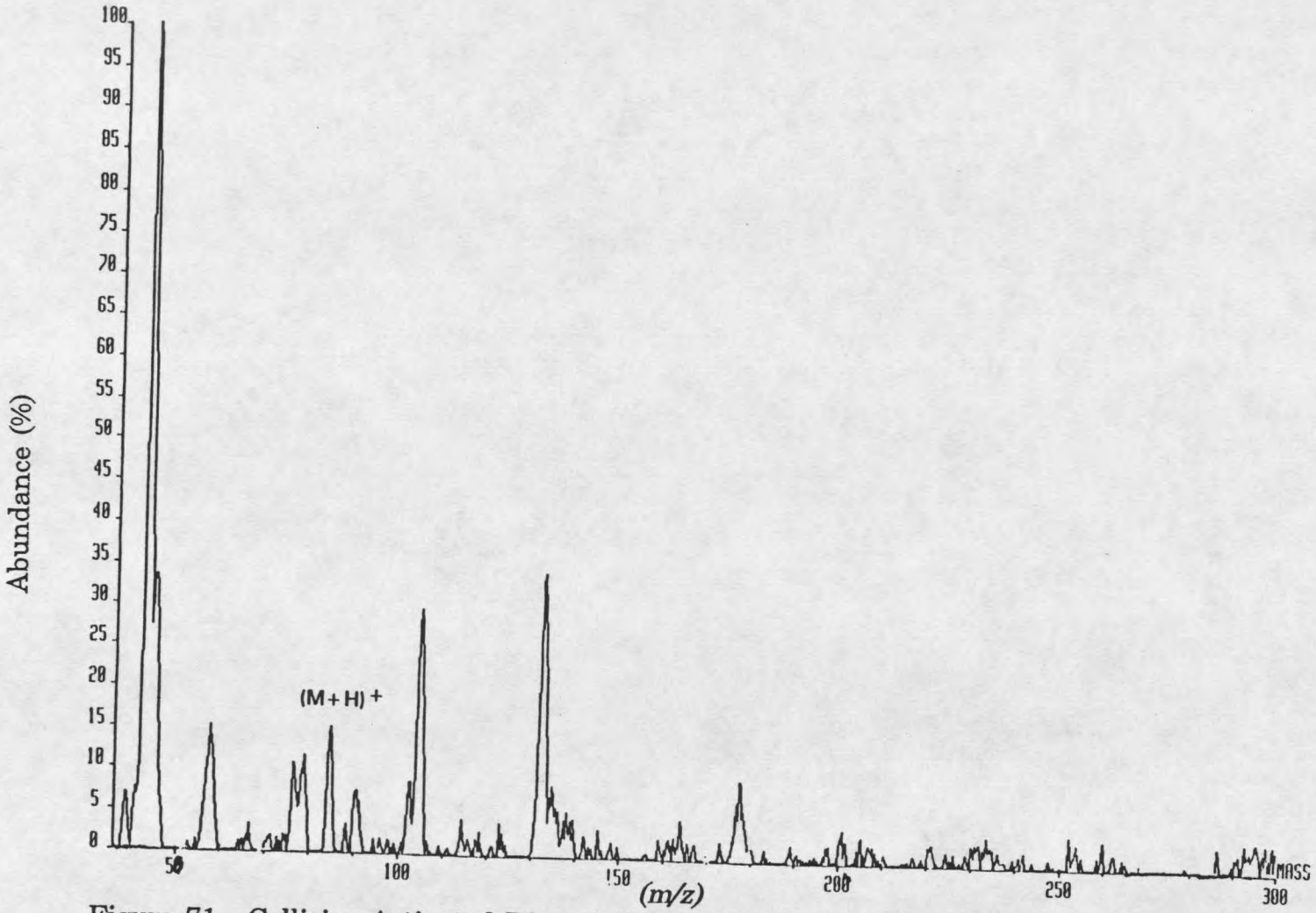


Figure 71. Collision-Activated Dissociation Spectrum of Amitrole. P. D. 135 Volts.

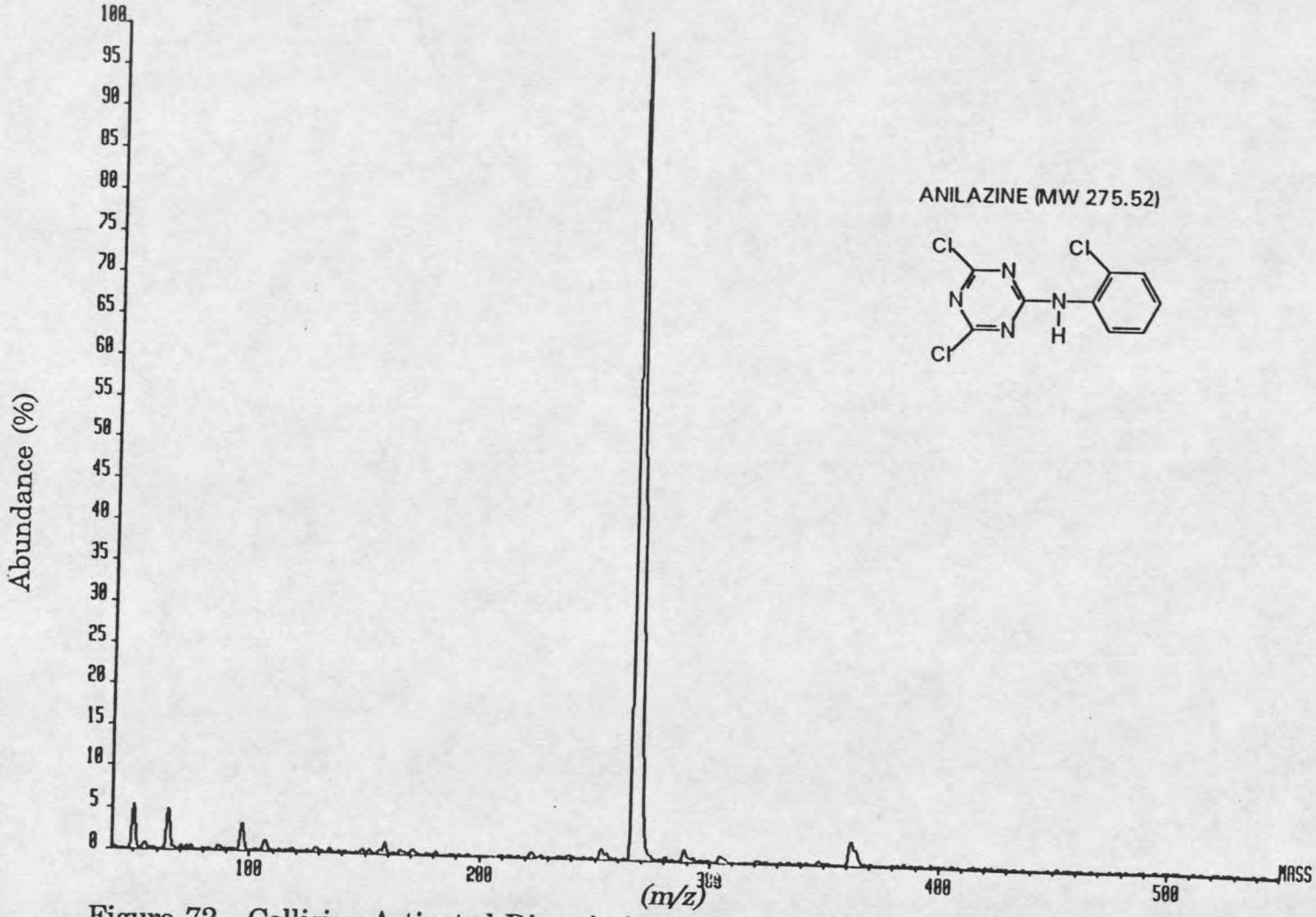


Figure 72. Collision-Activated Dissociation Spectrum of Anilazine. P. D. 35 Volts.

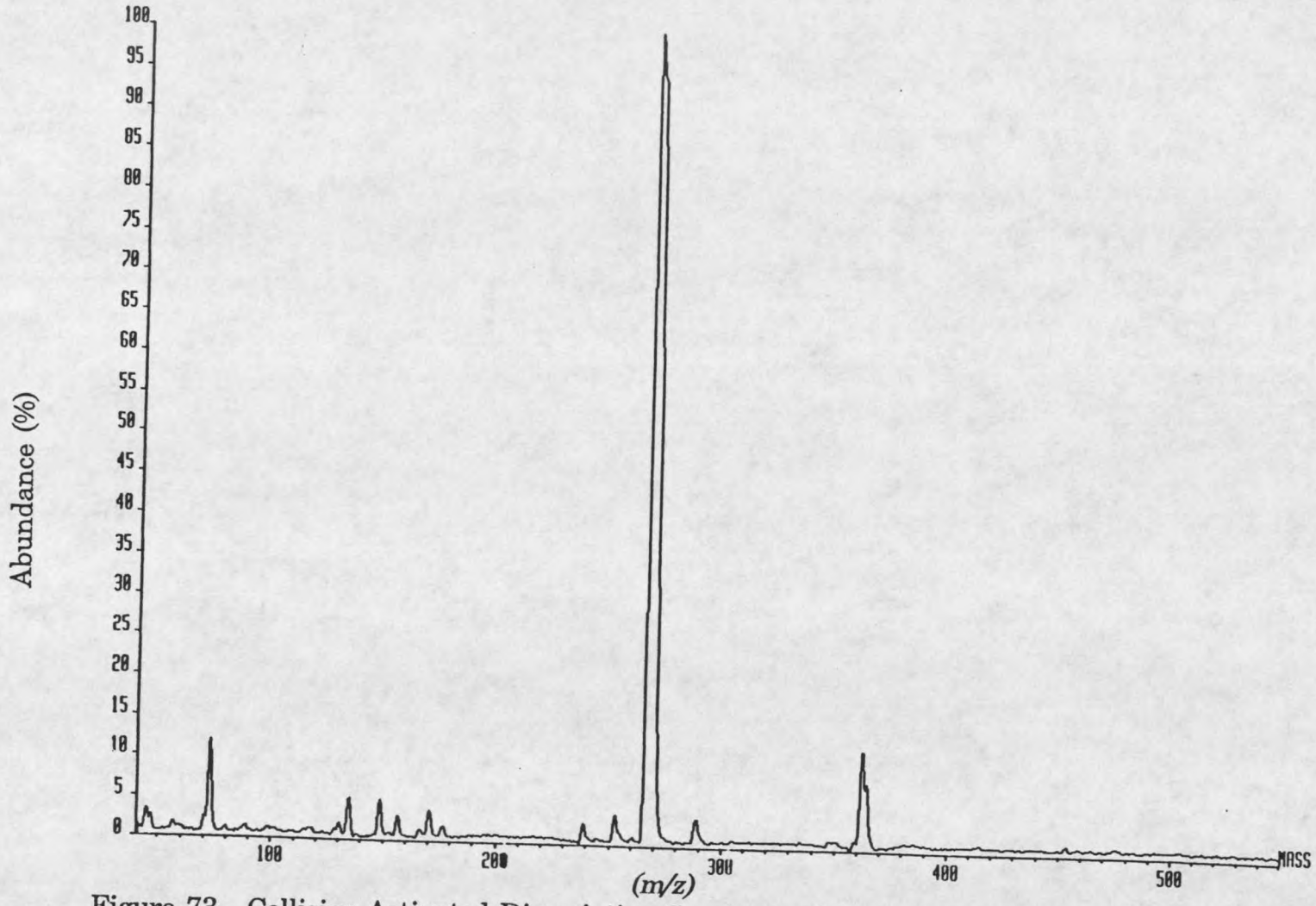


Figure 73. Collision-Activated Dissociation Spectrum of Anilazine. P. D. 85 Volts.

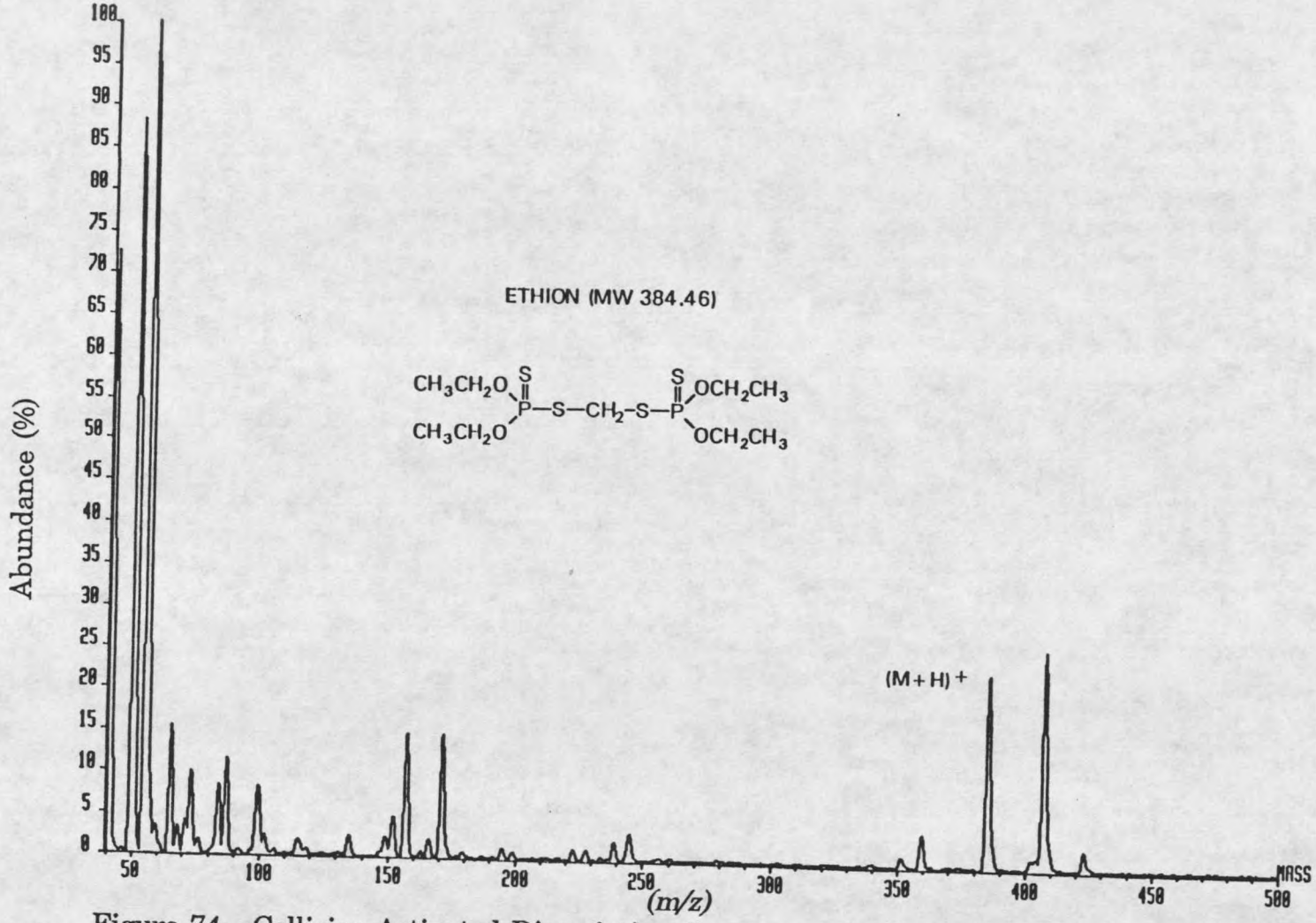


Figure 74. Collision-Activated Dissociation Spectrum of Ethion. P. D. 45 Volts.

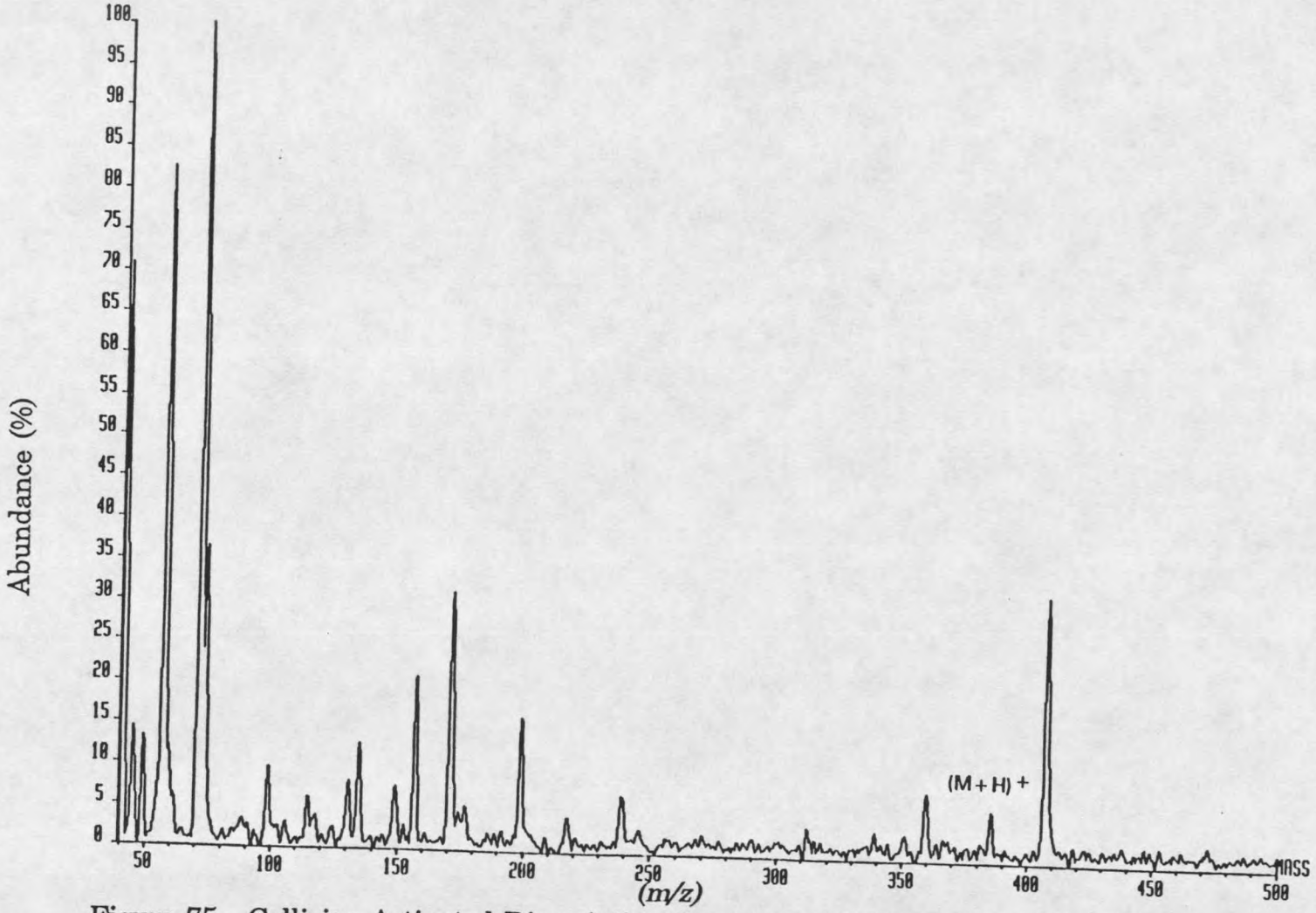


Figure 75. Collision-Activated Dissociation Spectrum of Ethion. P. D. 85 Volts.

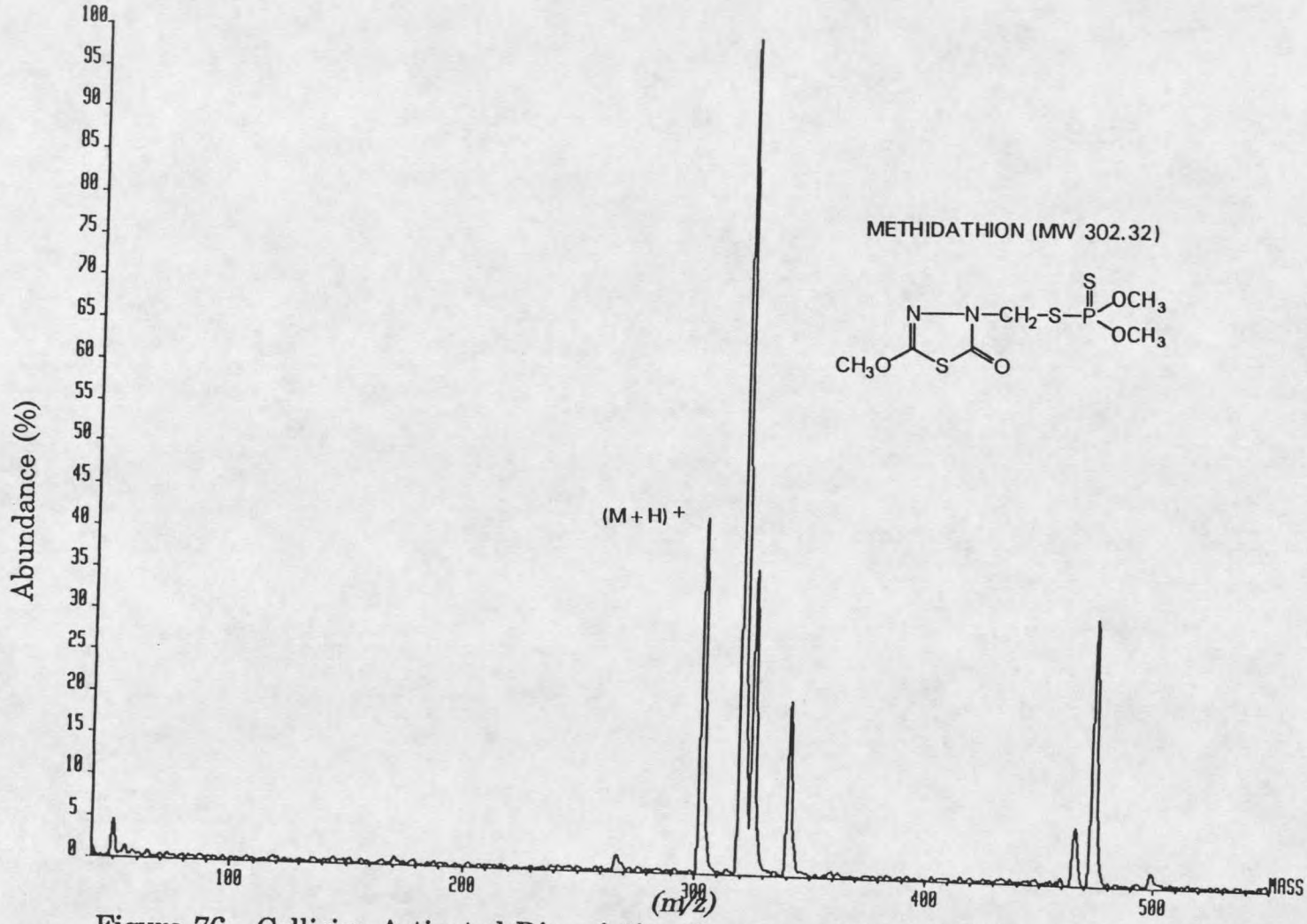


Figure 76. Collision-Activated Dissociation Spectrum of Methidathion. P. D. 45 Volts.

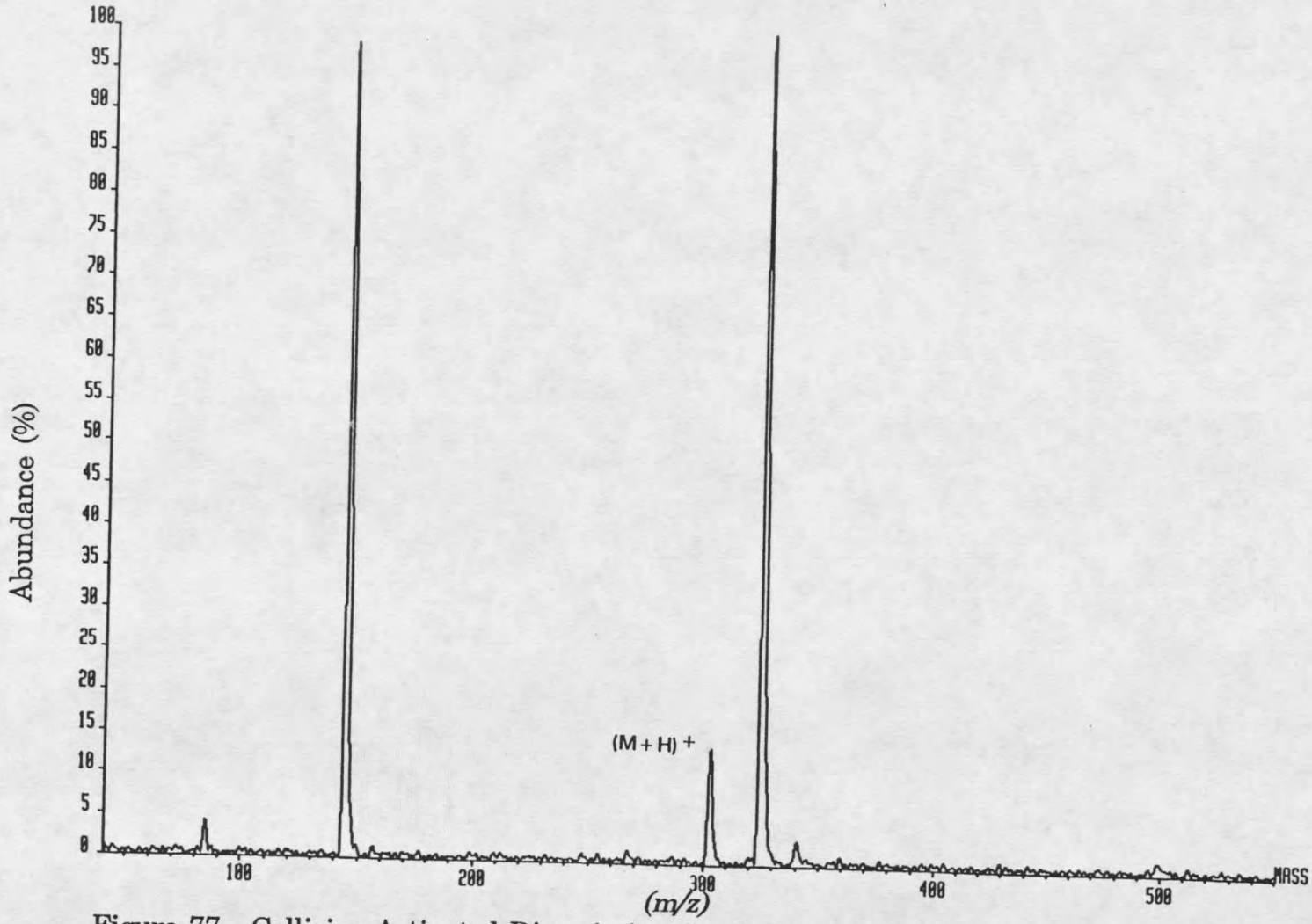


Figure 77. Collision-Activated Dissociation Spectrum of Methidathion. P. D. 85 Volts.

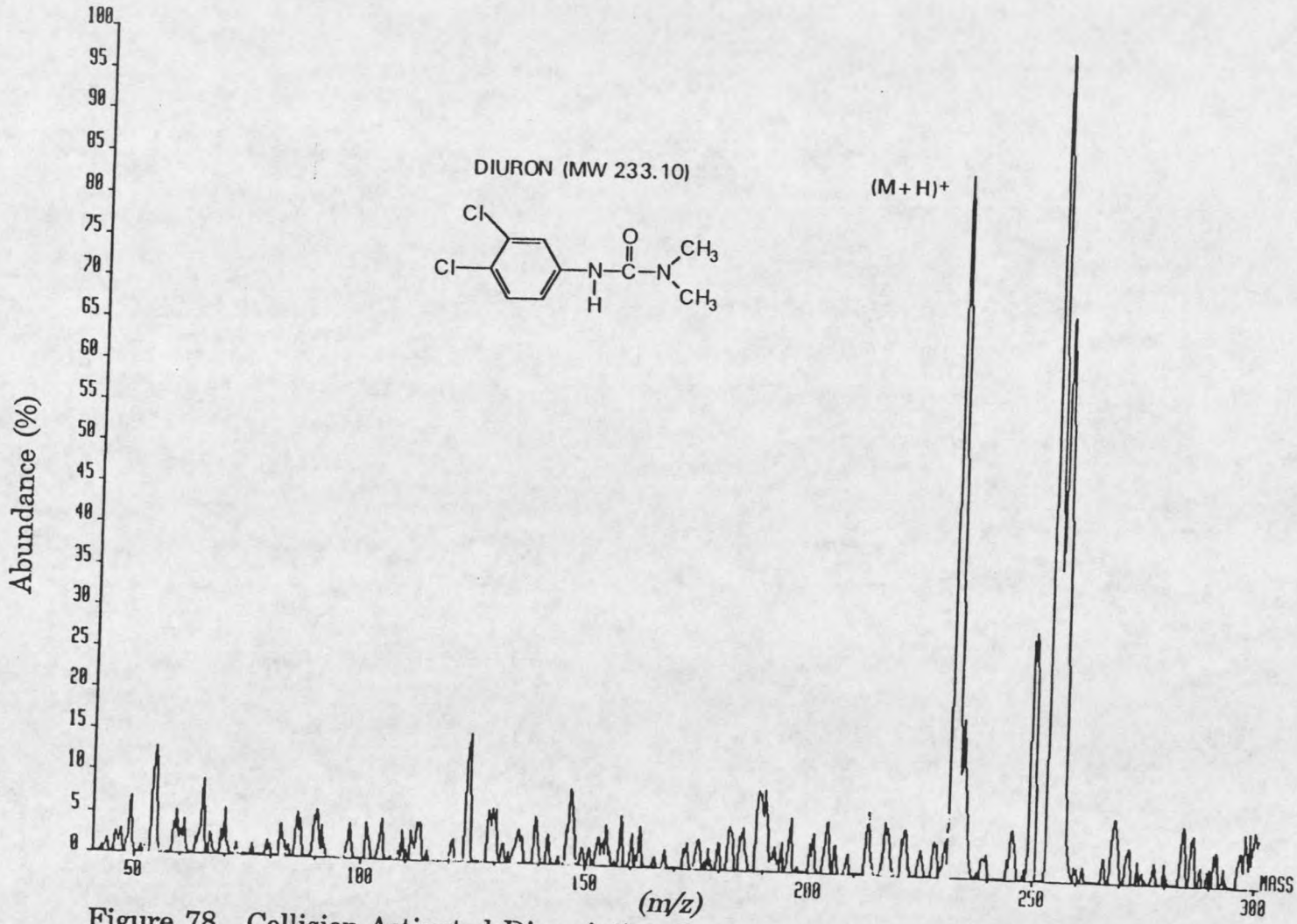


Figure 78. Collision-Activated Dissociation Spectrum of Diuron. P. D. 45 Volts.

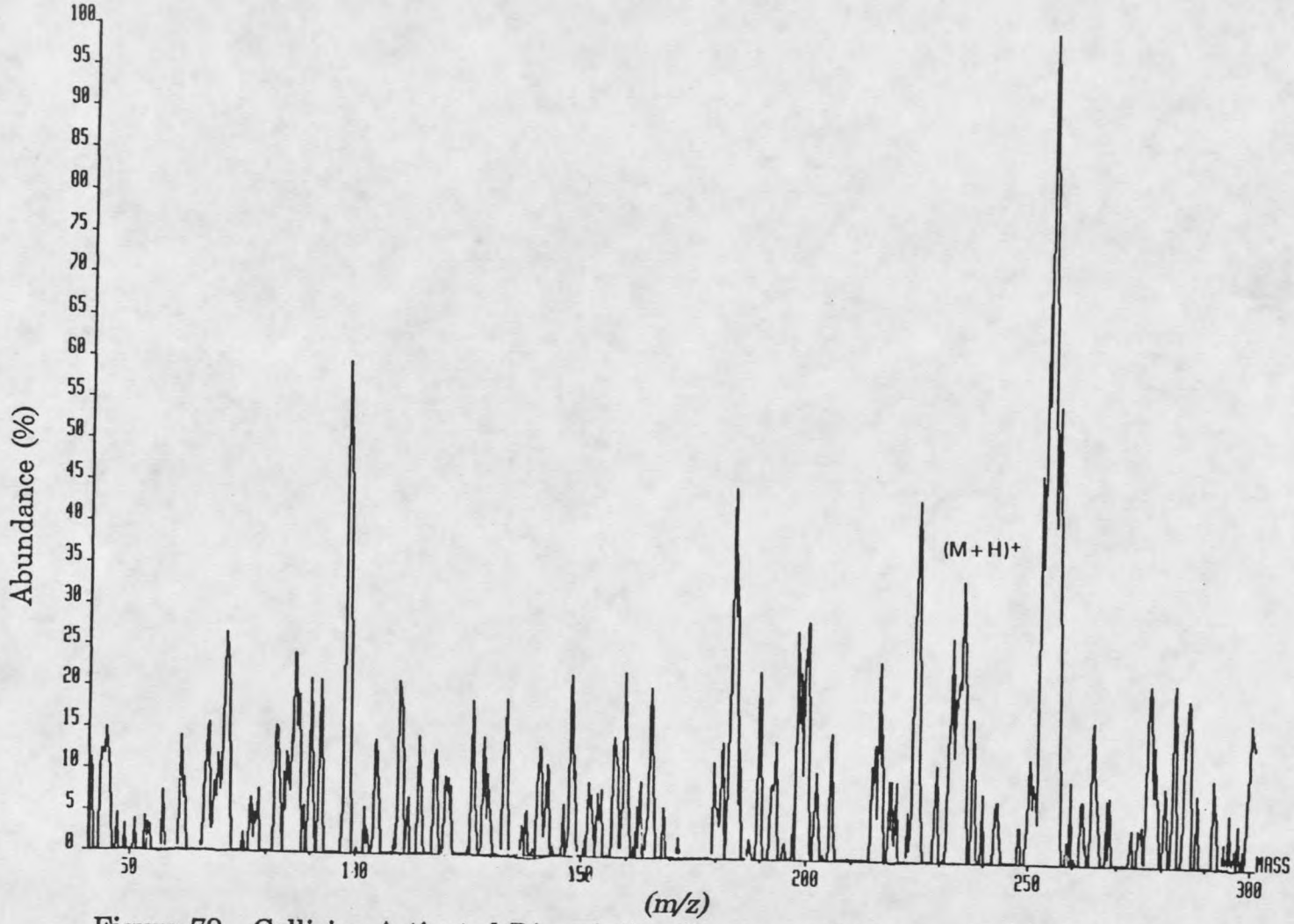


Figure 79. Collision-Activated Dissociation Spectrum of Diuron. P. D. 75 Volts.

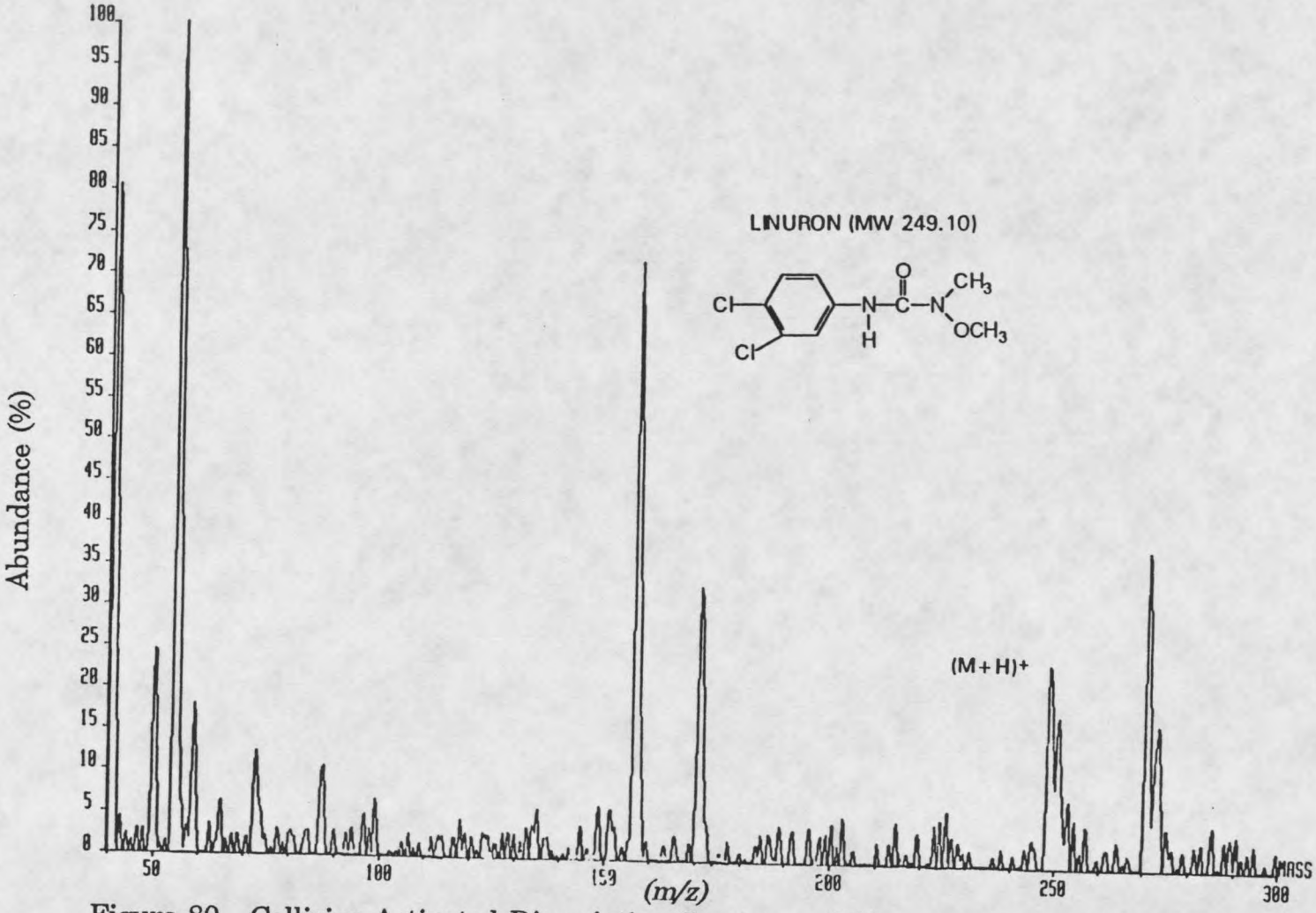


Figure 80. Collision-Activated Dissociation Spectrum of Linuron. P. D. 45 Volts.

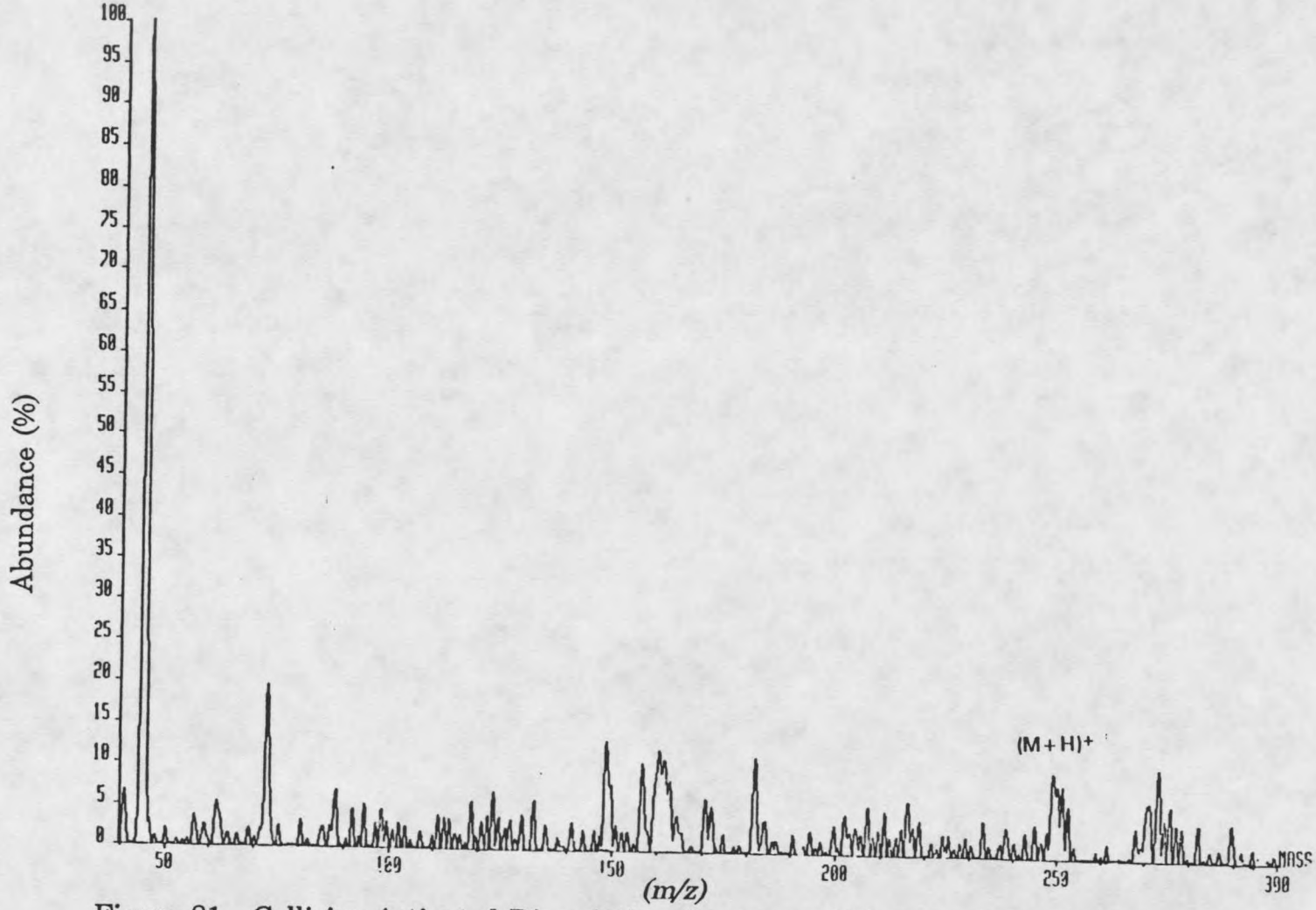


Figure 81. Collision-Activated Dissociation Spectrum of Linuron. P. D. 95 Volts.

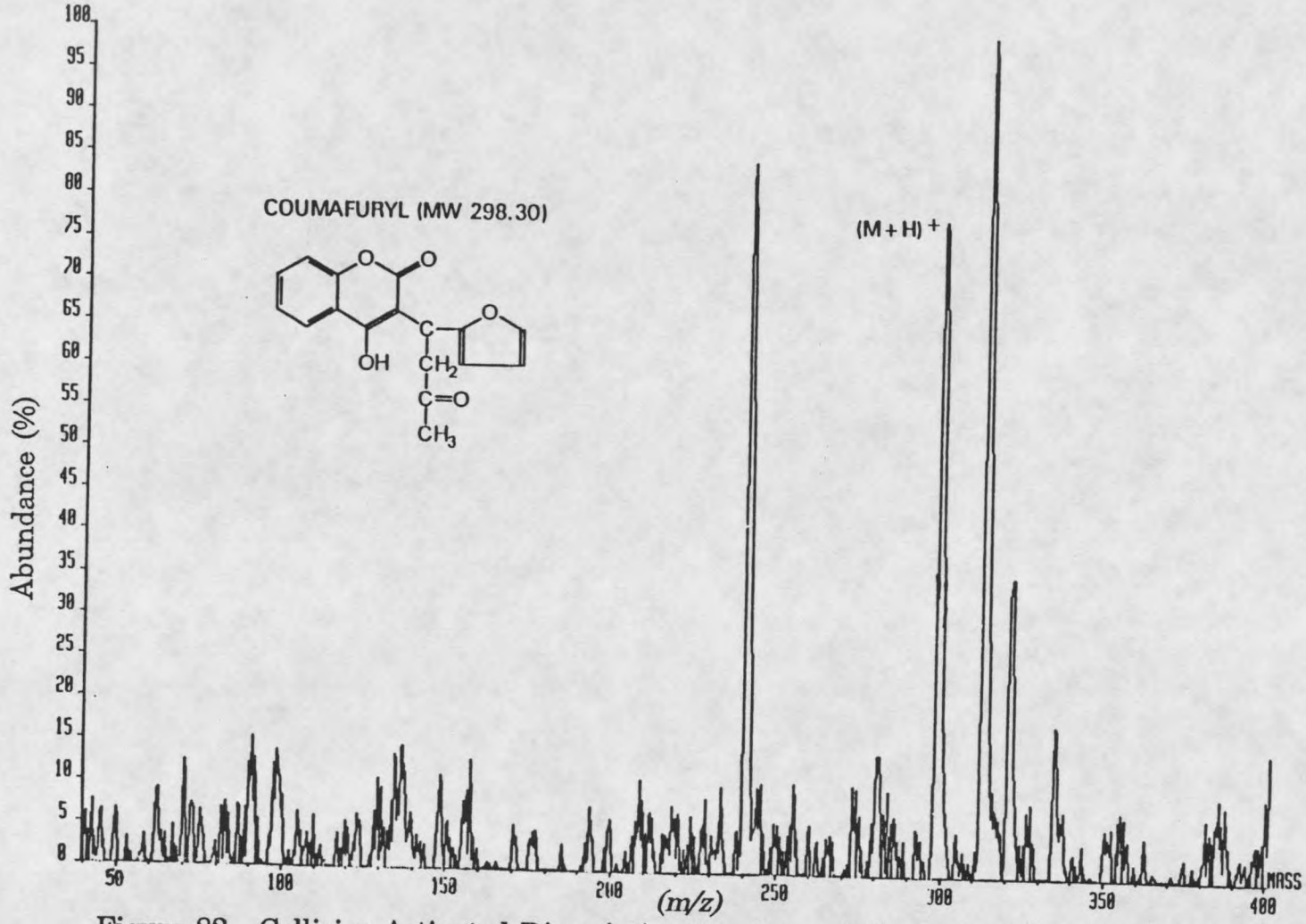


Figure 82. Collision-Activated Dissociation Spectrum of Coumafuryl. P. D. 55 Volts.

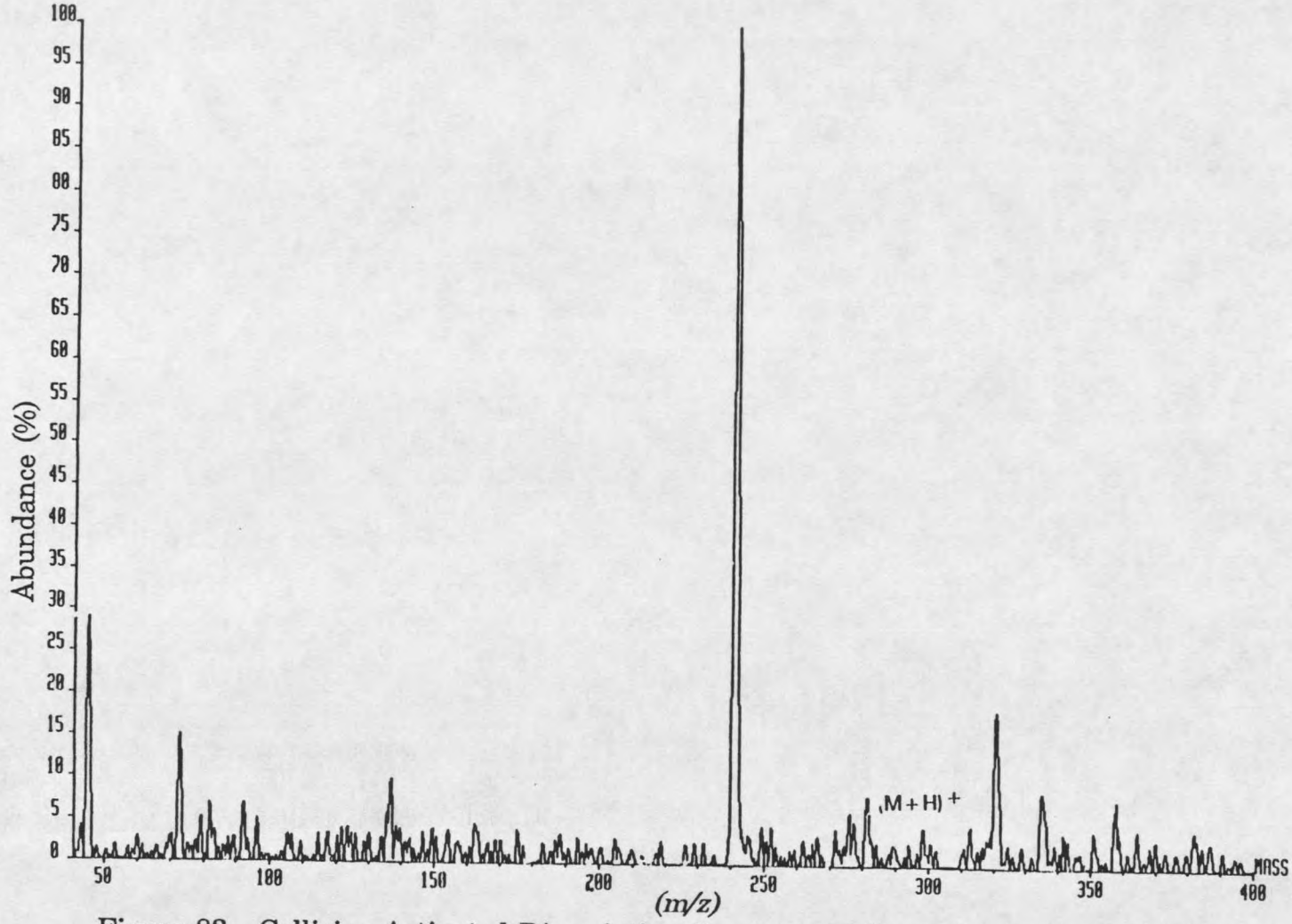


Figure 83. Collision-Activated Dissociation Spectrum of Coumafuryl. P. D. 85 Volts.

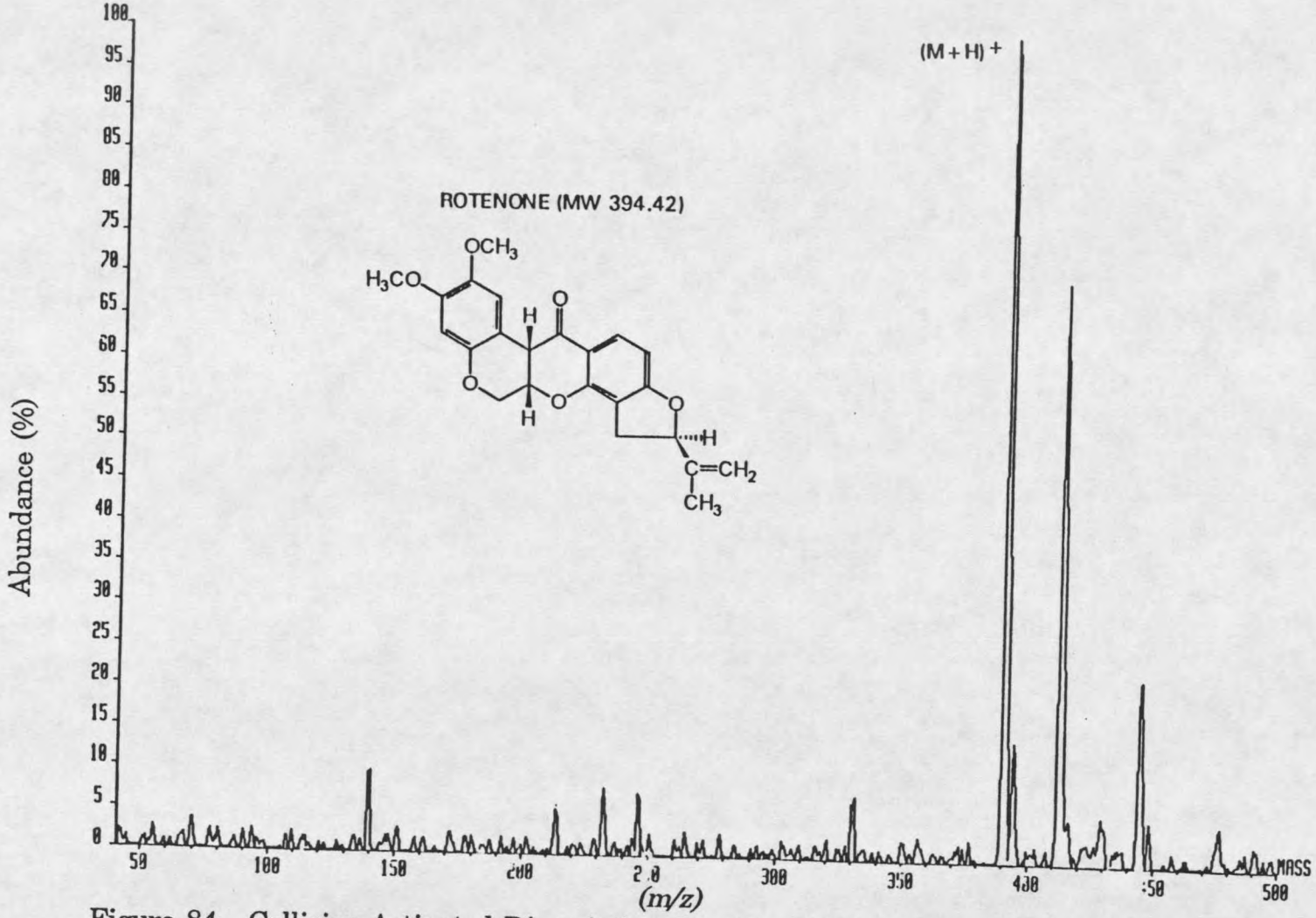


Figure 84. Collision-Activated Dissociation Spectrum of Rotenone. P. D. 55 Volts.

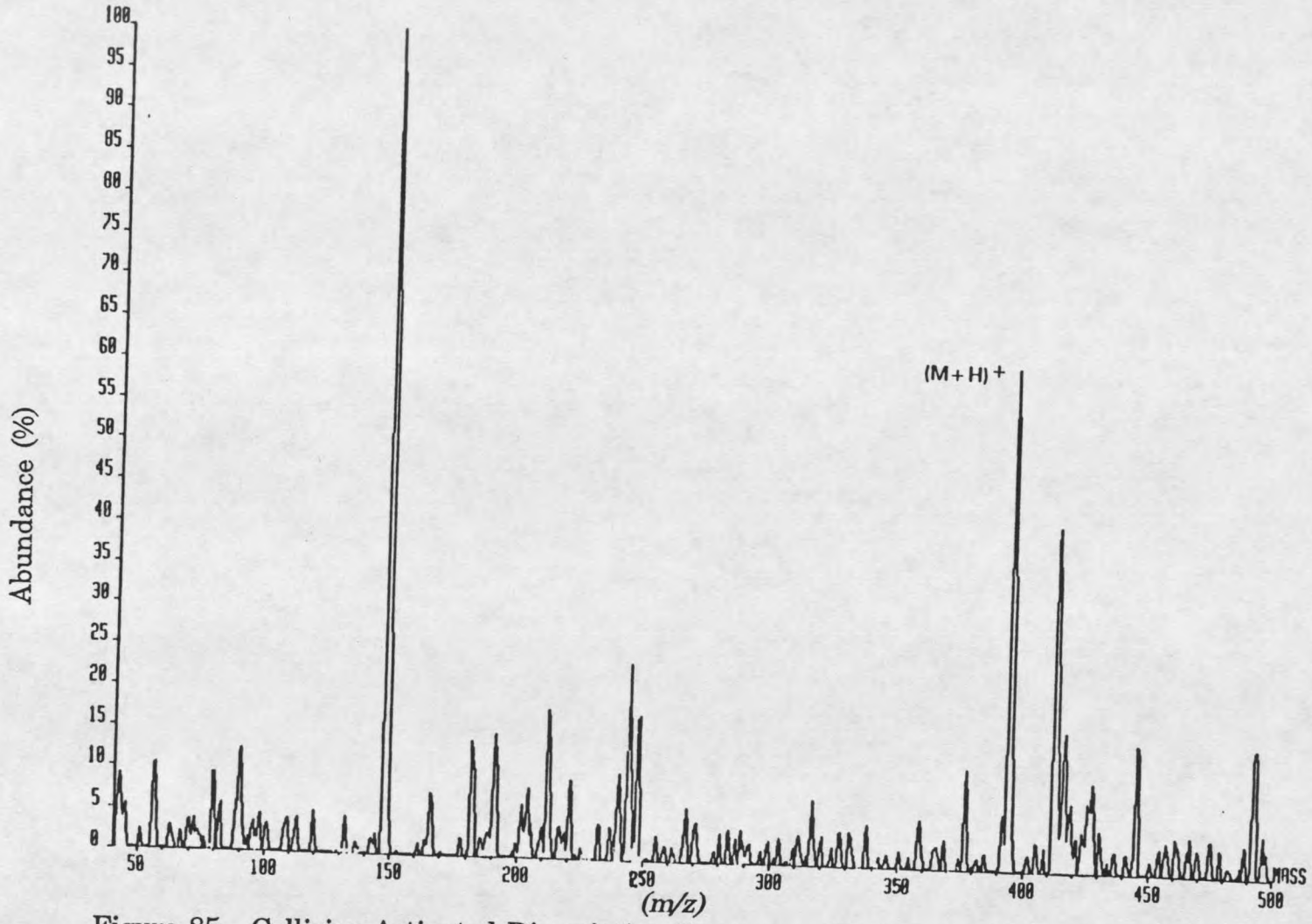


Figure 85. Collision-Activated Dissociation Spectrum of Rotenone. P. D. 120 Volts.

APPENDIX D

NEAT PESTICIDE RESPONSE AS A FUNCTION OF POTENTIAL DIFFERENCE

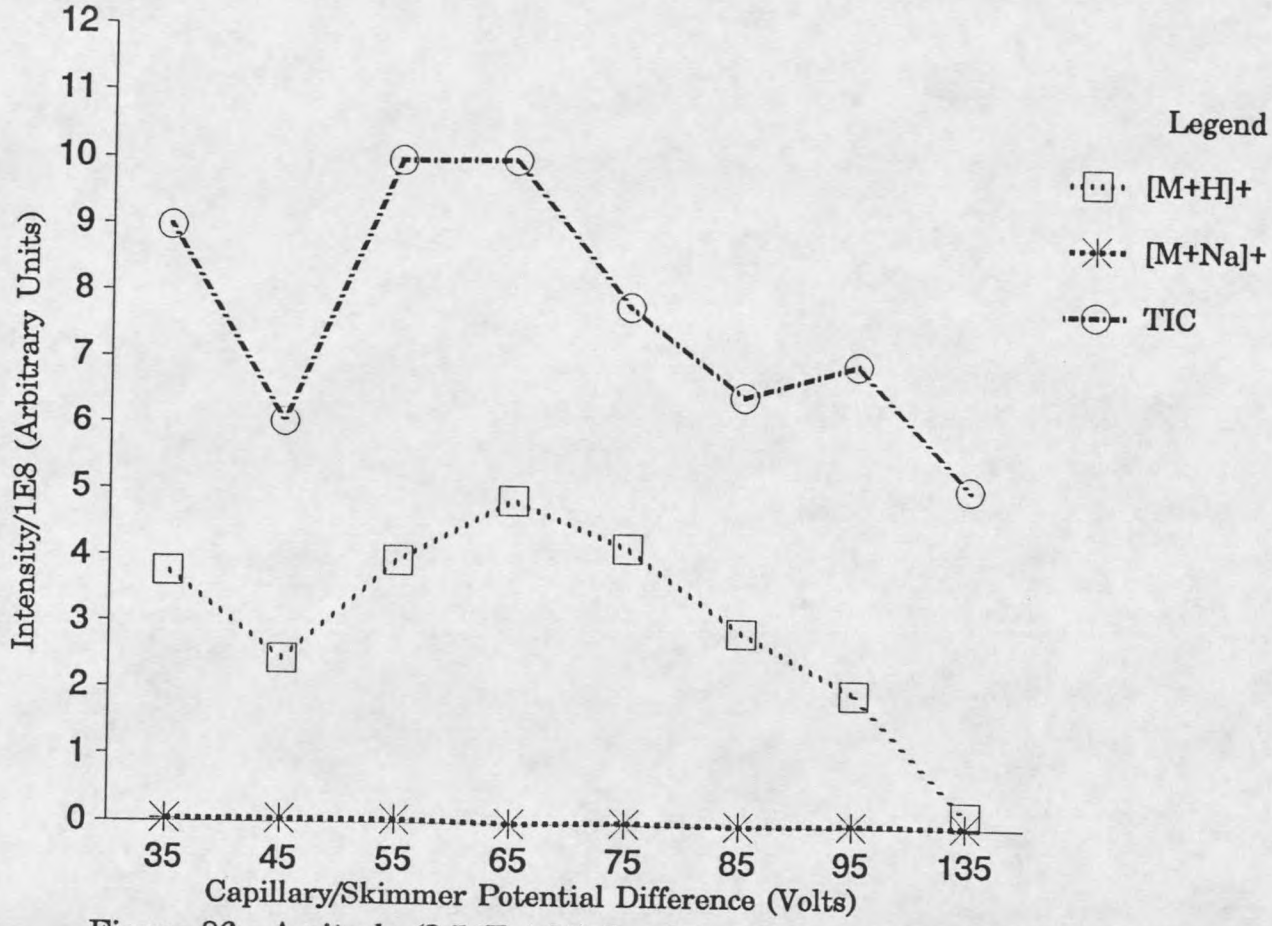


Figure 86. Amitrole (2.54E-4 M) Ion Intensity as a Function of Potential Difference.

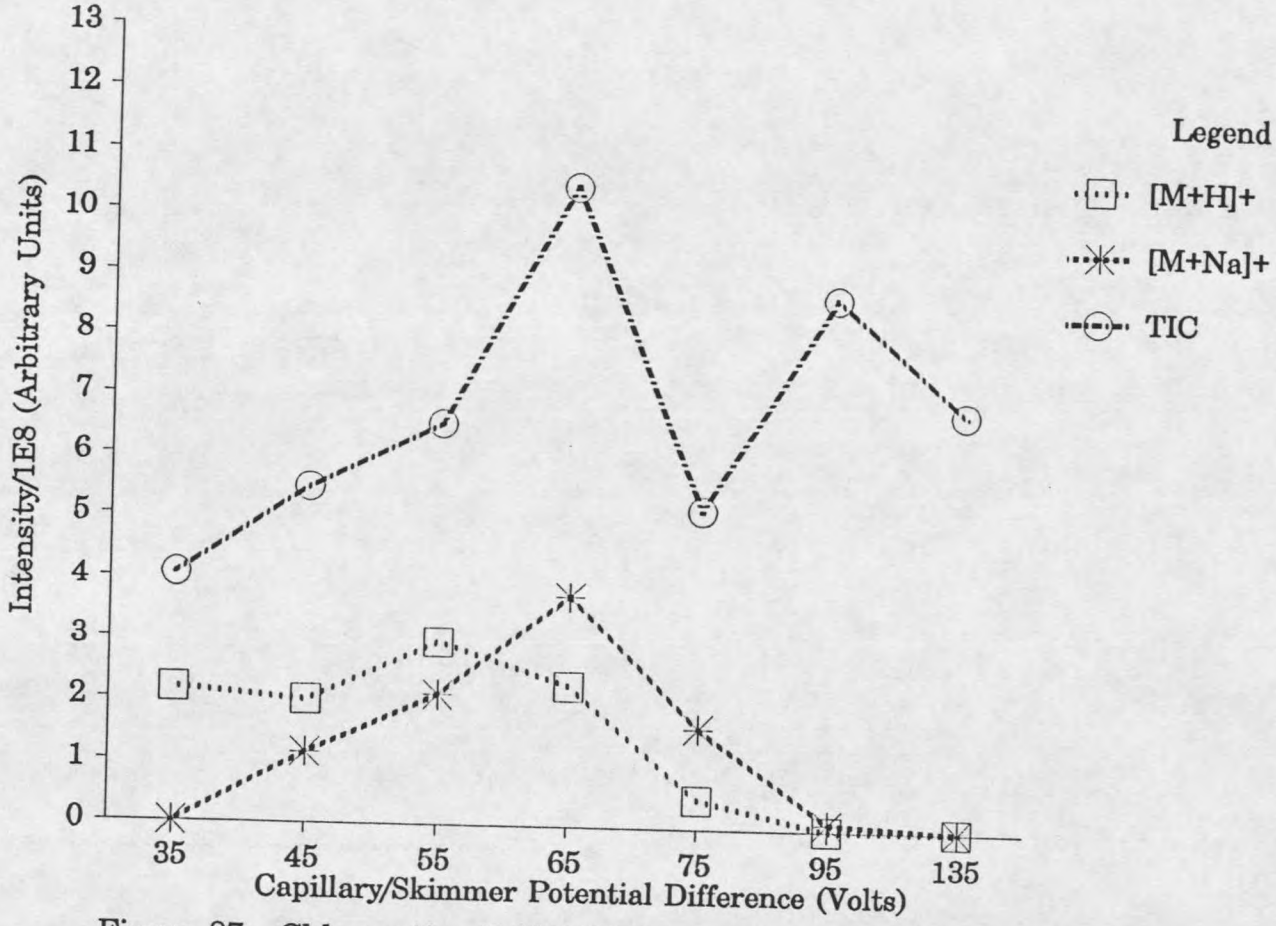


Figure 87. Chlorpyrifos (5.88E-5 M) Ion Intensity as a Function of Potential Difference.

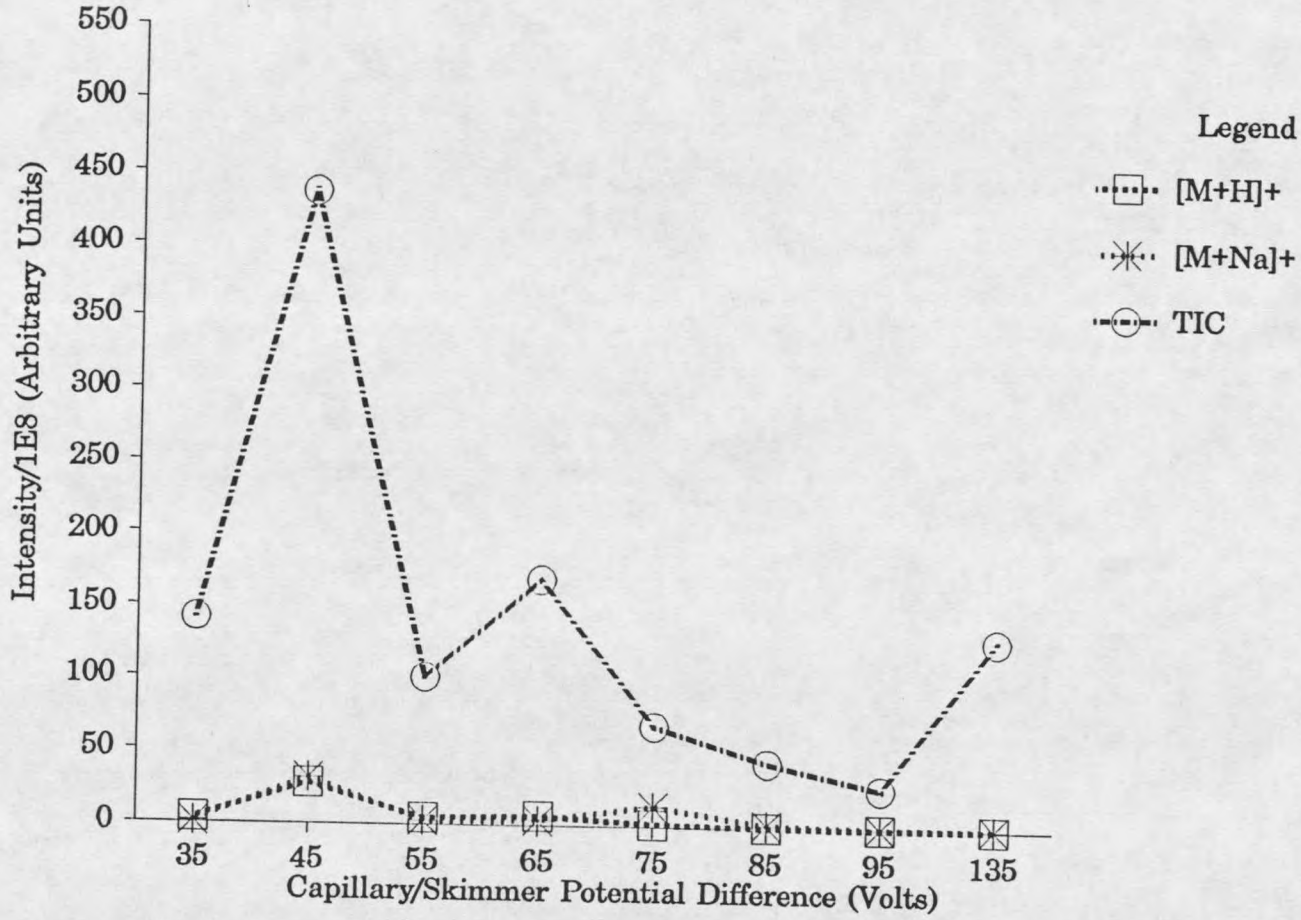


Figure 88. Ethion (1.44E-5 M) Ion Intensity as a Function of Potential Difference.

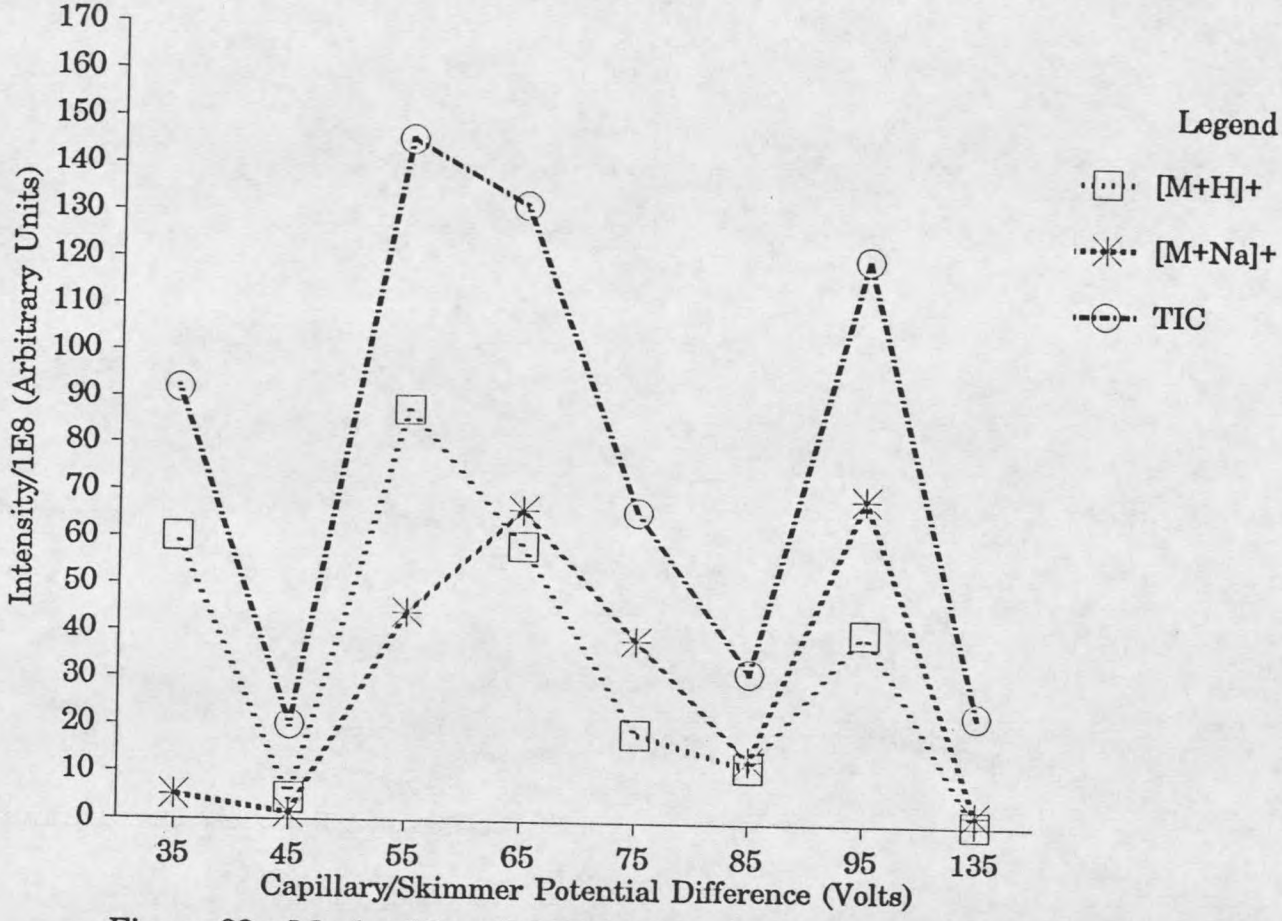


Figure 89. Mephosfolan (2.28E-5 M) Ion Intensity as a Function of Potential Difference.

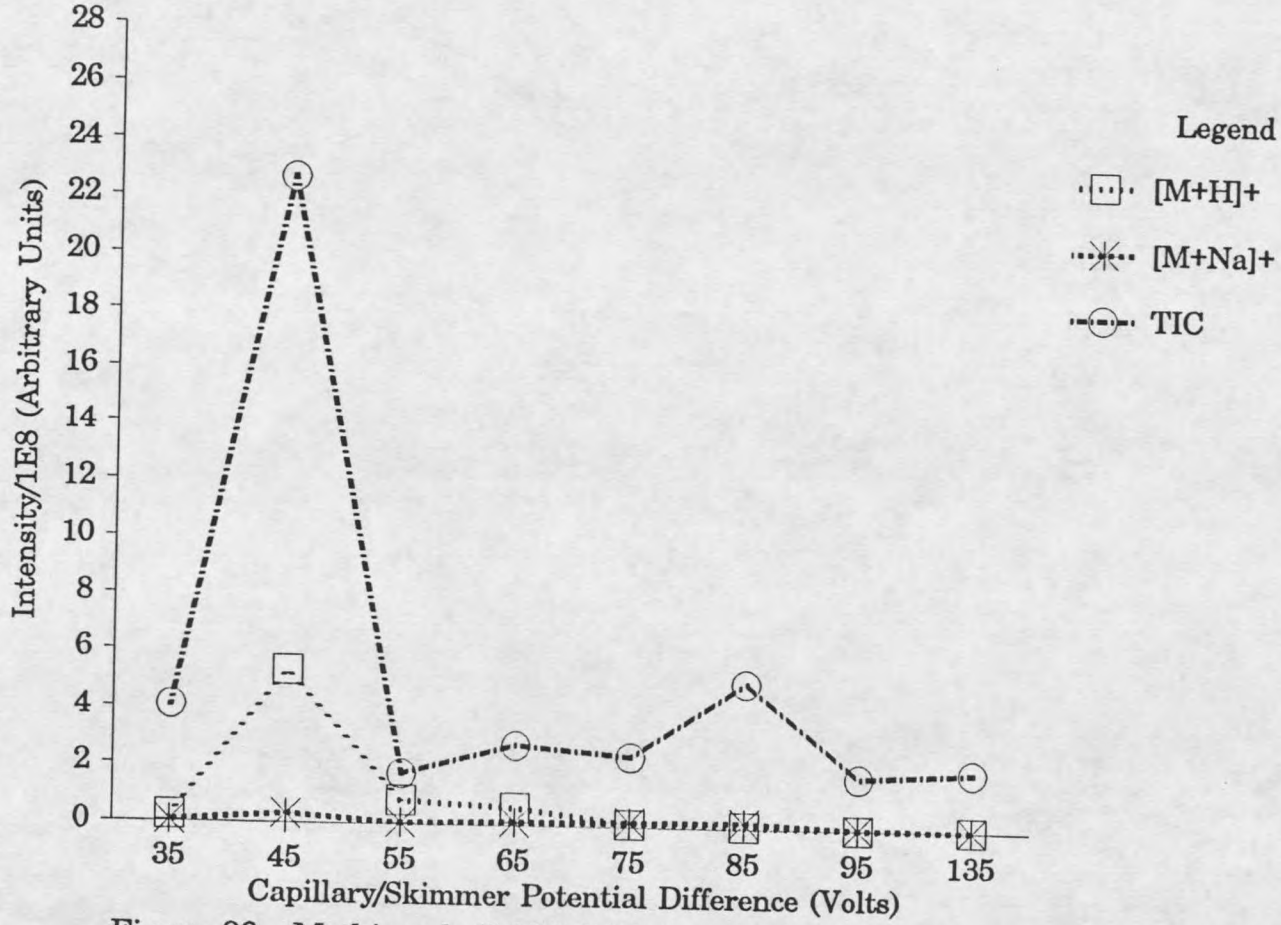


Figure 90. Methiocarb (9.98E-5 M) Ion Intensity as a Function of Potential Difference.

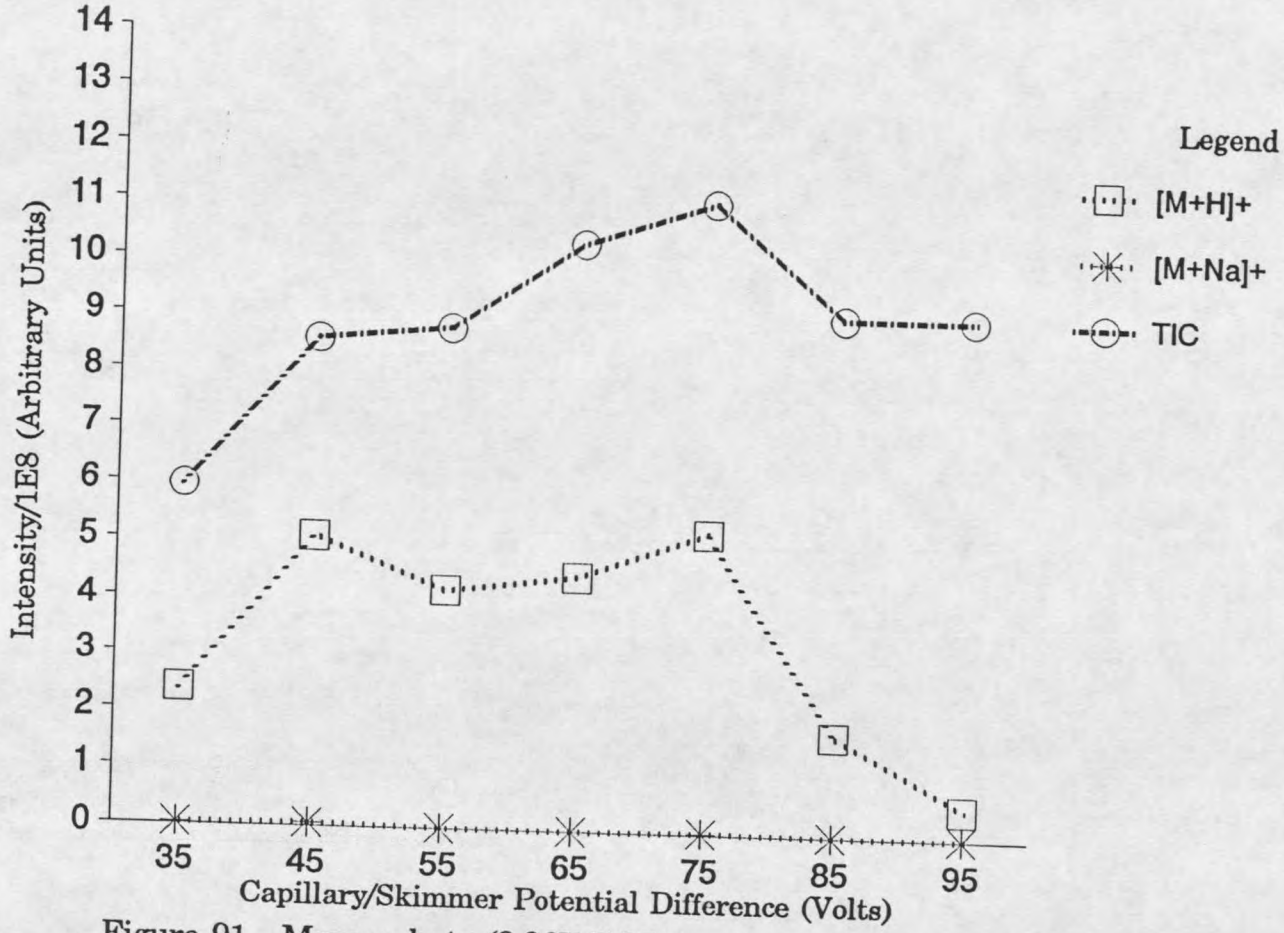


Figure 91. Mexacarbate (8.96E-5 M) Ion Intensity as a Function of Potential Difference.

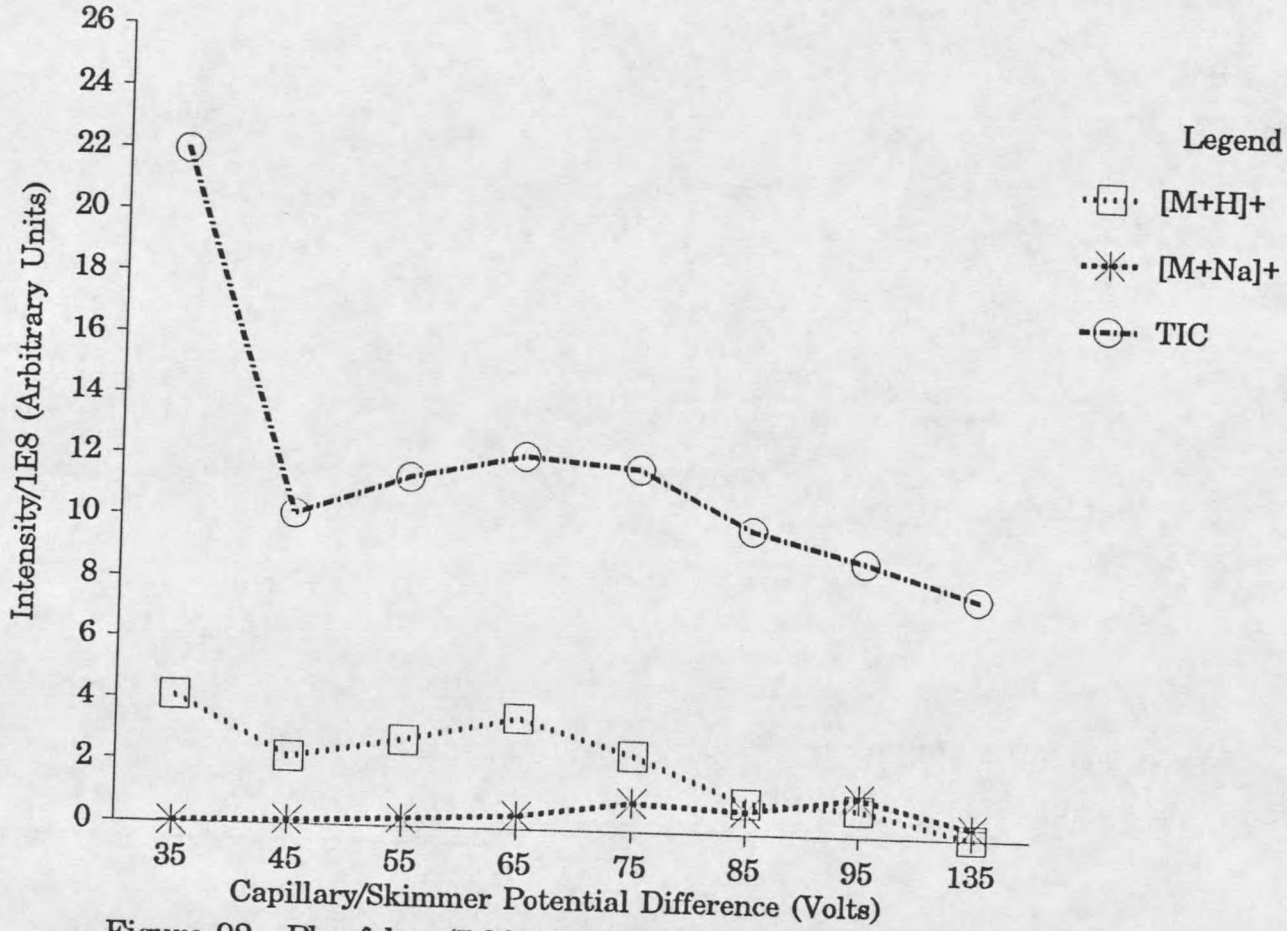


Figure 92. Phosfolan (7.90E-5 M) Ion Intensity as a Function of Potential Difference.

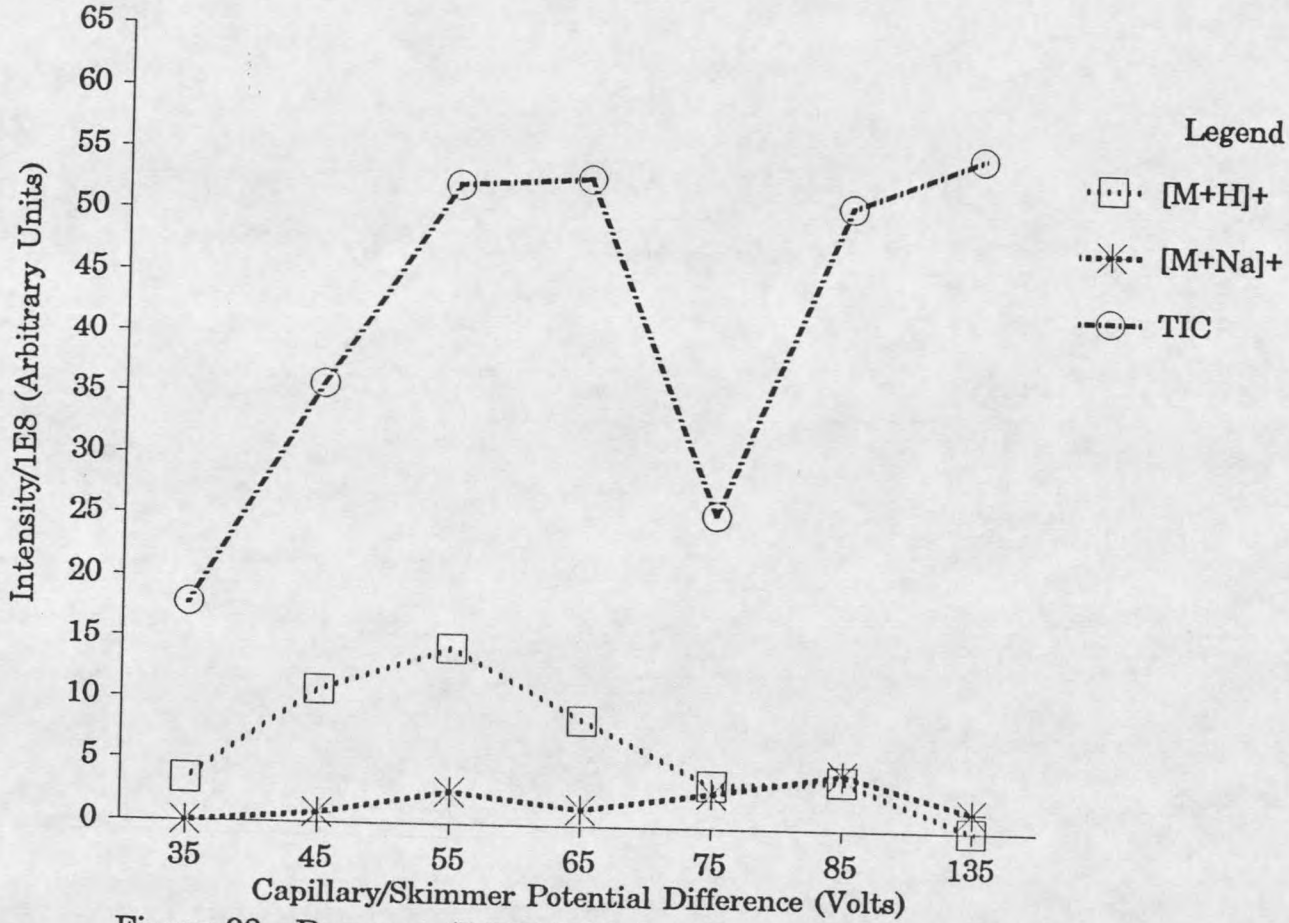


Figure 93. Propoxur (5.51E-5 M) Ion Intensity as a Function of Potential Difference.

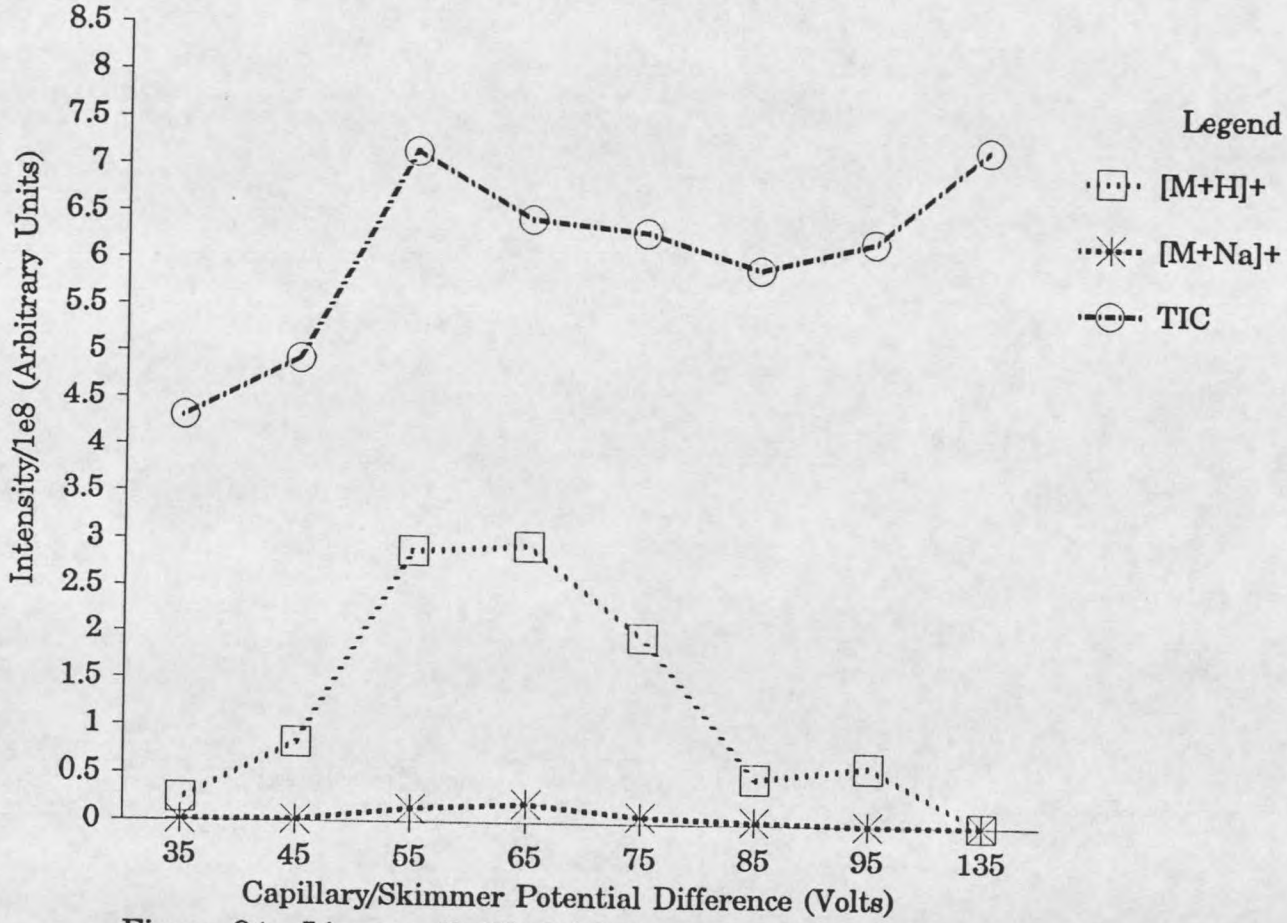


Figure 94. Linuron (8.40E-5 M) Ion Intensity as a Function of Potential Difference.

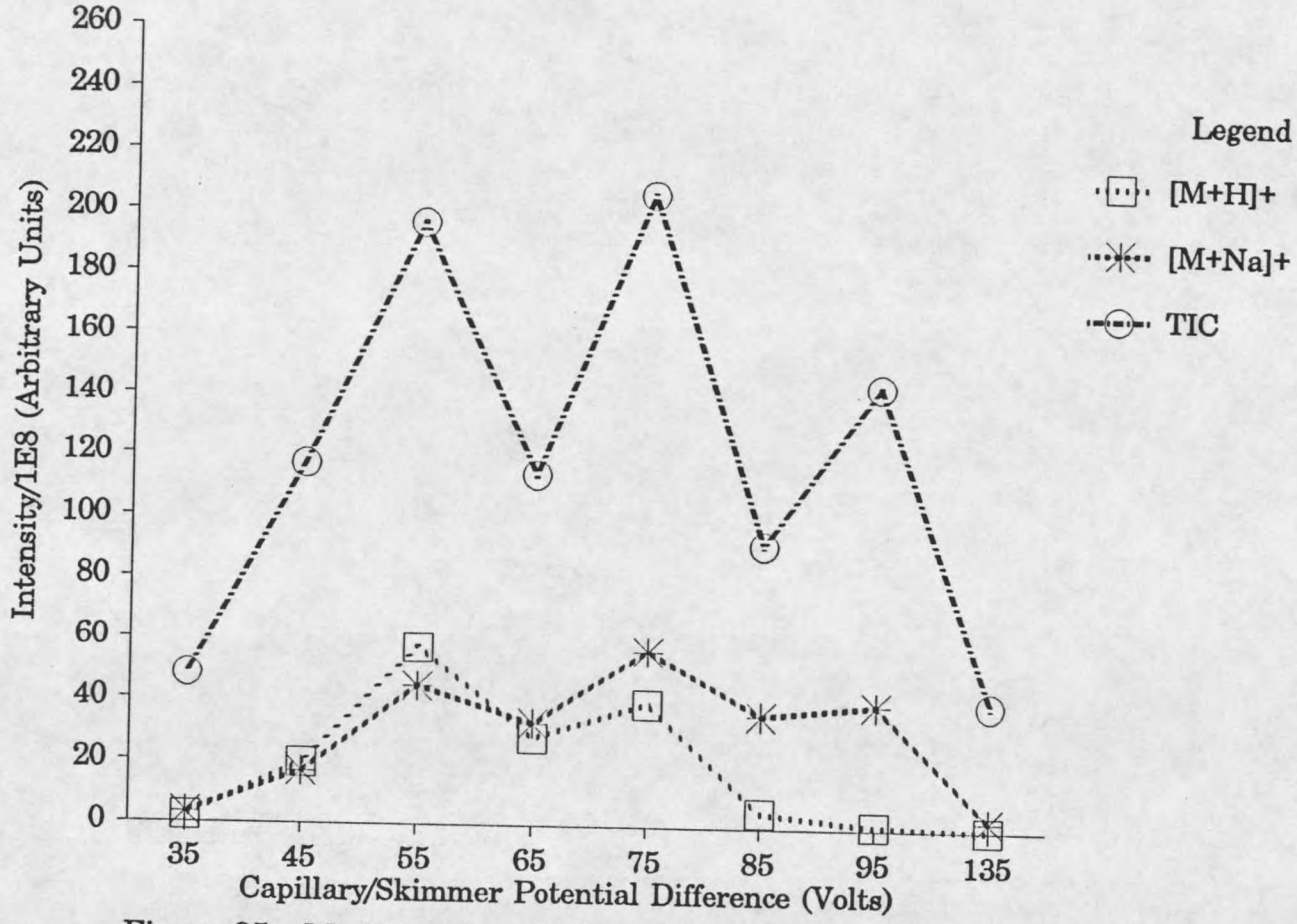


Figure 95. Methidathion (6.66E-5 M) Ion Intensity as a Function of Potential Difference.

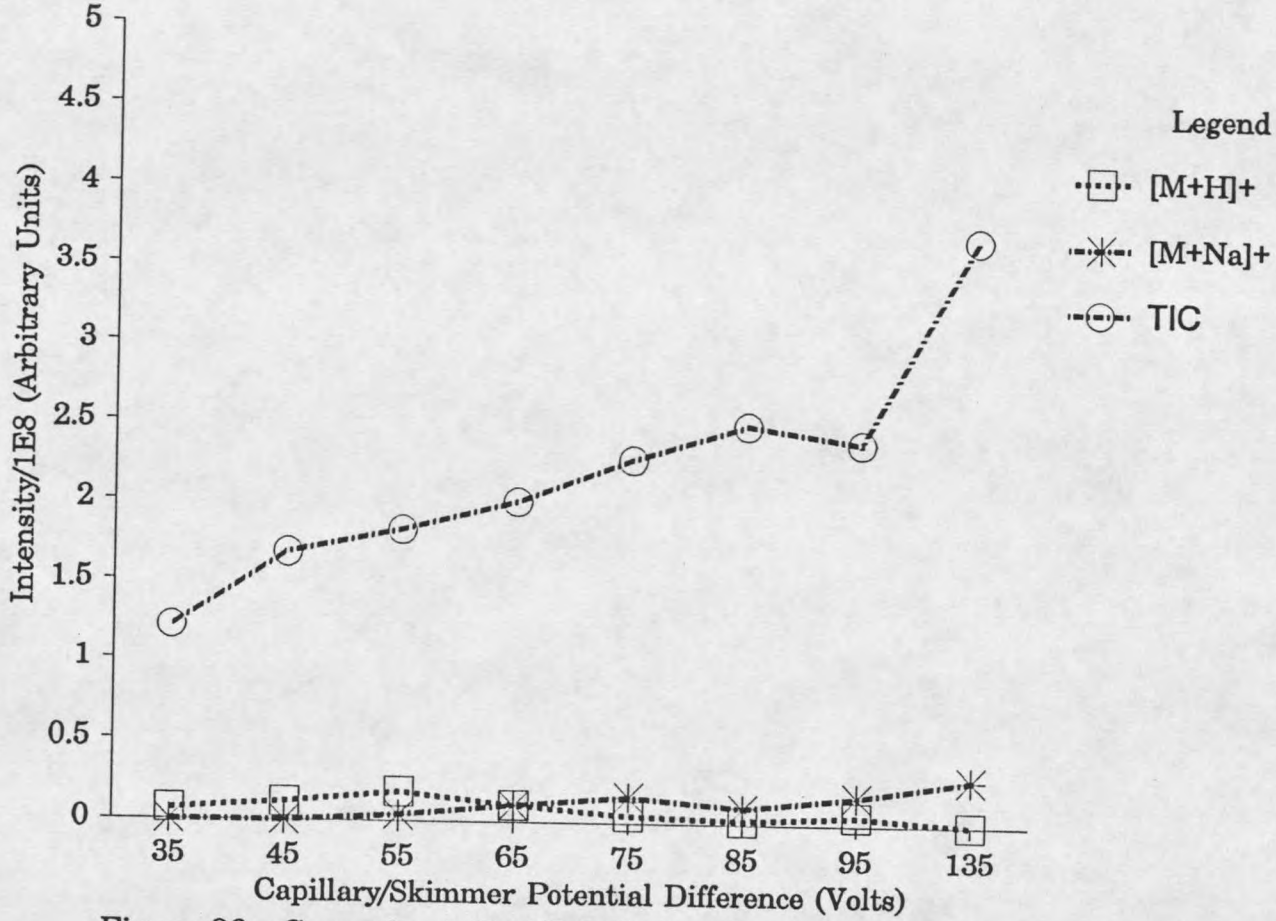


Figure 96. Coumafuryl (6.46E-5 M) Ion Intensity as a Function of Potential Difference.

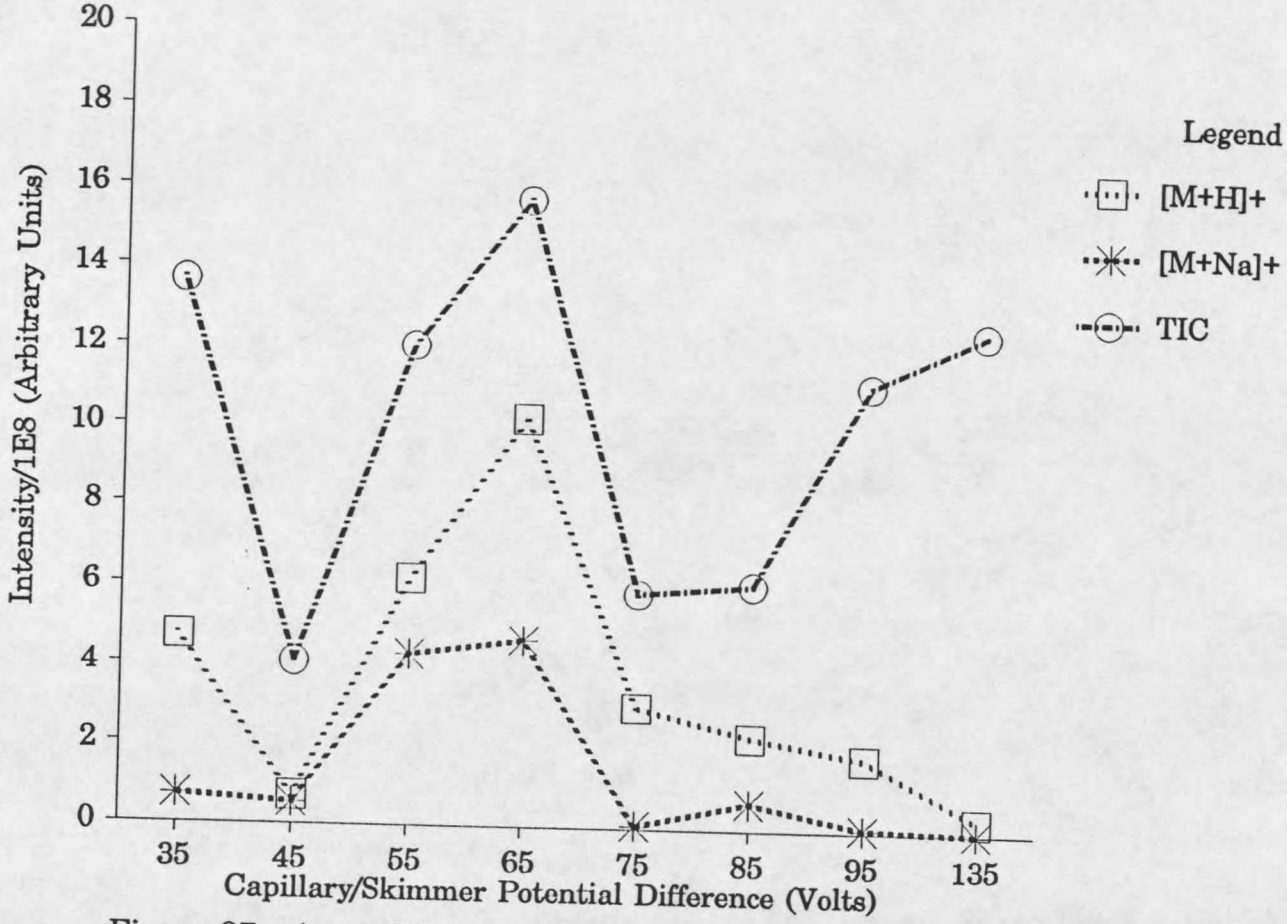


Figure 97. Antu (9.85E-5 M) Ion Intensity as a Function of Potential Difference.

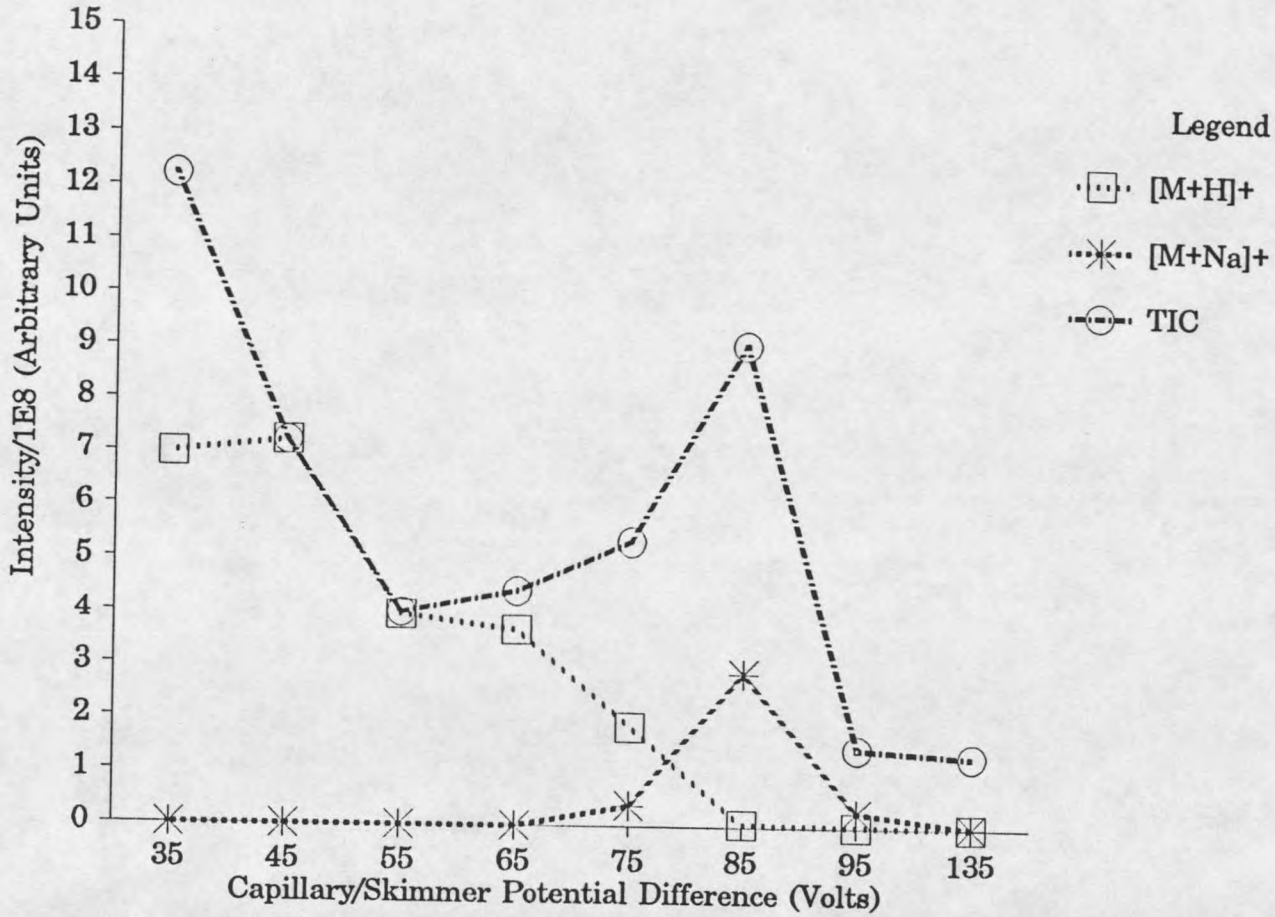


Figure 98. Carbofuran (9.38E-5 M) Ion Intensity as a Function of Potential Difference.

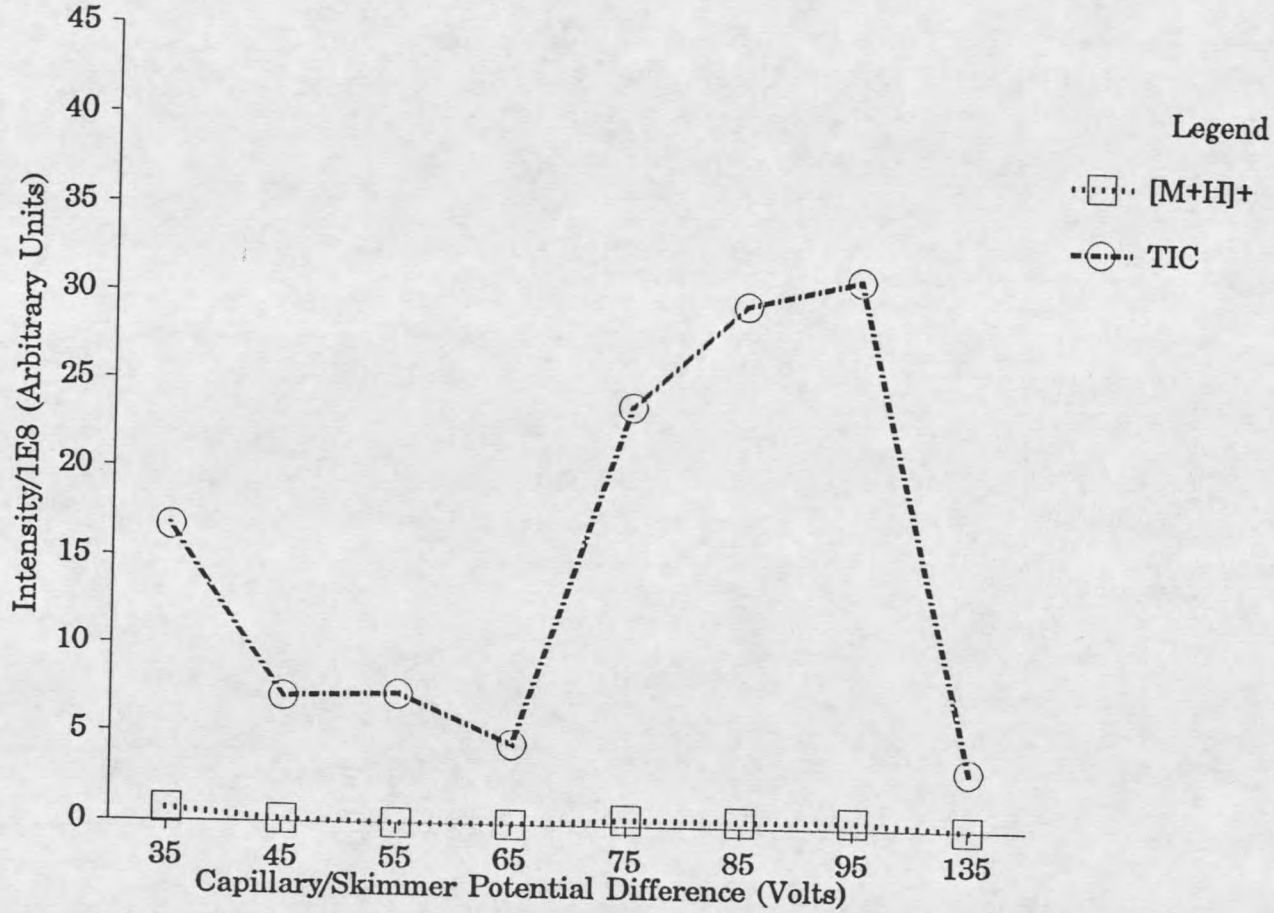


Figure 99. Endothall (1.00E-4 M) Ion Intensity as a Function of Potential Difference.

APPENDIX E

pH/SODIUM STUDIES

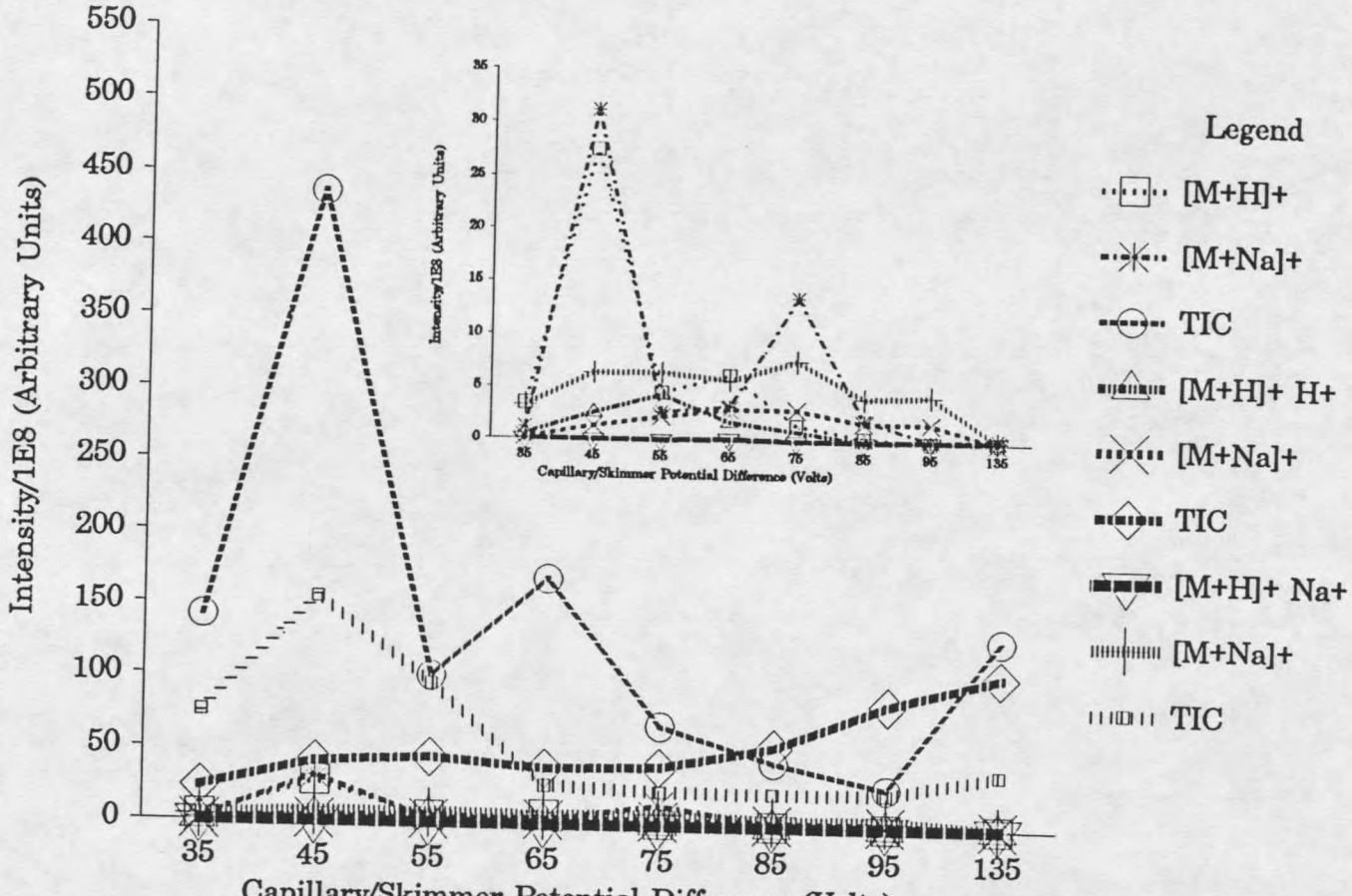


Figure 100. Ethion (1.14E-5 M) Ion Intensity as a Function of Potential Difference.

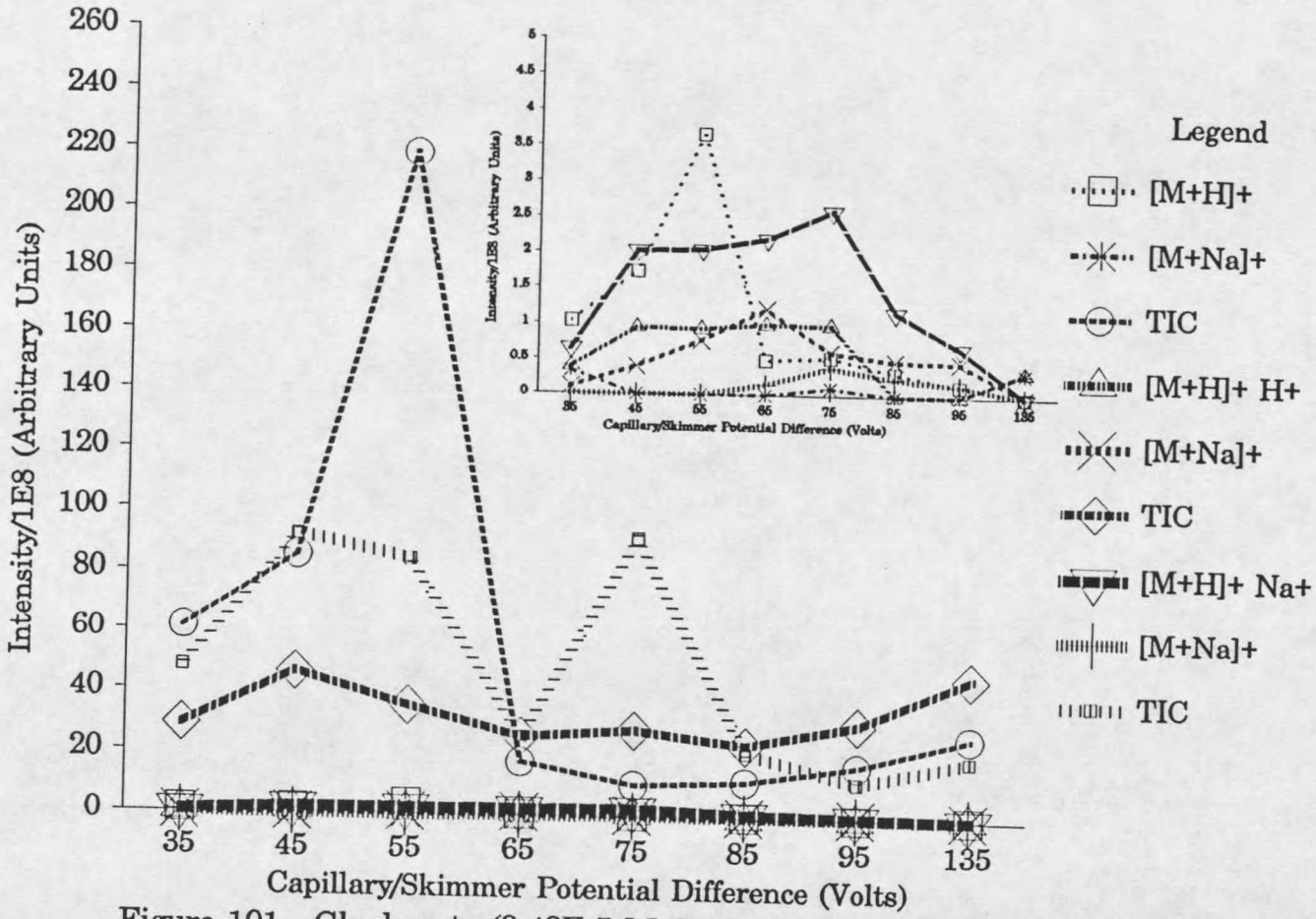


Figure 101. Glyphosate (9.48E-5 M) Ion Intensity as a Function of Potential Difference.

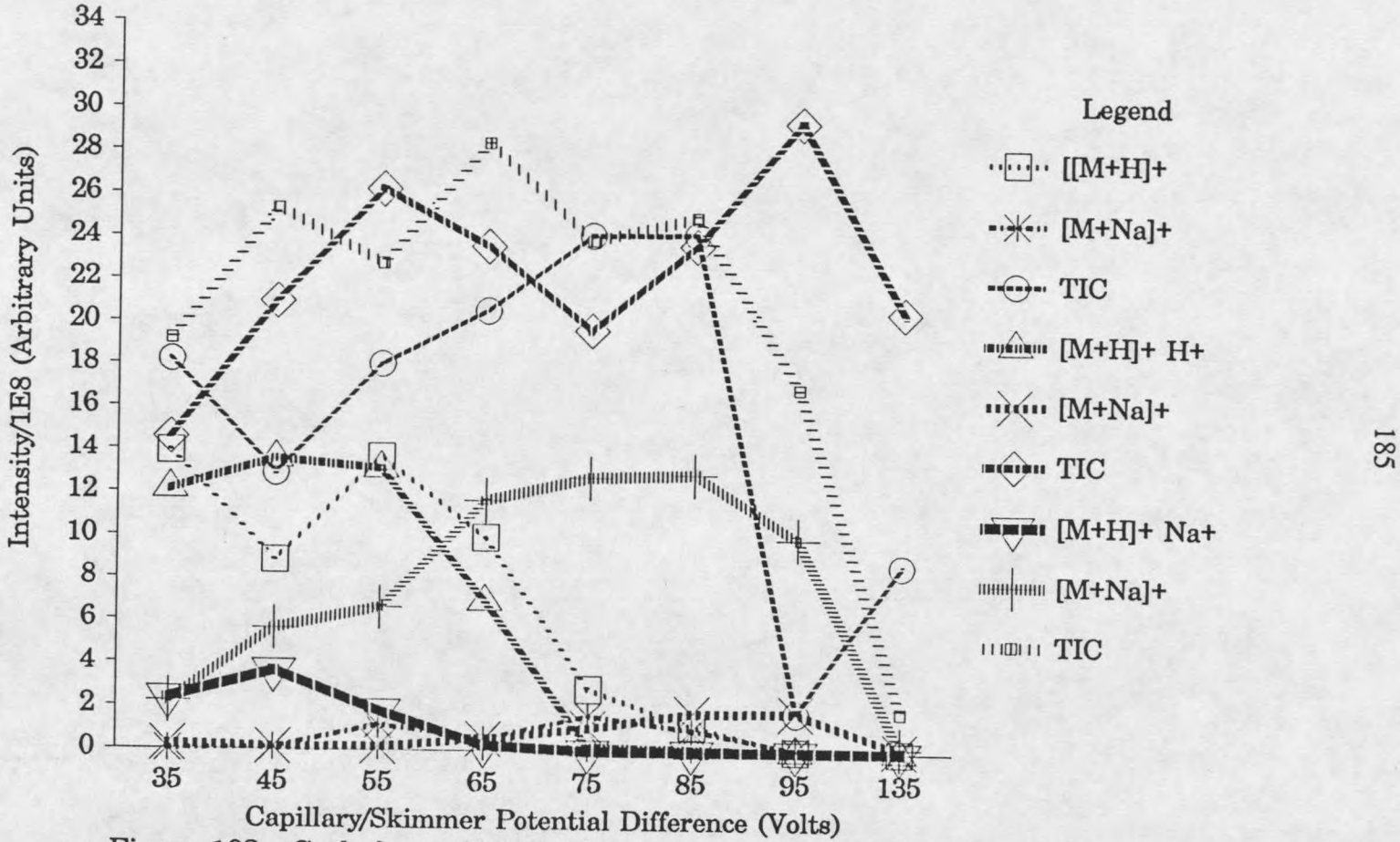


Figure 102. Carbofuran (7.41E-5 M) Ion Intensity as a Function of Potential Difference.

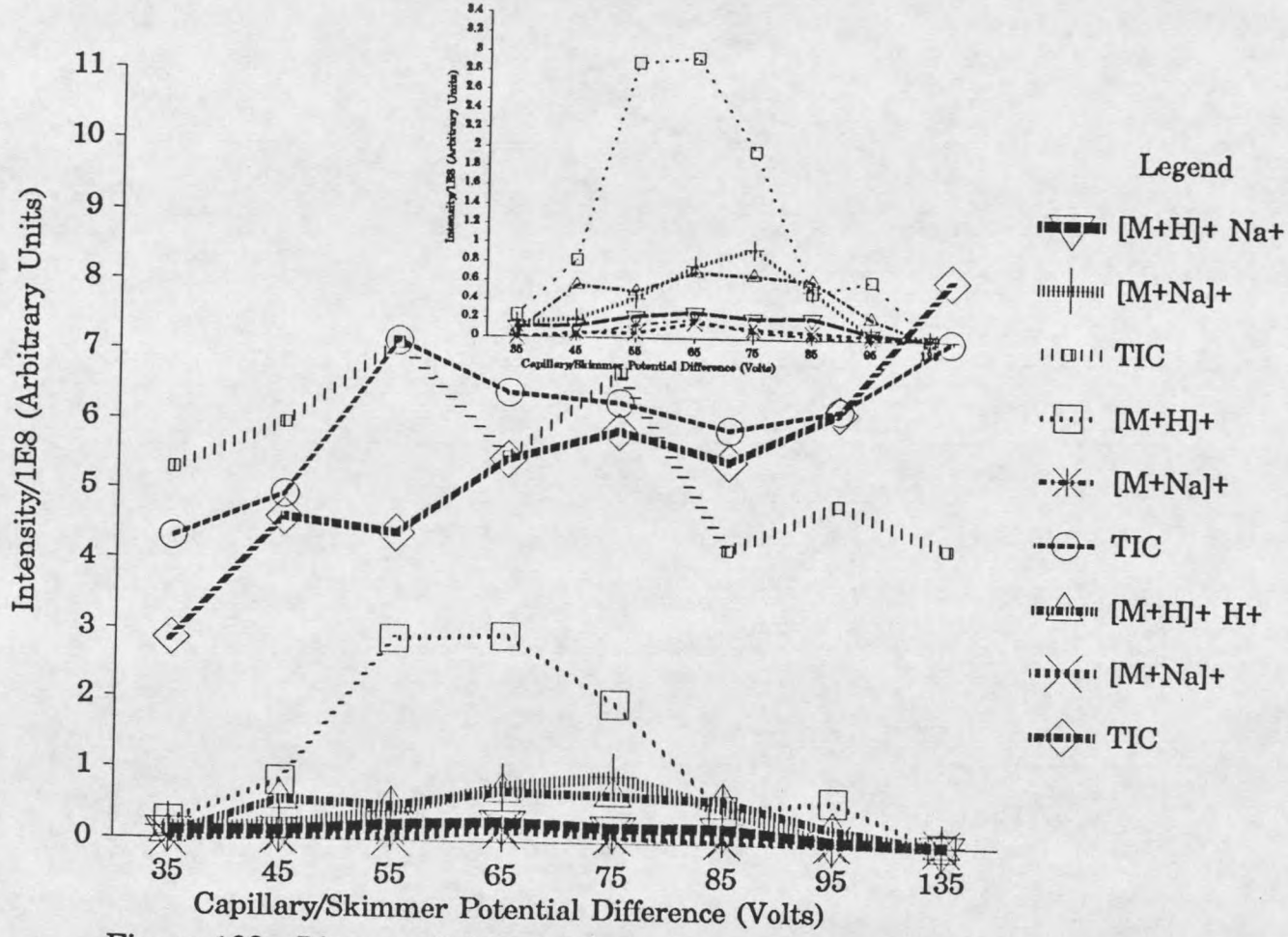


Figure 103. Linuron (6.64E-5 M) Ion Intensity as a Function of Potential Difference.

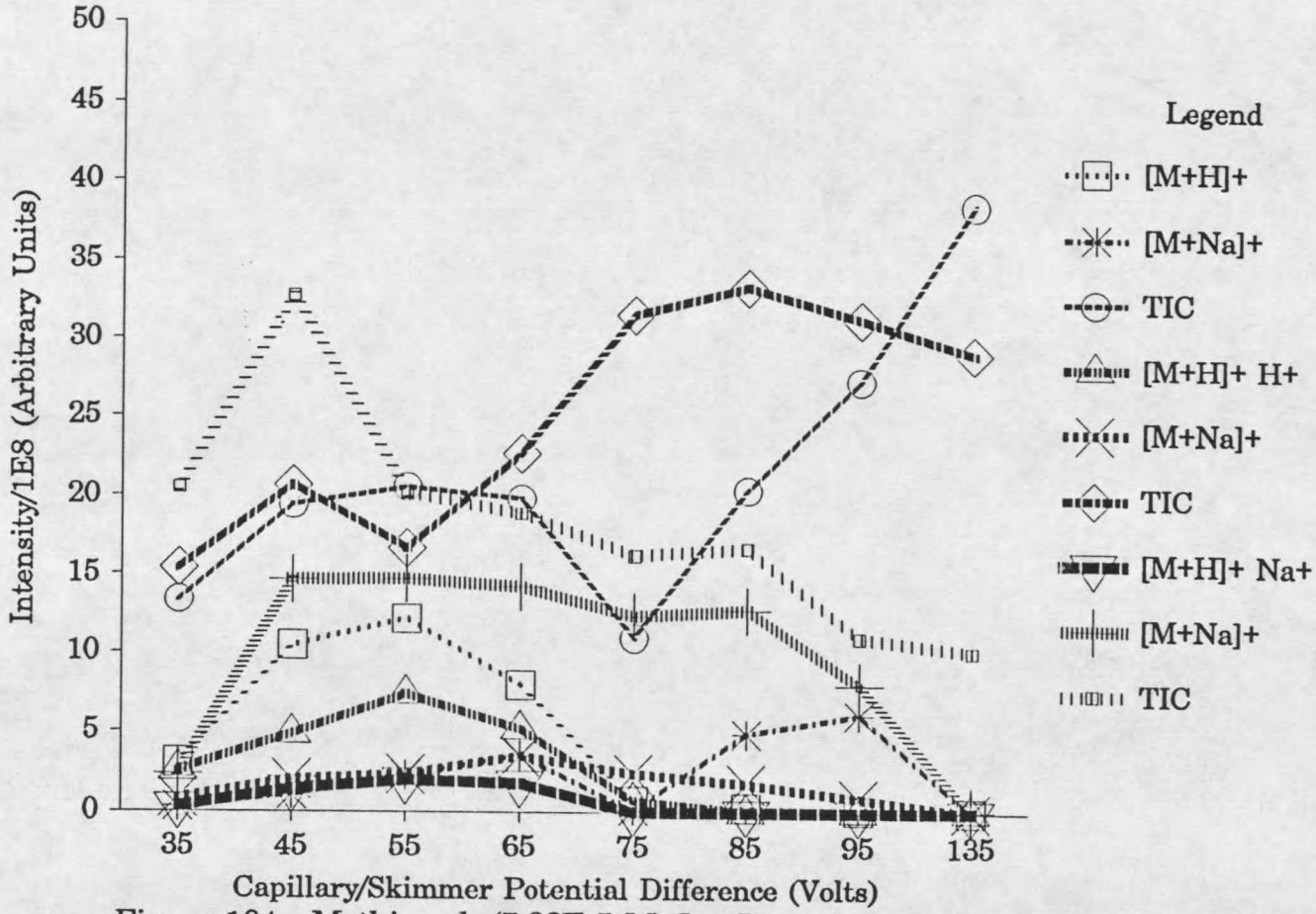


Figure 104. Methiocarb (7.88E-5 M) Ion Intensity as a Function of Potential Difference.

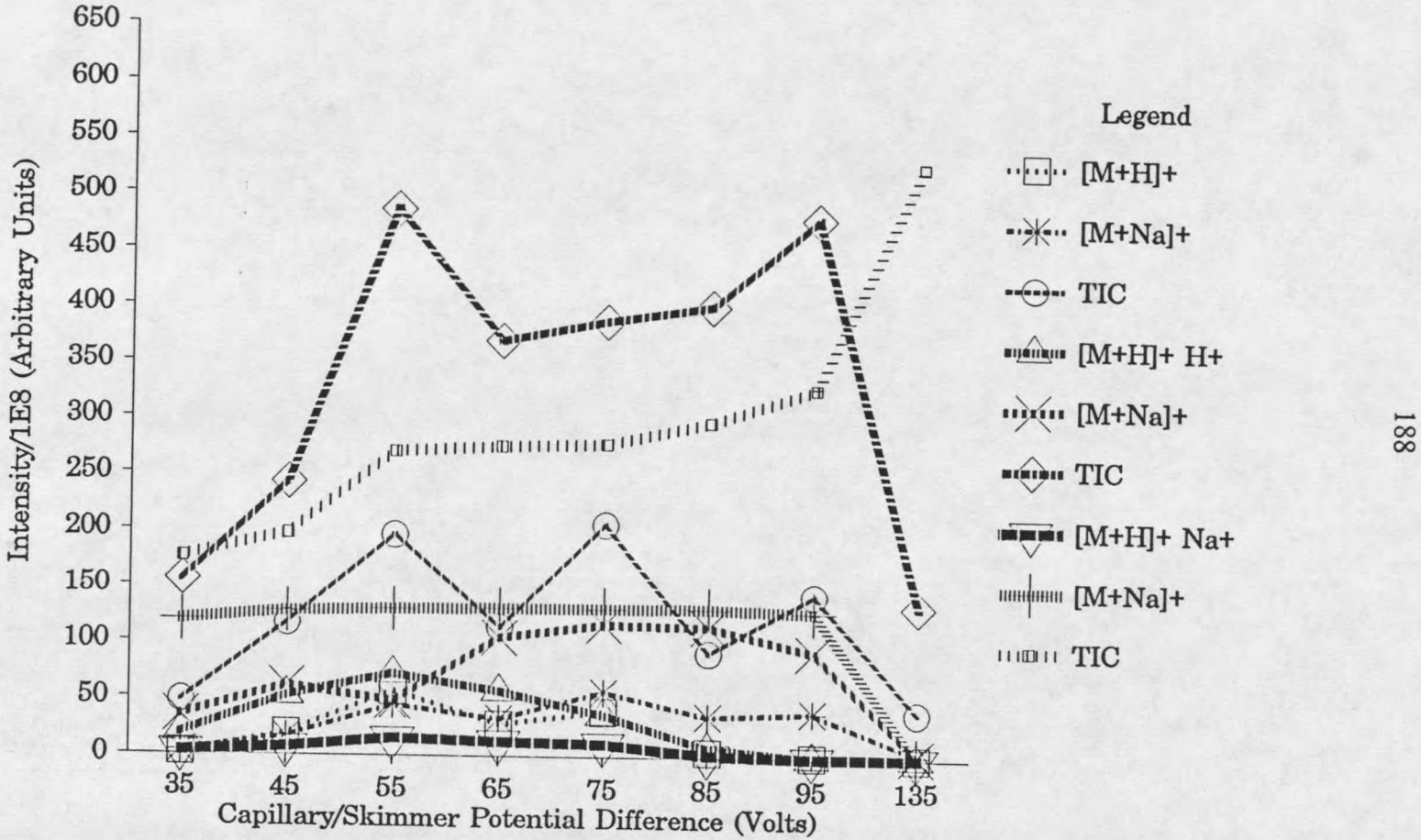


Figure 105. Methidathion (5.26E-5 M) Ion Intensity as a Function of Potential Difference.

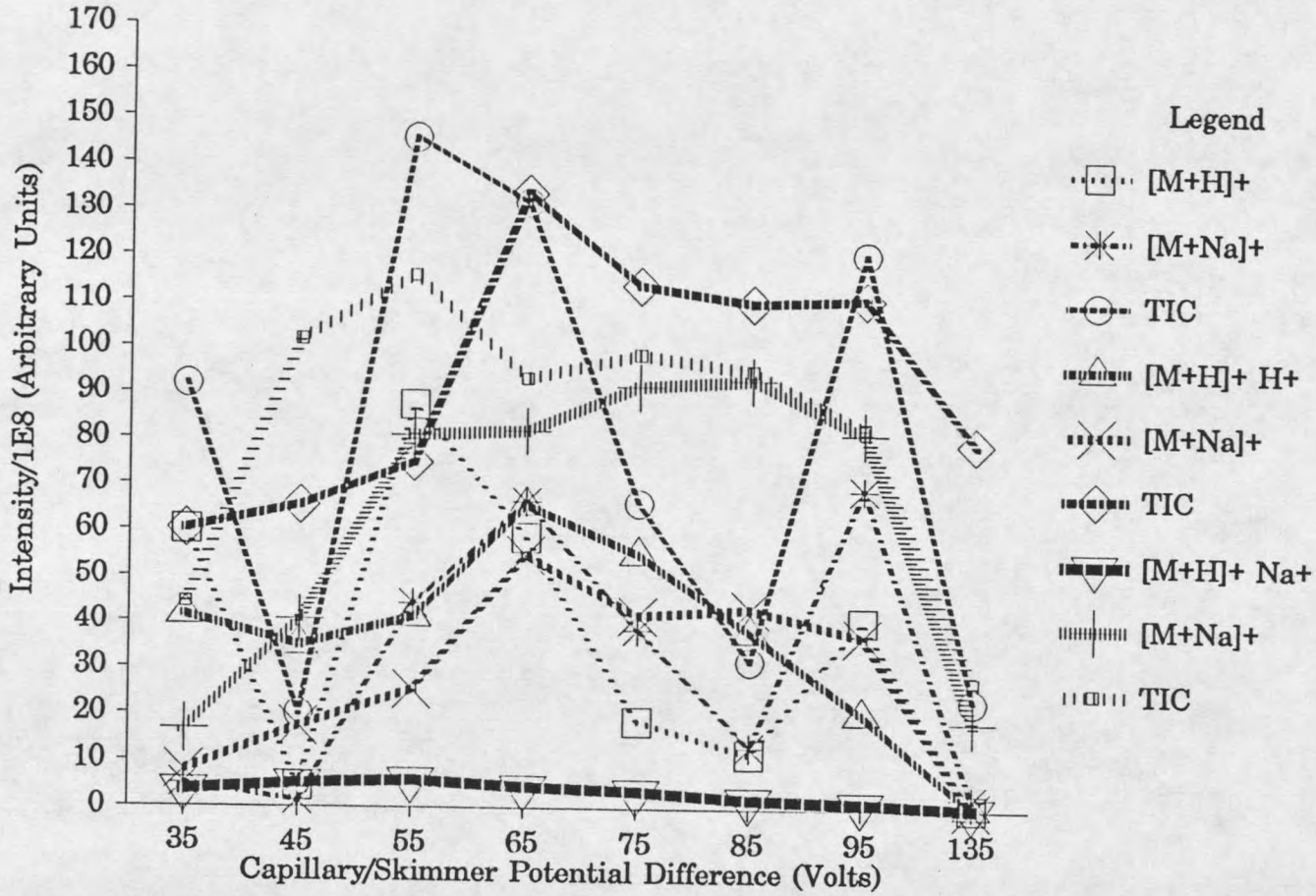


Figure 106. Mephosfolan (1.80E-5 M) Ion Intensity as a Function of Potential Difference.

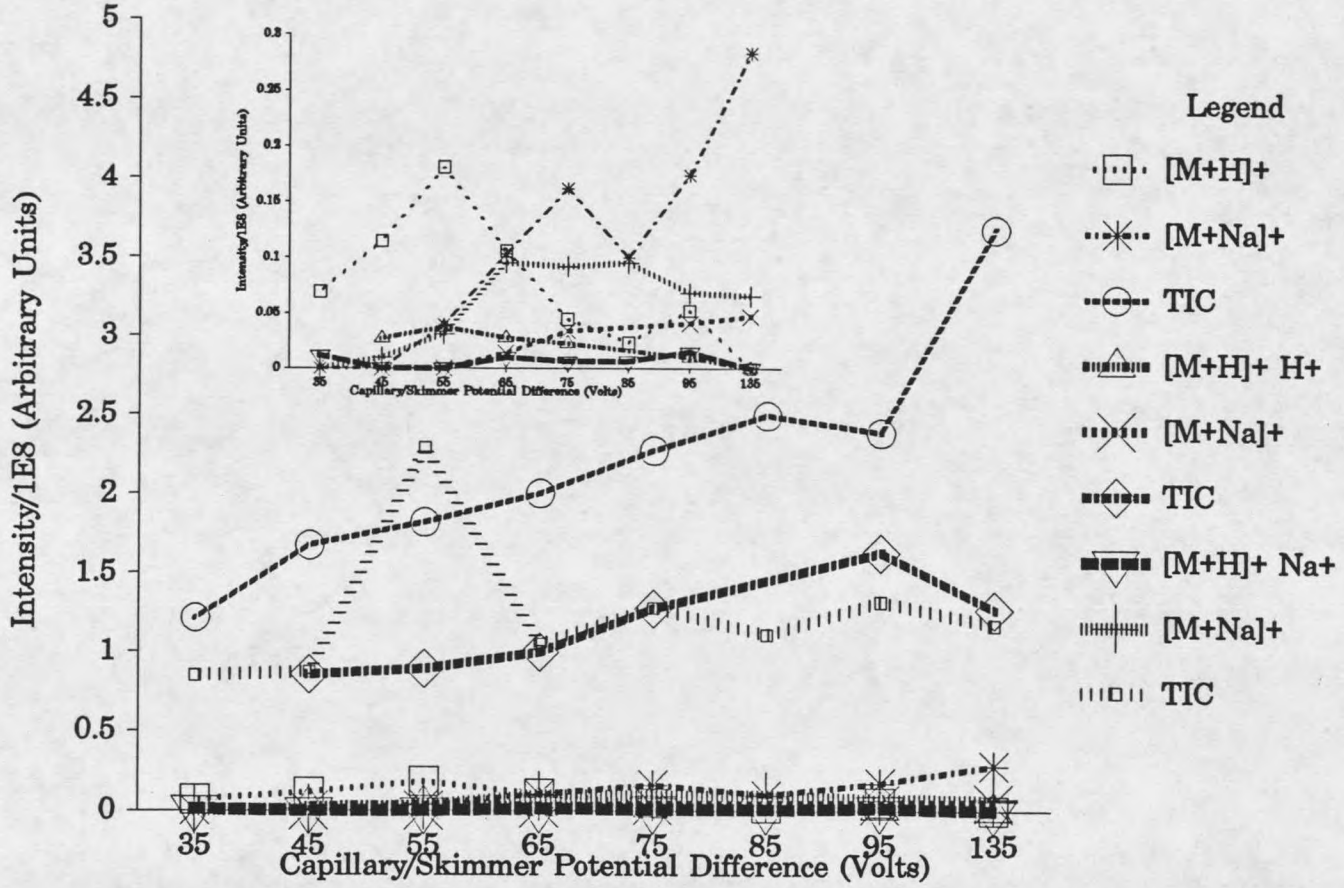


Figure 107. Coumafuryl (5.10E-5 M) Ion Intensity as a Function of Potential Difference.

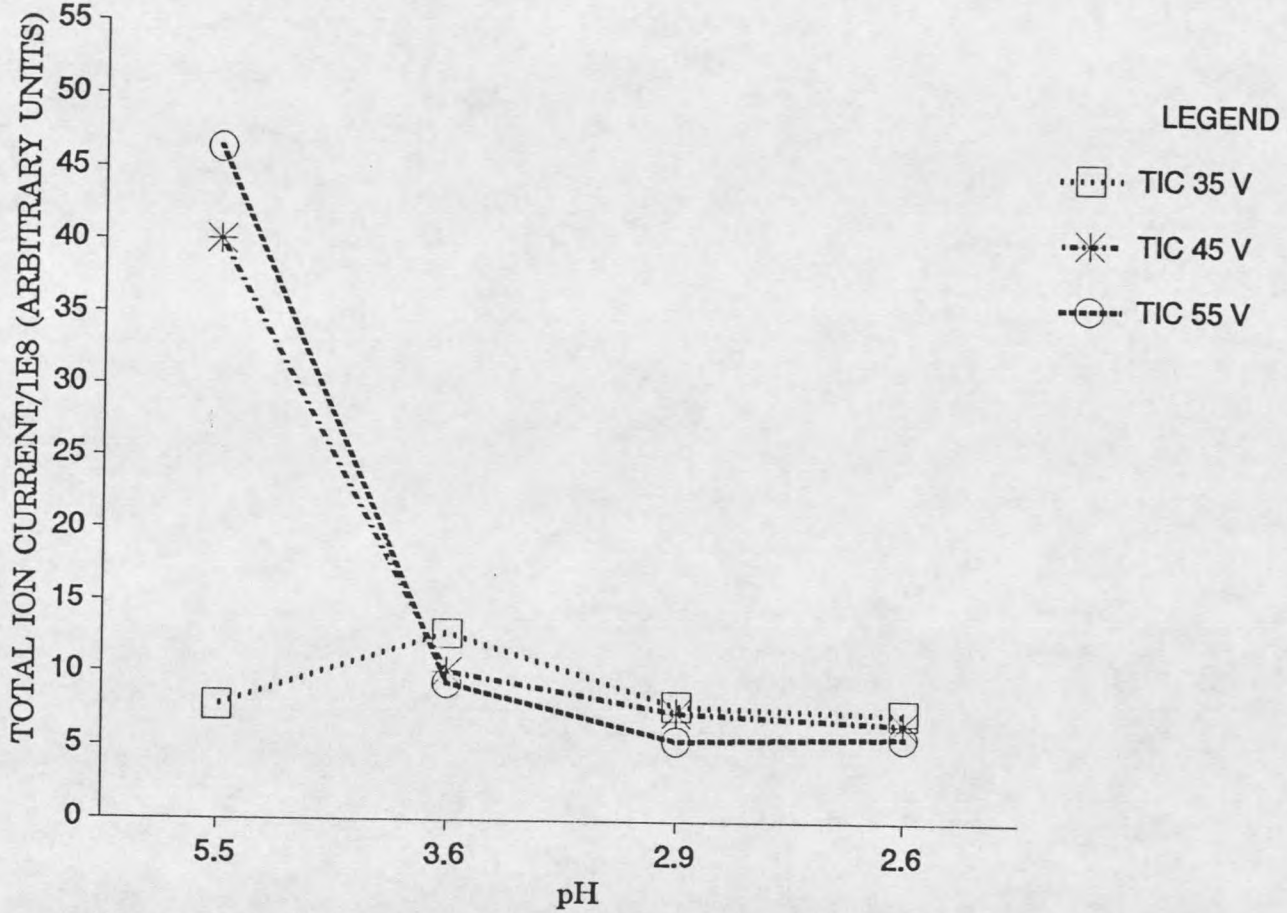


Figure 108. Total Ion Current as a Function of pH. Thiometon Concentration 1.2E-5 M.

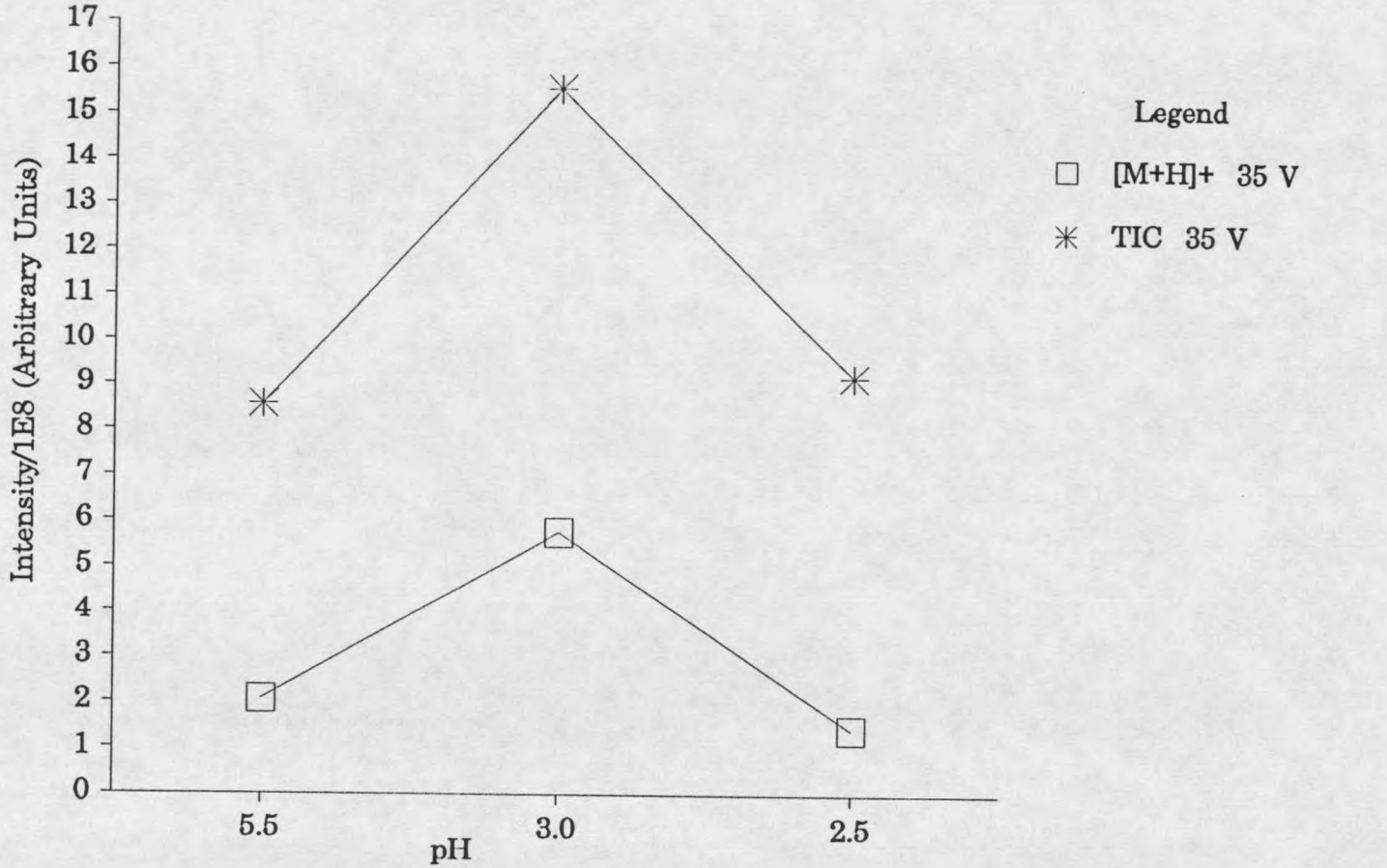


Figure 109. Total Ion Current as a Function of pH. Propoxur Concentration 5.0E-5 M.

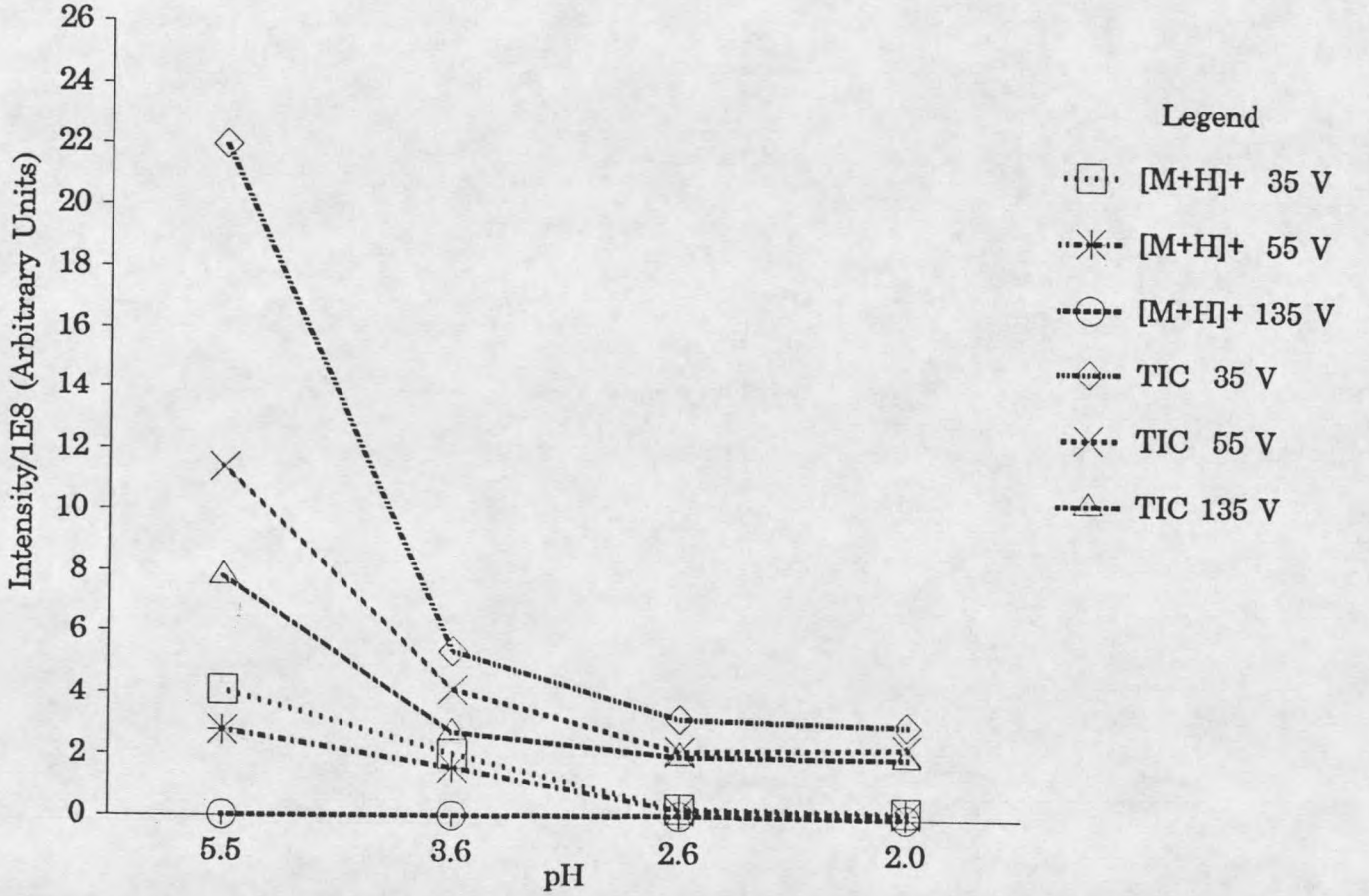


Figure 110. Intensity as a Function of pH. Phosfolan Concentration 1.58E-5 M.

APPENDIX F

SODIUM ADDUCT STUDY

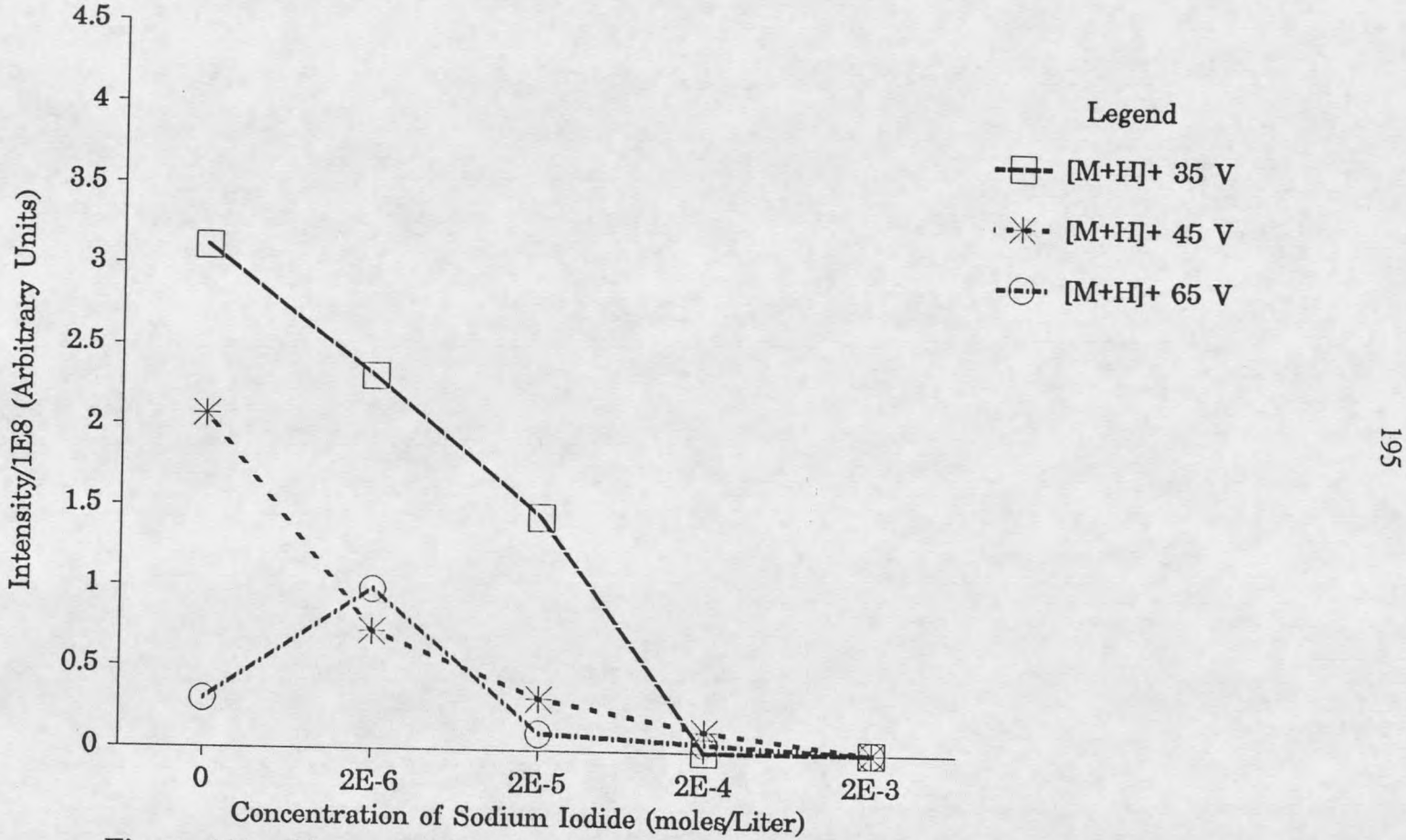


Figure 111. Diuron (1.73E-5 M) [M+H]+ Ion Intensity as a Function of NaI Concentration.

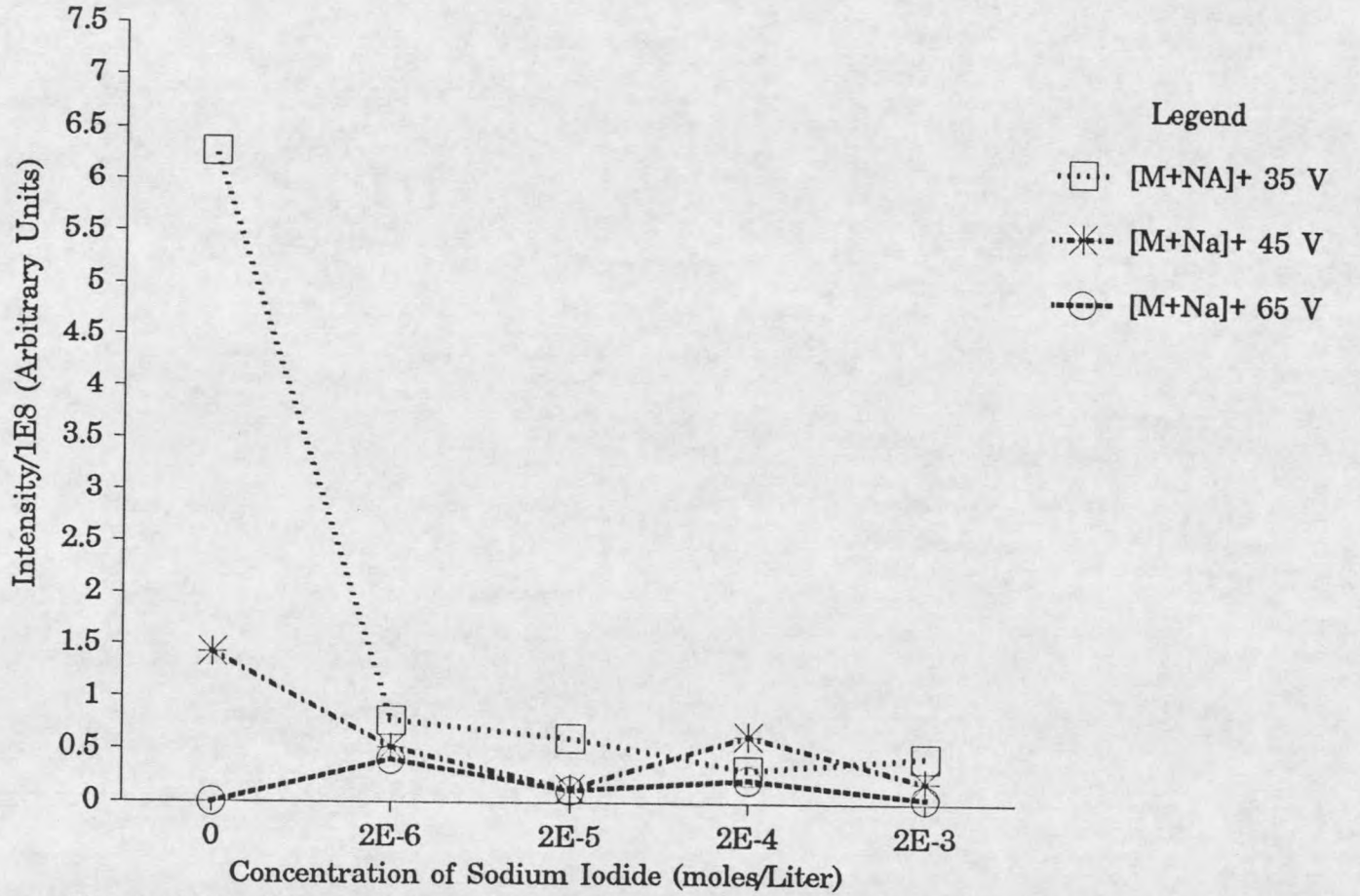


Figure 112. Diuron (1.73E-5 M) [M+Na]+ Ion Intensity as a Function of NaI Concentration.

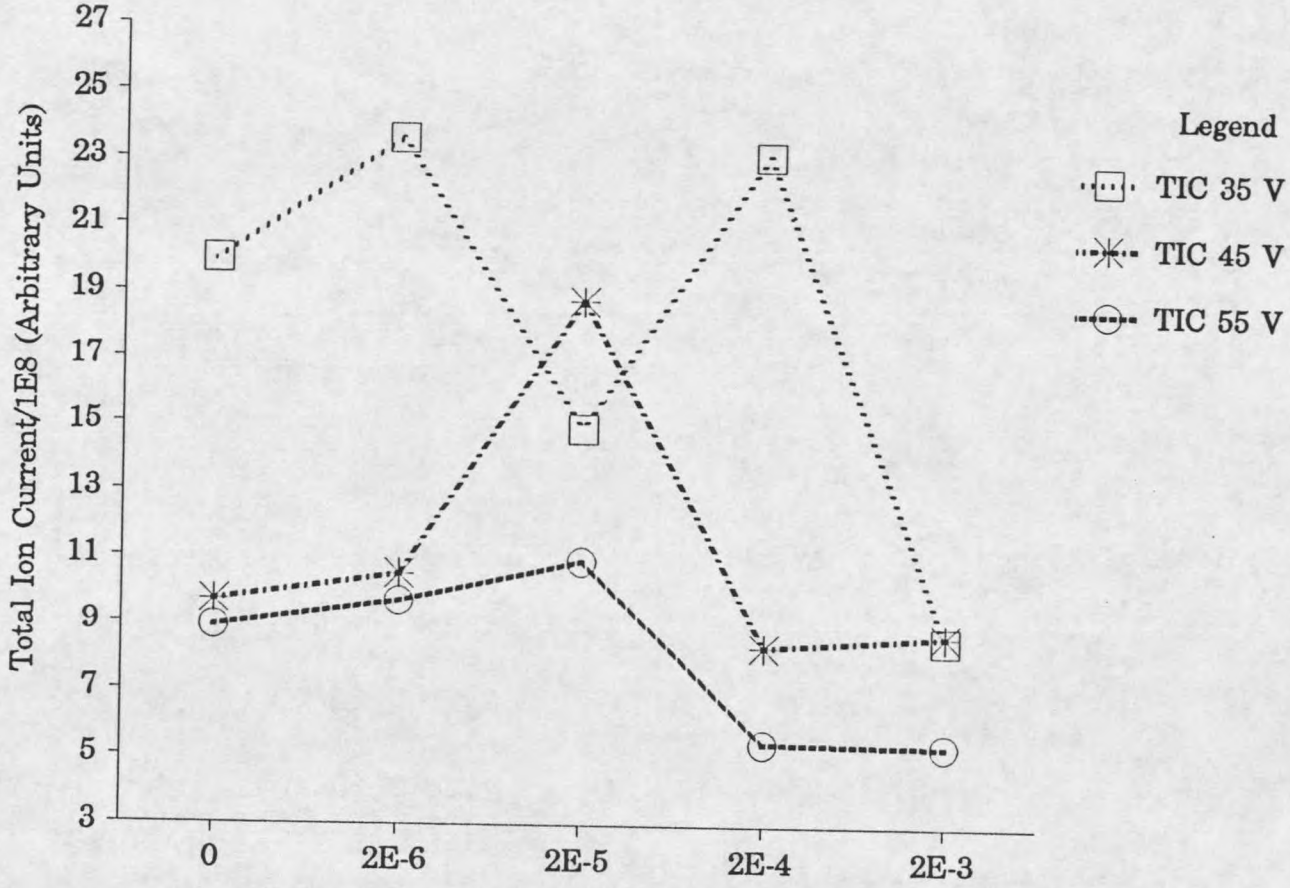


Figure 113. Diuron (1.73E-5 M) Total Ion Current as a Function of NaI Concentration.

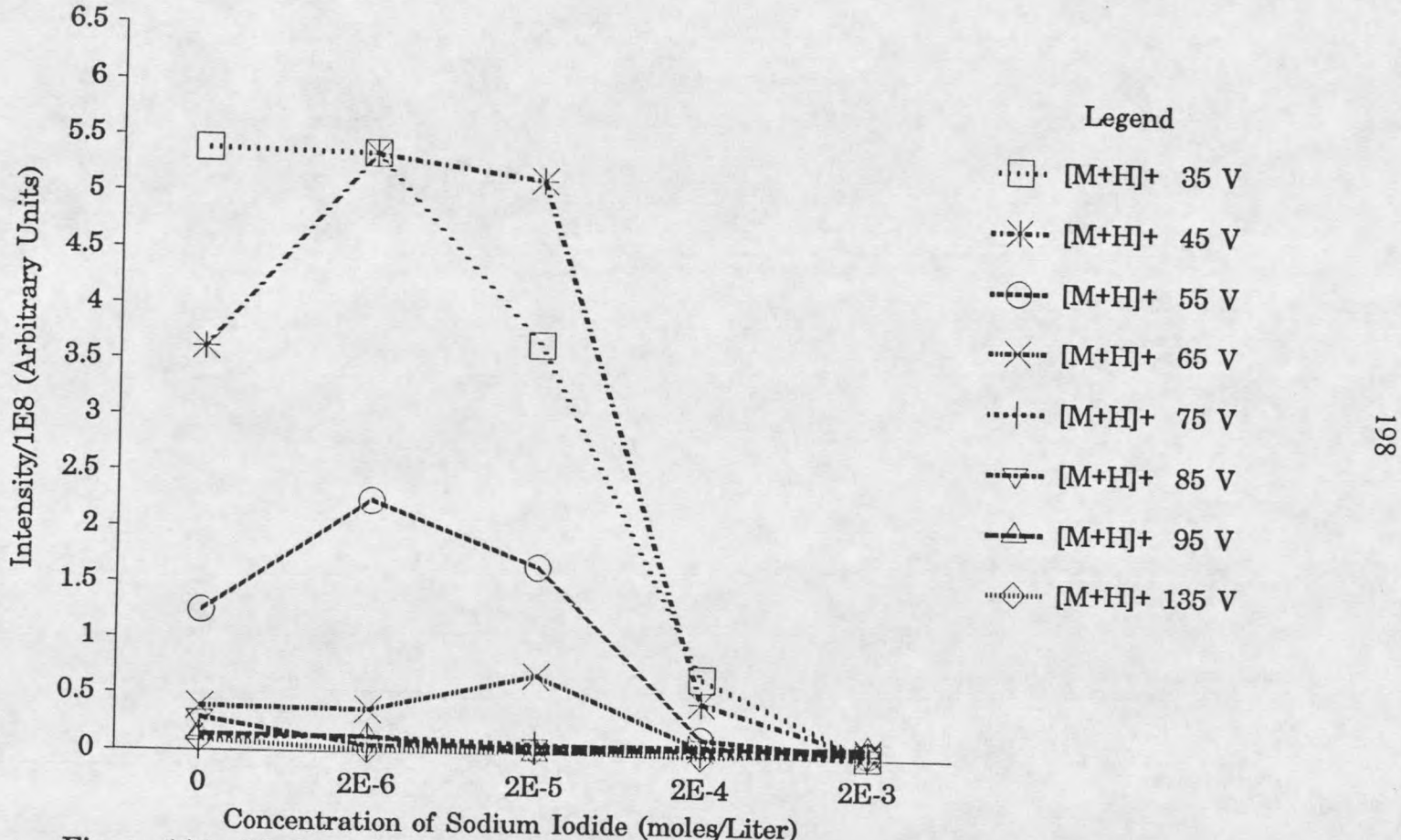


Figure 114. Methomyl (2.53E-5 M) [M+H]+ Ion Intensity as a Function of NaI Concentration.

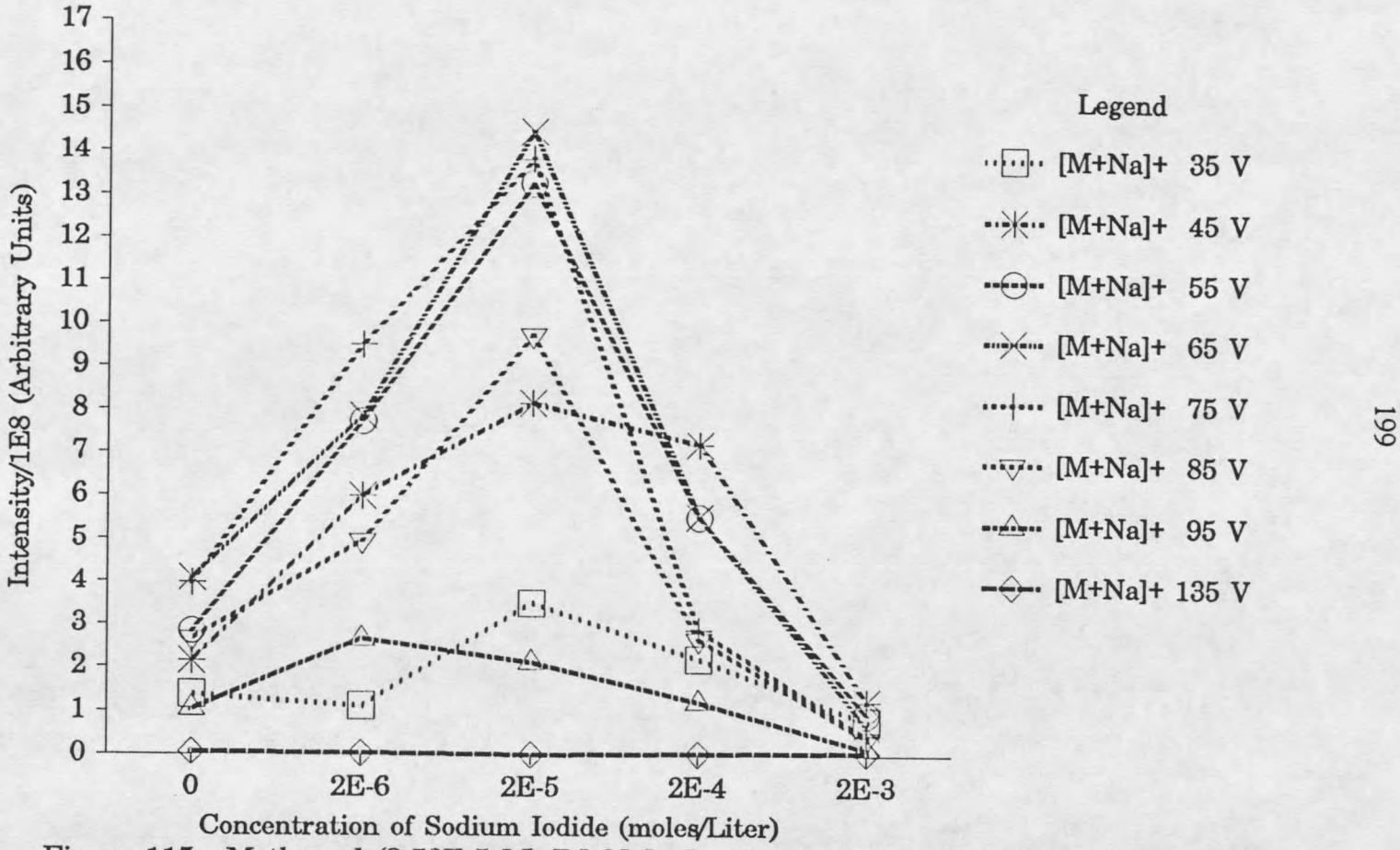


Figure 115. Methomyl (2.53E-5 M) [M+Na]+ Ion Intensity as a Function of NaI Concentration.

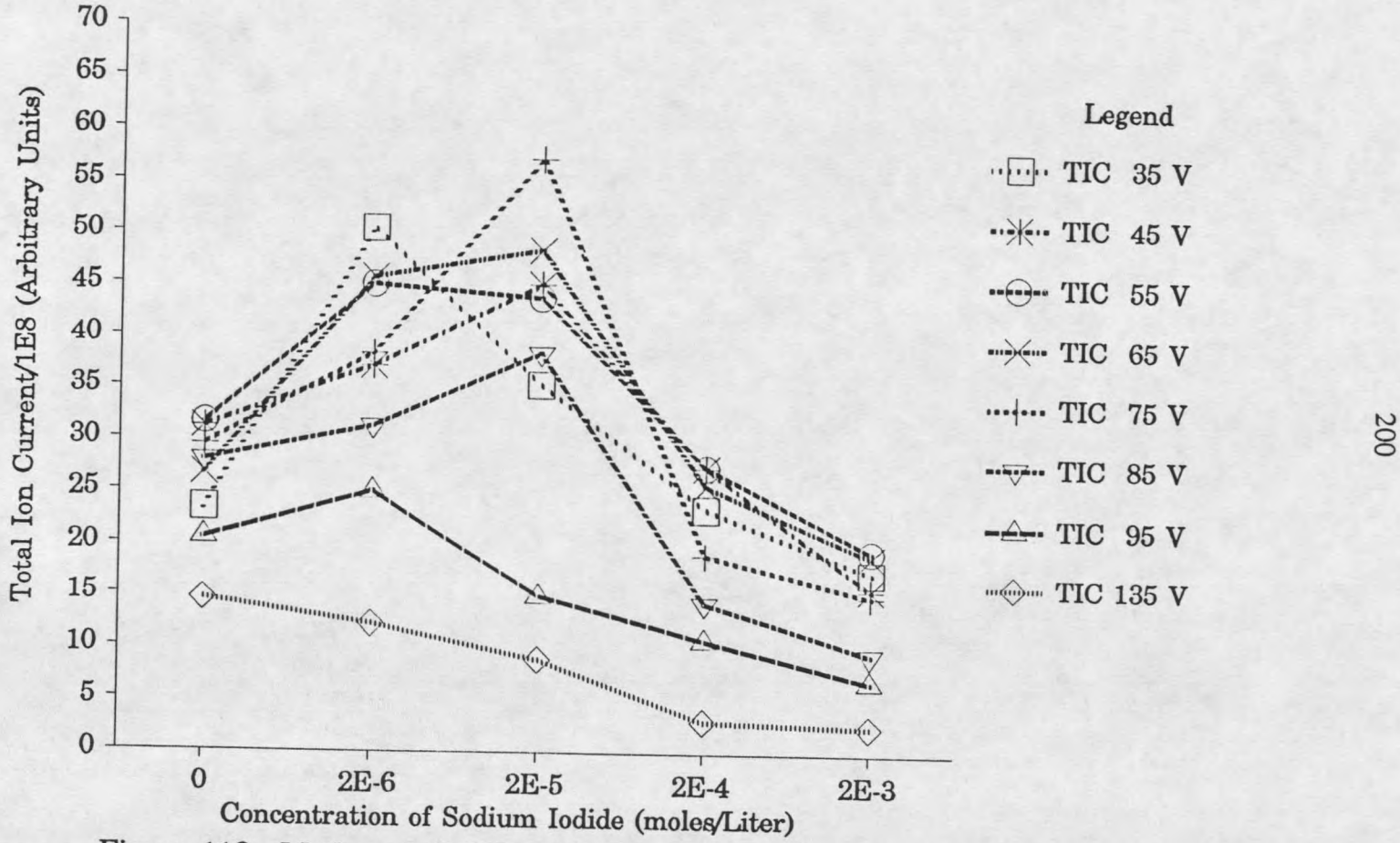


Figure 116. Methomyl (2.53E-5 M) Total Ion Current as a Function of NaI Concentration.

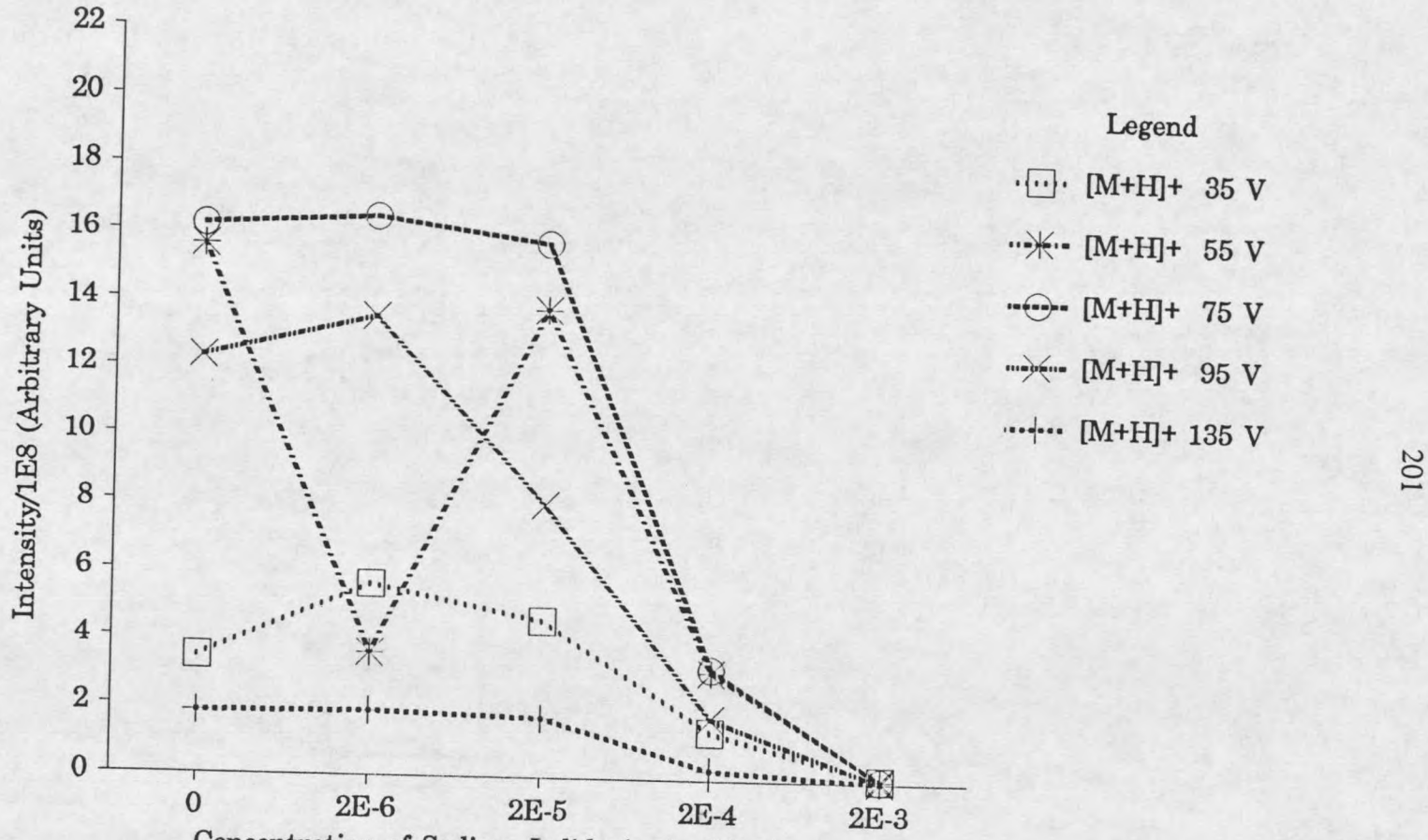


Figure117. Siduron (1.79E-5 M) [M+H]+ Ion Intensity as a Function of NaI Concentration.

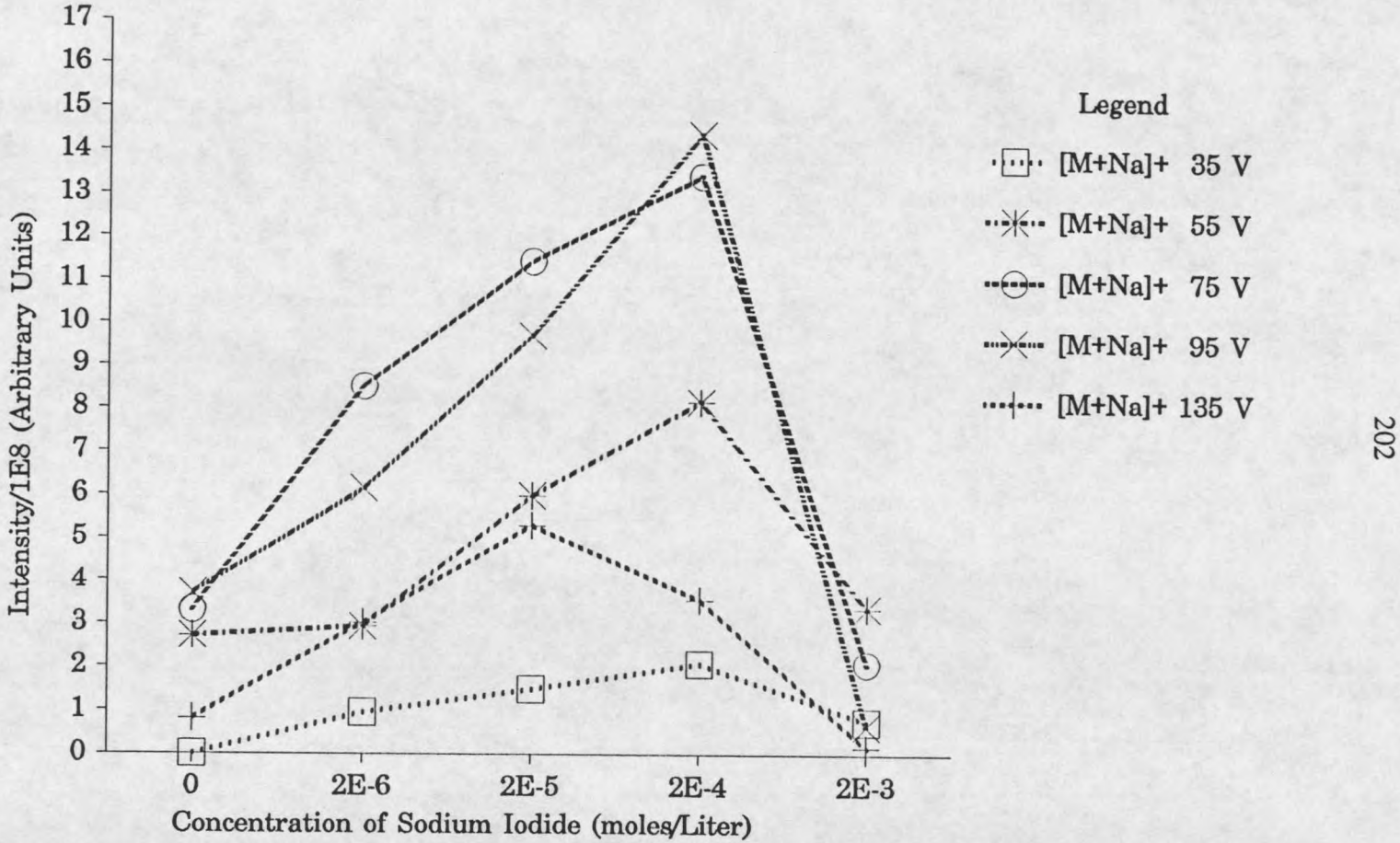


Figure 118. Siduron (1.79E-5 M) [M+Na]+ Ion Intensity as a Function of NaI Concentration.

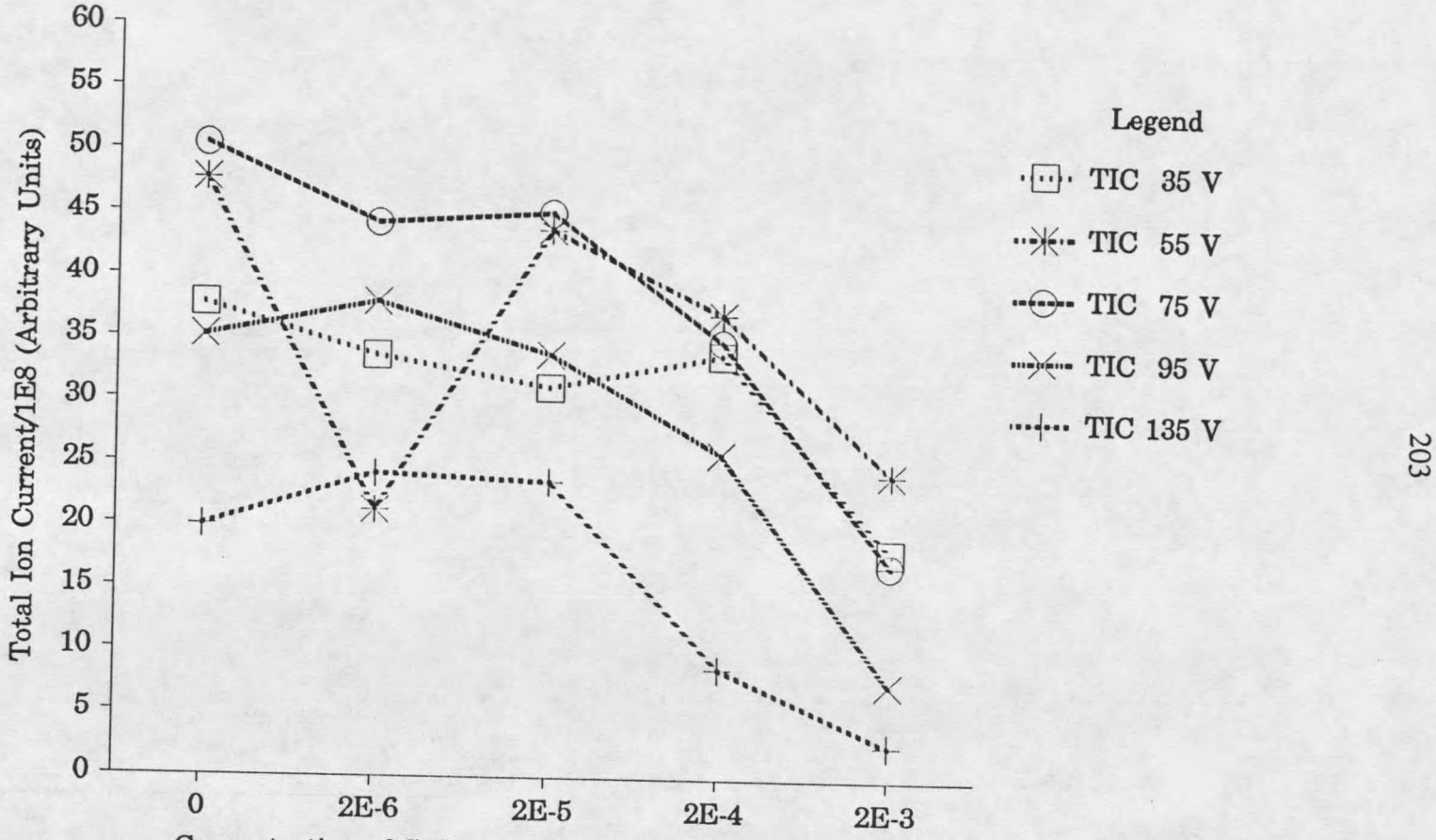


Figure 119. Siduron (1.79E-5 M) Total Ion Current as a Function of NaI Concentration.

APPENDIX G

AMMONIUM ACETATE STUDY

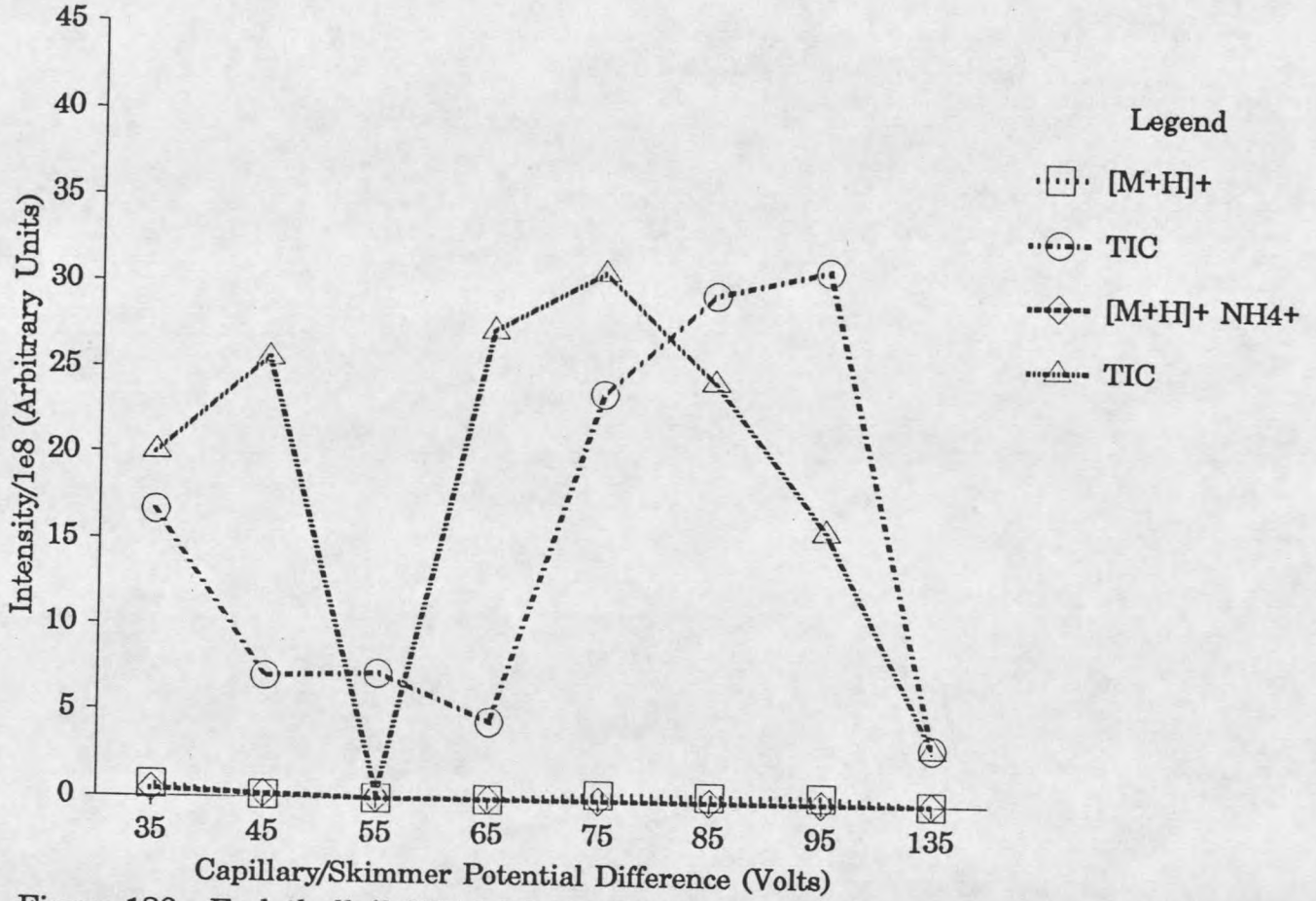


Figure 120. Endothall (8.00E-5 M) [M+H]+ Ion Intensity as a Function of Potential Difference.

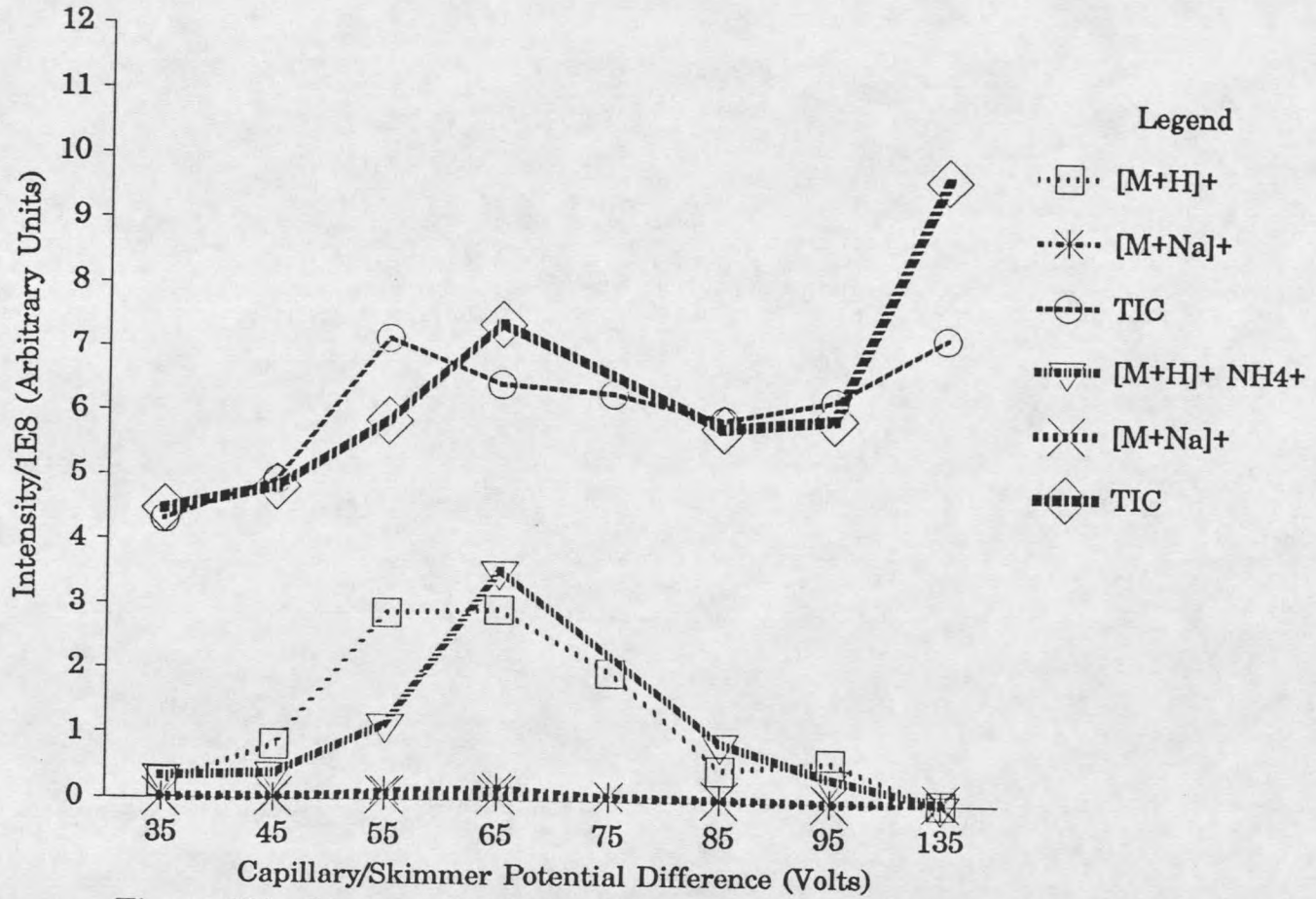


Figure 121. Linuron (6.72E-5 M) Ion Intensities as a Function of Potential Difference.

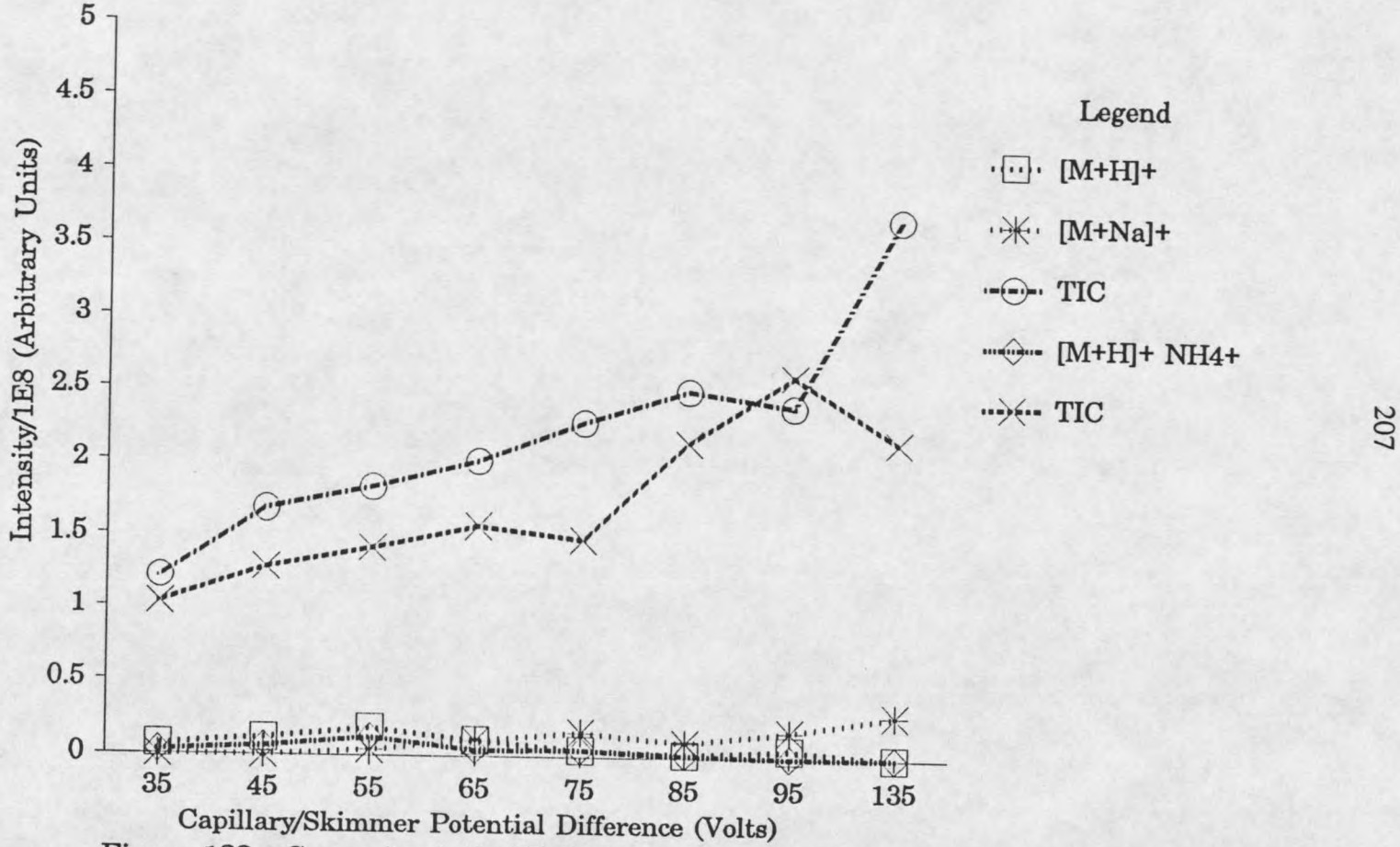


Figure 122. Coumafuryl (5.17E-5 M) Ion Intensities as a Function of Potential Difference.

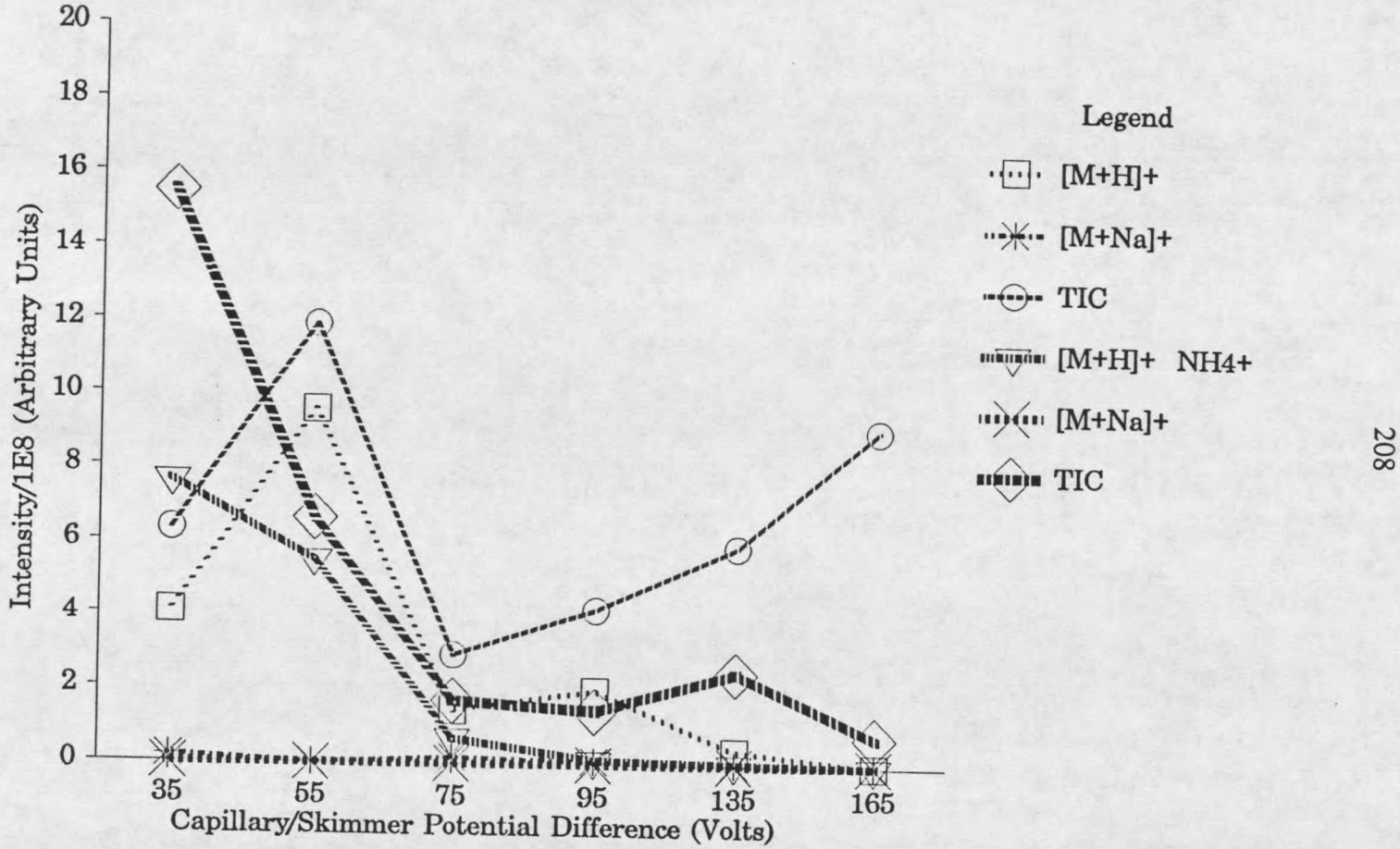


Figure 123. Antu (7.88E-5 M) Ion Intensities as a Function of Potential Difference.

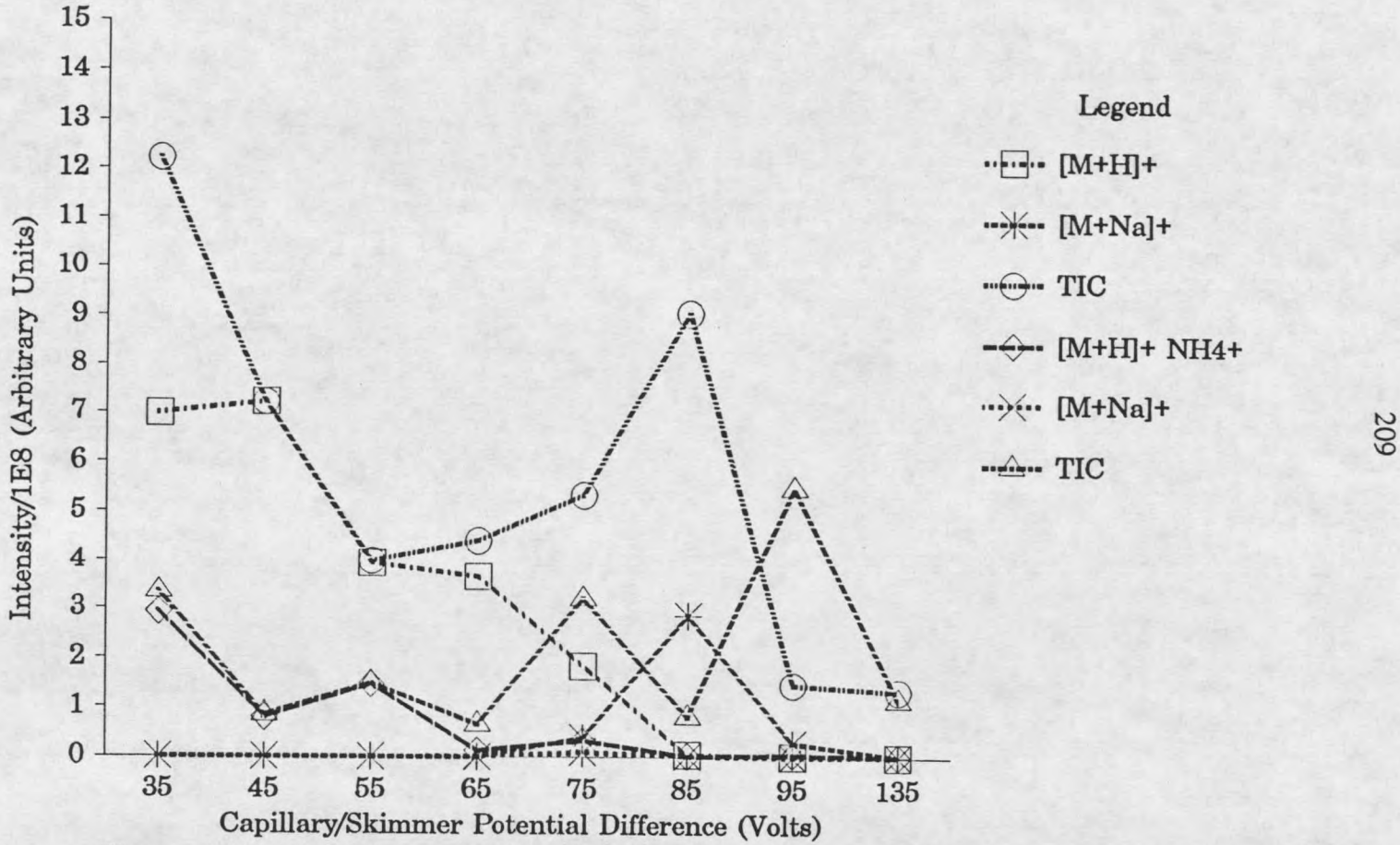


Figure 124. Carbofuran (7.50E-5 M) Ion Intensities as a Function of Potential Difference.

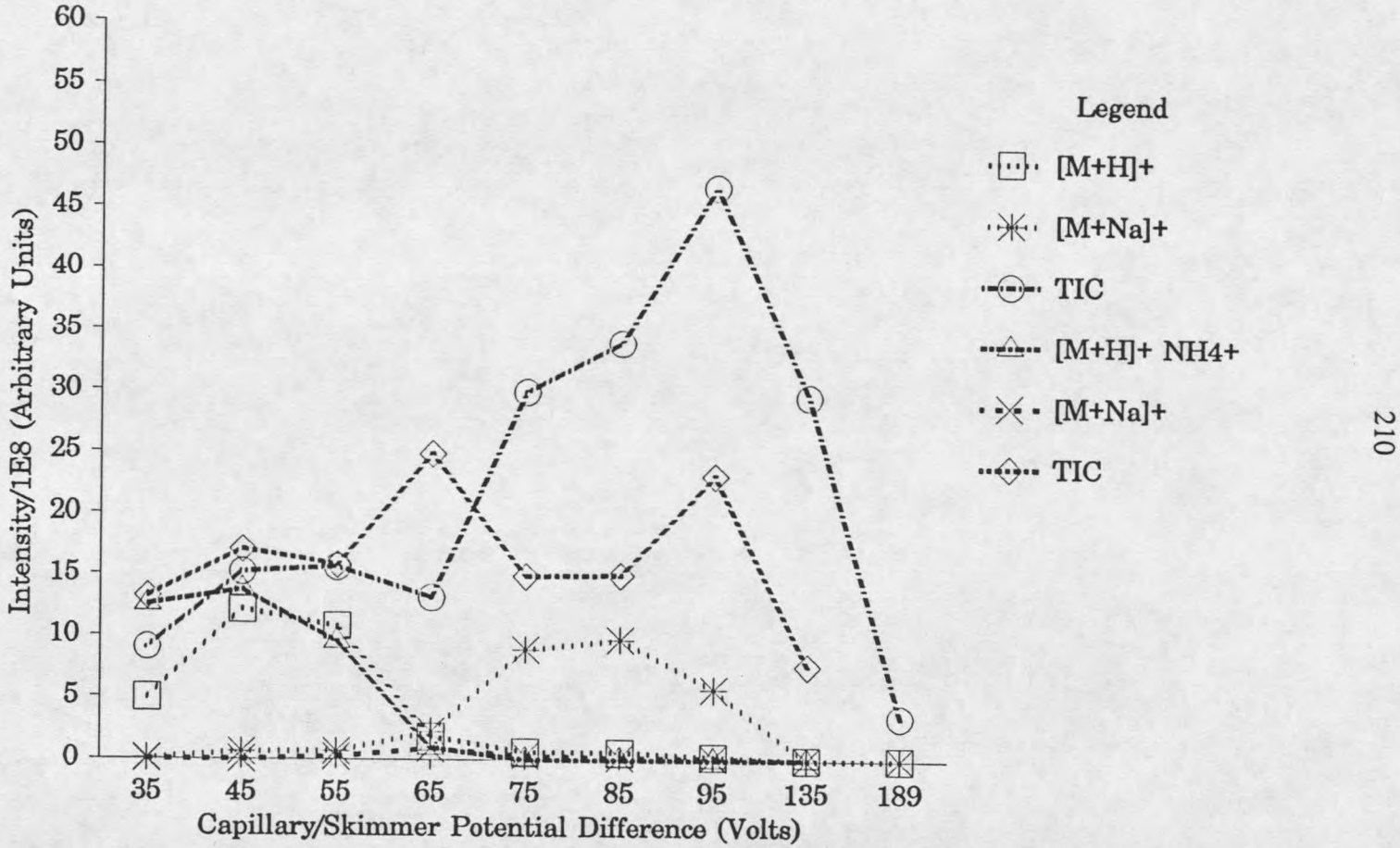


Figure 125. Propoxur (4.41E-5 M) Ion Intensities as a Function of Potential Difference.

APPENDIX H

SOLVENT STUDY

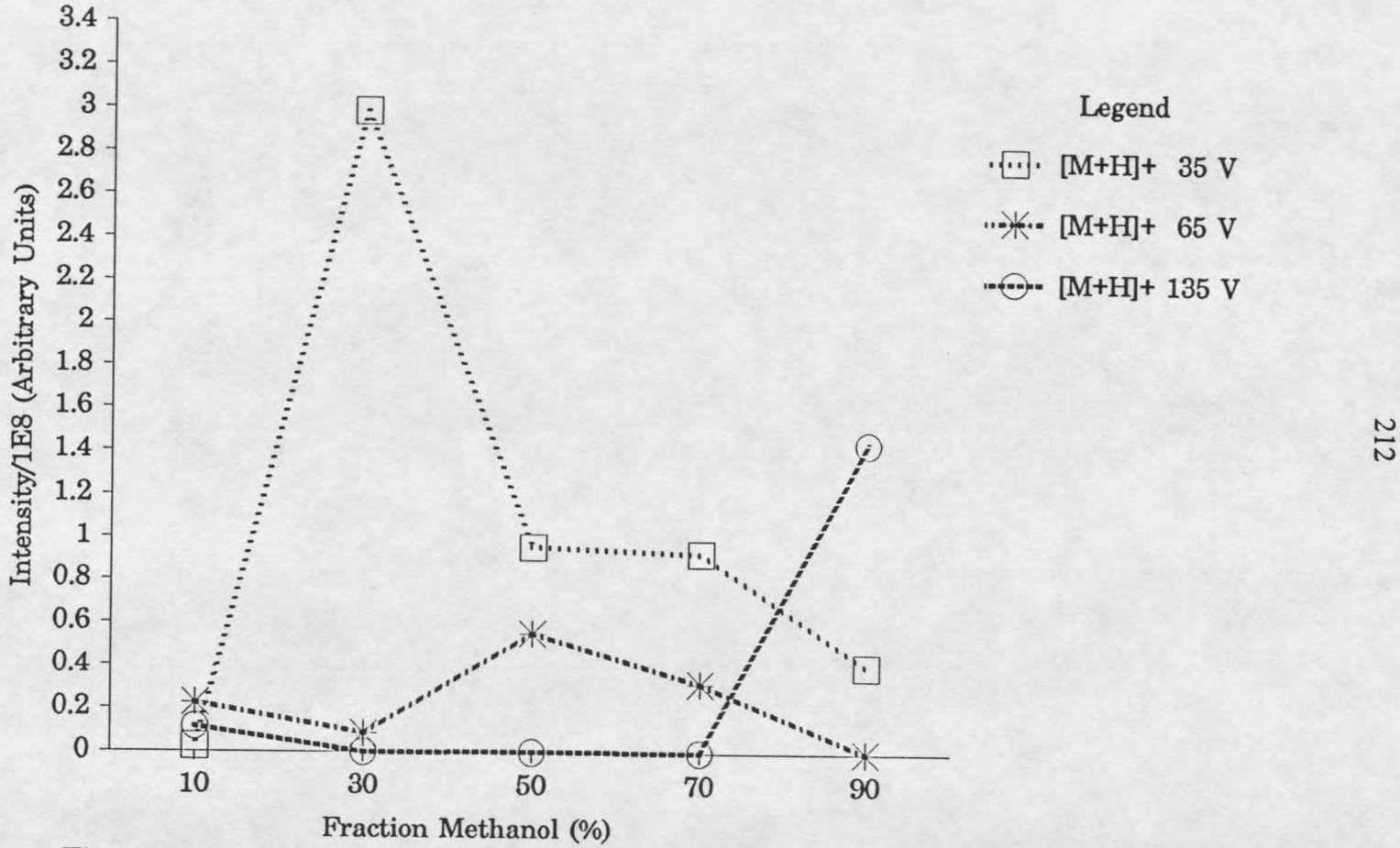


Figure 126. Methomyl (2.53E-5 M) [M+H]+ Ion Intensity as a Function of Methanol Fraction.

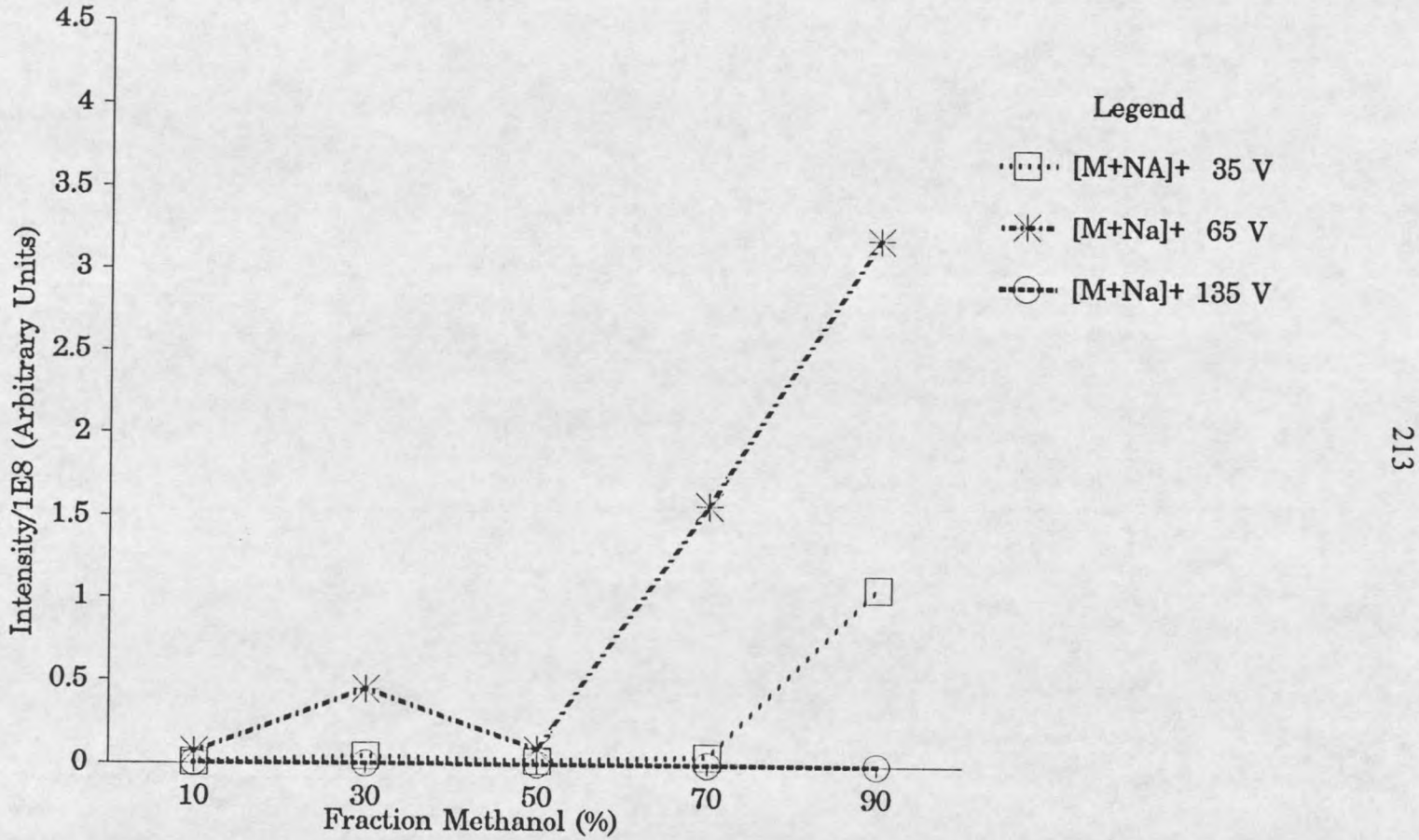


Figure 127. Methomyl (2.53E-5 M) [M+Na]+ Ion Intensity as a Function of Methanol Fraction.

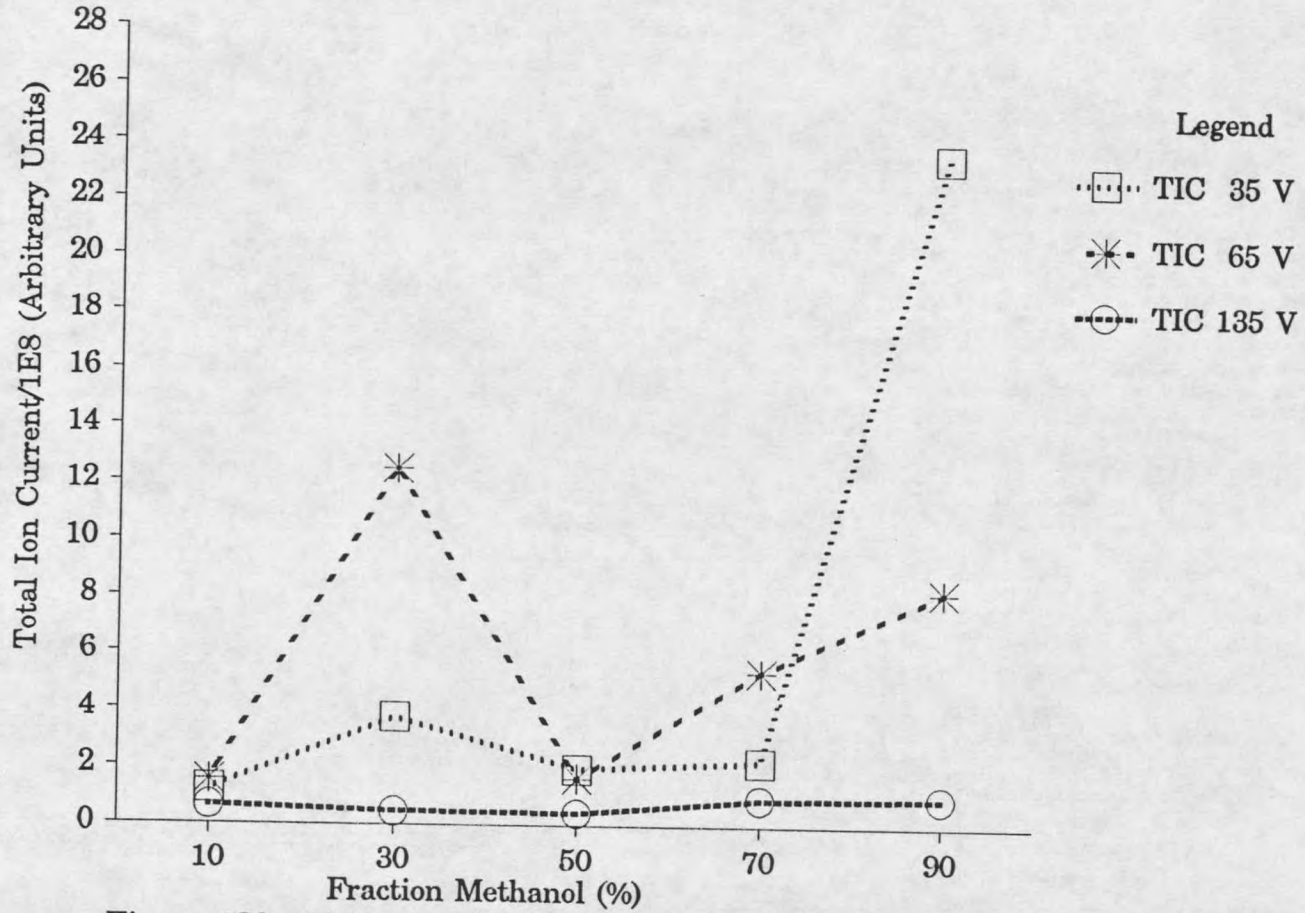


Figure 128. Methomyl (2.53E-5 M) Total Ion Current as a Function of Methanol Fraction.

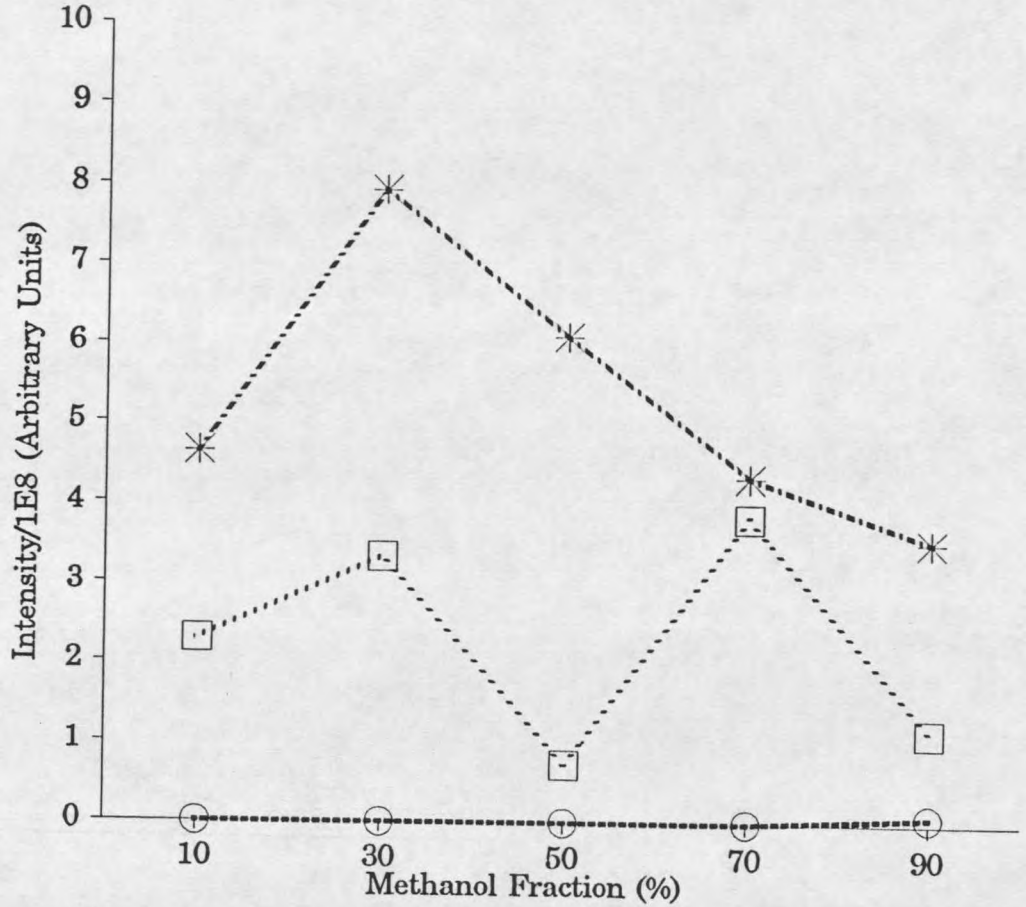


Figure 129. Phosfolan (1.58E-5 M) [M+H]+ Ion Intensity as a Function of Methanol Fraction.

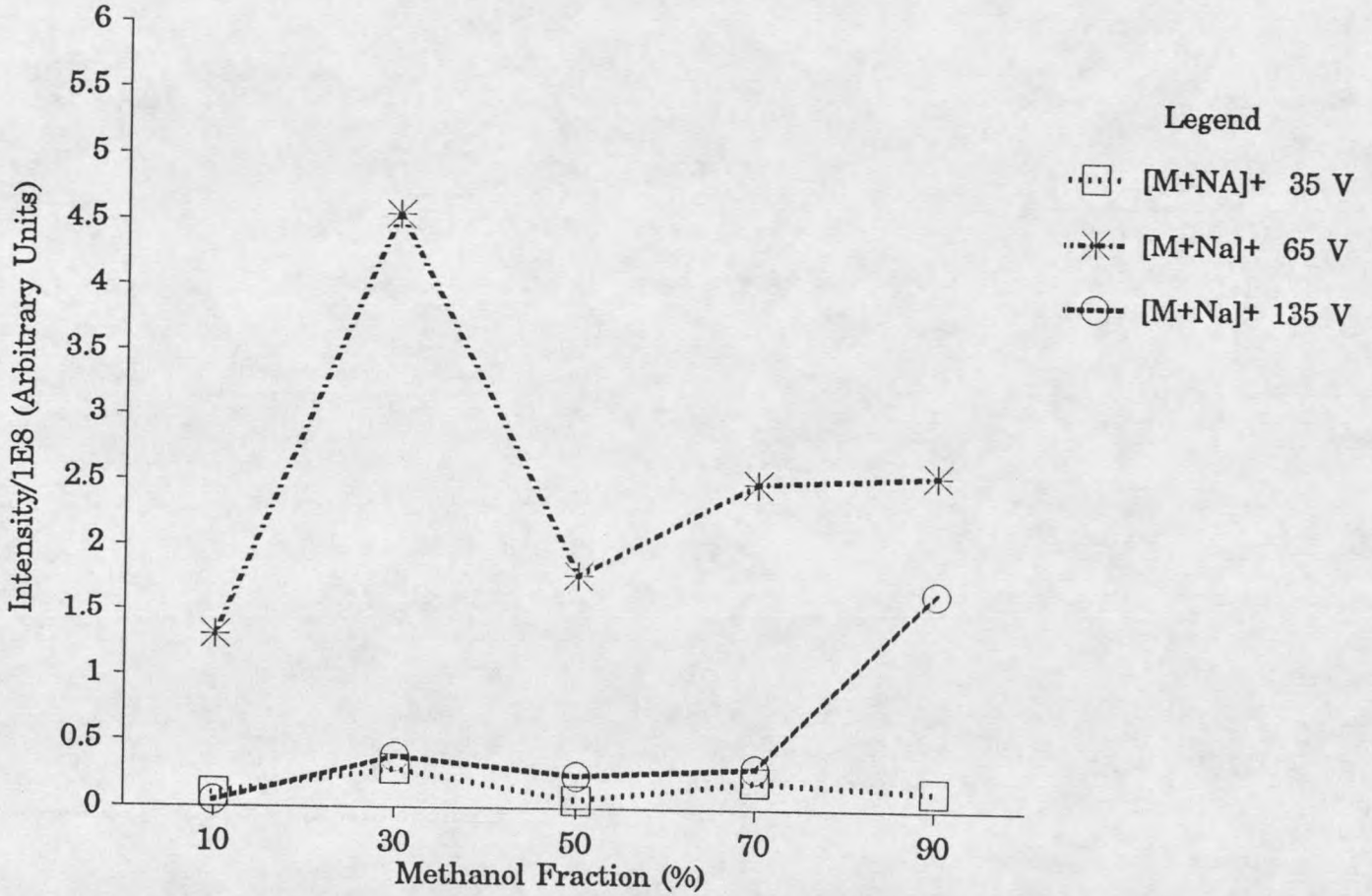


Figure 130. Phosfolan (1.58E-5 M) [M+Na]+ Ion Intensity as a Function of Methanol Fractionl.

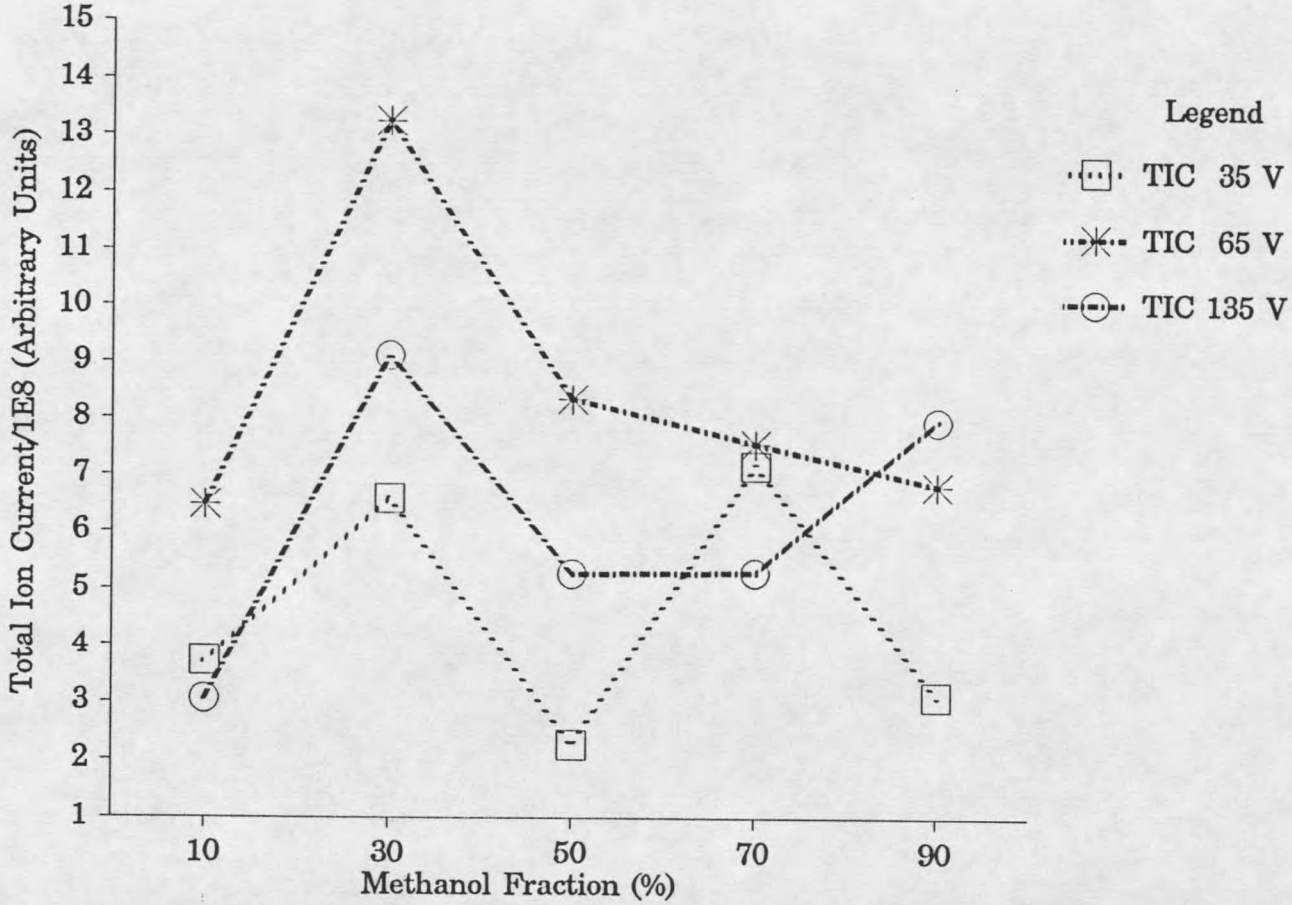


Figure 131. Phosfolan (1.58E-5 M) Total Ion Current as a Function of Methanol Fraction.

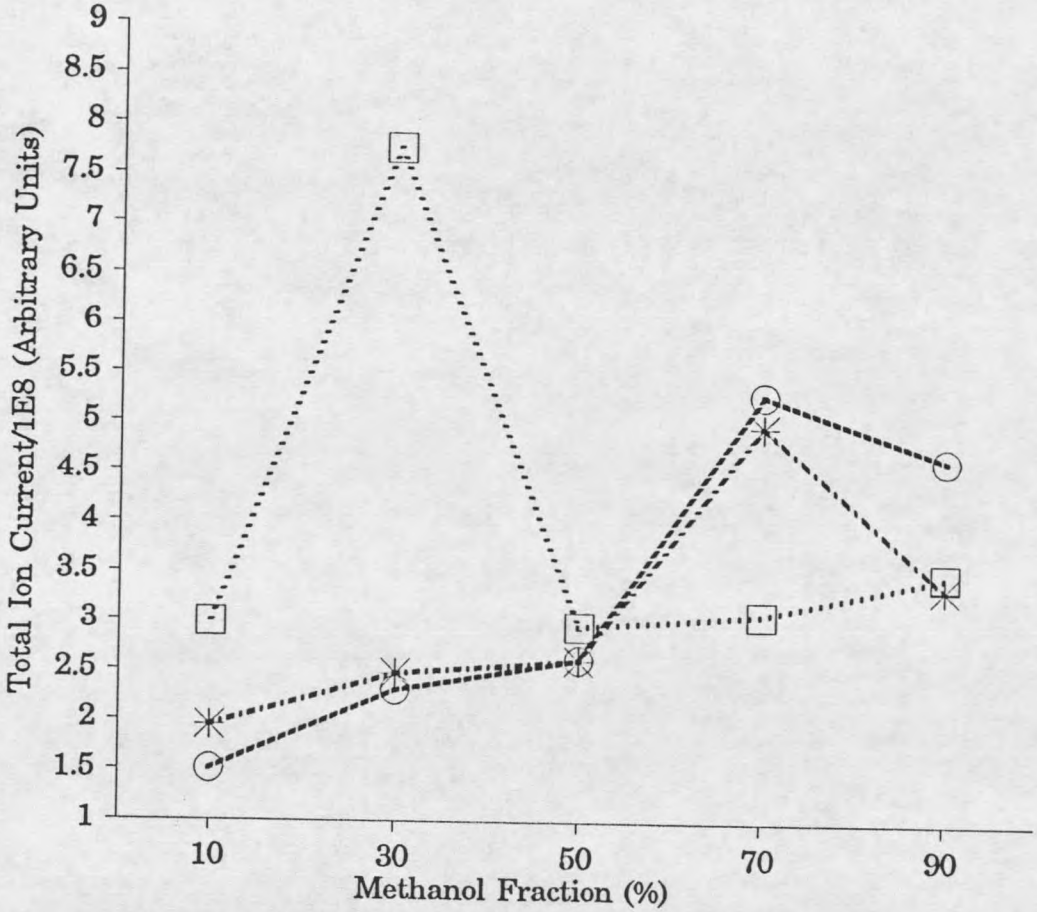


Figure 132. Folpet (1.43E-5 M) Total Ion Current as a Function of Methanol Fraction.

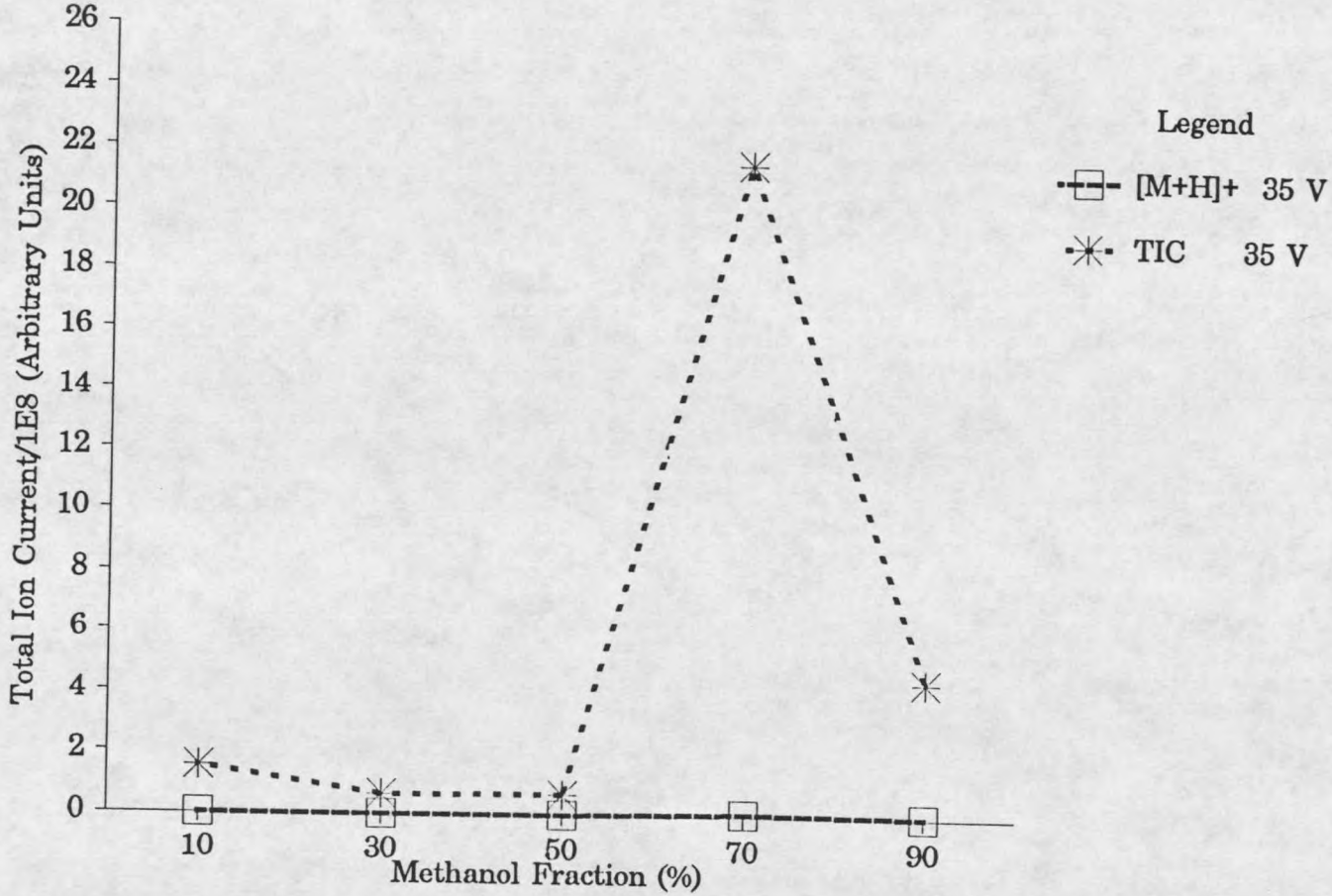


Figure 133. Trifluralin (1.25E-5 M) Total Ion Current as a Function of Methanol Fraction.

APPENDIX I

RAPID METHOD

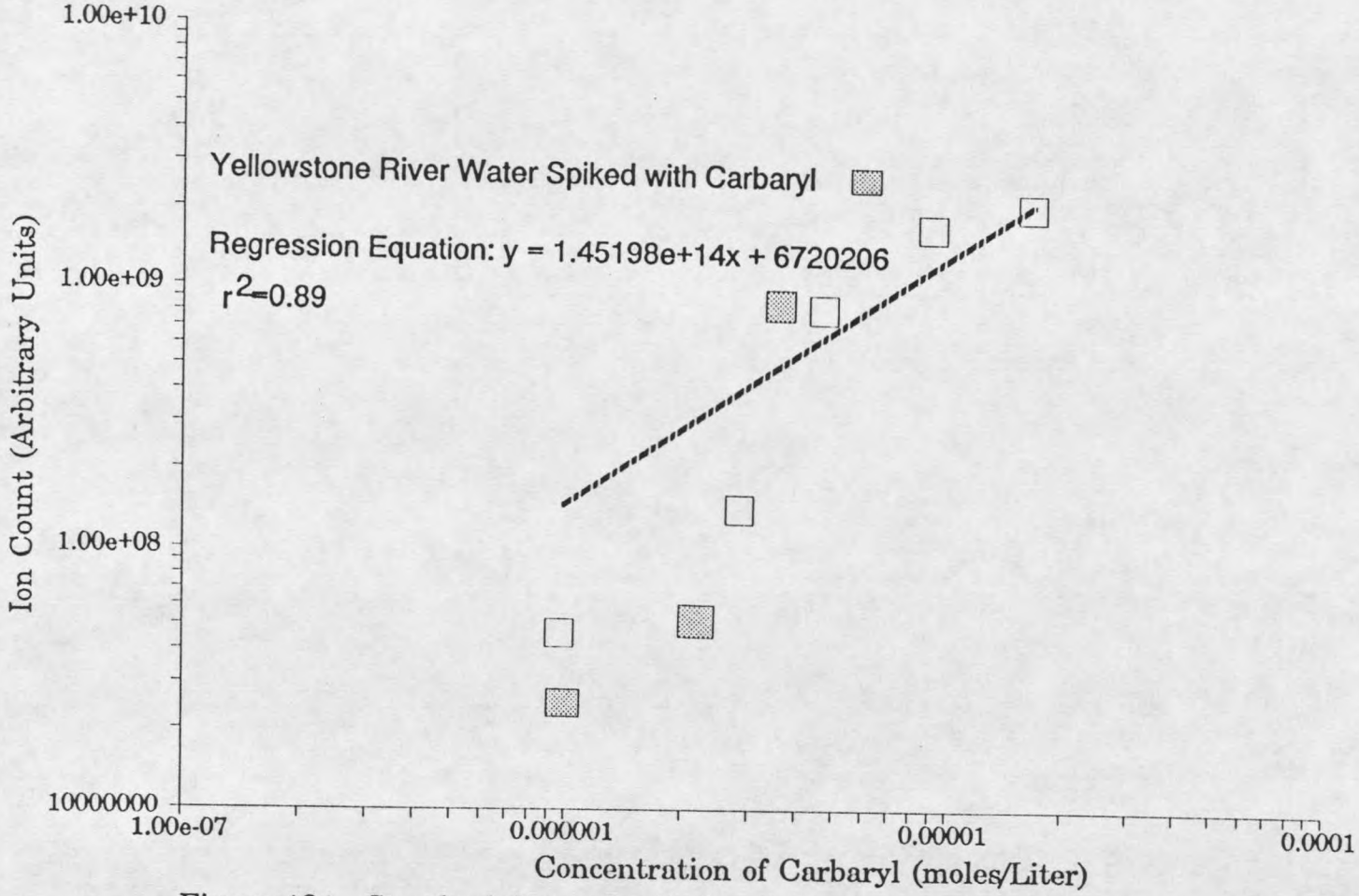


Figure 134. Standard Curve for Carbaryl Generated by Electrospray Ionization.

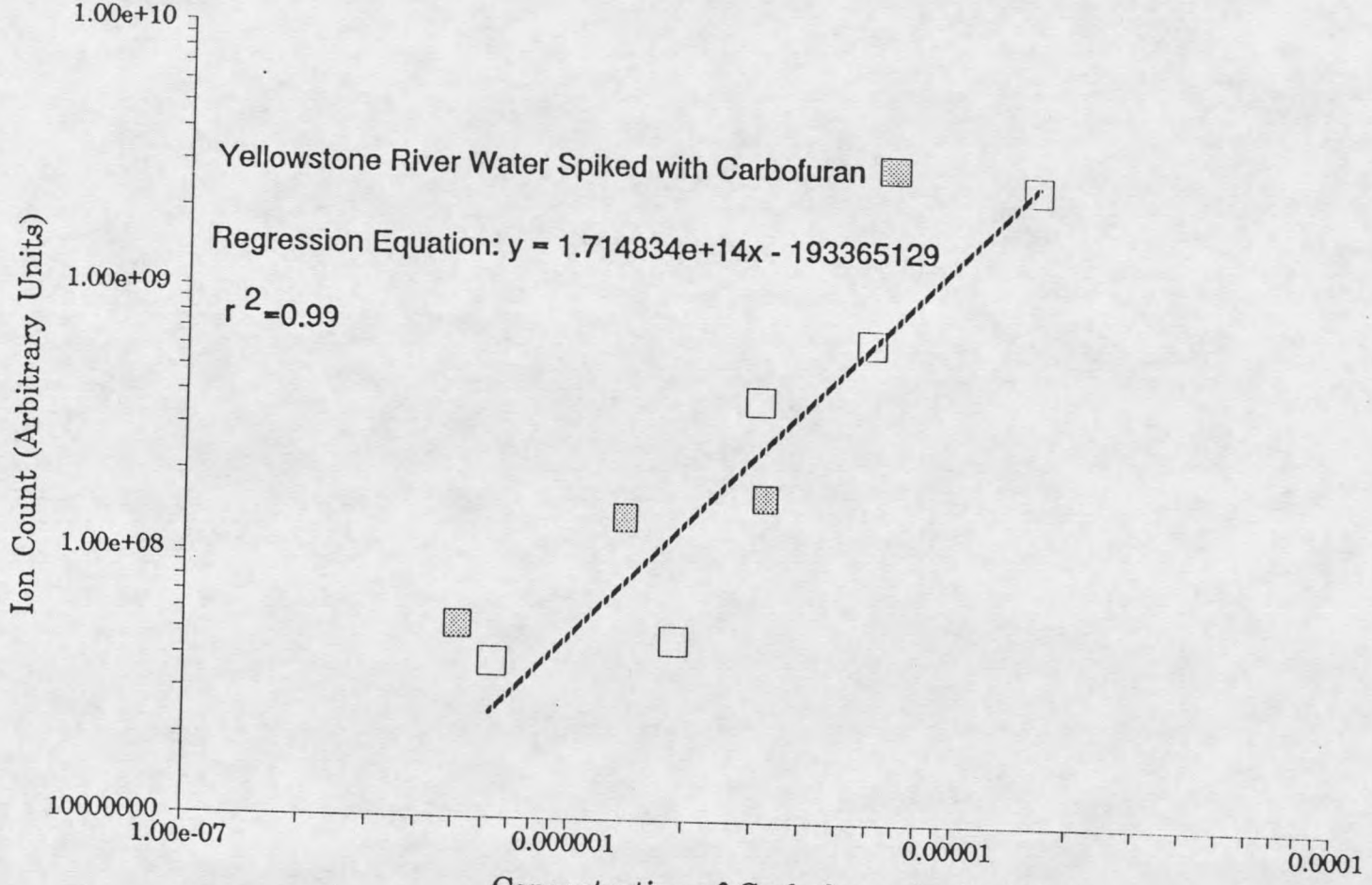


Figure 135. Standard Curve for Carbofuran Generated by Electrospray Ionization.

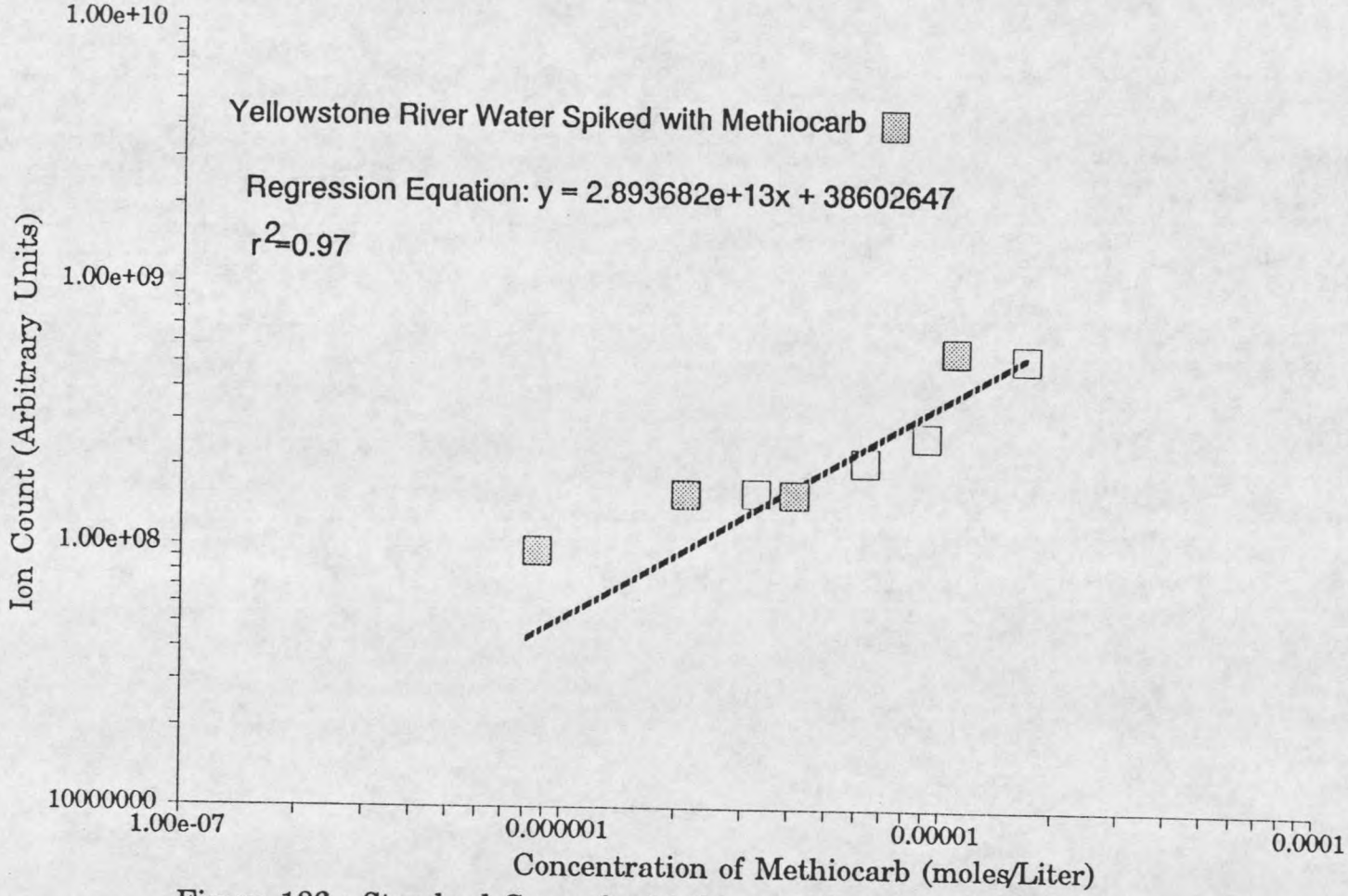


Figure 136. Standard Curve for Methiocarb Generated by Electrospray Ionization.

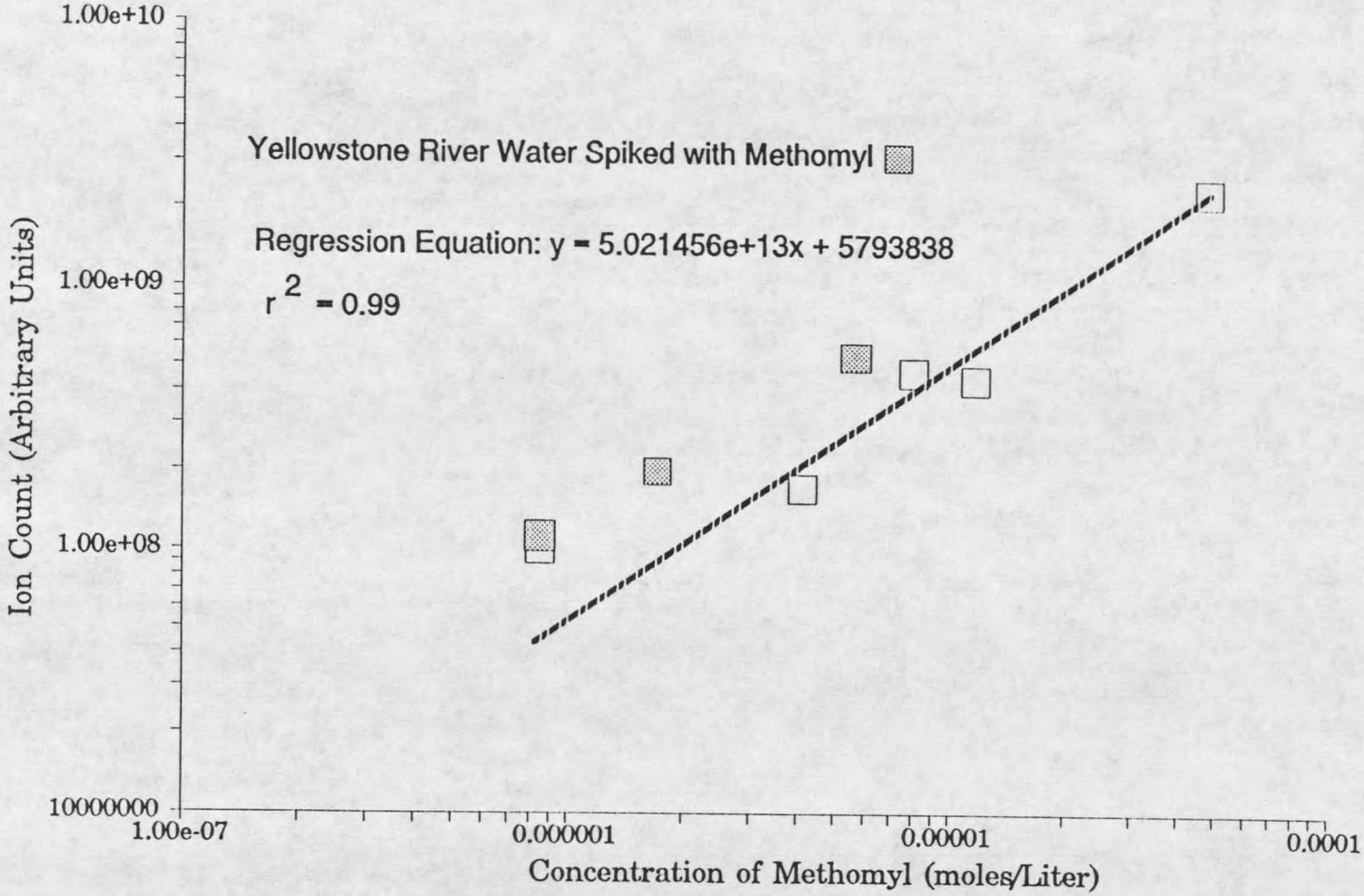


Figure 137. Standard Curve for Methomyl Generated by Electrospray Ionization.

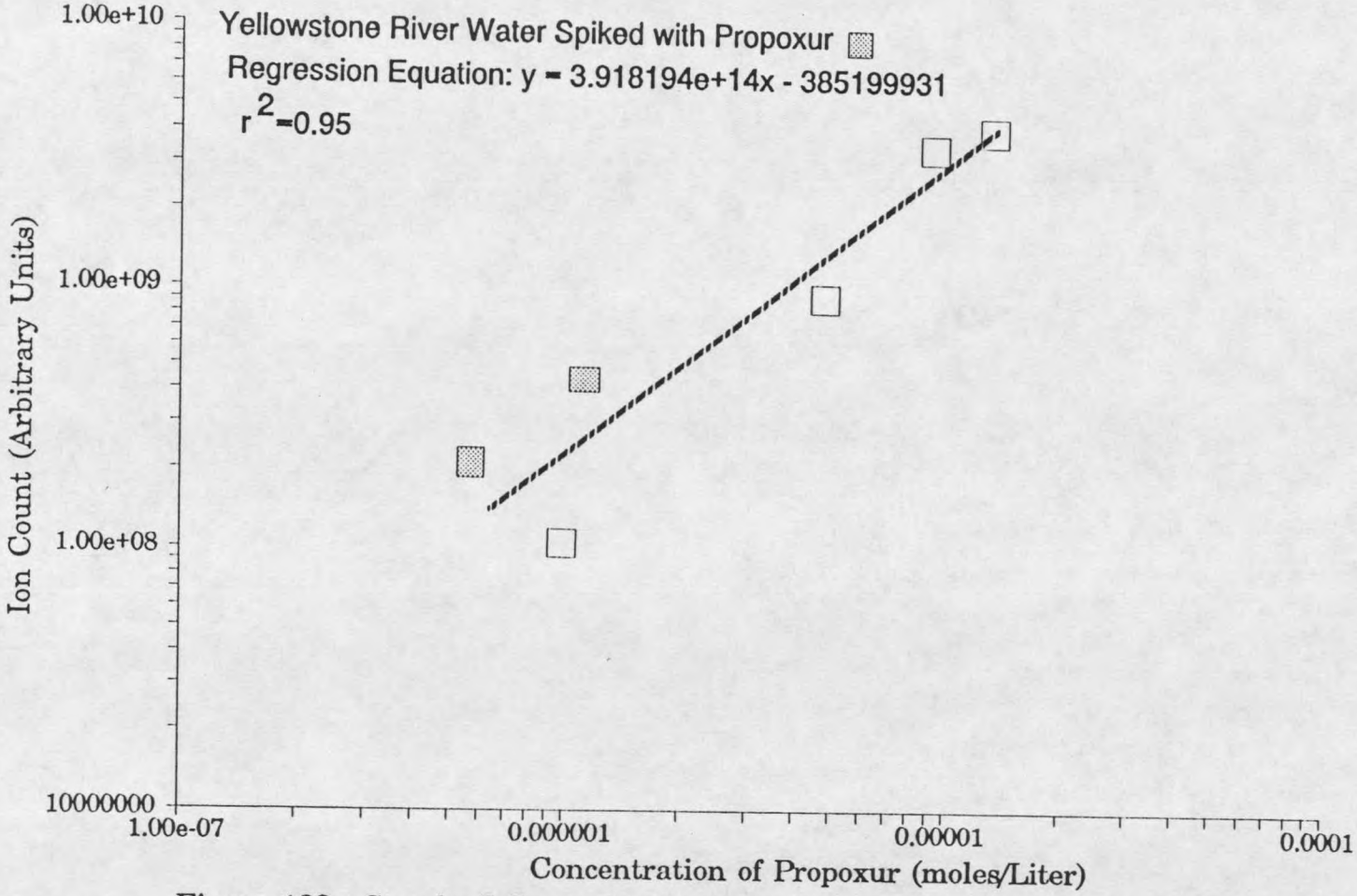


Figure 138. Standard Curve for Propoxur Generated by Electrospray Ionization.

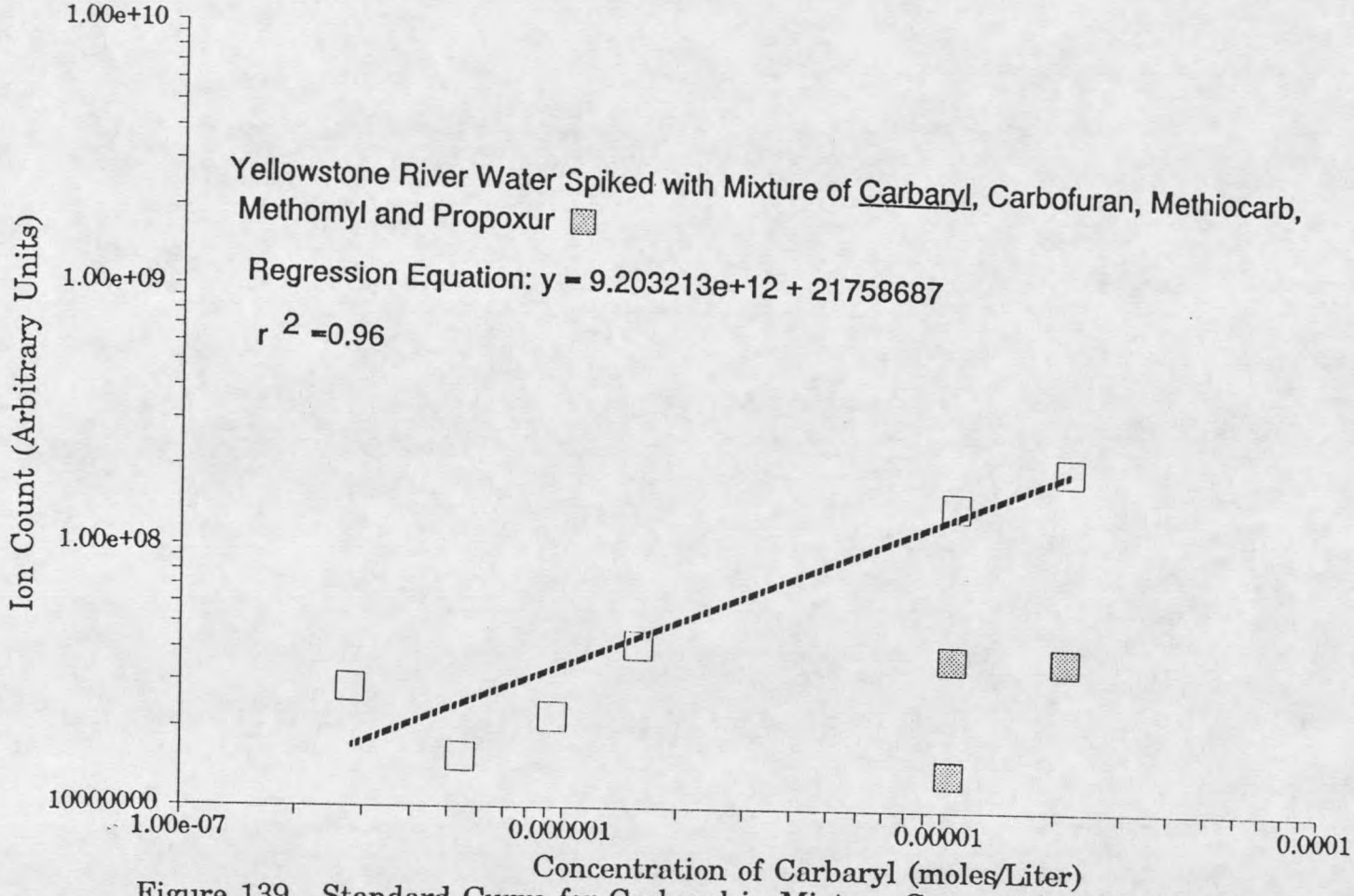


Figure 139. Standard Curve for Carbaryl in Mixture Generated by Electrospray Ionization.

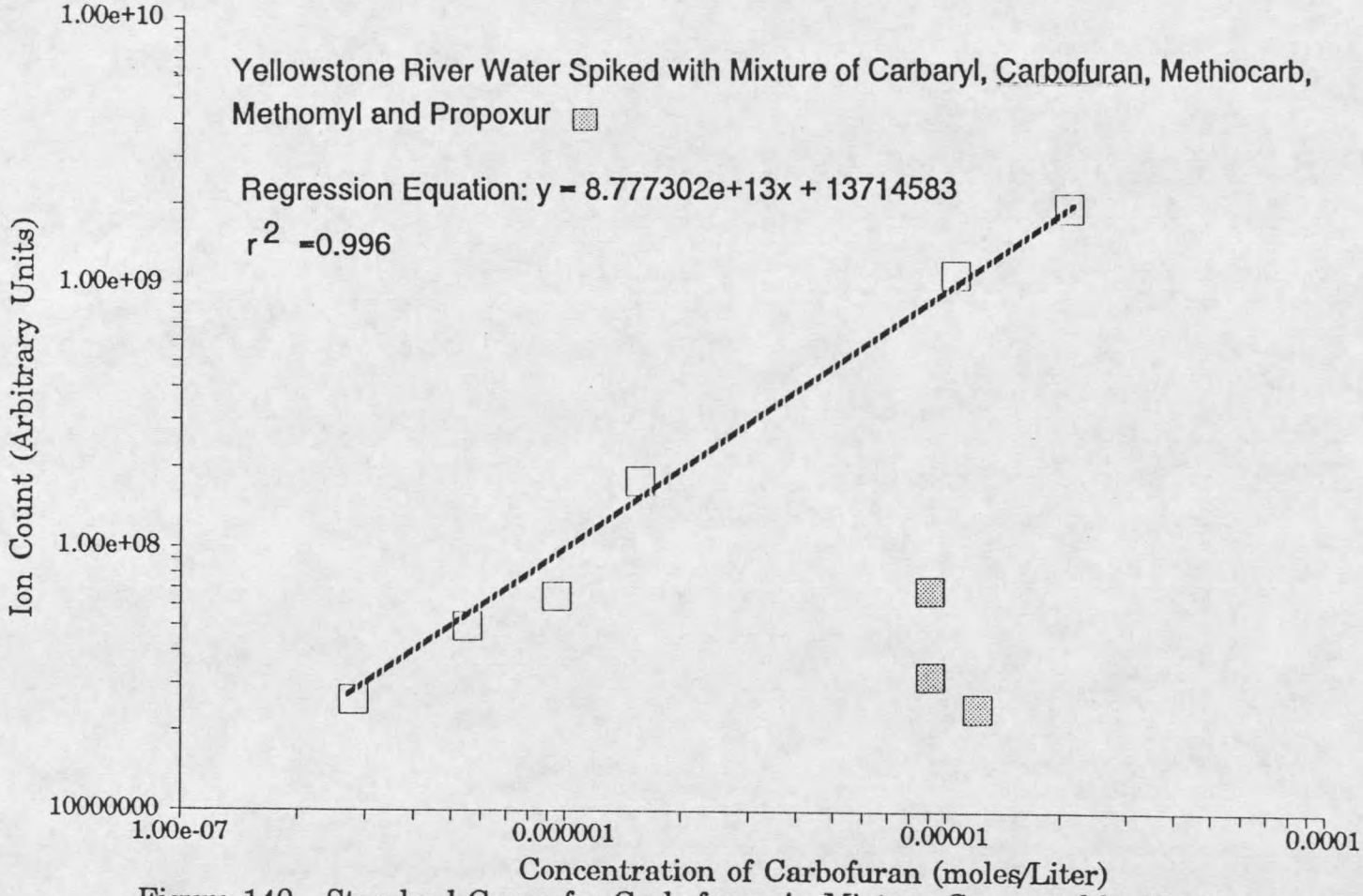


Figure 140. Standard Curve for Carbofuran in Mixture Generated by Electrospray Ionization.

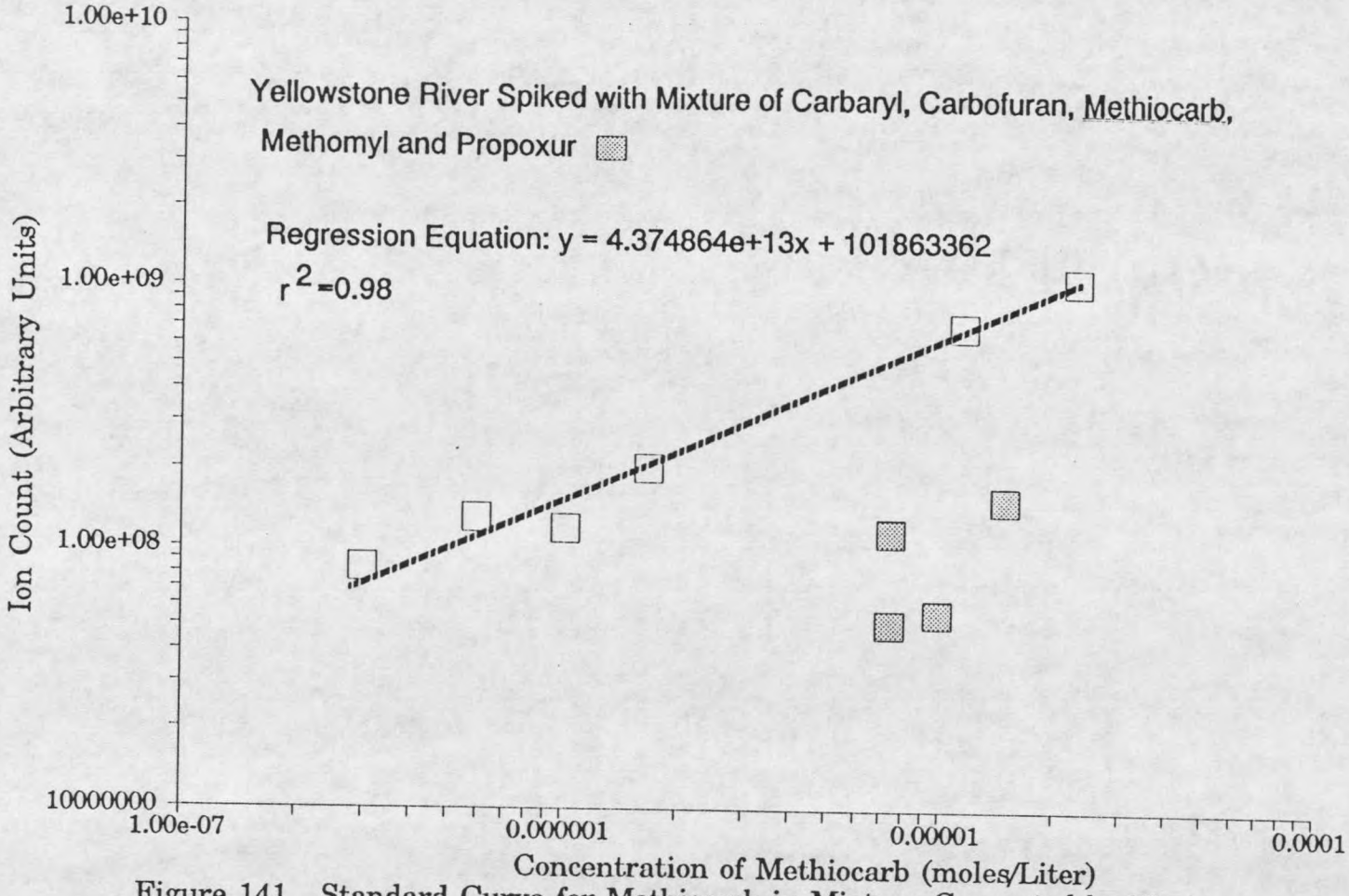


Figure 141. Standard Curve for Methiocarb in Mixture Generated by Electrospray Ionization.

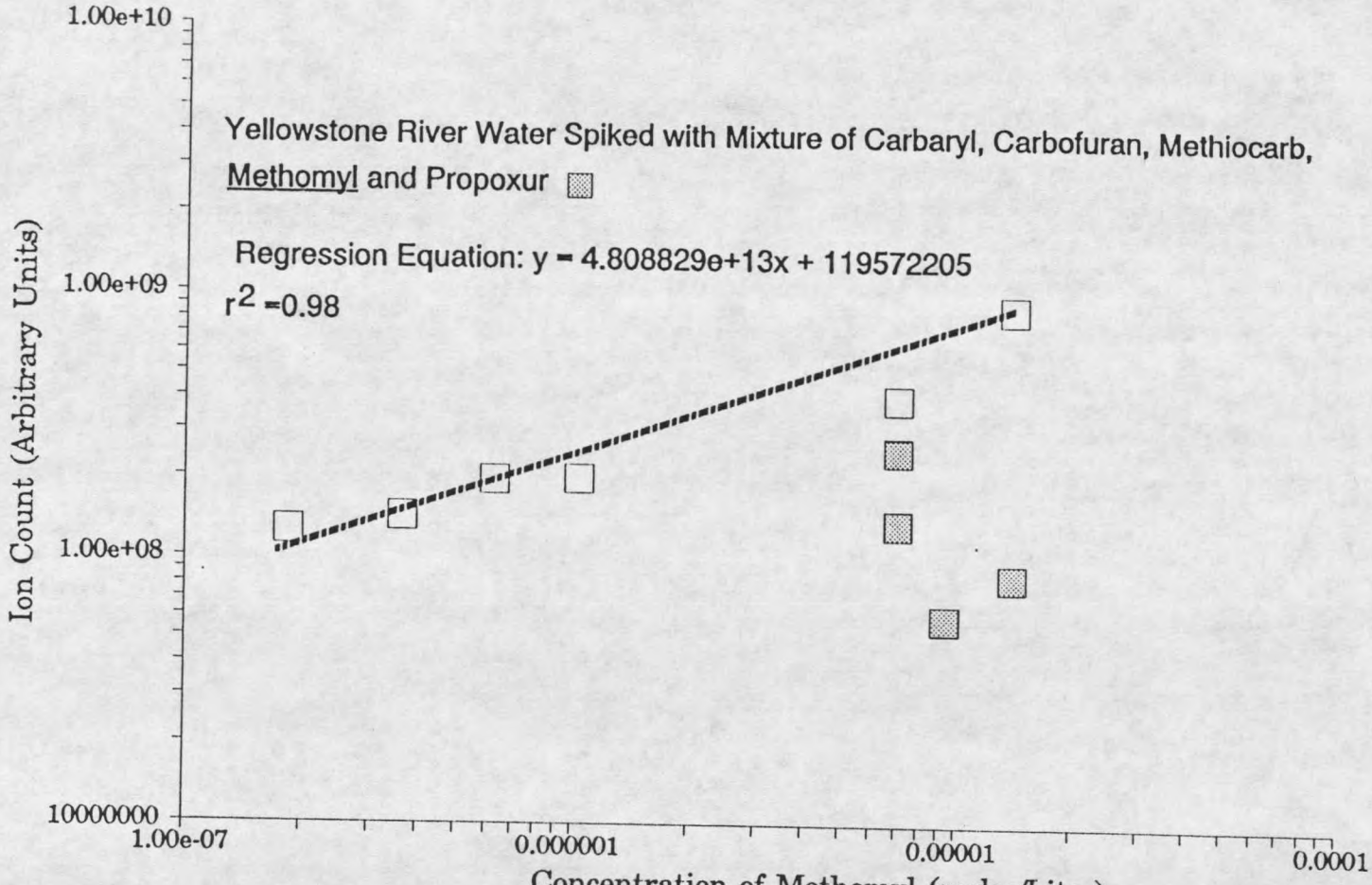


Figure 142. Standard Curve for Methomyl in Mixture Generated by Electrospray Ionization.

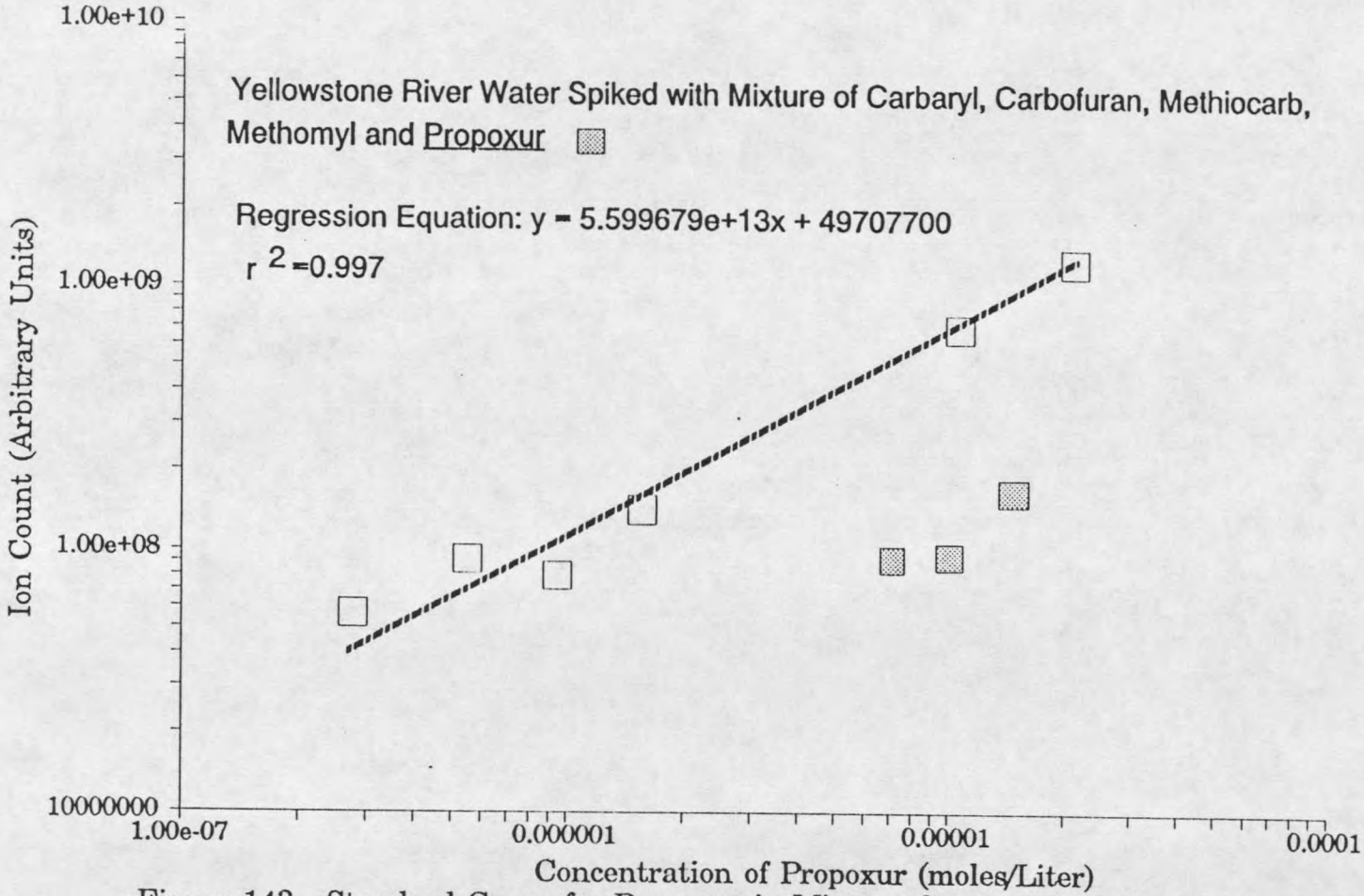


Figure 143. Standard Curve for Propoxur in Mixture Generated by Electrospray Ionization.

MONTANA STATE UNIVERSITY LIBRARIES
3 1762 10208475 1

HOUCHEN
BINDERY LTD
UTICA/OMAHA